

---

# **Behavioral, Electrocortical and Neuroanatomical Correlates of Egocentric and Allocentric Reference Frames during Visual Path Integration**

---

Inaugural-Dissertation  
zur Erlangung des akademischen Grades des  
Doktors der Philosophie

vorgelegt von

Markus Plank, geb. Müller  
aus Villingen-Schwenningen

2009



Ludwig-Maximilians-Universität München  
Fakultät für Psychologie und Pädagogik

Amtierender Dekan: **Prof. Dr. Joachim Kahlert**  
Gutachter: **PD Dr. Klaus Gramann**  
2. Gutachter: **Prof. Dr. Hermann J. Müller**  
3. Gutachter: **Prof. Dr. Ludwig Fahrmeir**  
Tag der mündlichen Prüfung: **26. März 2009**



***'Hope lies in dreams, in imagination and in the courage of those who dare to make dreams into reality.'***

Jonas Edward Salk  
(1914 – 1995)



# Contents

|  |           |
|--|-----------|
| <b>Preface</b>   | <b>x</b>  |
| <b>Acknowledgements</b>  | <b>xi</b> |
| <b>1 Theoretical Framework</b>   | <b>1</b>  |
| 1.1 Introduction .....   | 1         |
| 1.2 Updating Mechanisms – Piloting and Path Integration .....                    | 4         |
| 1.2.1 Piloting .....   | 4         |
| 1.2.2 Path Integration.....  | 4         |
| 1.2.2.1 Path Integration and Path Complexity.....                                | 7         |
| 1.3 Spatial Reference Frames and Representations.....                            | 10        |
| 1.3.1 Primitive and Derived Spatial Parameters.....                              | 12        |
| 1.3.2 Reference Frames and Acquisition of Spatial Knowledge....                  | 13        |
| 1.3.3 Reference Frames as Individually Stable Preferences.....                   | 16        |
| 1.4 Cortical Structures and Mechanisms .....                                     | 18        |
| 1.4.1 Cortical Substrates of Allocentric and Egocentric Reference<br>Frames..... | 18        |
| 1.4.1.1 Egocentric Processing along the Dorsal Pathway ..                        | 21        |
| 1.4.1.2 Allocentric Processing along the Ventral<br>Pathway .....                | 24        |
| 1.4.1.3 Retrosplenial Cortex as Transition Zone .....                            | 26        |
| 1.4.2 Spontaneous Electroencephalographic Oscillations.....                      | 27        |

|          |   |           |
|----------|---|-----------|
| 1.4.2.1  | Theta Activity (4 – 8 Hz) .....   | 28        |
| 1.4.2.2  | Alpha Activity (8 – 13 Hz) .....  | 29        |
| 1.4.2.3  | Rolandic Mu Activity (8 – 13 Hz) .....  | 30        |
| 1.4.3    | Identification of Human Brain Dynamics from Noninvasive Multi-Channel EEG Recordings..... | 30        |
| 1.4.3.1  | The ICA Model.....  | 32        |
| 1.4.3.2  | The ICA Algorithm.....  | 34        |
| 1.4.3.3  | Independence and Correlation .....  | 35        |
| 1.4.3.4  | ICA and PCA .....   | 35        |
| <b>2</b> | <b>Synopsis of the Present Thesis</b>   | <b>37</b> |
| 2.1      | Chapter 3.....  | 38        |
| 2.2      | Chapter 4.....  | 38        |
| 2.3      | Conclusions.....  | 39        |
| <b>3</b> | <b>Behavioral Analyses</b>  | <b>42</b> |
| 3.1      | Abstract.....   | 42        |
| 3.2      | Introduction .....  | 43        |
| 3.2.1    | Spatial Reference Frames and Individual Proclivities .....                                | 44        |
| 3.2.2    | Updating of Representation-Specific Information.....                                      | 44        |
| 3.2.3    | Aims of the Present Study .....   | 47        |
| 3.3      | Experiment 1.....   | 47        |
| 3.3.1    | Methods.....  | 48        |
| 3.3.1.1  | Subjects .....  | 48        |
| 3.3.1.2  | Task, Materials and Procedure .....   | 48        |
| 3.3.2    | Performance Measures.....   | 51        |
| 3.3.2.1  | Side Error .....  | 51        |
| 3.3.2.2  | Angular Fit.....  | 52        |
| 3.3.2.3  | Response Time .....   | 52        |
| 3.3.2.4  | Absolute Error .....  | 53        |
| 3.3.2.5  | Relative Error.....   | 53        |
| 3.3.3    | Results .....   | 53        |
| 3.3.3.1  | Side Error .....  | 53        |
| 3.3.3.2  | Other Incorrect Solutions – Arrowback Responses.....                                      | 54        |
| 3.3.3.3  | Angular Fit.....  | 55        |
| 3.3.3.4  | Response Time .....   | 55        |
| 3.3.3.5  | Absolute Error .....  | 56        |

|          |  |           |
|----------|--|-----------|
| 3.3.3.6  | Relative Error.....  | 57        |
| 3.3.4    | Discussion .....   | 58        |
| 3.4      | Experiment 2 – Same Direction .....                        | 60        |
| 3.4.1    | Methods.....   | 61        |
| 3.4.1.1  | Participants.....  | 61        |
| 3.4.1.2  | Task, Materials, and Procedure.....                        | 61        |
| 3.4.2    | Results .....  | 61        |
| 3.4.2.1  | Side Error .....   | 61        |
| 3.4.2.2  | Other Incorrect Solutions .....                            | 62        |
| 3.4.2.3  | Angular Fit.....   | 62        |
| 3.4.2.4  | Response Time .....  | 62        |
| 3.4.2.5  | Absolute Error .....                                       | 63        |
| 3.4.2.6  | Relative Error.....  | 64        |
| 3.4.3    | Discussion .....   | 65        |
| 3.5      | Experiment 3 – Opposite Directions .....                   | 68        |
| 3.5.1    | Methods.....   | 69        |
| 3.5.1.1  | Subjects .....   | 69        |
| 3.5.1.2  | Task, Materials, and Procedure.....                        | 69        |
| 3.5.2    | Results .....  | 70        |
| 3.5.2.1  | Side Error .....   | 70        |
| 3.5.2.2  | Other Incorrect Solutions .....                            | 70        |
| 3.5.2.3  | Angular Fit.....   | 70        |
| 3.5.2.4  | Response Time .....  | 70        |
| 3.5.2.5  | Absolute Error .....                                       | 71        |
| 3.5.2.6  | Relative Error.....  | 72        |
| 3.5.3    | Discussion .....   | 72        |
| 3.6      | Behavioral Data – General Discussion .....                 | 73        |
| 3.6.1    | Configural Updating of Primitive Parameters .....          | 74        |
| 3.6.2    | Co-Existence of Egocentric and Allocentric Representations | 75        |
| 3.6.3    | Conclusions and Upcoming Steps.....                        | 76        |
| <b>4</b> | <b>Electroencephalographic Analyses</b>                    | <b>77</b> |
| 4.1      | Abstract.....  | 77        |
| 4.2      | Introduction .....   | 78        |
| 4.2.1    | Path Integration.....                                      | 78        |
| 4.2.2    | Reference Frames in Spatial Navigation .....               | 79        |

|         |   |     |
|---------|---|-----|
| 4.2.3   | Cortical Differentiations between Egocentric and Allocentric Reference Frames.....                              | 81  |
| 4.2.4   | EEG Data Examination via Independent Component Analysis (ICA) .....   | 82  |
| 4.2.5   | Aims of the Present Study .....   | 84  |
| 4.3     | Experiment 1 – Same Direction .....   | 85  |
| 4.3.1   | Methods.....  | 85  |
| 4.3.1.1 | Participants.....   | 85  |
| 4.3.1.2 | Task, Materials, and Procedure .....  | 86  |
| 4.3.1.3 | Performance Measures.....   | 86  |
| 4.3.1.4 | EEG Recordings and Artifact Rejection .....   | 87  |
| 4.3.1.5 | Independent Component Analysis and Component Selection.....   | 88  |
| 4.3.1.6 | Component Power Spectra and Event-Related Spectral Perturbation (ERSP) .....                                    | 89  |
| 4.3.1.7 | IC (Pre-)Clustering .....   | 89  |
| 4.3.1.8 | ERSP Statistics.....  | 90  |
| 4.3.1.9 | Strategy- and Complexity-Difference ERSP Computation .....  | 91  |
| 4.3.2   | Results .....   | 91  |
| 4.3.2.1 | Behavioral Performance .....  | 91  |
| 4.3.2.2 | Source Reconstruction.....  | 92  |
| 4.3.2.3 | Cluster Dynamics.....   | 95  |
| 4.3.3   | Discussion .....  | 115 |
| 4.4     | Experiment 2 – Opposite Directions .....  | 121 |
| 4.4.1   | Methods.....  | 121 |
| 4.4.1.1 | Participants.....   | 121 |
| 4.4.1.2 | Task, Materials, and Procedure .....  | 122 |
| 4.4.1.3 | Performance Measures, EEG Recordings and Statistical Analyses .....   | 122 |
| 4.4.2   | Results .....   | 122 |
| 4.4.2.1 | Behavioral Performance .....  | 122 |
| 4.4.2.2 | Source Reconstruction.....  | 124 |
| 4.4.2.3 | Cluster Dynamics.....   | 126 |
| 4.4.2.4 | Discussion.....   | 141 |
| 4.5     | EEG Analyses – General Discussion.....  | 142 |
| 4.5.1   | Interaction of Environmental Complexity and Preferred Strategy in Occipito-Parietal and Parietal Cortices ..... | 144 |

|          |   |            |
|----------|---|------------|
| 4.5.2    | Activity in Common to Turners and Nonturners .....    | 145        |
| 4.5.3    | Conclusion.....                                       | 146        |
| <b>5</b> | <b>Deutsche Zusammenfassung</b>                       | <b>148</b> |
| 5.1      | Theoretischer Hintergrund .....                       | 148        |
| 5.2      | Zusammenfassung der durchgef hrten Untersuchung ..... | 150        |
| 5.2.1    | Zusammenfassung Kapitel 3 .....                       | 150        |
| 5.2.2    | Zusammenfassung Kapitel 4 .....                       | 151        |
| 5.3      | Schlussfolgerungen.....                               | 152        |
|          | <b>Bibliography</b>                                   | <b>155</b> |
|          | <b>Index of Figures and Tables</b>                    | <b>192</b> |
|          | <b>Tunnel Material</b>                                | <b>201</b> |
| A.1      | Instructions .....                                    | 201        |
| A.2      | Tunnel Configurations.....                            | 204        |
|          | <b>EEG-Cap Layout</b>                                 | <b>211</b> |
|          | <b>Eidesstattliche Versicherung</b>                   | <b>213</b> |
|          | <b>Curriculum Vitae</b>                               | <b>214</b> |

# Preface

This Ph.D. thesis has been written at the Ludwig-Maximilians-Universität München in the Department Psychology, General and Experimental Psychology. The project was located in the Research Group FOR480 'Temporal dynamics of visual processing', sponsored by the German Research Foundation (Deutsche Forschungsgemeinschaft). It was a major collaborative effort of PD Dr. Klaus Gramann (Department Psychology, LMU München; Swartz Center for Computational Neuroscience, UCSD San Diego), PD Dr. Stefan Glasauer and Prof. Dr. Dr. h.c. Thomas Brandt (Clinical Neurosciences and Department of Neurology, Center for Sensorimotor Research, LMU München). Travel grants of the *Boehringer-Ingelheim-Fonds*, the *German Academic Exchange Service*, and the *G.A.-Lienert-Foundation for Promotion of Young Researchers in Biopsychological Methods* made it possible to visit the Swartz Center for Computational Neuroscience. Main evaluators of this thesis were PD Dr. Klaus Gramann (LMU München; University of California San Diego) and Prof. Dr. Hermann J. Müller (LMU München).

The goal of this thesis was to identify the behavioral, neuroanatomical, and electrocortical correlates of human visual path integration within allocentric and egocentric reference frames by means of high density electroencephalography (EEG) during a virtual homing task. Experimental results are expected to further clarify the multifaceted interactions of pathway complexity and individual preferences for coding spatial information within either allocentric or egocentric reference frames. To integrate the psychophysiological experiments into the superordinate framework of research on path integration, results of behavioral, neuroanatomical, and neurophysiological experiments on spatial navigation are also reviewed.

# Acknowledgements

A number of people have contributed to the successful completion of this work. First of all, I want to thank my PhD mentor and supervisor PD Dr. Klaus Gramann. He gave me the unique opportunity to encounter fascinating frontiers in electroencephalographic research on spatial navigation based on cutting-edge data-mining methodology and technologies, and supported me throughout the last three years with invaluable expertise and knowledge. His dedication for high-quality research as well as his conscious pursuit of personal and intellectual growth took significant impact on my understanding of excellent scientific practice. In addition, I am grateful to Prof. Dr. Hermann Müller for involving me in an outstanding research group and supporting my personal advancement in multiple ways. I want to thank my colleagues and friends at the Ludwig-Maximilians-Universität München, foremost Dr. Davide Riccobon, for stimulating discussions. Additionally, I want to thank Lena Bur-bulla, Isabel Rätzel, Beate Killian, and Laura Voss for their vigilant help during the experiments.

Special thanks go to Dr. Scott Makeig and the research team of the Swartz Center for Computational Neuroscience, who provided me with unprecedented analysis algorithms, valuable words of advice, and a fascinating team-spirit. I want to particularly thank Dr. Julie Onton and Robert Buffington, who always had an open ear for my questions and suggestions.

This work would not have been possible without the help of my family. Christa and Albert, thank you for your endless support and inspiring experiences throughout the last years.

Conny, I am deeply thankful for your patience, faith, love, and much more that enabled me to always 'see light at the end of the tunnel'.

Markus Plank

München, March 2009

# Chapter 1

# Theoretical Framework

## 1.1 Introduction

Humans and other mobile organisms perceive, act upon and think about space. They localize threats, rewards and other agents in their proximal and distal surroundings by extracting spatial information from perceptual systems. This information is used to build up enduring spatial representations comprising information regarding the localization and relative position of starting points, landmarks and destinations, of routes and pathways, and environmental layouts. They are also capable to derive information regarding their own position and orientation with respect to the represented entities. This, further, enables humans to locomote within environments of varying scale and complexity as well as to interact with objects and other social agents located in their surroundings (Etchamendy & Bohbot, 2007; Tversky, 1993). These activities and mental processes would barely be possible without *spatial cognition*, a complex cognitive function defined as the capacity to acquire, organize, utilize, and revise knowledge about spatial environments in order to achieve a wide variety of goals fundamental to survival. Even if some functional components of spatial cognition are exclusively human – such as the ability to use gestures, verbal wayfinding directions, street signs, and maps – other aspects can be found in all mobile species, including the identification and manipulation of objects located in space, the ability to construct and utilize spatial representations, and spatial orientation and navigation (Landau & Jackendoff, 1993).

*Spatial navigation* comprises planning of travel through the environment by ‘determining and maintaining a course or trajectory from one place to another’ (Gallistel, 1990, p. 35). This course is chosen following various constraints (shortest distance, minimal travel time, maximum safety, etc. - Golledge, 1997;

Rieser, Guth, & Hill, 1982). Additional elements of spatial navigation consist of updating of position and orientation during travel, and, in the event of getting lost, reorienting and reestablishing a path towards the desired destination<sup>1</sup> (Loomis, Klatzky, Golledge, & Philbeck, 1999b). During navigation, the (moving) agent has to obtain and mentally store spatial information about the external world used at some later point to make predictions that constitute seminal foundations for the generation of (partially new) activity in space. For this purpose, polymodal sensory input from visual, vestibular, kinesthetic, and proprioceptive systems, information about the momentary position of the navigator, and long-term enduring action-plans have to be continuously updated, consolidated and integrated into more or less coherent and accurate mental representations of where we are with respect to our surroundings (Bryant, 1992; Kerkhoff, 2000; Tversky, 1993).

During the last decades, research on spatial navigation in psychology, cognitive neuroscience, and artificial intelligence led to a paradigm shift away from the existence of a global, rather amodal representational format (coming along with one global problem-solving mechanism) towards multiple domain-specific, flexible, and interchangeable representations and underlying mechanisms (Burgess, 2008; Tye, 1991). Potentially, there might exist as many different kinds of representations as there are possible solutions to the problem of wayfinding, ranging from rather inflexible route-based sequences of left and right turns to more map-like representations comprising metric parameters and inter-landmark distances (O'Keefe & Nadel, 1978). Although little is known about the spatial representations themselves, research coincides that these can be mounted within distinct but interacting spatial reference frames, including *egocentric* (body-centered) and *allocentric* (environment-centered) coordinate systems (Brewer & Pears, 1999; Klatzky, Loomis, Golledge, Cicinelli, Doherty, & Pellegrino, 1990; Mou, McNamara, Valiquette, & Rump, 2004). But whereas some studies suggested that the choice of either reference frame is obligatorily determined by task demands or external features, e.g., the perspective from which an environment is initially experienced (Bryant, 1992; Heft, 1979; Shelton & Gabrieli, 2002), or by developmental factors (Cousins, Siegel, & Maxwell, 1983; Siegel & White, 1975), recent investigations substantiated the importance of durable and intraindividually stable preferences for coding space

---

<sup>1</sup> In contrast to this ‘action-based’ definition of spatial navigation, *spatial orientation* denotes the predominately cognitive process of knowing about one’s current position as well as the spatial relations between (visible and nonvisible) landmarks. Generally, spatial orientation can be defined as the initial step of the navigational process: Spatial navigation imperatively requires spatial orienting, but spatial orienting is also possible without spatial navigation. However, humans do not explicitly sub-classify their navigation in this way; rather, they subsume the consecutive steps of constant gathering of environmental information, movement planning and simultaneous execution under ‘navigation’ in general (Bowman, Davis, Hodges, & Badre, 1999). This thesis will follow this rationale, and not further differentiate between spatial orientation and spatial navigation.

within distinct spatial reference frames (Gramann, Müller, Eick, & Schönebeck, 2005; Gramann, Müller, Schönebeck, & Debus, 2006). From an evolutionary perspective it seems plausible that humans are capable of learning and utilizing different representations in a flexible way, either in isolation or in combination (Aguirre & D'Esposito, 1999; Mou et al., 2004; Redish, 1999; Sholl, 2001; Touretzky & Redish, 1996).

Most importantly, these reference frames constitute the arena for bidirectional exchange between *bottom-up* information for updating position and orientation, and cognitive processes arising from spatial representations in a *top-down* manner. Whereas the former is determined by the amount and richness of the *array of perceptual inputs*, the latter is significantly affected by the comprehensiveness and detailedness of the enduring *spatial representation*. The behavioral and electrocortical consequences of this interplay between *external* (sensory) and *internal* (mental) processes constitute the central topic of the present PhD thesis:

*How is the external world represented on the neural level, and, how do environmental complexity and individual proclivities for coding space within allocentric and egocentric representations impact the updating processes during navigation, as analyzed by means of activation patterns within distinct cortical networks as well as resulting spatial behavior?*

This thesis combines approaches of general and experimental psychology with neuroscience, applying psychophysiological, i.e., electroencephalographic methods. It considers neither aspects of developmental or personality psychology, nor does it imply any neural modeling of structures and processes underlying spatial navigation as conducted within the fields of computational science or artificial intelligence. Although all these areas are subject to certain flaws and theoretical constraints, they – in sum – have contributed seminal and enriching insights into mechanisms and functions of spatial navigation. The present thesis will consider these fields of research but the primary focus is on psychological implications based on observations of human behavioral and neural responses to spatial structures

## 1.2 Updating Mechanisms – Piloting and Path Integration

As the subject is moving, the configuration of entities in space relative to the moving agent constantly changes. Accordingly, the navigator has to update his<sup>2</sup> position and orientation with respect to environmental space (Gallistel, 1993). The underlying spatial cues might be classified with respect to the type of information used: Position ('*position-based navigation*', or '*piloting*'), or velocity and acceleration ('*path integration*' or '*dead reckoning*') (Loomis, Klatzky, Golledge, Cicinelli, Pellegrino, & Fry, 1993).

### 1.2.1 Piloting

*Piloting*, also referred to as *position-based navigation*, denotes the utilization of visible, audible or otherwise perceivable exteroceptive cues, so-called 'landmarks' (distinct, stationary, and salient objects) in combination with a map of the surroundings in order to infer one's current position and orientation (Golledge, 1999b; Hunt & Waller, 1999). The spatial relations between one's current location and external landmarks are stored within *local vectors* (Merkle, Rost, & Alt, 2006). Whenever real maps are missing, the navigator might still be able to plan a goal-directed path connecting his current location and the destination by deducing a novel itinerary from the memorized spatial relationships between landmarks (Etienne, Maurer, & Georgakopoulos, 1999). During piloting, landmarks are linked by their temporal occurrence as well as their spatial relations that are associated with distinct movement decisions in order to proceed from one landmark to the next. The utilization of reference points and landmarks also allows for correction of errors in perceived position and orientation (position fixing), which qualifies piloting particularly for navigation within *vista space* (Montello, 1993).

### 1.2.2 Path Integration

The present research work will exclusively focus on navigation in the absence of fixed references and landmarks, so-called *path integration* (Loomis et al., 1993), or *dead reckoning*. Impressed by the fascinatingly precise navigation abilities of native guides who were able to keep track of a certain direction even in environments containing no landmark information, Darwin (1873) was the first to postulate the concept. He assumed unconscious processes, i.e., a 'sense of muscular movement' (p. 418), to constitute the driving forces behind

---

<sup>2</sup> The masculine form has been used solely for the purpose of readability and denotes the feminine as well.

path integration. Later on, it was described by Murphy (1873) as the integration of inertial signals along an outbound trajectory.

Path integration is widespread across various species, and has been found in insects (Bisetzky, 1957; Collett & Collett, 2000; Görner, 1958; Merkle et al., 2006; Mittelstaedt, 1985; Müller & Wehner, 1988, 2007; Wehner, Bleuler, Niervergelt, & Shah, 1990; Wehner & Wehner, 1986, 1990), birds (Collett & Collett, 1982; Regolin, Vallortigara, & Zanforlin, 1994), and mammals (Alyan & McNaughton, 1999; Etienne, Maurer, Berlie, Reverdin, Rowe, Georgakopoulos, & Seguinot, 1998; Klatzky, Beall, Loomis, Golledge, & Philbeck, 1999; Klatzky, Loomis, Beall, Chance, & Golledge, 1998; Loomis et al., 1999b; Mittelstaedt & Glasauer, 1991; Seguinot, Cattet, & Benhamou, 1998; Seguinot, Maurer, & Etienne, 1993).

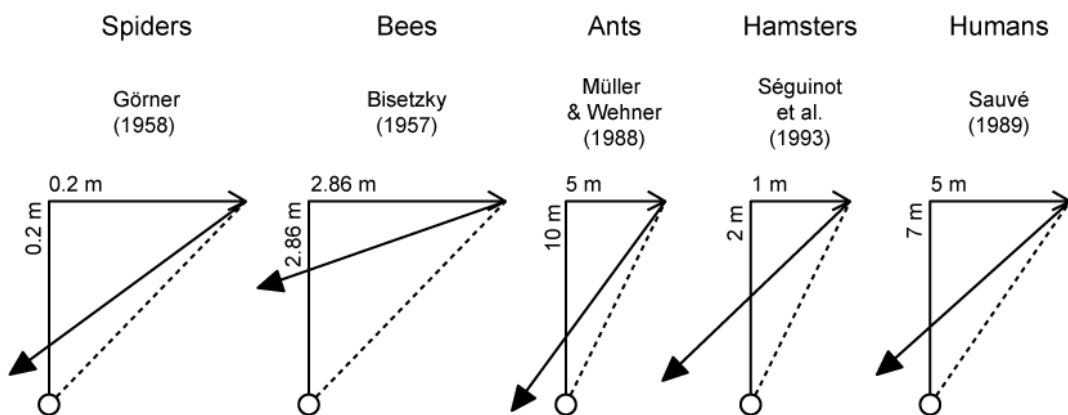


Figure 1.1: Path integration – Examples of systematic errors over species during homing after following L-shaped outbound trajectories (redrawn with permission from Maurer & Seguinot, 1995, p. 459). Circles indicate starting positions. The homing vector (solid black arrowhead) typically displays an inward-error, therefore crossing the previously traversed path.

As can be seen from Figure 1.1, path integration in these animals has most generally been tested by means of their *homing* or *triangle-completion abilities*. E.g., after traversing an outbound trajectory containing straight segments and turns, these animals are able to directly head back to the starting point. One arthropod with excellent spatial abilities is the Desert Ant *Cataglyphis Fortis*. Its navigation skills have been extensively studied by various scientific disciplines (e.g., neurobiology, engineering) with the initial systematic investigations dating back to the first decades of the 20th century (e.g., Cornetz, 1912). During foraging in the vast and virtually featureless environment of the Saharan desert, these arthropods cover distances of thousands of times their own body length to finally arrive pinpoint destinations. After uploading food, they display the characteristic, arthropod-specific homing behavior: They directly head back to their nest location in a straight line.

There is an ongoing debate about the sufficiency of path integration for human everyday navigation: Errors and uncertainty during navigation rise approximately exponential with increasing distance traveled. Therefore, cognitive psychology has accentuated its proneness to error (Dyer, 1998) and the ultimate need for corrective processes based on local vectors. Comparative psychology, by contrast, has emphasized the satisfactory quality of path integration for basic navigational processes (Ivanenko, Grasso, Israel, & Berthoz, 1997; Loomis et al., 1999b). Our daily city-dwellers' experience seemingly favors the active processing of landmarks and reference points (Foo, Duchon, Warren, & Tarr, 2007; Foo, Warren, Duchon, & Tarr, 2005). However, navigation solely based on local vectors holds the risk of being inflexible, unreliable and error-prone, since natural landmarks exposed to the forces of nature might disappear or alter their appearance due to seasonal or climatic changes over time (e.g., in the dark or during heavy fog). From an evolutionary perspective it might therefore be useful to apply a navigation strategy that runs independent of landmarks and does not require any (real or mental) map of the surrounding environment (Loomis et al., 1999b): Path integration ('velocity-based navigation') denotes the ability to infer one's current displacement (in terms of distance and direction) from a given origin by integrating velocity and acceleration and angular variation along a traversed trajectory into a *global* vector. Measurement of velocity and acceleration can be based on external (*allothetic*) and internal (*ideothetic*) signals (Mittelstaedt, 1985; Mittelstaedt & Mittelstaedt, 1982).

Allothetic signals include celestial cues such as skylight polarization (Merkle et al., 2006; Wehner, 2003), as well as compass cues, e.g., the geomagnetic field (Begall, Cervený, Neef, Vojtech, & Burda, 2008; Kimichi, Etienne, & Terkel, 2004) or constant wind direction (Müller & Wehner, 2007), and, additionally, minimal geographical slant (Restat, Steck, Mochnatzki, & Mallot, 2004; Steck, Mochnatzki, & Mallot, 2004). Optic and acoustic flow have also been shown to provide allothetic information (Frenz & Lappe, 2005; Kearns, Warren, Duchon, & Tarr, 2002; Kirschen, Kahana, Sekuler, & Burack, 2000; Mossio, Vidal, & Berthoz, 2008; Sun, Campos, Young, Chan, & Ellard, 2004; Warren, Kay, Zosh, Duchon, & Sahuc, 2001). Ideothetic signals, by contrast, comprise inertial vestibular information as provided by otoliths and semicircular canals (Chance, Gaunet, Beall, & Loomis, 1998; Fernandez & Goldberg, 197; Glasauer, Amorim, & Viaud-Delmon, 2002; Ivanenko et al., 1997; Klatzky et al., 1998; Peruch, Borel, Magnan, & Lacour, 2005; Yardley & Higgins, 1998), afferent proprioceptive signals from muscles, tendons, and joints, as well as efference copies of musculature commands (Bakker, Werkhoven, & Passenier, 1999). Recent studies suggest that visual flow also comprises ideothetic aspects (Winship, Pakan, Todd, & Wong-Wylie, 2006; Wylie, Glover, & Aitchison, 1999) and supplies sufficient information relevant for ideothetic updating of position and orientation (Gramann et al., 2005; Riecke, van Veen, & Bühlhoff, 2002).

Most suitable, continuous movement of a navigator along an outward path is represented as a sequence of steps (translations) of fixed step size, alternating

with changes of direction (rotations) (Benhamou, Sauve, & Bovet, 1990). As can be seen from Figure 1.2.A, path integration based on ideothetic cues is then described by formulas by which a *homing-vector* (*ideothetic azimuth value*) specifies the memorized home location after  $n+1$  steps ( $\omega_{n+1}; D_{n+1}$ ) as a function of its previous value computed after  $n$  steps ( $\omega_n; D_n$ ).

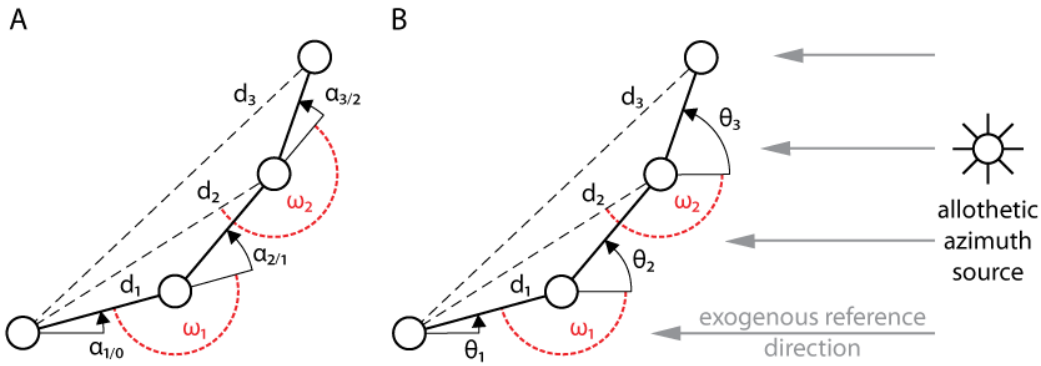


Figure 1.2: Path integration, polar coordinates – The navigator might estimate his position and angular orientation based on **(A)** ideothetic input, or **(B)** allothetic information (adapted and modified from Mittelstaedt, 2000, and Benhamou & Seguinot, 1995).

By contrast, when path integration is based on stationary *allothetic azimuth sources* (see Figure 1.2.B), e.g. skylight polarization, the total amount of rotation  $\theta$  after  $n$  steps is coded both with respect to the previously integrated rotations (idiothetic azimuth value) as well as with respect to the allothetic reference direction. The two inputs are subsequently weighted and added up for path integration. In other words, the navigator has to compute, at least approximately, length  $D$  and angle  $\omega$  of the global vector relative to an allothetic reference direction (Merkle et al., 2006; Mittelstaedt, 2000).

### 1.2.2.1 Path Integration and Path Complexity

The representation underlying path integration is a constantly updated abstraction derived from computations of route information. Speeds and turning angles along the outbound path are compared and subsequently summed up by vector addition (Etienne & Jeffery, 2004), resulting in a global vector, containing distance and direction of the current location with respect to the starting point (Merkle et al., 2006; Müller & Wehner, 1988). Even though not explicitly stated by Müller & Wehner (1988), the global vector concept may provide a basic idea of what is stored within an enduring spatial representation. The parameters retained in the generated *global vector* are seemingly determined by the frequency of the updating procedure, as suggested by distinctive modeling approaches to path integration (Benhamou & Seguinot, 1995; Maurer & Seguinot, 1995), that, most generally, characterize path integration as either being based on *history-free updating* (Müller & Wehner, 1988), or on *configurational updating* (Fujita, Klatzky, Loomis, & Golledge, 1993).

The *history-free model* or *moment-to-moment* updating (Müller & Wehner, 1988) assumes that the traveler is continuously monitoring sensations of linear and rotary velocity and acceleration. These sensations constantly refresh the computation of current position as well as the direction to an anchor point where the process was initiated. Data is fed into a global vector that contains only information regarding overall turning rate and distance required to reach the origin. With these two parameters the navigating subject should be able to orient at each point of an outbound path, without being affected by pathway complexity, e.g. by overall length of the passage, the number of segments or the direction of consecutive directional changes. Because history-free path integration is supposed to proceed online during the encoding of information, the homing vector should be available at all times during the passage, resulting in similar response times and comparable error scores independent of external factors, e.g., the layout of the traversed outbound trajectory. Following this minimalist definition of a global vector, the navigator would not be able to retrace the route just traveled or to proceed directly to any point along the route other than its origin.

Alternatively to the minimal vectorial information connecting two single points in 2D or 3D space, the navigator might store a more complete record of the traversed path (Foo et al., 2005). This has been proposed as *configural updating* (May & Klatzky, 2000), denoting a process that is strongly affected by shape and configurational parameters of the pathway. During configural updating, the traveler updates position and heading not in equidistant intervals, but only at significant points, e.g. when encountering a directional change. As a result, the representation of the traversed path is a sequence of straight segments intermitted by turns. Therefore, configural updating is strongly affected by path complexity with increasingly complex layouts resulting in higher cognitive load, i.e. remembering an increasing number of distinct points encountered during the path. Higher complexity in terms of more segments and more turns, or more gradual turns instead of, e.g., right-angled turns (Cornell & Bourassa, 2007), should lead to an increase in task difficulty, mirrored by measures of angular adjustment and reaction times (Jansen-Osmann & Wiedenbauer, 2006). For example, traversing a path with two segments connected by a 90° turn the navigator might represent the configuration of the path somewhere along the second leg as L-shaped. Following Loomis and colleagues (1999b), there might, however, exist gradual varieties on a continuum in between comprehensive representations, where the path is stored as a whole, and less extreme examples, where after an update the antecedent path representation of the previous segments are discharged from memory.

Several experiments support the predictions of the *configural updating* model (Loomis et al., 1993; May & Klatzky, 2000; Riecke et al., 2002). The first attempt to model *human* path integration abilities based on configural updating was made by Fujita and colleagues (1993), who posited an *encoding-error model of pathway completion* in the absence of vision, therefore excluding any allocentric information as sources of systematic error. The authors supposed

that errors emerge from systematic distortions in internal processing of ideothetic cues, e.g. from representational compression of lengths and turns along the pathway relative to their true values. The computation and execution of the homeward trajectory were not supposed to be afflicted with systematic error. Random error, by contrast, could arise at any stage of processing. Following Euclidean axioms, humans should encode the length of straight-line segments by a function providing a single value of segment length for each stimulus value (therefore, two straight passages of equal length should have equally encoded length values). The same should hold for the encoding of angular turns: Given that turning angles are internally encoded by a function providing single values for each stimulus turn, heading changes of equal angular magnitude should be encoded as equal. Based on these conceptualizations, Fujita and colleagues assumed the resulting internal representation to comprise not only a singular homing vector, but a comprehensive record of the path traversed. The model is quite successful in representing pathways consisting of isosceles triangles, but would have to integrate additional assumptions and variables in order to be applied to stimuli more complex than triangles, particularly when the outbound trajectory comprises crossovers or curved segments (Klatzky et al., 1990; Loomis et al., 1993).

However, only few studies exist investigating homing accuracy dependent on complexity parameters of the traversed path. In a homing task with blindfolded subjects Klatzky and colleagues (1990) systematically varied path complexity from one straight segment up to three segments, intersected by two turns. Analyses revealed a strong influence of path complexity on homing accuracy, with more pronounced distance and turn errors for more complex paths. Interestingly, Klatzky and colleagues also discussed the impact of configurational characteristics of the pathways. Their results suggested higher homing accuracy for trajectories with two turns bending into the same direction as compared to much lower homing accuracy for two contrary turns. Other studies also found participants to be quite accurate in directional estimations when traveling along paths containing one or two turns, but collapsing homing accuracy when the paths contained three turns (Ruddle, Payne, & Jones, 1998).

Pointing accuracy is assumed to decrease with increasing path length, defined by the numbers of segments (Loomis et al., 1993; but see Wiener & Mallot, 2006). Loomis et al. (1993) complemented the homing task of Klatzky et al. (1990) with an additional retracing task, where blindfolded subjects had either to make a shortcut back to the starting point or walk back along the path they came from. Whereas the latencies to initiate the homing response were significantly longer for routes of higher complexity, latencies for the retrace condition were comparable, suggesting that subjects not only updated an internal homing vector, but also formed a representation of the outbound path in memory. Following Loomis et al. (1993), the difficulty of a configuration can be determined by more than just the total length and number of legs of an outbound path.

As suggested by Merkle et al. (2006), homing accuracy may be afflicted with error, emerging from inaccurate measurements of rotations and/or translations while traversing the outbound path. Due to the iterative character of the updating process during path integration within an egocentric and an allocentric reference frame, errors tend to accumulate, resulting in a general misestimation of return distance or return direction with increasing path complexity.

The above described studies conceptualized path complexity in terms of number of segments and turns during an outbound path. However, several studies found human path integration to be differentially affected by translational and rotational information (Kearns et al., 2002; May, 2004). Additional support for this comes from Gramann et al. (2005), who applied a canonical correlation analysis on the relative contributions of rotational and translational information to measures of homing accuracy. The results demonstrated that rotational information had a higher impact on homing accuracy as compared to translational information. This result is also supported by connectionist network modelling (Etienne, Maurer, & Seguinot, 1996): Although the networks integrated directional information, they did not update return distance.

In sum, the depicted investigations on human path integration accuracy analyzed the influence of path complexity by varying the number of turns and segments demonstrating decreasing homing accuracy with increasing number of turns and segments. However, the cited studies have given little consideration to the influence of path complexity or the direction of consecutive heading changes on path integration based on distinct reference frames.

### 1.3 Spatial Reference Frames and Representations

Basically, a spatial reference frame can be defined as a ‘means of representing the locations of entities in space’ (Klatzky, 1998, p. 1). Reference frames allow the navigator to infer inter-object relations as well as self-to-object relations (Miller & Allen, 2001) by mounting distinct coordinate systems within which spatial information is encoded. Initially, this idea dates back to Trowbridge (1913), who aimed at the identification of factors supporting loss of orientation. According to the author some navigators may process spatial information within a ‘*domicentric*’ reference frame in which the current position of the navigator is coded with respect to his or her homing site. The navigator could be seen as connected to an elastic band attached to the home site. On the other hand, navigators apply an ‘*egocentric*’ method by orienting with respect to the cardinal directions (North, East, South, and West, respectively). The coordinate system originates in the Ego and also moves with the Ego. In this case, the elastic bands pointing into the cardinal directions have infinite lengths. Finding home within this egocentric method was supposed to be possible only if the traversed path is still memorized.

Although these conceptualizations have experienced fundamental transformations during the last century, research in spatial navigation agrees on the duality of representational systems. Most generally, a distinction is made between a self-centered *egocentric reference frame* and an environment-centered *allocentric reference frame*<sup>3</sup> (Brewer & Pears, 1999; Burgess, 2006; Klatzky, 1998; Klatzky et al., 1990; McNamara & Valiquette, 2004; Mou et al., 2004; Neggers, Schölvinck, van der Lubbe, & Postma, 2005; Sholl & Nolin, 1997; Wang & Spelke, 2002).

In an *egocentric reference frame*, established by self-to-object relations, locations are represented with respect to a reference point on the navigator's body (Vogeley & Fink, 2003). This so-called '*egocenter*' (Klatzky & Wu, 2008) as well as a reference direction being aligned with the subject's heading, or orientation. The location of the egocenter within the body of the navigator has been investigated and found to vary with the sensory modality and other task-related factors (Soechting & Flanders, 1992). The egocenter of binocular vision, for example, has been found to lie between the eyes (Enright, 1998; Ono, Mapp, & Howard, 2002; Wade, 1992), whereas for touch, the egocenter varies with posture (Haggard, Newman, Blundell, & Andrew, 2000). This thesis will refer to any frame of reference as '*egocentric*' as long as its origin is located on the navigator and space relative to his or her location. Since humans almost always move along their line of sight, alignment of the three reference systems (eye-centered, head-centered, and torso-centered) can be expected, and thus space is coded based on the three intrinsically defined axes of the navigator: front-back, right-left, and up-down (Bryant & Tversky, 1999; Franklin & Tversky, 1990). Distance and direction of entities in space are estimated independently of each other, solely related to the body of the navigator (Aguirre & D'Esposito, 1999; van Asselen, Kessels, Kappelle, Neggers, Frijns, & Postma, 2006). As the navigator moves, he has to update these representations with each consecutive step by vector summation (see section 1.2.2). Updated egocentric positions of objects are computed by adding the displacement vector of an object (relative to the navigator) to their previous egocentric position vectors. The resulting spatial representation therefore can be characterized as being dynamic and transient. In other words, the world constantly changes, whereas the navigator remains spatially fixed in the center of the reference system (Wang & Spelke, 2000).

---

<sup>3</sup> Often, egocentric and allocentric are conceptualized to mirror the distinction of subjective vs. objective view points. However, both egocentric and allocentric reference frames imply a certain (subjective) perspective. Therefore, some researchers, mostly in philosophy, have tempted to identify reference frames that are entirely independent of any perspective (e.g., Campbell, 1994). Grush (2000) refers to these as *nemocentric*.

By contrast, an *allocentric reference frame*, also referred to as ‘*exocentric*’ or ‘*geocentric*’, establishes a polar or Cartesian coordinate system with an origin external to the navigator and an external reference direction, e.g., as defined by allothetic azimuth sources, or the initial view of an environmental space (Benhamou, 1997; Burgess, 2006; Mou, McNamara, Rump, & Xiao, 2006; Wang & Spelke, 2002). Object-to-object relations are represented independently of the position and orientation of the navigator, implying a map-like survey view of the surroundings with coordinate axes corresponding to cardinal directions (‘University is about 2 km north of Marienplatz.’), or, alternatively, to the global layout of the environment, such as the intrinsic axis of a rectangular room or an array of objects (Mou & McNamara, 2002; Mou et al., 2004; Shelton & McNamara, 2001; Shelton & McNamara, 2004). Also, natural boundaries such as coastal shores and mountain ranges can provide allocentric reference directions (Jonsson, 2002). Representing the moving navigator within an allocentric reference frame implies constant updating of his position (but not his orientation) within stable, enduring spatial relations between salient objects (comparable to a fixed figural map in which the navigator’s position is indicated by a single ‘you-are-here’-point without any orientation; Klippel, Freksa, & Winter, 2006).

### 1.3.1 Primitive and Derived Spatial Parameters

Following the remarks of the previous section, significant points in the environment can be represented within either an egocentric or an allocentric reference frame, with each reference system comprising a specific set of *primitive parameters*.

*Egocentric distance* and *egocentric bearing* (distance and angle relative to the navigator’s axis) are primitives of the egocentric reference frame that have to be continually updated as the navigator moves within space. When confronted with two objects in space, the inter-object direction is coded with respect to the navigator’s current directional axis, resulting in an *ego-oriented bearing* from one object to the other, i.e., the angle between Ego’s intrinsic axis and the vector connecting A and B (see Figure 1.3 for details). The allocentric reference frame, by contrast, codes every point in space relative to a given reference direction and origin (*allocentric distance*, *allocentric bearing*). The navigator is represented solely by means of locational, but without directional information. Therefore, the direction from A to B is represented as angular difference between the vector connecting A and B and the reference direction, referred to as *allocentric bearing* (Klatzky & Wu, 2008). *Allocentric heading* denotes a specific case of allocentric bearing, namely the angle between the navigator’s axis and the reference direction. Ego-oriented bearing then is nothing else but the difference between allocentric bearing and allocentric heading (see Klatzky, 1998 for further details).

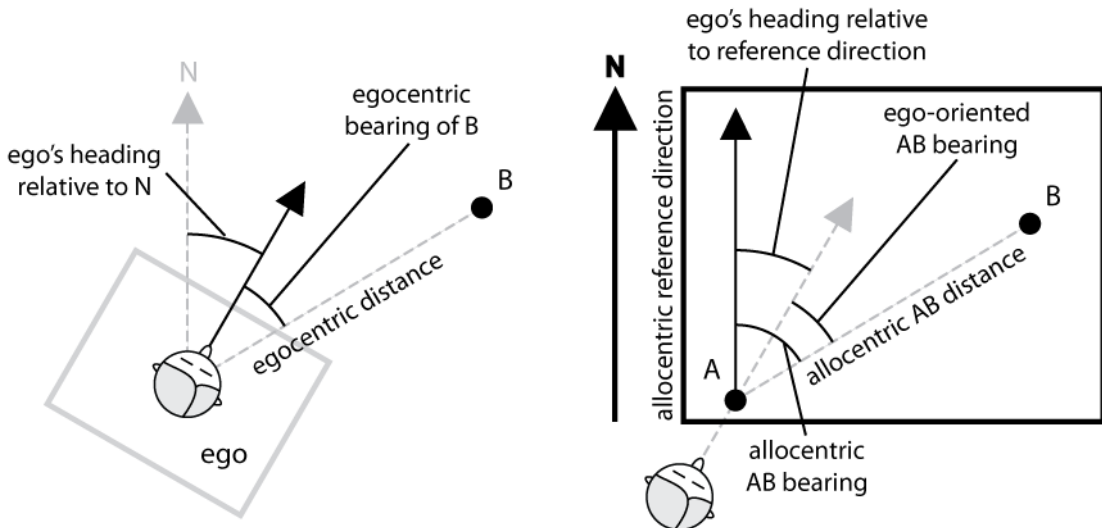


Figure 1.3: Egocentric (left) and allocentric (right) reference frames – Ego's intrinsic axis of orientation defines angles in a polar coordinate system, and Ego's egocenter establishes the origin of a vector that connects Ego with an object in the environment. Object-to-object relations (distances and directions) may also be defined with respect to an allocentric reference frame as established by the reference direction of the environment and an extrinsically defined origin (adapted from Klatzky & Wu, 2008).

An object in egocentric space (e.g., the tea mug to my right) can be represented within an allocentric reference frame (e.g., being located on a desk in the south-eastern corner of my office), and vice versa. The systems are mathematically equivalent. But whereas primitive parameters within their respective reference frame are immediately available, they are accessible to the alternative reference frame only via derivation. Computational costs due to the transformation may result in prolonged response times, increased response variability, or accumulation of error. To avoid computational costs it would be necessary for the navigator to compute and maintain two reference frames in parallel to successfully retrieve any desired spatial information necessary for orienting. Recent findings support this assumption demonstrating that egocentric and allocentric reference frames co-exist in parallel (Burgess, 2006; Gramann et al., 2005; Riccobon, 2007; Schönebeck, Thanhäuser, & Debus, 2001; Waller & Hodgson, 2006). But which are the factors determining the choice of a reference frame? This question will be addressed in the following sections.

### 1.3.2 Reference Frames and Acquisition of Spatial Knowledge

Spatial knowledge is acquired from various sources, e.g., maps, spatial language, or by active exploration (Tversky, 1993). Several studies have shown that the choice of an allocentric or egocentric reference frame depends on the kind of information available, e.g., whether an environment is experienced directly or indirectly (Montello, Waller, Hegarty, & Richardson, 2004). Also, Thi-

nus-Blanc & Gaunet (1997) provided evidence that map-based knowledge acquisition fosters allocentric survey representations, whereas self-exploration enabled the navigator to build up egocentric route knowledge, due to the egocentric nature of incoming signals on early visuo-perceptive processing levels. This thesis will focus on direct acquisition of spatial knowledge, as available during day-to-day locomotion and navigation, where navigators utilize various sources of information (visual, vestibular, kinesthetic, and proprioceptive systems) in parallel.

Systematically controlled experiments allow for an investigation of specific quantitative and qualitative contributions of each of these information sources for updating of spatial representations. Sensory input can be controlled to diminish the contributions of spatial cues that could be used for piloting, e.g., by excluding landmarks via perceptive restraints (blindfolding), therefore fostering spatial processing based on path integration. Additionally, progress in high-performance computer technology has contributed to the emergence of *Virtual Reality* (VR) as additional medium for the exploration of human navigation performance (Bowman & McMahan, 2007; Gillner & Mallot, 1998; Jansen-Osmann & Berendt, 2002; Peruch, Gaunet, Thinus-Blanc, & Loomis, 2000; Ruddle et al., 1998; Wiener, Schnee, & Mallot, 2004). In contrast to real world experiments, VR qualifies for objective, reliable and valid experiments on the impact of different input information, sensory modalities, and spatial processes and strategies (Cutting & Vishton, 1995; Hunt & Waller, 1999; Loomis, Blasovich, & Beall, 1999a; Riecke, 2003; Sanchez-Vives & Slater, 2005; Tarr & Warren, 2002).

In natural environments visual flow provides the navigator with rich arrays of spatial information (Mossio et al., 2008). A large body of studies suggests that even in absence of proprioceptive or vestibular cues optic flow (Gibson, 1954) as solitary source of self-motion information (Dichgans & Brandt, 1978; Goldstein, 2007; Hettinger, 2002; Riecke & Schulte-Pelkum, 2006) supports effective spatial updating as well as the construction of spatial representations (Gramann et al., 2005; Gramann et al., 2006; Kearns et al., 2002; Lappe, Bremmer, & van den Berg, 1999; Loomis & Beall, 1998; May, Wartenberg, & Peruch, 1997; Riecke, Cunningham, & Bühlhoff, 2007; Stankiewicz, Legge, Mansfield, & Schlicht, 2006; Wartenberg, May, & Peruch, 1998). Visual flow patterns can be achieved by presenting arrays of indistinguishable objects that can only be tracked over a short distance (Riecke, 2003), mirroring real-life situations of moving in heavy fog or heavy snowfall.

In a study of Klatzky and colleagues (1998), subjects had to perform a speeded triangle-completion task, i.e., they ‘experienced’ an outbound trajectory containing an initial straight segment, a turn, and a second leg. Spatial experience was varied in terms of presence or absence of vestibular information, e.g., real walking vs. imagined walking (verbal description, virtual environment). Subsequently they were asked to perform a homing response, i.e., to turn to face the origin as they would if they had walked the path and were at the end of the

second segment. Results revealed that only when rotations were physically performed (i.e., walk and real-turn conditions) and vestibular information was present, participants did accomplish the homing turn correctly. In all remaining conditions, participants systematically overturned by the amount of the turn between the path segments. In other words, physical movement including vestibular input guarantees for successful integration of translations and rotations, allowing the navigator to infer egocentric bearing back to the starting point. In absence of vestibular cues, i.e., imagined movement, only translational changes are integrated into the spatial representation, and heading is not updated automatically (Loomis et al., 1993; Loomis et al., 1999b; May, 1996; Presson & Montello, 1994).

Wraga (2003) suggested an explanation for the failure of the ‘imagined walking’ in updating of heading, arising from conflicts between reference systems of the imagined self-motion during the task and the subsequent bodily response. In order to perform the physical body turn for the homing response, participants in the imagined condition had to realign the egocentric frame of their *real body* with the *imagined* egocentric frame corresponding to the viewpoint at the end of the imagined outbound path, therefore requiring effortful cognitive processing<sup>4</sup>. By contrast, during physical movement updating occurred ‘automatically’ and without cognitive effort, since imagined and physical egocentric frames were aligned during the whole passage. When participants had to perform the imagined homing task verbally, e.g. by describing the direction (left or right) and the number of degrees they would have to turn in order to face home (Avraamides, Klatzky, Loomis, & Golledge, 2004a), no systematic underestimation occurred any more.

Taken together, bodily responses such as manually pointing, turning, or walking may induce a body-centered egocentric reference frame, whereas other response modalities, such as verbal descriptions, do not imply a body-centered reference frame. With respect to the terminology of egocentric and allocentric reference frames these results read as follows: During the confrontation with vestibular information (translations and rotation), self-to-object relations are updated within an egocentric reference frame, i.e., the navigator successfully updates egocentric return bearing, and – in case of more than one object being located in the environment – ego-oriented bearings of object-to-object relations (e.g., A-to-B, B-to-C, and A-to-C). However, these pairwise object-to-

---

<sup>4</sup> These findings also bear resemblance to results of studies in mental rotation (Kassin, 2003), that, generally, found self-to-object pointing performance to be slower for imagined rotations as compared to physical rotations, resulting in response latencies that vary with respect to the angular deviation between imagined and physical facing direction of the participant. Rieser (1989) suggested that due to the missing vestibular and proprioceptive signals during imagined movements spatial updating is not accomplished automatically, but requires additional cognitive effort.

object relations are not subsumed within a coherent reference system, but solely set in relation to the navigator. In the imagined walking condition, by contrast, an allocentric reference frame is activated that integrates solely allocentric bearings between start and end points (regarding translational, but not rotational information).

Taking into account that the choice of distinct reference frames for navigation and for experimental responses is associated with different primitive parameters it can be argued that participants in the study of Klatzky and colleagues did not respond incorrectly (overestimated their homing response). Rather, they responded adequately within the reference frame they chose to solve the task. Which reference frame is finally chosen, seems in part to be dependent on the response mode. This result is in accordance with several studies assuming the coexistence of egocentric and allocentric spatial representations (Aguirre & D'Esposito, 1999; Burgess, 2006; Burgess, Spiers, & Paleologou, 2004; Riccobon, 2007; Sholl, 2001; Waller & Hodgson, 2006). Neuropsychological and lesion studies supporting this notion will be further discussed in section 1.4.1.

### 1.3.3 Reference Frames as Individually Stable Preferences

In addition, the choice of one or another reference frame may depend on enduring and intraindividually stable proclivities and trait-like preferences (e.g., for route-based vs. survey-based orientation strategies - Denis & Loomis, 2007; Denis, Pazzaglia, & Cornoldi, 1999; Lawton, 1996; Pazzaglia & de Beni, 2001; Pazzaglia & Taylor, 2007). Generally speaking, this differentiation resembles the duality of representational systems, with survey and route knowledge being encoded within an allocentric or an egocentric reference frame, respectively (Gramann et al., 2005; Gramann et al., 2006; Müller & Gramann, 2007; Riccobon, 2007; Schönebeck et al., 2001). Which factors determine the preferred use of either frame is still an open issue in spatial navigation research. From a developmental perspective, it might be established within the interplay of heredity transmissions and learning history (e.g., affected by socio-cultural imprint) (Pick, 1999; Siegel & White, 1975).

However, these personal affinities for specific reference frames only come to bear when experimental conditions are carefully set up. Both acquisition and reproduction phase allow participants to experience and respond to space within their preferred reference frame. Based on the results of Klatzky et al. (1998) and Avraamides et al. (2004), advantages should result when participants were able to not only encode space within their preferred reference frame but also to respond accordingly. Since verbal or bodily responses imply the use of an allocentric or an egocentric reference frame respectively, research is facing novel challenges in applying appropriate experimental material.

An innovative approach has been proposed by Schönebeck et al. (Gramann, 2002; Gramann et al., 2005; Gramann et al., 2006; Schönebeck et al., 2001). After visual flow stimulation of virtual turning tunnels (no vestibular input was provided) subjects had to adjust a simulated 3D-arrow to point directly back to the starting point of the trajectory ('homing-task', see Figure 1.4 for details).

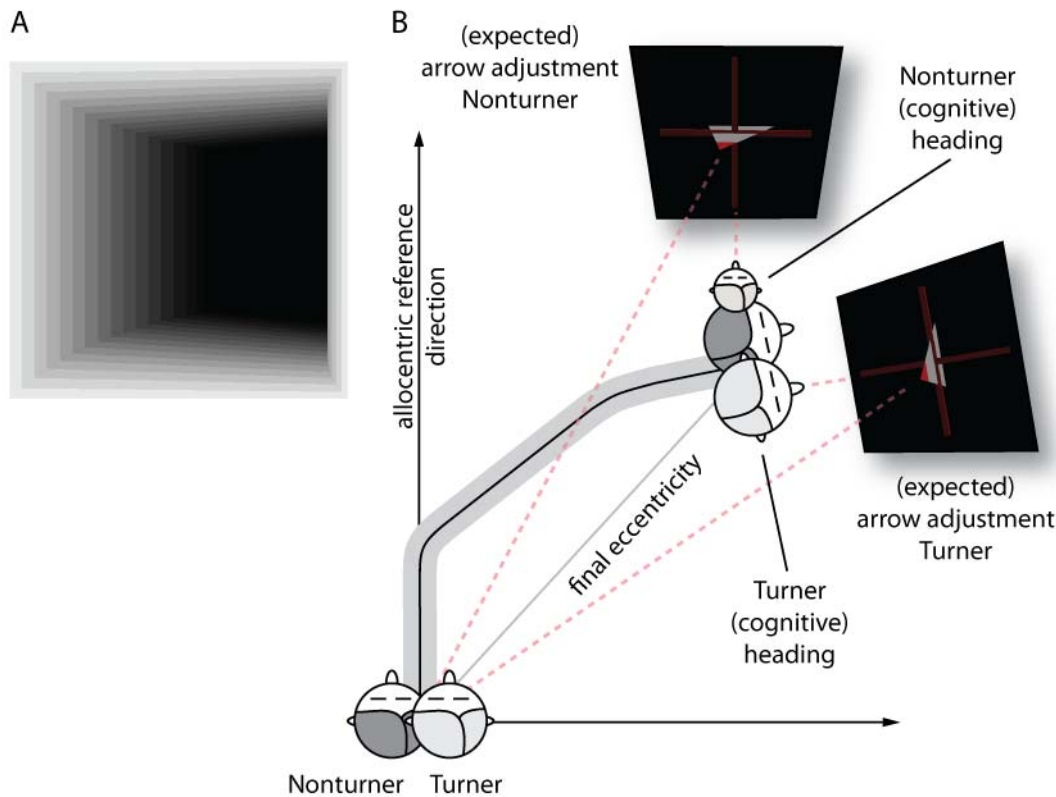


Figure 1.4: Tunnel-task (Gramann et al., 2005; 2006) – **(A)** Visual flow stimulation of virtual turning tunnels; right-turning segment; **(B)** Proposed model of spatial encoding within an allocentric reference frame ('Nonturners', dark grey heads) and an egocentric reference frame ('Turners', light grey head), respectively (see text for explanation). Detailed sketches will be provided in section 3.

Despite identical visual experience and task instructions, homing responses of two groups of subjects differ significantly. One group of participants, so-called *Turners*, using an egocentric reference frame, adopt a spatial representation that includes updating of cognitive heading according to the perceived heading changes during the passage. Therefore, their arrow adjustment following a tunnel to the *right* points to their *right* behind them. In contrast, *Nonturners*, using an allocentric reference frame, base their homing reactions on a heading representation that is aligned with the orientation of the initial tunnel segment (reference direction) and does not include an updated cognitive heading. After traversing the very same *right* turning tunnel, Nonturners typically adjust the homing arrow pointing back to their *left* revealing systematic overestimations by the amount of the turning angles along the outbound trajectory. The strik-

ing differences in homing vector adjustments of Turners and Nonturners cannot be attributed to differences in the feeling ofvection since both groups consistently reported a feeling of moving forward through the tunnel and into different directions according to the tunnel turns.

Due to the egocentric nature of incoming signals (the visual flow provided egomotion information from a first-person perspective), participants have to basically establish an egocentric reference frame, as applied by the Turner group. For Nonturners, by contrast, two different assumptions can be made: They encode either spatial information during the outbound path – comparable to Turners – within an egocentric reference frame, and derive an additional allocentric reference frame after the tunnel ends. Alternatively, they transfer the egocentric parameters into allocentric coordinates already during the passage. Riccobon (2007) provided initial results for egocentric and allocentric reference frames being active in parallel during visual path integration, bearing resemblance to conceptualizations of Burgess (2006).

The following section will give a brief introduction into psychophysiological considerations on reference frames and spatial representations.

## 1.4 Cortical Structures and Mechanisms

### 1.4.1 Cortical Substrates of Allocentric and Egocentric Reference Frames

The variety of cognitive processes involved in spatial processing (uptake of sensory information, integration within distinct reference frames, retrieval of enduring spatial representations, spatial actions) necessitates innovative and holistic psychophysiological approaches based on methodological and technological innovations, enabling the researcher to analyze cortical activities in each subject's data, not by direct spatial filtering for activities generated in a set of pre-defined cortical locations (comparable to the ROI-approach for the analysis of fMRI data, as described in Brett, Anton, Valabregue, & Poline, 2002), but rather by using the information content of the data itself (Onton & Makeig, 2006). Further, novel approaches to data-mining of neural dynamics have to be able to detect cortical processes that act upon a time range of milliseconds. However, in order to properly discuss the results obtained with these seminal technologies the following section provides previous findings from several fields of study regarding the cortical structures as well as their task-related dynamics when performing spatial tasks, particularly during spatial navigation (based on allocentric and egocentric reference frames). It is important to note that these studies varied with respect to the species investigated (human, nonhuman), as the availability of sensory input (real vs. virtual navigation), and the applied recording techniques (invasive and noninvasive elec-

troencephalography, magnetoencephalography, (functional) magnetic resonance imaging, positron emission tomography, lesion studies). This thesis will evaluate the current state of knowledge with respect to cortical structures and spatial dynamics accompanying spatial navigation within egocentric and allocentric reference frames.

During everyday locomotion in natural environments, vision provides the major source of information for the processing and active determination of self-movement (Lappe et al., 1999). Visual information is initially processed within primary and secondary visual areas (BA 17, 18, and 19 following Brodmann; areas V1-V5 following the functional classification). Subsequent information processing is gated into two distinct streams of projection, with *location*-, or *action-based* information being processed along the *dorsal stream* ('where pathway') projecting into posterior parietal cortex, and further into prefrontal areas (Aguirre & D'Esposito, 1997; Diwadkar, Carpenter, & Just, 2000; McIntosh, Grady, Ungerleider, Haxby, Rapoport, & Horwitz, 1994; Miller & D'Esposito, 2005; Ungerleider & Mishkin, 1982). By contrast, *object-based* information of a stimulus such as color, shape, size, and orientation, is processed along the *ventral stream* ('what pathway') projecting into inferior temporal cortex with efferent projections into parahippocampal and hippocampal areas (Haxby, Grady, Horwitz, Ungerleider, Mishkin, Carson, Herscovitch, Schapiro, & Rapoport, 1991; Mishkin, Ungerleider, & Macko, 2001). Figure 1.5 provides a selective survey of areas involved in spatial processing. Subsequent sections will further discuss the anatomical and functional properties as well as network interlinkage of these areas.

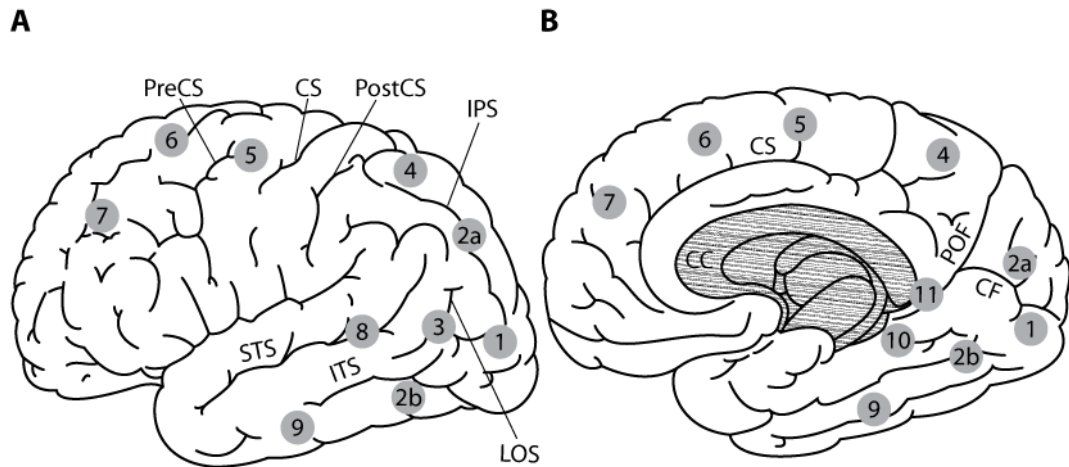


Figure 1.5: Brain areas involved in spatial processing – **(A)** Lateral view of the left cerebral hemisphere and **(B)** medial view of the right cerebral hemisphere showing major sulci and fissures e.g., precentral sulcus (PreCS), central sulcus (CS), postcentral sulcus (PostCS), superior (STS) and inferior temporal sulci (ITS), intraparietal sulcus (IPS), and, lateral occipital sulcus (LOS), respectively. Additionally, in medial view are depicted the corpus callosum (CC), as well as parieto-occipital (POF) and calcarine fissures (CF). Colored numbers represent approximative centroids of areas involved in processing of spatial information: (1) Primary/secondary visual cortices (V1/V2, BAs 17/18); (2) associative visual cortex V3, subarea V3A within dorsal V3 (2a) and ventral aspects (2b); (3) MT+ cluster, at the junction of the ITS and LOS; (4) posterior parietal cortex, precuneus (BA 7); (5) premotor cortex (BA 6); (6) frontal eye fields (BA 8); (7) dorsolateral prefrontal cortex (BA 9/46); (8) superior temporal gyrus (BA 22); (9) inferior temporal gyrus (BA 20); (10) (para-)hippocampal gyrus; (11) retrosplenial cortex (BA 29/30) (adapted and modified from Culham, He, Dukelow, & Verstraten, 2001; Sunaert, Van Hecke, Marchal, & Orban, 1999; Waxman, 2002).

Areas along the dorsal pathway as well as their further projections to prefrontal areas have been found to be involved in egocentric processing of spatial information such as encoding of object location with respect to one's own body (Committeri, Galati, Paradis, Pizzamiglio, Berthoz, & LeBihan, 2004; Galati, Committeri, Sanes, & Pizzamiglio, 2001; Vallar, Lobel, Galati, Berthoz, Pizzamiglio, & Le Bihan, 1999; Wilson, Woldorff, & Mangun, 2005). By contrast, activation along the ventral pathway is closely linked to allocentric processing of spatial information (Brandt, Schautz, Hamilton, Bruning, Markowitsch, Kalla, Darlington, Smith, & Strupp, 2005; King, Trinkler, Hartley, Vargha-Khadem, & Burgess, 2004; Maguire, Frackowiak, & Frith, 1997; Mayes, Montaldi, Spencer, & Roberts, 2004; Parslow, Rose, Brooks, Fleminger, Gray, Giampietro, Brammer, Williams, Gasston, Andrew, Vythelingum, Loannou, Simmons, & Morris, 2004).

### 1.4.1.1 Egocentric Processing along the Dorsal Pathway

#### ***Visual Perception***

Neuroanatomical studies have suggested that information processing within the dorsal stream is accomplished by several different though interacting routes from area V1 to higher-level visual association areas in posterior parietal cortex. One set of inputs arrives via areas V2/V3 (Culham et al., 2001; Stiles, 2001). Cortical areas along this pathway display increasing sensitivity for motion-related stimuli with maximally selective neural responses to movement-related stimuli in area V3A (cuneus, BA 19 following Brodmann), anterior to dorsal V3 near the junction of occipital and intraparietal sulci (Tootell, Mendoza, Hadjikhani, Ledden, Liu, Reppas, Sereno, & Dale, 1997). This area has been identified by retinotopic mapping of stimuli presented on the contralateral hemifield to code spatial information within a retino-centered egocentric reference frame (Merriam, Genovese, & Colby, 2003; Morland, Baseler, Hoffmann, Sharpe, & Wandell, 2001).

Another pathway from occipital to posterior parietal regions arises via area MT+/V5 (lateral occipital cortex) and adjacent area MST. Middle temporal area MT+, was initially discovered by Zeki and colleagues (Zeki, Watson, Lueck, Friston, Kennard, & Frackowiak, 1991), who characterized this area as the human homolog of monkey areas MT, MST, and neighboring motion-selective cortex. Area MT has been found to encode basic elements of motion, e.g., velocity and direction of visual stimuli as provided by means of changes in luminance (Maunsell & van Essen, 1983), whereas area MST assumes processing of higher-order motion, e.g., 3-D object and self-motion via optic flow (Britten & van Wezel, 2002; Duffy, Page, & Froehler, 2005; Duffy & Wurtz, 1991a, 1991b; Froehler & Duffy, 2006; Tanaka, Sugita, Moriya, & Saito, 1993). An alternative route from V1 to posterior parietal cortex leads via area PO, located medially in the parieto-occipital sulcus. This area is specialized for processing of stimuli presented in peripheral visual fields (Galletti, Battaglini, & Fattori, 1995). Whereas in monkey studies area MST seemingly processes moving objects relative to the background, area PO codes self-motion relative to the environment (Lui, Bourne, & Rosa, 2006). However, human area MT+ seemingly undertakes both tasks.

This sub-differentiation was also replicated in recent human studies (e.g., Peuskens, Sunaert, Dupont, Van Hecke, & Orban, 2001). Visual tracking of a moving stimulus resulted in neural activation in MT+ which continued to respond during pursuit eye movements even when the visual stimulus itself disappeared, suggesting an anticipatory function of this area for higher-level processing of spatial information. Interestingly, neural activity was not only associated with eye movements but also with head movements (Brotchie, Andersen, Snyder, & Goodman, 1995; Stricanne, Andersen, & Mazzoni, 1996; Thier & Erickson, 1992). Microstimulation in area MST has been shown to bias a monkey's perceived direction of heading (Britten & van Wezel, 1998; van Wezel & Britten, 2002). In several psychophysiological studies, subportions of

MT+ have also been found to allow subjects to accurately judge heading from certain components of optic flow, such as circular and radial motion (Fetsch, Wang, Gu, Deangelis, & Angelaki, 2007; Morrone, Tosetti, Montanaro, Fiorentini, Cioni, & Burr, 2000).

### ***Visuomotor Coordination and Retrieval of Episodic Memory in Precuneus***

The different dorsal routes converge in posterior parietal cortex, particularly within precuneus (BA 7, posteromedial parietal cortex), where visuospatial coordinate transformations between various egocentric reference frames are accomplished (Cavanna & Trimble, 2006; Dean & Platt, 2006; Xing & Andersen, 2000). In concert with several areas along the intraparietal sulcus (anterior, posterior, intermediate IPS), postcentral sulcus, and parieto-occipital fissure, the precuneus primarily coordinates retino-, eye-, and head-centered spatial processing with visuo-motor control of body- and extremity-centered actions into a coherent egocentric representation of the surroundings (Aguirre & D'Esposito, 1997, 1999; Andersen, Snyder, Bradley, & Xing, 1997; Dupont, Orban, De Bruyn, Verbruggen, & Mortelmans, 1994; Rizzolatti, Riggio, & Shellinga, 1994; Sunaert et al., 1999; Vogeley & Fink, 2003; Vogeley, May, Ritzl, Falkai, Zilles, & Fink, 2004). Additionally, precuneus activity has been associated with concepts of self-consciousness and experience of agency (Farrer & Frith, 2002), as well as retrieval of episodic memory, which constitutes a central prerequisite for enduring action plans guiding spatial behavior, e.g., when trying to find the shortest way back home (Aguirre, Zarahn, & D'Esposito, 1998; de Jong, Shipp, Skidmore, Frackowiak, & Zeki, 1994; Fletcher, Shallice, Frith, Frackowiak, & Dolan, 1996; Ghaem, Mellet, Crivello, Tzourio, Mazoyer, Berthoz, & Denis, 1997; Maguire, Frith, Burgess, Donnett, & O'Keefe, 1998b; Shallice, Fletcher, Frith, Grasby, Frackowiak, & Dolan, 1994).

Lesion studies provided rich evidence for parietal structures playing the crucial role for viewpoint-dependent processing, as reviewed by Aguirre & D'Esposito (1999). Lesions of parietal structures generally result in so-called '*heading disorientation*' as well as '*egocentric disorientation*'. Patients with parietal lesions not only display pronounced deficits in visuomotor coordination ('optic ataxia', Perenin & Vighetto, 1988; Rossetti, Pisella, & Vighetto, 2003), or inability to explore the contralateral spatial hemisphere ('unilateral neglect', Vallar, 1998). They may also fail to properly estimate self-to-object relations. Particularly, in mental rotation tasks patients with parietal lesions have been found to significantly underestimate rotation angles (Farrell & Robertson, 2000) due to problems in perceiving their body midsagittal plane (Pizzamiglio, Committeri, Galati, & Patria, 2000), or deficits in encoding their '*heading*' (Bremmer, Duhamel, Ben Hamed, & Graf, 2002), a central prerequisite for egocentric processing (Committeri et al., 2004).

A recent lesion study of Seubert and colleagues (2008) further corroborated the central role of cortical areas along the dorsal pathway for egocentric processing. Participants traversed the previously depicted virtual tunnels (Gramann, 2002; Gramann et al., 2005; Schönebeck et al., 2001) with single

turns of varying angularity. Patients with lesions in parietal areas made significantly more qualitative and quantitative errors (i.e., left-right inversions and less accurate directional estimations) as compared to patients with lesions located in frontal areas, suggesting a fundamental contribution of parietal structures to spatial processing within an egocentric reference frame.

### ***Spatial Actions and Parietofrontal Modules***

Results of comparative studies suggested that posterior parietal cortex blends in anatomically and functionally distinct circuits into specific areas within prefrontal and premotor regions (Cavada & Goldman-Rakic, 1989a, 1989b; Foxe & Simpson, 2002). The latter has generally been associated with planning of voluntary movements as well as composition of complex action scripts from basic and rather prototypical elements (Bremmer, Schlack, Duhamel, Graf, & Fink, 2001; Bremmer, Schlack, Shah, Zafiris, Kubischik, Hoffmann, Zilles, & Fink, 2001; Cisek & Kalaska, 2005; Colby & Goldberg, 1999; Kalaska & Crummond, 1992). Graziano and colleagues (1994) were the first to report neuronal activity in premotor cortex (BA 6) being correlated with motor preparation and controlling movements on the basis of somatosensory information. This finding has been constantly replicated in several experimental conditions and tasks, e.g., line bisection (Vallar et al., 1999), motor response tasks such as pointing and grasping (Astafiev, Shulman, Stanley, Snyder, Van Essen, & Corbetta, 2003), and mental rotation (Lamm, Windischberger, Leodolter, Moser, & Bauer, 2001). In a mental rotation task of Windischberger and colleagues (2003), participants showed enhanced activity within bilateral premotor, dorsolateral prefrontal, as well as parietal areas during stimulus presentation, reflecting cognitive processing. By contrast, after performing the subsequent motor task (button press) only premotor areas contralateral to the effective hand displayed significant activation. Because neurons were found to be responsive to visual stimuli adjacent to the effective arm or hand, and arm movements resulted in spatial remapping, premotor cortex seemingly codes spatial information within an arm- or hand-centered egocentric reference frame, respectively (Bousaoud, 1995, 2001; Peuskens et al., 2001).

Comparative tracer studies in monkey provided rich evidence that particularly within dorsal premotor cortex (PMd) neuronal assemblies reveal distinct anatomic connectivity. Whereas rostral parts (PMdr) primarily interact with dorsolateral prefrontal cortex (BAs 9 and 46) as well as frontal eye fields (BA 8) (Colby & Goldberg, 1999), caudal aspects (PMdc) are exclusively interconnected to parietal regions, i.e., precuneus (Ghosh & Gattera, 1995; Matelli, Govoni, Galletti, Kutz, & Luppino, 1998). Since microstimulation of monkey PMdr resulted in saccadic eye movements, this area has consequently been associated with aspects of visual attention. By contrast, PMdc stimulation evoked forelimb or body movements, which has been taken as indicator of intention-related processes, e.g., motor preparation (Fujii, Mushiake, & Tanji, 2000).

Taken together, spatial processing within an egocentric reference frame is established within a parieto-premotor network, with further projections into dor-

solateral prefrontal cortex, as validated by human studies utilizing variations of the line bisection paradigm (Fink, Marshall, Shah, Weiss, Halligan, Grosse-Ruyken, Ziemons, Zilles, & Freund, 2000; Fink, Marshall, Weiss, Stephan, Grefkes, Shah, Zilles, & Dieterich, 2003), as well as during navigation and orientation in complex virtual environments (Committeri et al., 2004; Gramann et al., 2006).

#### 1.4.1.2 Allocentric Processing along the Ventral Pathway

##### ***Object Specificity in Lateral Temporal Cortices***

Within the ventral pathway, visual information passes areas V1/V2 to ventral aspects of area V3 and extrastriate area V4, as well as MT+, with further interconnections to superior and inferior temporal cortex (Barbas & Blatt, 1995; Fuster, 2008; Miller, Li, & Desimone, 1993; Miyashita, 1993; Ranganath, Cohen, Dam, & D'Esposito, 2004; Wilson, Scalaide, & Goldman-Rakic, 1993; Wilson & McNaughton, 1993) (see also Figure 1.5). Neural selectivity for highly specific complex objects such as hands or faces gradually increases from early visual areas to later ventral areas, particularly for neurons in inferior temporal cortex (Desimone, Albright, Gross, & Bruce, 1984; Kanwisher, McDermott, & Chun, 1997; Malach, Reppas, Benson, Kwong, Jiang, Kennedy, Ledden, Brady, Rosen, & Tootell, 1995; Tanaka et al., 1993). Neural firing of these cells has been found to be exclusively determined by intrinsic figural and surface properties of objects, and not by self-to-object properties such as relative location (Kobatake & Tanaka, 1994; Perrett, Smith, Potter, Mistlin, Head, Milner, & Jeeves, 1984, 1985; Tanaka, Saito, Fukada, & Moriya, 1991). These neurons reveal large receptive fields covering the fovea and extending into both visual hemifields, therefore allowing for object recognition as well as object generalization across several viewing perspectives (Milner & Goodale, 1996). In other words, lateral temporal structures support the construction of object representations that remain stable as the observing subject moves along through the environment.

##### ***Place Cell Coding in Hippocampal Structures***

Lateral temporal areas are closely interlinked with dorsolateral, ventrolateral and anterior prefrontal cortices, as well as medial temporal structures, particularly parahippocampal gyrus and hippocampus<sup>5</sup>. Neurons in the hippocampus of the rat, so-called '*place cells*', have been characterized by their location-specific firing as the animal traverses the environment (Foster, Castro, & McNaughton, 1989; Maaswinkel, Jarrard, & Whishaw, 1999; McNaughton,

---

<sup>5</sup> There are also connections from inferior temporal cortex to the amygdala, primarily associated with learning processes (stimulus-response) in social and emotional contexts (Gaffan, Gaffan, & Harrison, 1988), which will not be considered further.

Barnes, Gerrard, Gothard, Jung, Knierim, Kudrimoti, Qin, Skaggs, Suster, & Weaver, 1996; Wilson & McNaughton, 1993).

Comparable neurons have been discovered in non-human primates (Georges-Francois, Rolls, & Robertson, 1999; Rolls, 1999) as well as in human epileptic patients (Ekstrom, Kahana, Caplan, Fields, Isham, Newman, & Fried, 2003; Hartley, Maguire, Spiers, & Burgess, 2003; Iaria, Chen, Guariglia, Ptito, & Petrides, 2007; Iaria, Petrides, Dagher, Pike, & Bohbot, 2003). Place cells fire maximally when the subject moves into a distinct region of the environment, i.e., the ‘place field’, and display virtually no activity in other areas.

Spatial coding of these cells is independent of the subject’s current orientation as well as stimuli available at a certain place. Instead, place cells code viewpoint-independently for the position of the subject itself in a space-fixed allocentric reference frame (Georges-Francois et al., 1999; Matsumura, Nishijo, Tamura, Eifuku, Endo, & Ono, 1999; O’Keefe & Nadel, 1978; Rolls, 1999; White & McDonald, 2002; Wilson & McNaughton, 1993). Environment-based encoding provides the prerequisite for an enduring map-like representation of the environment that can be flexibly retrieved and allow for place recognition whenever re-encountering the same environment from different viewpoints (Maguire, Burgess, Donnett, Frackowiak, Frith, & O’Keefe, 1998a; Milner & Goodale, 1996; Muller, 1996; Squire, Stark, & Clark, 2004; Wolbers & Büchel, 2005). Based on these findings, hippocampal structures as well as lingual/posterior parahippocampal areas play a crucial role for the construction of an enduring spatial representation within an allocentric reference frame from episodic memory (Bohbot, Iaria, & Petrides, 2004; Bohbot, Kalina, Stepankova, Spackova, Petrides, & Nadel, 1998; Burgess, Maguire, & O’Keefe, 2002; Ekstrom et al., 2003; Epstein, Parker, & Feiler, 2007; Fowler, Saling, Conway, Semple, & Louis, 2002; Lambrey, Amorim, Samson, Noulhiane, Hasboun, Dupont, Baulac, & Berthoz, 2008; Maguire, Burgess, & O’Keefe, 1999; McCarthy, Evans, & Hodges, 1996; Smith & Mizumori, 2006; van Asselen et al., 2006; Wolbers & Büchel, 2005). Neuropsychological studies on humans also associated lesions within the ventral pathway with deficits in viewpoint-independent allocentric processing of spatial structures, termed ‘*landmark agnosia*’, as well as impaired ability in constructing new environmental representations, so-called ‘*anteriograde topographical disorientation*’ (Aguirre & D’Esposito, 1999; Turriziani, Carlesimo, Perri, Tomaiuolo, & Caltagirone, 2003). In a study of Maguire and colleagues (Maguire, Burke, Phillips, & Staunton, 1996), patients with lesions in either right or left temporal lobes were provided with videotape presentations of overlapping routes. Interestingly, both right and left lesion groups were comparably impaired on topographical orientation tasks, i.e., landmark recognition and sketch map drawing. However, only patients with lesions in the right hippocampus made erroneous proximity judgments, whereas patients with lesions in the left hemisphere were commonly able to accomplish the task. Recent studies support the notion that particularly right hippocampal as well as parahippocampal structures are responsible for storing the locations of objects encountered in spatio-temporal sequence with-

in an enduring allocentric representation (Burgess, Maguire, Spiers, & O'Keefe, 2001; Ghaem et al., 1997; Gramann et al., 2006; Grön, Wunderlich, Spitzer, Tomczak, & Riepe, 2000; Johnsrude, Owen, Crane, Milner, & Evans, 1999; Parslow, Morris, Fleminger, Rahman, Abrahams, & Recce, 2005; van Asselen et al., 2006; Wolbers, Wiener, Mallot, & Büchel, 2007).

#### 1.4.1.3 Retrosplenial Cortex as Transition Zone

Following Burgess and colleagues (2001), spatial processing along the dorsal stream coordinates the continuous update of self-to-object relations within an egocentric reference frame, suggesting its crucial role for the coordination of spatial actions (e.g., locomotion, grasping, pointing or gazing) that heavily rely on short-term memory. With respect to spatial navigation, posterior parietal areas extract self-to-object-relations from direct perceptual experiences and enable the navigator to flexibly respond to the stimuli present in a given situation. By contrast, processing along the ventral pathway and subsequent medial temporal structures has been associated with long-term storage of spatial information within allocentric coordinates. Since allocentric representations must arise indirectly via transformation of sensory input, and allocentric coordinates have to be re-transferred into egocentric ones in order to allow spatial actions, the question arises, how the brain accomplishes the transformations between egocentric and allocentric representations (Byrne & Becker, 2008).

An area that has been identified as transition zone for bidirectional exchange of egocentric and allocentric information is retrosplenial cortex, located within posterior cingulate gyrus, extending posteroventrally around and below the eponymous splenium of the corpus callosum (Morris, Paxinos, & Petrides, 2000; Morris, Petrides, & Pandya, 1999). Particularly the posteroventral aspects labeled as Brodmann Areas 29 and 30 (Brodmann, 1925) have been found to mediate between dorsal and ventral pathways. In general, BA 30 reveals afferent and efferent projections to mid-dorsolateral prefrontal areas (e.g., BAs 9 and 46, Goldman-Rakic, Selemon, & Schwartz, 1984; Kobayashi & Amaral, 2000, 2003; Kobayashi & Amaral, 2007; Shibata, Kondo, & Naito, 2004), parahippocampal structures (Suzuki & Amaral, 1994), as well as presubiculum and entorhinal cortex (Buckwalter, Schumann, & Van Hoesen, 2008; Parvizi, Van Hoesen, Buckwalter, & Damasio, 2006). Additionally, retrosplenial cortex stays in communication with superior temporal sulcus, posterior parietal cortex (Pandya, Hoesen, & Mesulam, 1981), as well as subcortical structures, e.g., the thalamic nuclei.

Lesions studies have provided evidence for retrosplenial participation in episodic memory (e.g., Cooper, Manka, & Mizumori, 2001; Masuo, Maeshima, Kubo, Terada, Nakai, Itakura, & Komai, 1999; Vogt, Absher, & Bush, 2000). Whereas lesions within left retrosplenial cortex have been associated with general memory deficits such as autobiographical amnesia, right retrosplenial lesions have been found to specifically affect *spatial* memory. E.g., although recognition of single landmarks was possible, patients were not able to inte-

grate a series of landmarks into a coherent global spatial network, therefore restraining them from learning novel routes, not to mention their inability in retracing or describing a previously encountered route. This finding of particularly right retrosplenial involvement in spatial memory processing has been corroborated by neuroimaging studies (Epstein et al., 2007; Maguire et al., 1998a; Maguire, Gadian, Johnsrude, Good, Ashburner, Frackowiak, & Frith, 2000; Maguire, Mummery, & Büchel, 2000).

The question arises, what is processed within retrosplenial cortex. Maguire (2001) proposed that patients suffering from retrosplenial lesions seemingly lose their ‘heading’ (Aguirre & D’Esposito, 1999) within the environment. Interestingly, portions of heading cells exist in rodent retrosplenial cortex (Chen, Lin, Green, Barnes, & McNaughton, 1994; Chen, Lin, Barnes, & McNaughton, 1994), with neural firing patterns signalling the heading of the animal within the environment. These heading cells have also been found in ventral intraparietal areas (Bremmer et al., 2002), as well as thalamic structures, therefore suggesting pronounced interactions between these areas both during encoding and retrieval of spatial information (Iaria et al., 2007). Retrosplenial cortex transposes self-motion cues arising from posterior parietal regions with enduring spatial information established within hippocampal areas (Cavanna & Trimble, 2006; Dean & Platt, 2006), as suggested by recent imaging studies (e.g., Ino, Inoue, Kage, Hirose, Kimura, & Fukuyama, 2002; Wolbers & Büchel, 2005), as well as electroencephalographic studies (Gramann, Onton, Riccobon, Müller, Bardins, & Makeig, submitted).

### 1.4.2 Spontaneous Electroencephalographic Oscillations

Once the structures involved in spatial navigation are identified, their spectral dynamics during the acquisition, consolidation, and retrieval of spatial knowledge may be further investigated. Analysis of spontaneous EEG activity allows for an identification of consecutive stages of information processing as indicated by quantitative and qualitative involvement of distinct cortical areas associated with various forms of sensory and cognitive processes on a subsecond time scale (Basar, Basar-Eroglu, Karakas, & Schürmann, 2000). Generally, spontaneous EEG activity is constituted by uncoupled (sub-)cortical sources producing random oscillatory activity in a wide frequency range. Sensory stimulation causes a coupling of these generators, resulting in temporally synchronous and coherent oscillations. This oscillatory synchronization is also referred to as (phase-locked or time-locked) ‘event-related EEG activity’ (Basar et al., 2000).

Due to the associative strength between stimulation and oscillatory response, generally, a distinction is made between evoked and *induced* oscillatory activity. Whereas evoked activity is characterized by its occurrence in direct temporal relation (i.e., time-locked) to a stimulus (particularly discrete, salient stimuli with a transient, punctual onset), induced activity denotes fluctuating activity with rather weak time-locking to a presented stimulus (Bullock, 1992),

e.g., in case of ongoing visual stimulation as applied in the depicted Tunnel-task of Gramann et al. (2005; 2006). Induced activity has also been found to accompany a wide variety of cognitive processes.

#### 1.4.2.1 Theta Activity (4 – 8 Hz)

Initially defined within the frequency range of 3 to 7 Hz by Walter (1953), and recorded in rabbit hippocampus by Green & Arduini (1954) about a year later, oscillation within the 4 – 8 Hz frequency range is referred to as *theta rhythm* (Niedermeyer & da Silva, 2005). Several studies have reported frontal theta activity to correlate with the difficulty of mental operations (Manzey, 1998), further supported by results of Asada, Fukuda, Tsunoda, Yamaguchi, & Tonoike (1999), who localized the generator sources of theta activity during focused attention in or near medial prefrontal cortex. Subsequently, theta has been associated with cognitive processes in general, e.g., locomotion, orienting and other voluntary behaviors (Kahana, Seelig, & Madsen, 2001; Klimesch, 1999), and with different aspects of working memory in particular (Klimesch, 1996; O'Keefe & Burgess, 1999; Schack, Klimesch, & Sauseng, 2005). During the last decade, the cohesive concept of theta activity arising primarily in frontal sides has experienced a distinctive transformation. Recent studies on working memory have suggested that theta emanates not only from prefrontal but also from central, parietal, and medial temporal neuronal assemblies (Boston & Charlestown, 2001; Sarnthein, Petsche, Rappelsberger, Shaw, & von Stein, 1998; Sauseng, Klimesch, Schabus, & Doppelmayr, 2005; Schack et al., 2005) establishing a dynamic framework for intercommunication between spatially segregated cortical areas in order to support cognitive processing (Mizuhara, Wang, Kobayashi, & Yamaguchi, 2004).

With respect to the aims of the present thesis two characteristics of theta activity are of importance: First, theta is directly related to memory maintenance and increases with task difficulty (Gevins & Smith, 2000; Gevins, Smith, McEvoy, & Yu, 1997; Jensen & Tesche, 2002; Onton, Delorme, & Makeig, 2005). E.g., subjects in a study of Kahana and colleagues (1999) showed increased (4 – 8 Hz) theta activity when navigating within more complex maze systems, as well as during the recall phase. Second, theta activity has not only been found during memory storage and retrieval, but also at earlier stages of cognitive processing, serving as feed-forward gating mechanisms during the encoding phase (Klimesch, 1999; Klimesch, Doppelmayr, Schimke, & Ripper, 1997b). Referring to these central functions, recent studies investigating human navigation abilities in virtual environments have provided profound evidence for theta activity being associated with the encoding of spatial information (Caplan, Kahana, Sekuler, Kirschen, & Madsen, 2000; Caplan, Madsen, Raghavachari, & Kahana, 2001). Riccobon (2007), applying the tunnel paradigm as described above, also provided evidence for interrelations of (4 – 8 Hz) theta activity with cognitive effort during visual path integration.

Both electroencephalographic (EEG) and magnetoencephalographic (MEG) studies in humans have consistently reported increased oscillatory power in the (4–8 Hz) theta band when confronted with increased environmental complexity (Bischof & Boulanger, 2003; Caplan et al., 2001; Kahana et al., 1999). Particularly at critical time points, e.g., when navigators have to decide which way to take, pronounced theta activity has been detected (Bischof & Boulanger, 2003), suggesting that this frequency band specifically correlates with memory retrieval and action-based pursuance of self-determined navigational goals (Caplan, Madsen, Schulze-Bonhage, Aschenbrenner-Scheibe, Newman, & Kahana, 2003; Cornwell, Johnson, Holroyd, Carver, & Grillon, 2008; de Araujo, Baffa, & Wakai, 2002; Ekstrom et al., 2003).

#### 1.4.2.2 Alpha Activity (8 – 13 Hz)

The term *alpha rhythm* was introduced by Berger (1929), denoting a global cerebral rhythm with peak frequency of 10 – 11 Hz. Today, alpha is defined as rhythmic oscillatory activity within the frequency interval of 8 – 13 Hz and mean amplitude of 20 – 60  $\mu$ V (Niedermeyer & da Silva, 2005). Generator sources of alpha activity have been localized in posterior sites, including occipital, parietal, and posterior temporal regions. Within this distributed network alpha waves have several different functional correlates reflecting sensory, motor, and memory functions (Basar & Schürmann, 1997; Lehmann & König, 1997). Alpha also extends into central areas, the vertex, and midtemporal regions. However, in central areas alpha has to be distinguished from coexisting *mu* activity (see following section). Alpha is generally registered during mental and physical resting states with eyes closed, and is blocked or reduced during mental or bodily activity in terms of *event-related desynchronization* (ERD)<sup>6</sup> (Klimesch, Doppelmayr, Pachinger, & Ripper, 1997a; Pfurtscheller, 2001; Pfurtscheller & Lopez da Silva, 1999), also referred to as alpha suppression (Schwartz, Salustri, Kaufman, & Williamson, 1989). Central mu, by contrast, does not display the alpha-specific blocking with eye opening (Niedermeyer & da Silva, 2005). Therefore, reduction of alpha activity constitutes a valid signature of states of mental activity and engagement, e.g., focused attention (Pfurtscheller & Aranibar, 1977), and can be used as marker of activation or cognitive preparedness of the cortical domain for processing of task-related information (Angelakis, Lubar, Stathopoulou, & Kounios, 2004; Pfurtscheller, 2001; Pfurtscheller & Lopez da Silva, 1999).

However, the functional aspects of alpha desynchronizations remain an open issue. In this context it seems to be appropriate to distinguish between func-

---

<sup>6</sup> Event-related synchronizations (ERS, increased alpha band activity) are commonly referred to as being linked to an idling of the cortical source domain (Angelakis et al., 2004; Pfurtscheller, 2001; Pfurtscheller and da Silva, 1999).

tionally independent alpha sub-bands with a (7 – 10 Hz) lower alpha and a (10 – 13 Hz) upper alpha band, as suggested by means of various principal component analyses on EEG data (Bartussek & Gräser, 1980; Herrmann, Fichte, & Kubicki, 1980; Mecklinger, Kramer, & Strayer, 1992), further corroborated by several experimental studies (Klimesch, Schimke, & Pfurtscheller, 1993; Pfurtscheller & Lopez da Silva, 1999). Whereas the upper alpha band has been found to be involved in semantic memory storage (Klimesch, 1997), the lower alpha band is involved in the allocation of attentional resources during search and retrieval (Klimesch, 1996; Klimesch, Doppelmayr, Russegger, Pachinger, & Schwaiger, 1998). With respect to spatial navigation, recent studies have provided evidence for activity of the lower alpha band correlating with attentional encoding of spatial information (de Araujo et al., 2002; Riccobon, 2007).

#### **1.4.2.3 Rolandic Mu Activity (8 – 13 Hz)**

Jasper & Andrews (1938) were the first postulating a special alpha rhythm, both in terms of topography and functionality. This variation of alpha, so-called *mu rhythm* typically reveals spectral peaks at approximately 10 Hz and around 20 Hz (first harmonics), emanating from central cortex, particularly in or near primary somato-motor cortex (Salmelin & Hari, 1994; Schnitzler, Salenius, Salmelin, Jousmäki, & Hari, 1997). It gets desynchronized during (sensori-)motor-related task demands, e.g., real movements or motor planning (Caplan et al., 2003; Koshino & Niedermeyer, 1975; Pfurtscheller, 2001; Pfurtscheller, Neuper, Andrew, & Edlinger, 1997). Within the context of *motor imagery*, several studies on self-locomotion in (real and virtual) environments have utilized online recordings of somato-motor mu for vehicle steering based on brain-computer-interfaces, enabling persons to ‘walk from thought’ (e.g., Leeb, Scherer, Keinrath, Guger, & Pfurtscheller, 2005; Pfurtscheller, Leeb, Keinrath, Friedman, Neuper, Guger, & Slater, 2006).

Importantly, mu does neither display the typical suppression effects of the central alpha band (Niedermeyer & da Silva, 2005), nor does it correlate with alpha activity. Whereas earlier studies implied mu and alpha activity to behave in concert during visual stimulation (i.e., attenuation of alpha to be related to simultaneous increase of mu activity, reflecting a resting state of the sensori-motor cortex) (Pfurtscheller, 1992), Vanni, Portin, Virsu, & Hari (1999) provided evidence for independent activity patterns of general alpha and rolandic mu rhythms.

#### **1.4.3 Identification of Human Brain Dynamics from Noninvasive Multi-Channel EEG Recordings**

As depicted in section 1.4.1, hemodynamic imaging studies have provided evidence for task-related metabolic activities in equivalent brain areas during navigation. However, the high spatial resolution of these methodologies comes along with costs in temporal resolution. Electroencephalographic studies as characterized in section 1.4.2, by contrast, benefitted from the excellent tem-

poral resolution of the EEG, which has been misleadingly neglected for spatial reconstruction purposes, since most current EEG studies analyze electrical potential differences recorded between scalp surface electrodes and a distant scalp reference electrode – both ‘located relatively far from the brain itself’ (Onton & Makeig, 2006, p. 99). Additionally, multi-channel EEG recordings from electrodes located at the scalp surface have been characterized by highly correlated signals at neighboring channels (e.g., Haalman & Vaadia, 1997).

However, the recorded signals do not originate on-site (e.g., within the scalp, or in brain areas directly located beneath the electrode position). Instead, they originate from partially synchronized local field potentials in distinct cortical domains – with ‘domain’ being defined as a cortical patch of unknown extent (Onton, Westerfield, Townsend, & Makeig, 2006). The cytoarchitecture of pyramidal cells (Niedermeyer & da Silva, 2005) within these domains, as well as their perpendicular orientation with respect to the cortical surface, corroborate the assumption of an additive effect of temporally synchronous extra-neuronal potentials that – in terms of summed ‘far-field’ potentials – further spread towards scalp electrodes via volume conduction. In case of non-synchronous local activity or non-parallel orientation of neighboring pyramidal neurons, local domain activities would cancel each other out – and far-field potentials would be prevented from gaining enough strength to be measured on the scalp surface.

Most intriguingly, but following basic principles of electrical conductance, far-field potentials arising in spatially distinct cortical (and noncortical) domains emanate to and sum linearly at nearly every surface electrode. As a result, the retrieved EEG signal at each electrode is a sum, or *weighted linear mixture* of the underlying cortical source signals, with the weights being determined by the distance between electrode and cortical source domain, their relative orientation, as well as the conduction properties of the intermediate structures (cortex, intra-ventricular cerebro-spinal fluid, skull, and skin, respectively). In other words, it is possible to compose EEG scalp signals as the linear sum of distinct, phase-independent, and spatially stationary signals arising from cortical areas that – over sufficient time – act as single, distinct, and temporally independent neural compound generating locally synchronous EEG activity.

Based on the assumption of temporal independence, as well as spatial stationarity of EEG signals generated within distinct cortical domains (Makeig, Bell, Jung, & Sejnowski, 1996a; Makeig, Jung, & Sejnowski, 1996b), Independent Component Analysis (ICA) is able to reveal the driving forces (sources) underlying a set of observed phenomena (EEG activity recorded at the scalp surface). The working-hypothesis:

*‘If different signals arise from different physical processes then the signals have to be statistically independent.’*

is reversed by ICA, which is, however, logically unwarranted, but works in practice (Stone, 2004):

*'If statistically independent signals can be extracted from signal mixtures then these extracted signals must stem from different physical processes'.*

In other words, ICA allows to *un-mix* the mixtures retrieved from scalp electrodes, thereby enabling the reconstruction of temporally as well as functionally independent activities of multiple brain and non-brain sources. Because ICA does not incorporate any knowledge about source localization or specifications beside temporal independence, ICA is often referred to as *blind source separation* (BSS) technique (Hyvärinen, 1999; Hyvärinen & Oja, 2000). However, in combination with information regarding the distribution of the electrode array, source signals, or *Independent Components* (ICs) can be spatially localized. This so-called 'inverse-modeling' (Akalin-Acar & Gencer, 2004; Onton & Makeig, 2006) utilizes either normalized individual structural magnetic resonance (MR) brain images of the participants, or normalizes the subject's head shape to a standard head model (Onton & Makeig, 2006). The following section will provide a brief introduction into the philosophy and mathematical fundamentals of Independent Component Analysis. Sections 4 and 5 will go into further detail with respect to the consecutive steps from EEG recordings to the analysis of spectral dynamics within reconstructed source clusters and will provide the parameters as applied for ICA.

#### 1.4.3.1 The ICA Model

Consider a simple example of exactly two intracortical sources and two electrodes located at the scalp. Following the remarks of previous section, the data obtained at each electrode is a result of the combination of source signals, with the precise nature of this combination being determined by a set of so-called *mixing coefficients* (a, b, c, d; see Figure 1.6 for details).

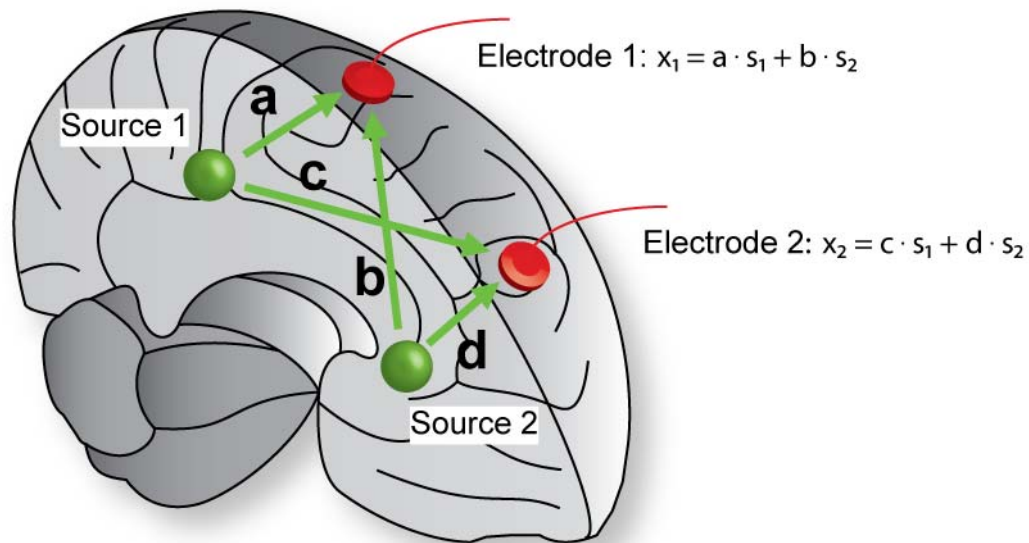


Figure 1.6: Mixing process – The EEG outputs of two electrodes  $x_1$  and  $x_2$  can be conceptualized as linear mixtures of (at most) two IC source signals  $s_1$  and  $s_2$ . The relative proportions of each source signal in the signal mixtures depend on the distance from the electrodes to the sources, as well as properties of the conducting in-between structures.

The mixing coefficients ( $a, b, c, d$ ) linearly transform the vector variable  $s$  to another vector variable  $x$ . By recombining the signal mixtures the mixing process can be reversed. The reversion process is thereby determined by a set of *unmixing coefficients* ( $\alpha, \beta, \gamma, \delta$ ; see Figure 1.7 for details).

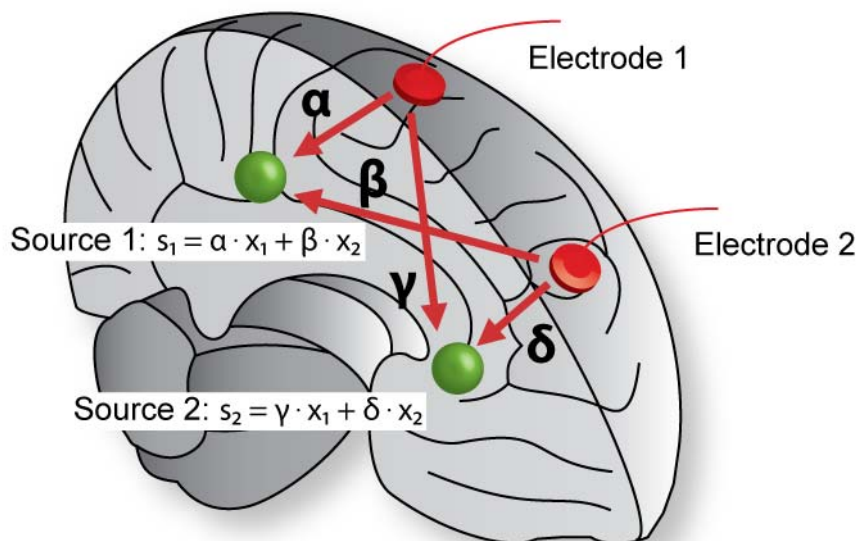


Figure 1.7: Unmixing process – The goal of ICA consists of the identification of *unmixing coefficients* in order to convert the signal mixtures  $x_1$  and  $x_2$  to form the two estimated source signals  $s_1$  and  $s_2$ .

ICA algorithms are able to identify an *unmixing matrix*  $\mathbf{W}$  that comprises the unmixing coefficients ( $\alpha, \beta, \gamma, \delta$ ),

$$\mathbf{W} = \begin{pmatrix} \alpha & \beta \\ \gamma & \delta \end{pmatrix} \quad (1.1)$$

such that – by multiplication with the signal mixture matrix  $\mathbf{x} = [x_1, x_2 \dots x_n]$  – the matrix  $\mathbf{s} = [s_1, s_2 \dots s_n]$  of independent component (IC) time courses can be reconstructed

$$\mathbf{s} = \mathbf{W} \cdot \mathbf{x}. \quad (1.2)$$

$\mathbf{s}$  and  $\mathbf{x}$  are  $n \times t$  matrices (number of channels  $\times$  number of time-points, for EEG data), and  $\mathbf{W}$  is an  $n \times n$  matrix (Onton et al., 2006; Rajapakse, Cichocki, & Sanchez, 2002). In our example, we would be able to reconstruct at most two sources from two electrode channels, therefore  $\mathbf{W}$  is a  $2 \times 2$  matrix (containing four unmixing coefficients).

#### 1.4.3.2 The ICA Algorithm

Given a set of signal mixtures and an unmixing matrix, how do we know that the extracted signals are source signals? A plausible solution seems to consist of checking the extracted sources for independence. However, independence can only be measured indirectly via *entropy*, that is, the uniformity of a distribution of a bounded set of values. Complete uniformity corresponds to *maximum entropy*. In case of a discrete set of  $N$  signal values the entropy of this set depends on the uniformity of the values in the set. Further on, the entropy of multiple variables is denoted as *joint entropy* (Stone, 2004) and can be depicted as the degree of uniformity in multidimensional space.

One way to reconstruct mutually independent signals is to find, by natural gradient ascent, an unmixing matrix  $\mathbf{W}$  that maximizes the entropy  $H$  of the distribution of  $\mathbf{Y} = g(\mathbf{y})$ , where  $g$  is assumed to be the *cumulative density function* (cdf) of the source signals. Interestingly, the unmixing matrix not only maximizes the entropy of the signals but also the shared entropy, or *mutual information* between them and the set of signal mixtures. The identification of independent signals by maximizing entropy is also known as *infomax* (Bell & Sejnowski, 1995a, 1995b; Lee, Girolami, Bell, & Sejnowski, 2000), based on a logistic neural network (Linsker, 1992; Nadal & Parga, 1994).

If  $g$  is the cdf of the source signals then the extracted signals  $\mathbf{y} = \mathbf{W}\mathbf{x}$  approximate the source signals. In other words, if  $\mathbf{W}$  is the optimal unmixing matrix then the signals  $\mathbf{y}$  extracted by  $\mathbf{W}$  from  $\mathbf{x}$  are the source signals  $\mathbf{s}$ , and the signals  $\mathbf{Y} = (Y_1, Y_2)$  obtained by transforming  $\mathbf{y}$  by a model cdf  $g$  (with  $\mathbf{Y} = g(\mathbf{y})$ ) have a uniform (*maximally entropy*) joint distribution (for further details, see Makeig, Jung, Bell, Ghahremani, & Sejnowski, 1997).

After identification of  $\mathbf{W}$ , the columns of the inverse matrix  $\mathbf{W}^{-1}$  (also an  $n \times n$  array) entail the relative weights with which the independent components project to each of the scalp electrodes. Mapping these weights to the according electrodes on a head model allows the construction of a graphical solution, i.e., the visualization of the scalp projections or scalp maps of each independent component.

#### 1.4.3.3 Independence and Correlation

Independence can be characterized best by comparison with uncorrelatedness. Someone might posit that ‘variables  $x$  and  $y$  are absolutely uncorrelated’, with the intention to imply that  $x$  and  $y$  are completely unrelated, which – per se – is not guaranteed. However, unrelatedness is captured by *statistical independence* as defined by probability density functions (pdfs). With  $p_x$  being the pdf of variable  $x$  ( $p_y$  being the pdf of  $y$ ), and  $p_{xy}$  being the joint pdf of variables  $x$  and  $y$ , then the two variables  $x$  and  $y$  are independent if and only if

$$p_{xy}(x,y) = p_x(x)p_y(y), \quad (1.3)$$

where the pdfs  $p_x(x)$  and  $p_y(y)$  are the marginal pdfs of the joint pdf  $p_{xy}(x,y)$ . In case of independent variables the joint pdf can be obtained from the product of the marginal pdfs. If two variables are not independent then it is not possible to obtain their joint pdf from the marginal pdfs of the joint pdf.

For independent variables  $x$  and  $y$  Equation (1.3) also implies the following expectation  $E$ :

$$E[x^p y^q] = E[x^p] E[y^q] \quad (1.4)$$

If  $p = 1$  and  $q = 1$  then the *expectation*  $E[x^p y^q] = E[xy]$  denotes the first moment of the joint pdf  $p_{xy}$ , also known as the covariance between  $x$  and  $y$ . Importantly, correlation (being the standardized covariance) assumes  $p = q = 1$ , so if  $x$  and  $y$  are uncorrelated then the first moment of the joint pdf  $p_{xy}$  equals the product of the first moments of the marginal pdfs  $p_x$  and  $p_y$  of  $p_{xy}$

$$E[xy] = E[x] E[y] \quad (1.5)$$

In contrast, independence not only involves the first moment but *all* positive integers of  $p$  and  $q$ . Since independence comprises uncorrelatedness (but not vice versa) many ICA methods constrain the estimation procedure reducing the number of free parameters, and simplifying the problem (Hyvärinen & Oja, 2000; Stone, 2004).

#### 1.4.3.4 ICA and PCA

Although ICA and PCA are both linear decomposition techniques, their mathematical principles vary as their biological interpretations are quite different. PCA aims at the identification of communalities between channels by finding

temporally orthogonal directions in a given set of joint channel data space (obligatory, scalp maps have to be orthogonal) that successively explain as much of the residual data variance as possible. ICA, on the other hand, identifies directions in the joint data (generally, scalp maps are non-orthogonal) whose activation profiles are as distinct as possible from each other. This minimization process not only involves a de-correlation, but also the elimination of higher-order joint statistics. The assumption of non-orthogonality of the component scalp maps (which is also biologically plausible) allows ICA to separate phase-uncoupled activities emanating either from spatially fixed cortical domains or non-brain artifact sources. In case of non-orthogonal scalp maps, PCA would just re-arrange the original signal mixtures to form new mixtures that, again, would be intercorrelated, whereas ICA would be able to truly extract mutually independent components that neither are correlated nor share any other joint characteristics (Onton et al., 2006).

Taken together, ICA has proven to reliably and validly reveal the driving forces of cortical activity without necessitating assumptions beside temporal independence of IC activity. Recently, co-registered EEG-fMRI recordings further demonstrated that ICA successfully reconstructs spatial sources with high temporal accuracy, and further, that major temporal characteristics of ICs dynamics are directly coupled to the BOLD-signal (Debener, Ullsperger, Siegel, Fiehler, von Cramon, & Engel, 2005).

Applying ICA for the analysis of EEG data allows examination of the underlying information sources in the data (without minimal assumptions regarding the nature of the signals), rather than their summed effects at the scalp electrodes. By means of removing or minimizing the effects of volume conduction, detailed examination of the separate dynamics and dynamic interrelationships of distinct cortical areas are possible (Delorme & Makeig, 2003; Makeig, Westerfield, Jung, Enghoff, Townsend, Courchesne, & Sejnowski, 2002).

## Chapter 2

# Synopsis of the Present Thesis

Based on the previously depicted conceptualizations, this Ph.D. thesis combined two central lines of spatial navigation research that, *per se*, have been shown to moderate neural substrates and behavioral outcomes of human visual path integration ability: Complexity of the traversed environment and preferred use of either an allocentric or an egocentric reference frame for building up a spatial representation. However, there exists, hitherto, no study on behavioral performance and/or spectral dynamics during visual path integration at different complexity levels taking into consideration individual preferences for building up a spatial representation within either an egocentric or an allocentric reference frame. Therefore, the primary aim of the present thesis consisted in the identification of behavioral, neuro-anatomical, and electrocortical correlates of human visual path integration within allocentric and egocentric reference frames during the confrontation with outbound paths of varying complexity. Additionally, it was of interest, whether spatial updating within the respective reference frames is accomplished in a configural or history-free manner.

For this purpose, behavioral (response latencies, absolute and signed error scores) and electrophysiological methods were applied. Information-based spatial filtering of high-density EEG recordings into maximally independent component (IC) processes allowed for investigation of differences in mean IC brain source spectral dynamics between navigation strategies during visual path integration.

## 2.1 Chapter 3

The initial behavioral results of Gramann and colleagues (2005) and Riccobon (2007) provided strong evidence for homing accuracy of subjects preferentially using an egocentric reference frame during path integration (*Turners*) as well as subjects preferentially using an allocentric reference frame (*Nonturners*) being comparably affected by increased complexity in terms of numbers of turns. However, in these studies overall length of the passages has been kept constant, so that subjects could determine whether traversing a tunnel with one, two, or three turns, respectively, from estimating distance and/or time until encountering the first turn. This might have influenced the absence of complexity effects. Furthermore, direction of successive heading changes during turns was not explicitly controlled for. As a consequence, data averaging of angular adjustments for tunnels with two turns into the same and into opposite directions might have masked strategy-specific errors in homing accuracy and latency.

In order to circumvent these limitations, a set of virtual turning tunnels was constructed that allowed for investigation of specific effects of number and direction of successive heading changes on homing accuracy/ latency of Turners and Nonturners. In Experiment 1, participants traversed tunnels with either one turn, two turns into the same direction, or two turns of similar angularity into opposite directions. By contrast, in Experiment 2 only tunnels with one turn or with two turns bending into the same directions was presented. In Experiment 3, finally, tunnels with one turn and two opposite turns of equal angularity were presented. At the end of a passage participants indicated their momentary position relative to the starting point (point to origin). Turners and Nonturners were found to display comparable error patterns (regression to the mean) supporting the notion of path integration being based on configural updating of distance and direction. Importantly, behavioral data supported the notion of an extended configural updating mechanism subserving path integration (Klatzky et al., 1999). Due to memory-loss and ambiguity during paths of higher complexity, participants seemingly built up representation-based expectancies of complexity-specific ‘average paths’, resulting in shifted regression tendencies for tunnel configurations of higher complexity. Results elaborated previous findings (Gramann et al., 2005), corroborating the consideration of individual strategies in spatial navigation.

## 2.2 Chapter 4

The question was if the comparable behavioral performance was also mirrored in terms of comparable cortical processes during encoding and retrieval of spatial information. Therefore, high-density scalp EEG (128-channels) record-

ings of Experiments 2 (same direction) and 3 (opposite directions) were analyzed using Independent Component Analysis (ICA, Makeig, Debener, Onton, & Delorme, 2004). Subsequently, the generator sources of the obtained independent component (IC) processes were spatially localized within the cortical source domain based on equivalent current dipole model reconstruction (Anemüller, Sejnowski, & Makeig, 2003; Makeig et al., 2004). In contrast to classical ERP-studies analyzing induced electrocortical activity within delimited frequency bands within a few hundred milliseconds, event-related spectral perturbations provide insight into continuous brain dynamics covering a wider range of the frequency spectrum (ranging from 3 to 45 Hz).

Consistent with recent imaging studies on spatial navigation (Committeri et al., 2004; Galati, Lobel, Vallar, Berthoz, Pizzamiglio, & Le Bihan, 2000; Maguire et al., 1998a; Wolbers et al., 2007) and processing of visual flow information (Culham et al., 2001; Sunaert et al., 1999), the experiments resembled a wide-ranging cortical network of IC source locations with spectral dynamics mirroring the processing of translational and rotational information during curved tunnel segments from a first-person perspective, accompanied by alpha (near 10 Hz) blocking in occipito-parietal areas and lateral temporal/ frontal midline theta (near 6-Hz) activation. Turners encoded spatial information primarily within occipito-parietal and parietal cortices subserving the construction of the egocentric reference frame, whereas for Nonturners ventral activation was increased (allocentric reference frame), complemented by retrosplenial activation, the transition zone between reference systems (Maguire, 2001). Additional to the reference-frame-specific activation patterns in the depicted regions, both Turners and Nonturners displayed increased frontal midline theta activity when traversing tunnels with two turns. EEG results replicated and extended previous findings on electrocortical activity during path integration (Gramann et al., 2006; Riccobon, 2007), and shed light on the cortical mechanisms that guided configural coding.

## 2.3 Conclusions

The results of chapters 3 and 4 provided evidence for egocentric and allocentric referential systems to encode spatial information based on *extended configural updating* (Klatzky et al., 1999), i.e., the update of reference-frame-specific primitive parameters during critical stages of travel such as upcoming heading changes. E.g., based on configural updating an outbound path consisting of two straight segments separated by an on-spot turn of 90° might be represented as being L-shaped. However, as pathway complexity is increased, navigators are confronted with ambiguity and memory-loss due to the increasing number of elements that have to be updated with each successive translation/ rotation. Behavioral data provided evidence that spatial encoding is not purely ‘object-based’ but rather moderated by route expectancies retrieved

from the representational level. In other words, the previously described path layout might not always be encoded as being L-shaped. Instead, as the navigator traverses various trajectories, their layout is gradually accumulated into an ‘average pathway’. Under ambiguity, the navigator might resort to this rough estimation in order to identify the approximate distance and direction of the starting point of travel. However, the represented set of previously traversed paths determines the encoding of the actually traversed trajectory. With respect to the present findings, Turners’ and Nonturners’ homing responses implied that they built up complexity-specific ‘average paths’ whenever confronted with multiple, unpredictably varying complexity levels (Experiment 1). As variability was reduced (Experiments 2 and 3), it depended on the configuration of the traversed pathways whether both complexity-levels were merged into a single ‘average path’ (one turn and two turns bending into the same direction), or each complexity level was coded with respect to distinct ‘averages’ (one turn and two opposite turns).

Importantly, analysis of event-related spectral perturbations (ERSPs) suggested that egocentric and allocentric processing share communalities in processing rotational and translational information, but that each strategy group resembles to distinct neural circuits as environmental complexity is increased, which might be interpreted with respect to conceptualizations of egocentric and allocentric reference frames conveying distinct primitive parameters (Klatzky, 1998) that are most likely processed within areas responsible for updating these variables, e.g., heading information in retrosplenial or posterior parietal cortex (Calton & Taube, 2009; Nitz, 2009). Additionally, spatial encoding might have been altered by frontal executive processing. Based on findings addressing the association of theta band activation with memory retrieval at important time points of travel (Kahana et al., 2001), these theta deflections might have marked the updating of representational primitives. Additionally, theta activation supposedly coordinated the above mentioned memory-based retrieval of ‘average pathways’ resulting from recorded experiences with tunnels of similar complexity. Present findings suggested that the update of strategy-specific information could be characterized as being monitored by processes that are activated irrespective of the preferred use of an egocentric or an allocentric reference frame. Taken together, results supported the assumption of co-existing allocentric and egocentric reference frames as implied by neuropsychological investigations (Aguirre & D’Esposito, 1999; Burgess, 2006; Burgess et al., 2004; Byrne, Becker, & Burgess, 2007; Hartley et al., 2003; Mou et al., 2004; Redish, 1999; Sholl, 2001).

Future research has to address how the present results would transfer to more general navigation tasks, e.g., when additional ideothetic information from the vestibular system is present, or allothetic cues such as landmarks are available. Spatial encoding should be significantly altered, as suggested by Foo and colleagues (2007). However, these near-real-world tasks require the precise control of experimental stimulation. Immersive VE systems utilizing mobile brain imaging (Makeig, Gramann, Jung, Sejnowski, & Poizner, accepted; Makeig,

Onton, Sejnowski, & Poizner, 2007) might constitute the seminal basis for further investigation of complexity effects on behavioral and electrocortical correlates of allocentric and egocentric navigation under more natural conditions. Further, these systems would extend present results on homing accuracy in terms of directional estimations by active production of homing trajectories.

# Chapter 3

# Behavioral Analyses

## 3.1 Abstract

Whenever landmarks are unavailable during navigation, humans are forced to use path integration, i.e., the continuous consolidation and integration of sensory input on velocity and acceleration from different sensory modalities within distinct but complementary reference frames. The present study investigated differences in homing accuracy based on an egocentric or an allocentric reference frame by systematically varying the complexity of a virtual outbound path. In three experiments, participants preferentially using an allocentric or an egocentric reference frame (Nonturners vs. Turners, respectively) traversed virtual tunnels with either one turn, two turns into the same direction, or two turns of similar angularity into opposite directions. At the end of a passage participants indicated their momentary position relative to the starting point (point to origin). Turners and Nonturners were found to display comparable error patterns attributable to the variation in path complexity. The results support the assumption that path integration was based on configural updating of distance and direction. Participants built up representation-based expectancies incorporating a complexity-dependent ‘average path’, resulting in varying regression tendencies for the tested complexity levels. These findings highlight the central role of individual strategies in spatial navigation and support the assumption that encoding of spatial information for different complexity levels is moderated by the preferred reference frame.

## 3.2 Introduction

Spatial cognition is a core competence for everyday survival and successful interaction with our environment. This multifaceted cognitive function is defined as the capacity to acquire, organize, utilize, and revise knowledge about spatial environments allowing the construction and utilization of mental representations of where we are with respect to our surroundings (Bryant, 1992; Kerkhoff, 2000; Tversky, 1993). For this purpose, polymodal sensory input from visual, vestibular, kinesthetic, and proprioceptive systems, information about the momentary position of the navigator, and long-term enduring action-plans have to be continuously updated, consolidated and integrated within distinct but interacting reference frames (Avraamides & Sofroniou, 2006; Golledge, 1999a; Mou et al., 2004). During spatial navigation the moving agent has to obtain and store spatial information about the external world by updating spatial relations from sensory input in order to keep track of his current position and orientation during travel (Gallistel, 1993).

The underlying mechanisms might be classified with respect to the type of information used: Piloting, also referred to as position-based navigation, denotes the utilization of visible, audible or otherwise perceivable allothetic cues, so-called ‘landmarks’ (distinct, stationary, and salient objects) in combination with a map of the surroundings (Golledge, 1999b; Hunt & Waller, 1999). In the absence of landmarks, humans, like other mobile species, have been found to be capable of path integration, i.e., the processing of allothetic (e.g., optic flow) or ideothetic (e.g., proprioceptive, vestibular, and kinesthetic) information on velocity and acceleration in order to infer distances and directions to relevant sites, e.g., the starting point of an excursion (Biegler, 2000; Cornell & Heth, 2004; Loomis et al., 1999b).

Previous studies have investigated ideothetic path integration abilities in triangle completion tasks ('homing') where blind or sighted blindfolded participants are led or passively transported along outbound trajectories containing two, or more, straight segments, separated by on-spot turns of varying angularity. Subsequently, participants were asked to perform a short-cut, e.g., by manually pointing or bodily turning towards, and/or walking back to the starting point of the passage (Klatzky, 1998; Klatzky et al., 1999; Klatzky et al., 1990; Loomis et al., 1993; Loomis et al., 1999b; Peruch, May, & Wartenberg, 1997). The results demonstrated that ideothetic signals allow for proper updating of position and orientation in space (Ivanenko et al., 1997; McNaughton et al., 1996). Further, if no vestibular or proprioceptive cues were given visual flow information as exclusive input for path integration was sufficient for the construction of an enduring spatial representation (Kearns et al., 2002; Kirschen et al., 2000; Riecke et al., 2007; Wraga, Creem-Regehr, & Proffitt, 2004).

### 3.2.1 Spatial Reference Frames and Individual Proclivities

Such enduring spatial representations comprise the locations of significant objects (Etchamendy & Bohbot, 2007; Tversky, 1993), as well as one's position with respect to the represented entities within either a (body-centered) *egocentric* or an (environment-centered) *allocentric* reference frame (Brewer & Pears, 1999; Klatzky, 1998; Klatzky et al., 1990; McNamara, Rump, & Werner, 2003; Mou et al., 2004). During the last decade several investigations using neuropsychological methods demonstrated that the use of an egocentric or an allocentric reference frames is based on activity within distinct brain areas (Committeri et al., 2004; Galati et al., 2001; Vallar et al., 1999; Wilson et al., 2005). Importantly, the choice of one or another reference frame during spatial navigation is affected by enduring and individually stable preferences (Denis & Loomis, 2007; Gramann et al., 2005; Lawton, 1996; Pazzaglia & de Beni, 2001). Lesion studies and electroencephalographic investigations further support the assumption of reference frame proclivities and showed that distinct brain areas subserve the computation and use of an allocentric or an egocentric reference frame (Gramann et al., 2005; Gramann et al., 2006; Gramann et al., submitted; Riccobon, 2007; Seubert et al., 2008).

### 3.2.2 Updating of Representation-Specific Information

The use of distinct reference frames as a means to represent entities in space leads to differences in the primitive parameters stored in the spatial representation (Klatzky, 1998). The aim of the present investigation was to investigate whether homing accuracy dependent on the use of distinct reference frames is differentially influenced by path complexity. If reference frame specific parameters are updated on a *moment-to-moment* basis, as proposed in history-free models of spatial updating (Benhamou & Seguinot, 1995; Hartmann & Wehner, 1995; Merkle et al., 2006; Müller & Wehner, 1988) overall bearings and distances between the navigator's current position and an arbitrary starting point should be available irrespective of path complexity (Loomis et al., 1999b). History-free updating also implies that the navigator is neither able to retrace the path nor to determine the layout of the trajectory, as observed in arthropods (Merkle et al., 2006; Müller & Wehner, 1994, 2007). However, there is empirical evidence that humans are capable of these tasks (Cornell & Greidanus, 2006; Cornell & Heth, 2004; Loomis et al., 1993). Therefore, it seems plausible to assume that the resulting representation contains more than just the distance and direction to the starting point of an excursion.

The *encoding-error model* (Fujita et al., 1993) as representative of models based on *configural updating* proposes that spatial updating is not only executed in constant intervals, but includes significant time-points of travel. Therefore, the resulting spatial representation contains not only information regarding overall distance and direction between current position and starting point, but also the layout of the traversed outbound path on the representa-

tional level. However, rotational information has been found to have a higher impact on updating as compared to translational information (Kearns et al., 2002; May, 2004). Therefore, heading changes constitute the critical time points of a passage where spatial updating is accomplished (Loomis et al., 1993; May & Klatzky, 2000; Riecke et al., 2002). Since turning locations are stored as points that determine the path layout, more complex pathways, i.e., containing more turns, require increasing cognitive resources due to the increasing number of relations to be encoded. This results in prolonged homing latencies and more pronounced errors during retrieval (Jansen-Osmann & Wiedenbauer, 2006; Kearns et al., 2002; Loomis et al., 1993; Maurer & Seguinot, 1995).

During history-free spatial updating the navigator has to refresh only overall return bearing and distance to the starting point. Both parameters are primitives within the egocentric and the allocentric locational representation. In contrast, configural updating within an egocentric reference frame requires the navigator to update *egocentric return distance* and *bearing* of the starting point, but also *egocentric self-to-object* relations (and distances) of all objects encountered along the outbound pathway. Since egocentric bearings vary with each directional change of the navigator's intrinsic axis of orientation the egocentric system is instable and updating of egocentric bearings becomes more difficult with increasing number of turns. More importantly, the direction of subsequent turns might impact egocentric updating, since represented elements have to be shifted/rotated with respect to the intrinsic axis of the navigator (see Figure 3.1).

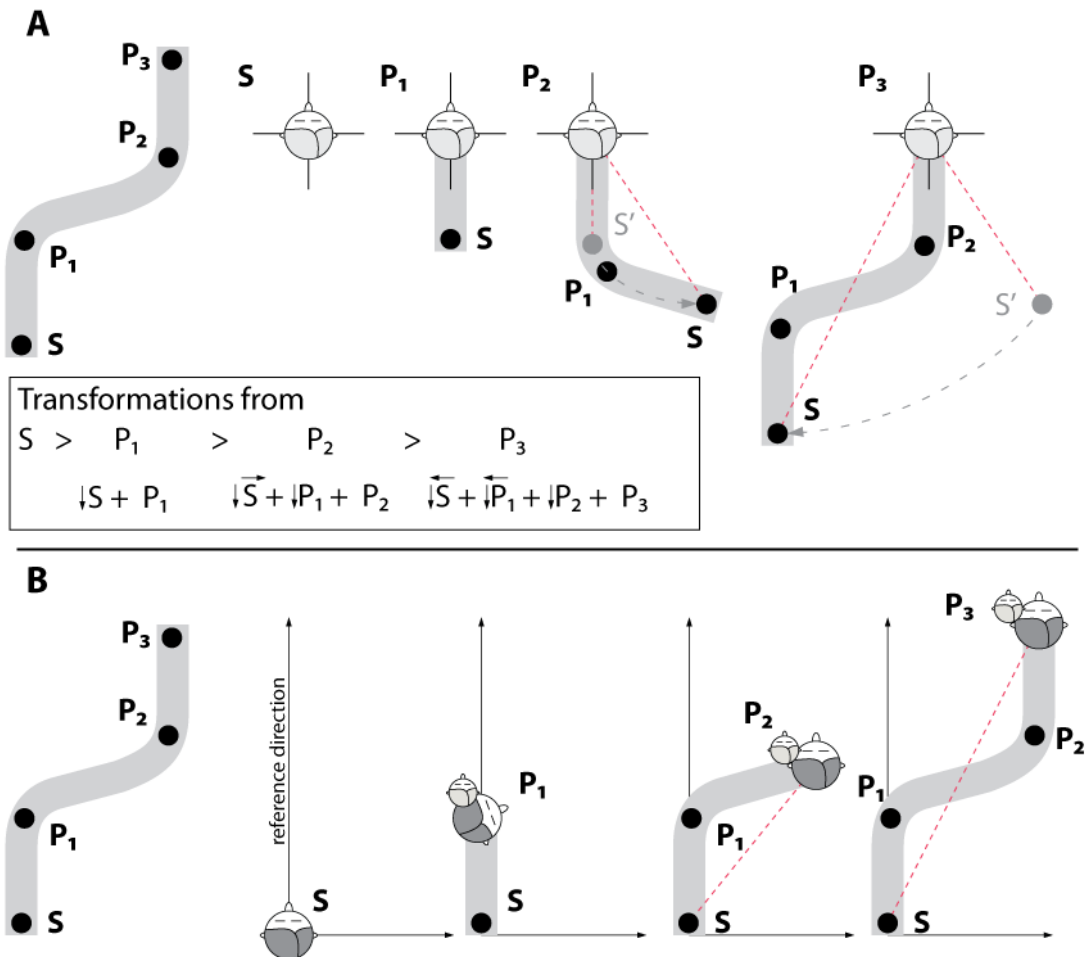


Figure 3.1: **(A)** Configural updating within an egocentric reference frame. As the subject moves along the outbound trajectory, egocentric distances and bearing are updated at significant time points of travel, e.g., during rotations. Thus, the path is partitioned into straight segments separated by turns. During the initial translation from S to P<sub>1</sub>, only the return distance has to be updated while the bearing remains identical. However, during the curve, bearing as well as distance change. As a result, S moves to the right side with respect to the navigator's intrinsic axis of orientation. Between turns, distances and bearings have to be updated accordingly. During the curve at P<sub>2</sub>, the starting point again moves from the right to the left side. **(B)** By contrast, within an allocentric reference frame, traversing the outbound trajectory based on configural updating denotes the updating of allocentric distance and bearing with respect to the reference direction. In order to process rotational information, the navigator has to update the allocentric heading, i.e., the relative direction of travel with respect to the reference direction. Since within an allocentric reference frame the navigator moves within the array of stationary objects, the return bearing does not change sides. If the allocentric bearing after the first turn is to the left, it is still on left as the path continues with an opposing turn.

Similarly, increasing errors due to increasing number of elements should also be present for allocentric configural coding. However, since within the allocentric reference frame the navigator's changes in orientation are computed with

respect to an external reference direction, providing information about the *allocentric heading* of the moving agent, the relative direction of changes in the navigator's intrinsic axis should have no impact on allocentric coding. Thus, within an allocentric reference frame successive heading changes should have no impact on accuracy and response latencies.

Taken together, whereas history-free updating supposedly results in comparable errors and response latencies for homing responses based on distinct reference frames, configural updating should lead to strategy-specific deteriorations due to differences in updating of primitive parameters.

### 3.2.3 Aims of the Present Study

The present study investigates the influence of path complexity dependent on the use of an allocentric or an egocentric reference frame during spatial navigation. In order to examine these questions, the tunnel paradigm was used (Gramann, 2002; Schönebeck et al., 2001), providing subjects with visual flow stimulation of 3D virtual turning tunnels with straight and curved segments (no vestibular input). After passages through virtual tunnels participants have to adjust a virtual 3D-arrow to point directly back to the starting point of the passage (point to origin). Path complexity was operationalized as the number and directions of successive heading changes (of varying angularity) along an outbound trajectory, and representational accuracy was captured in terms of accuracy in homing vector adjustment as well as response latencies. In *Experiment 1*, participants preferentially using an egocentric or an allocentric reference frame were confronted with multiple complexity levels, i.e., tunnels of different length and number of turns. In order to dissociate the effects between the different complexity levels of the outbound paths, in *Experiment 2* tunnels with one and two turns bending into the same directions were used. Participants in *Experiment 3*, by contrast, traversed tunnels with one turn or tunnel with two turns with identical angles bending into opposite directions.

## 3.3 Experiment 1

In *Experiment 1*, participants were confronted with multiple complexity levels, i.e., tunnels with one turn, two turns bending into the same direction, and two opposite turns with parallel start- and end-segments. Given that the encoding of an allocentric and an egocentric spatial representation is based on configural updating, the number of elements that have to be integrated rises with increasing overall length as well as number of consecutive heading changes along the outbound trajectory. Since within an egocentric reference frame all self-to-object relations have to be continuously updated with respect to the navigator's intrinsic axis of orientation, Turners were expected to show more pronounced regression tendencies as well as prolonged response latencies for

tunnels of higher complexity. Further, spatial updating of Turners should be more demanding in case of opposite turns as compared to turns bending into the same direction. Nonturners, by contrast, were supposed to display a comparable increase in regression to the mean between complexity levels, while response time should be unaffected by path complexity since the positional updating of the navigator within an allocentric reference frame was supposed to result in comparable computational demands independent of the path layout.

### 3.3.1 Methods

#### 3.3.1.1 Subjects

Due to gender-specific differences in spatial navigation (Coluccia & Louse, 2004; Grön et al., 2000; Lawton & Morrin, 1999; Ohnishi, Matsuda, Hirakata, & Ugawa, 2006; Sakthivel, Patterson, & Cruz-Neira, 1999; Sandstrom, Kaufman, & Huettel, 1998; Shelton & Gabrieli, 2004) only male subjects participated in the experiment. Twenty male subjects of the Ludwig-Maximilians-University Munich, Germany, took part in Experiment 1 (age ( $M \pm SD$ ) =  $25.60 \pm 3.42$  years). Participants were either paid 8€ per hour or received course credit for taking part in the experiment. The experiment followed the American Psychological Association's (APA's) Ethical Principles of Psychologists and Code of Conduct (American Association of Psychology, 2002). All subjects had normal or corrected to normal vision and reported no history of neurological disorder. All but one subject were right-handed.

#### 3.3.1.2 Task, Materials and Procedure

Participants were seated in a dimmed and sound-attenuated black cubicle equipped with electromagnetic shielding in front of a 37.7 cm x 37.7 cm (approx. 21 in. screen size) Eizo Flexscan F77s TCO 99 (resolution of 1280 x 1024 pixels, 102 Hz), placed 100 cm (approx. 39 in.) in front of the observers with the screen center being aligned with the participant's horizontal straight ahead of sight. The visual angle of the presented tunnel passages was approximately 21°.

#### *Categorization*

Prior to the main experiment a categorization task was applied in order to classify the preferred spatial strategy of the subject (Nonturner vs. Turner). Participants traversed 30 tunnels with one single turn of varying angle. Tunnels were composed of an initial straight segment followed by a curved segment and two final straight segments. At the end of a passage through the tunnel two arrows were displayed that represented the correct homing response based on an allocentric or an egocentric reference frame (see Figure 3.2). In a forced-choice task, participants had to spontaneously decide which of the two arrows pointed back to the starting point of their passage. Within three blocks of 10 trials each turning angles gradually decreased, so that egocentric

and allocentric arrows converged, resulting in increasing task difficulty. In order to take part in the main experiment, participants had to consistently (i.e., more than 83% of the trials) select the allocentric or egocentric arrow to be categorized as Nonturner or Turner, respectively. All subjects selected for the main experiment demonstrated consistent choice of one or the other reference frame (Turners  $M \pm SD = 29.6 \pm 0.7$  categorization trials ( $99\% \pm 0.02\%$ ), Nonturners  $M \pm SD = 28.7 \pm 1.3$  trials ( $96\% \pm 0.04\%$ ); correlation between Preferred Strategy and strategy-specific arrow choice:  $r(19) = .997$ ,  $p < .00001$ ).

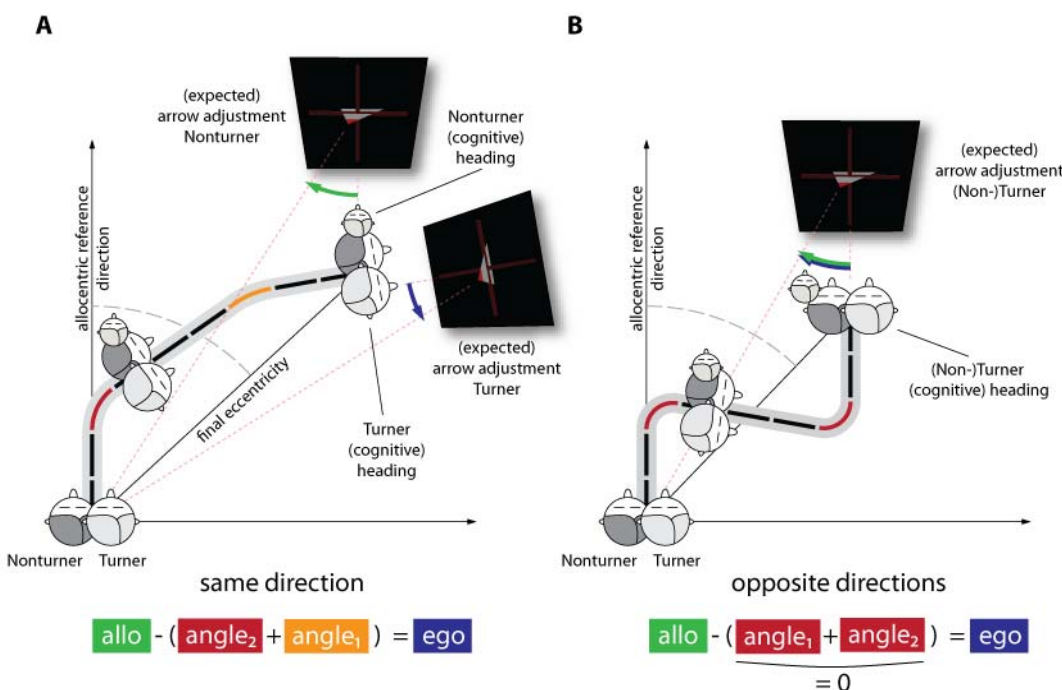


Figure 3.2: Cognitive headings of Turners and Nonturners differ with respect to the tunnel configuration. **(A)** Tunnels with one and two turns bending into the same direction result in distinct cognitive headings at the end of the passage. **(B)** By contrast, tunnels with two opposite turns of equal angularity result in identical final cognitive headings for Turners and Non-turners.

After categorization, subjects underwent a brief training block of approximately 10 minutes traversing 16 tunnels (8 tunnels with one turn; 4 tunnels with two turns bending into the same direction; 4 tunnels with opposite turns of equal angularity). End positions differed from the ones used in the main experiment. Tunnels with one turn were generated of five segments, with the two initial and two final straight segments enclosing the turning segment. Tunnels with two turns had a total of six segments (turns in segments 2 and 5). In contrast to the forced choice task of the categorization, subjects now had to adjust the homing arrow (initially in  $180^\circ$  position) so that it pointed back to the origin of the tunnel passage. By pressing the right or left mouse button, the arrow was rotated continuously. When the adjustment of the subjectively correct

homing vector was completed, the setting was confirmed by pressing the middle mouse button. Participants were allowed to adjust the homing arrow without time limit. After subjects confirmed their response, the adjusted arrow was presented simultaneously with the expected strategy-specific response. Because participants' responses on tunnels with two turns were of special interest for the current study, feedback was provided only for tunnels with one turn.

### Main Experiment

The main experimental session included 21 blocks of 8 tunnels each and 1 final block with 12 tunnels with minor breaks between the blocks. During the experiment tunnels with one turn and two turns were presented. The task of the subjects was to keep up orientation during the tunnel passage and to adjust the homing vector at the end of the passage. The time line of a single trial is depicted in Figure 3.3.

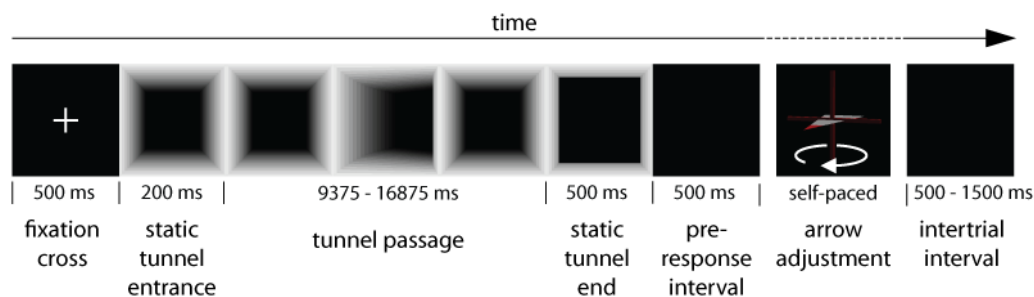


Figure 3.3: Experiment 1 – Time line of a single trial without feedback. After 500 ms presentation of a fixation cross, a static image of the tunnel entrance was displayed (200 ms). Thereafter, the tunnel passage was presented, lasting either 9400 ms for tunnels with one turns or 16920 ms for tunnels with two turns. A snapshot of the tunnel end was presented for another 500 ms, followed by a 500 ms blank screen pre-response interval. The arrow appeared, pointing into the depth of the screen, which could be adjusted without time limit. Upon response confirmation, feedback could be provided (2000 ms). A consecutive 500 – 1500 ms blank screen announced the next trial.

Each trial started with a fixation cross for 500 ms, followed by the presentation of a static display of the first tunnel segment for 200 ms. Then, tunnel movement started. Length of tunnels and positions of turning segments were identical to the training trials. Tunnels with one turn comprised five segments, with the two initial and two final straight segments enclosing the turning segment of varying angles. Tunnels with two turns had a total of nine segments (turns located in segments 3 and 7). After the passage along the outbound path participants had to adjust the homing vector so that it pointed back to the origin of the tunnel passage. In 10% of the trials and only for tunnels with one turn or two turns bending into the same direction strategy-specific feedback on the subject's homing accuracy was displayed for 2000 ms. A blank screen (500 – 1000 ms) marked the onset of the next trial.

The placement of turns in segments 3 and 7 ensured that subjects could not determine if traversing a tunnel with five or with nine segments until either the end of the passage showed up or the tunnel continued with a second turn. Further, stimulus turns of tunnels with nine segments could bend into the same direction (2 turns, sd), or into opposite directions with equally angled turns (2 turns, od). The angle of turns was varied such that the eccentricity of end positions of the outbound paths reached 15°, 30°, 45°, and 60° ( $\pm 2^\circ$  deviation to avoid categorical reactions during arrow adjustment) to the left and right relative to the starting position. Eccentricity of end position was conceptualized within an allocentric reference frame. For tunnels with one turn as well as tunnels with two turns bending into the same direction, the egocentric eccentricity could be retrieved by reversing signs. For tunnels with two opposite turns of equal angularity, end positions were identical within both reference systems. Due to geometric-mathematical constraints in the construction of the tunnel material (segments of uniform length, constant movement speed), it was not possible to program tunnels with two opposite turns in segments 3 and 7 (of equal angularity) that ended at the categorical eccentricity of 60°. This condition only would have been possible with longer turning segments (as compared to straight ones). There were a total of 144 'experimental' tunnels, randomly interlaced by 36 'filler' tunnels, consisting of tunnels with one and two turns ending up at the eccentricity of 60°, always bending into the same direction. Participants received feedback on every tenth trial with one turn or two turns bending into the same direction.

### 3.3.2 Performance Measures

The tunnel paradigm follows the logic of analyzing cognitive processes during spatial orientation using psychophysiological measures. One critical point is the distinction between correct and incorrect solutions. In this context, incorrect solutions, meaning the navigator loses his orientation during the tunnel passage, were omitted from the further analysis, so only correct reactions were incorporated.

#### 3.3.2.1 Side Error

One basic indicator for valid reactions in the tunnel paradigm is the correct indication of the side of the starting point relative to the end position, left or right within the preferred reference frame. Previous studies (Gramann et al., 2005; Riecke & Wiener, 2007; Riecke, 2008) conceptualized reactions indicating the wrong side of end position as *side errors*. This type of error might reflect ambiguities caused either by inattentiveness during the experimental procedure (e.g. simple mixing up of right and left) and/or by complete loss of orientation. However, the number of side errors has been suggested to be related to path complexity interacting with strategy-specific preferences for an egocentric or an allocentric reference frame (see Gramann, 2005, Experiment 1). Therefore, side errors were analyzed separately and eliminated from further analyses. In addition to side errors arrow adjustments erroneously pointing

into the depth of the monitor ( $90^\circ$  -  $180^\circ$  to both sides) instead of back ( $0^\circ$  -  $90^\circ$  to both sides) were rejected from further analyses.

### 3.3.2.2 Angular Fit

Participants should not only be able to differentiate between left and right, but also to discriminate fine-tuned eccentricities of end position within the virtual environment. The Pearson correlation between the adjusted homing vector for each eccentricity of end position and the objective angular vector was used for statistical analysis of this criterion for building up a correct spatial representation. Correlations were subsequently standardized using the Fisher transformation, in order to conduct pairwise comparisons of the resulting correlation coefficients within and between strategy groups, as well as within and between complexity levels (tunnel layouts).

### 3.3.2.3 Response Time

Response time was calculated as the delay between the onset of the response arrow and the initial button press of one of the mouse buttons. Since the homing vector adjustment is no speeded task, subjects could press the right or left mouse button without explicitly having a spatial representation in mind but constructing it during the arrow adjustment phase, e.g., while rotating the virtual arrow into the approximative position. However, response time is conceptualized to be a weighted sum of *random* and *systematic* processes. In this case, the depicted pattern of spatially reasoning after initiating the response should be randomly, and therefore equally, distributed over *all* presented tunnels. As a result, differences in response time can be attributed solely to additional systematic processes. Nevertheless, if the response latency to initiate the arrow adjustment was among the slowest 2.5% of strategy-group specific response times, the trial was excluded from the further analyses.

Response time was analyzed by means of mixed design ANOVAs with *Preferred Strategy* (Turner, Nonturner) as the between-subjects factor, and *Tunnel Layout* (1 turn; 2 turns, sd; 2 turns, od), *Side of End Position* (left or right relative to starting point), and, additionally, *Eccentricity of End Position* ( $15^\circ$ ,  $30^\circ$ ,  $45^\circ$ ), as the within-subject factors. Whenever the factor *Side* did not show any significant main effects the data was aggregated over left and right sides. In case of violations of homoscedasticity, Greenhouse-Geisser correction was applied. Effect size was computed using generalized eta squared,  $\eta_G^2$  (Bakeman, 2005; Olejnik & Algina, 2003). Significant terms were further analyzed with post-hoc tests using the iterative *Holm-Bonferroni* adjustment (for

further applications see Krauth & Lienert, 1973)<sup>7</sup>. The same analyses were applied for the following dependent measures.

### 3.3.2.4 Absolute Error

The absolute error provides information about the absolute difference between the subject's reaction and the expected reaction. Because eccentricity of end position is defined within an allocentric coordinate system, for subjects using an allocentric frame of reference (Nonturners) the absolute error is computed as the difference between eccentricity of end position and angular adjustment. For participants using an egocentric reference frame (Turners), the numerical value of the subject's reaction is composed of the (allocentric) eccentricity of end position and the angle between the (allocentric) reference direction and the heading direction of the last segment. For tunnels with parallel start-end segments the difference is Zero. Because error tendencies are incorporated absolutely disregarding the direction of the error, over- and underestimations do not neutralize each other but sum up, providing information about reaction accuracy.

### 3.3.2.5 Relative Error

Following the above described computation of allocentric into egocentric coordinates, signed error scores were analyzed, reflecting possible differences in angular adjustments between Turners and Nonturners with respect to the direction of error. The relative error score takes the direction of the error in angular reaction dependent on the eccentricity of end position into account (underestimations or overestimations, respectively).

## 3.3 Results

Subjects demonstrated a spontaneous and stable preference for choosing an egocentric or an allocentric reference frame as reflected in highly positive correlations between adjusted and expected homing vectors. Overall, subjects were able to keep up orientation and to adjust the reaction format within their preferred reference frame. In detail, the results were as follows.

### 3.3.3.1 Side Error

Tunnel Layout was found to be the only factor revealing an influence on the number of side errors [ $F(1.01, 36) = 8.180, p < .010, \eta^2_G = .181$ ]. Side errors for tunnels with two opposite turns ( $M \pm SD = 12.19\% \pm 18.60\%$ ) was found to dif-

---

<sup>7</sup> For the purpose of readability, non-significant p-values were multiplied by the number of tests instead of comparing an obtained (non-significant) p-value with a Holm-Bonferroni adjusted significance level.

fer significantly ( $p < .01$ ) from both tunnels with one turn as well as tunnels with two turns leading into the same direction (one turn:  $M \pm SD = 0.63\% \pm 1.19\%$ ; two turns, sd:  $M \pm SD = 0.31\% \pm 0.76\%$ ; comparison between one and two turns, sd: n.s.), as obtained by subsequent pairwise comparisons (see Figure 3.4).

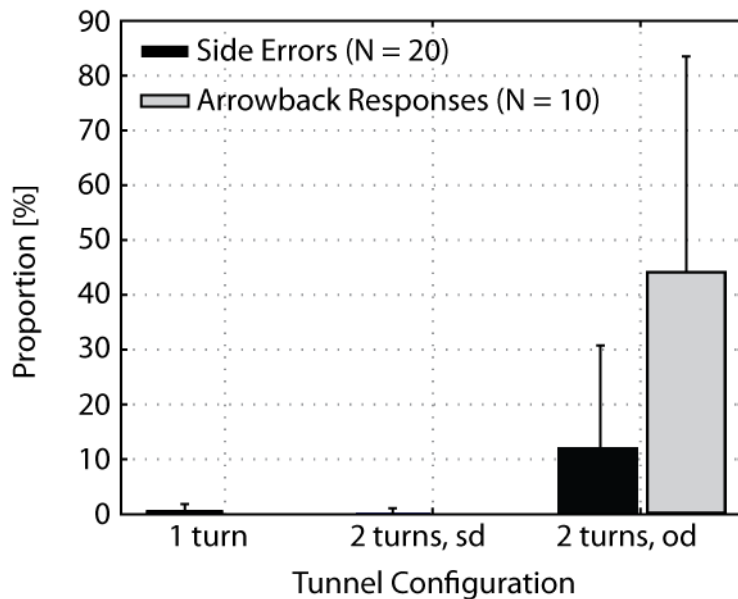


Figure 3.4: Experiment 1 – Percentaged mean side errors ( $\pm 1$  SD, depicted by black boxes;  $N = 20$ ), and percentaged mean arrowback reactions ( $\pm 1$  SD, depicted by grey boxes;  $N = 10$ ), for tunnels with one turn, two turns bending into the same direction (sd), and two opposite turns (od).

### 3.3.3.2 Other Incorrect Solutions – Arrowback Responses

For some of the tunnels with two opposite turns in Experiment 1, ten participants (5 Turners, 5 Nonturners) demonstrated underestimations as large as the current eccentricities of the tunnel passages themselves. Although the tunnel layout always included a parallel offset between the starting point and the end of the tunnel passage, subjects adjusted homing vectors pointing back more or less  $180^\circ$ . E.g., after an outbound path with a turn of  $70^\circ$  to the right in segment 3 and opposing turn of  $70^\circ$  to the left in segment 7, the correct angular adjustment at the end of the passage would point approximately  $30^\circ$  to the left. As a result, an arrow adjustment of  $0^\circ$  is an underestimation of 30. Analyses of these so-called ‘arrowback responses’ for the 10 subjects revealed a main effect of Tunnel Layout to be significant [ $F(1.00, 16) = 11.582, p < .009, \eta^2_G = .475$ ]. There were no arrowback reactions for tunnels with one turn and tunnels with two turns bending into the same direction, but an average of  $M \pm SD = 44.38\% \pm 39.16\%$  arrowback reactions for tunnels with two opposite turns (see Figure 3.4). There were no significant correlations between side error and arrowback scores.

### 3.3.3.3 Angular Fit

Correlations of observed angular response with strategy-specific expected angular response revealed highly significant interrelationships for both Nonturners,  $r(172) = .926$ ,  $p < .0001$ , and Turners,  $r(177) = .897$ ,  $p < .0001$ , with comparable correlations for Turners and Nonturners. With respect to the number and direction of turns, both groups displayed significant interrelationships between expected and observed angular responses. For Nonturners, decreasing correlations were obtained with higher path complexity (one turn:  $r(60) = .965$ ; two turns, sd:  $r(60) = .953$ ; two turns, od:  $r(52) = .865$ ,  $ps < .0001$ ). Standardized correlations coefficients of tunnels with one turn and tunnels with two turns bending into the same direction were found to be comparable, but both differed significantly from angular fit for tunnels with two opposite turns ( $ps < 0.005$ ). Turners displayed a similar declining pattern (one turn:  $r(60) = .967$ ; two turns, sd:  $r(60) = .935$ ; two turns, od:  $r(57) = .873$ , respectively,  $ps < .0001$ ; difference between 1 turn and 2 opposite turns:  $p < .0003$ )<sup>8</sup>.

### 3.3.3.4 Response Time

Analysis of response times revealed a significant main effect of Preferred Strategy [ $F(1, 16) = 8.921$ ,  $p < .010$ ,  $\eta_G^2 = .248$ ], as well as a significant interaction of Preferred Strategy  $\times$  Tunnel Layout [ $F(2, 32) = 4.758$ ,  $p < .016$ ,  $\eta_G^2 = .032$ ]. As can be seen from Figure 3.5, Nonturners retained a constant response time level throughout all complexity levels. Turners, by contrast, displayed slightly increasing mean response times with increasing complexity. However, *Holm-Bonferroni* adjusted post-hoc t-tests revealed this increase to be non-significant ( $ps > .129$ ). Mean response times of Turners and Nonturners differed significantly only for tunnels with two turns into the same direction ( $p < .003$ ).

---

<sup>8</sup> Correlation coefficients of Turners and Nonturners differed due to the differential exclusion of trials with side errors, arrowback reactions, and reaction slips. Some subjects produced either erroneous adjustment at individual eccentricities, resulting in missing correct values.

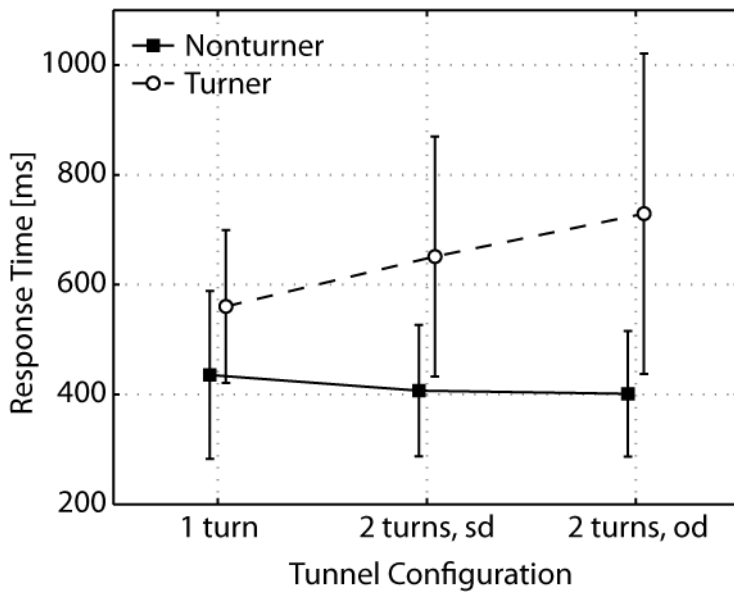


Figure 3.5: Experiment 1 – Mean RT ( $\pm 1$  SD, depicted by the error bars) of the adjusted homing vector for tunnels with one turn, two turns bending into the same direction (sd), and two opposite turns (od), separately for Nonturners (solid line, boxes) and Turners (dashed line, circles).

### 3.3.3.5 Absolute Error

The absolute error was significantly influenced by Tunnel Layout [ $F(1.41, 32) = 6.506, p < .011, \eta_G^2 = .148$ ], and Eccentricity of End Position [ $F(2, 32) = 62.52, p < .0001, \eta_G^2 = .344$ ]. Additionally, a significant interaction was found for Tunnel Layout  $\times$  Eccentricity of End Position [ $F(2.41, 32) = 15.001, p < .0001, \eta_G^2 = .176$ ], which was further analyzed with Holm-Bonferroni adjusted pairwise comparisons. As depicted in Figure 3.6, for tunnels with one turn and two turns bending into the same direction absolute error scores at the end position of  $45^\circ$  eccentricity differed significantly from absolute error scores at eccentricities of  $15^\circ$  and  $30^\circ$  (all  $p < .005$ ). For tunnels with two opposite turns, mean absolute error differed between all eccentricities (all  $p < .0002$ ).

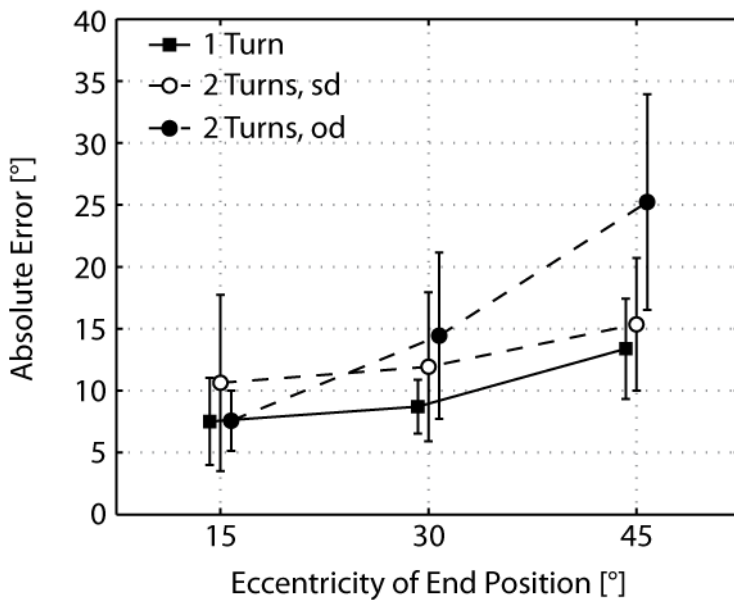


Figure 3.6: Experiment 1 – Mean absolute error ( $\pm 1$  SD, depicted by the error bars; solid line) of the adjusted homing vector at different eccentricities (sides were concatenated), separately for tunnels with one turn (solid line), two turns bending into the same direction (dashed line, open circles), and two opposite turns (dashed line, filled circles).

Absolute error scores for tunnels with one turn and tunnels with two turns bending into the same direction were comparable at all eccentricities. However, mean absolute error of tunnels with one turn and tunnels with two opposite turns differed at the end positions of 30° and 45° eccentricity ( $p < .002$ ), whereas differences between the two tunnel layouts with two turns were found only at the most eccentric end position of 45° ( $p < .003$ ).

### 3.3.3.6 Relative Error

Significant main effects on signed error scores were found for Tunnel Layout [ $F(2, 32) = 22.690, p < .0001, \eta_G^2 = .352$ ], as well as for Eccentricity of End Position [ $F(1.40, 30) = 89.555, p < .0001, \eta_G^2 = .300$ ]. Additionally, the interaction of Tunnel Layout  $\times$  Eccentricity of End Position showed a significant interaction [ $F(2.80, 64) = 13.037, p < .0001, \eta_G^2 = .077$ ] (see Figure 3.7). Subsequent post hoc tests revealed a comparable trend in signed error rates for all tunnel layouts, with decreasing values with increasing eccentricity of end position. For tunnels with one turn signed error scores differed significantly between the eccentricity of 15° and the more lateral end positions of 30° and 45° eccentricity ( $p < .0001$ ). For tunnel passages with two turns signed error scores differed at all tested eccentricities ( $p < .011$ ). This difference in signed error scores was even more pronounced for tunnels with two opposite turns ( $p < .00001$ ).

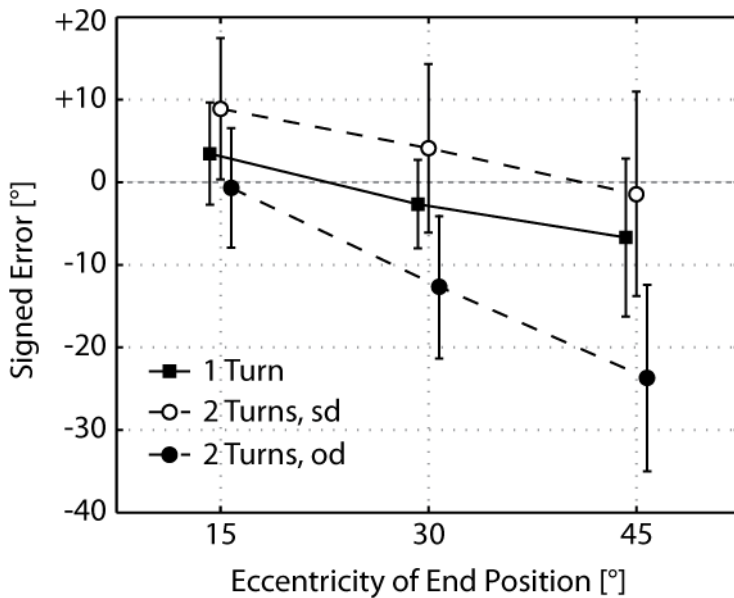


Figure 3.7: Experiment 1 – Mean signed error ( $\pm 1$  SD, depicted by the error bars) of the adjusted homing vector at different eccentricities (sides were concatenated), separately for tunnels with one turn (solid line), two turns bending into the same direction (dashed line, open circles), and two opposite turns (dashed line, filled circles).

Further, between the tunnel layouts signed error scores differed significantly at all eccentricities ( $p < .003$ ), except for the comparison between tunnels with one turn and two opposite turns at the innermost eccentricity of  $15^\circ$ , as well as between tunnels with one turn and two turns bending into the same side at  $45^\circ$  eccentricity.

### 3.3.4 Discussion

The aim of Experiment 1 was to determine the influence of pathway complexity in terms of overall length as well as number and direction of consecutive turns along an outbound path on homing accuracy and response latency of Nonturners and Turners, using an allocentric or an egocentric reference frame, respectively. Since the primitive parameters of the reference frames differ, it was of particular interest whether these were updated in a history-free or configurational manner, as measured on the basis of angular adjustments and response latencies.

Subjects were able to solve the task, as corroborated by the pronounced correlations between adjusted and expected arrow adjustment. Also, the absence of side effects proved egocentric and allocentric spatial representations to enclose right and left sides into a coherent representation space (Andersen, 1995; McNaughton et al., 1996). In several ways, the present experiment provided strong evidence for the rejection of history-free updating during visual path integration. Number and direction of successive heading changes as well as laterality of end position revealed an impact on measures of homing accura-

cy and latency, suggesting configural updating (Fujita et al., 1993) of distance and direction during visual path integration. This was the case for both strategy groups using either an allocentric or an egocentric reference frame. Absolute error scores indicated that Nonturners and Turners were more accurate at inner end positions as compared to more lateral end positions. This deterioration of accuracy was most pronounced for tunnels with two opposite turns ending at the outmost eccentricity, bearing resemblance to results of complexity-related increases of absolute error by Klatzky et al. (1990). With respect to the direction of error, specific patterns of under- and overestimations of eccentricity of end position were observed. Whereas inner end positions were overestimated, more lateral end positions were underestimated. Interestingly, only when traversing tunnels with one turn the mean of adjusted homing arrows corresponded to the mean of the presented eccentricities, suggesting that this configuration was encoded more or less correct. For paths of higher complexity, the mean of the adjusted values was shifted dependent on the relative direction of the second turn. Whereas eccentricities of tunnels with two turns bending to the same direction were overestimated, end positions of tunnels with opposite turns were underestimated. This linear shift only fits the encoding-error model of Fujita and colleagues (1993) under the assumption that encoding of incoming visuo-spatial information is not a context-independent process but, rather, that it takes the previously traversed paths into consideration. Therefore, encoding is additionally determined by expectations of the ‘average’ pathway pervading the encoding process in a top-down manner, as proposed by Klatzky et al. (1999).

Both strategy groups displayed comparable error patterns although the underlying primitive parameters should differ. For longer and more complex outbound paths configural updating implies an increase of elements that have to be stored (and updated) as the navigator proceeds. Comparable error scores might therefore indicate that Turners and Nonturners encode the same amount of elements along the outbound trajectory, supporting the assumption of qualitative equivalence of representation systems (Avraamides, Loomis, Klatzky, & Golledge, 2004b; Burgess, 2006; Mou et al., 2006). Therefore, it seems reasonable to assume that within allocentric and egocentric reference frames identical objects are chosen for constructing an enduring representation.

Response latencies were small overall, suggesting that updating of object bearings and distances was already accomplished during the passage (Riecke & Wiener, 2007). Importantly, Turners and Nonturners response latencies differed. Nonturners' response latency was found to be unaffected by pathway complexity, whereas Turners needed longer to initiate their homing response when paths contained more turns, particularly, when turns were bending into opposite directions. The complexity-related increase in response latency for Turners replicated results of Loomis et al. (1993). The update of multiple egocentric distances and directions within an egocentric reference frame is computationally more demanding as compared to the update of allocentric direc-

tions, since an increasing number of represented objects has to be updated with each successive step and rotation. Therefore, Turners might have taken longer to initiate the homing response since spatial relations within the egocentric reference frame had to be updated until the very end of the passage, whereas for Nonturners the spatial layout might have been already present during the last segment (Riecke & Wiener, 2007).

Difficulties with opposite turns also became manifest in side error scores, replicating findings on side errors for more complex pathways of Riecke & Wiener (2007). The question was where these side errors emerge from. Post-experimental interviews revealed that subjects experienced increased difficulties when traversing tunnels with two opposite turns, resulting in high ambiguity and uncertainty with respect to the side the homing arrow should point to. This stands in marked contrast to real-world navigation, where subjects can distinguish right and left turns easily, even with eyes closed (Cornell & Greidanus, 2006). Since both strategy groups displayed increasing side errors, it seems plausible to assume that side errors arose at information-processing stages common to Turners and Nonturners, e.g., during the uptake and encoding of visuo-spatial information, as suggested by the configural updating model of Fujita and colleagues (Fujita et al., 1993).

### 3.4 Experiment 2 – Same Direction

Based on the above described findings, Experiment 2 investigated the influence of reduced path complexity and more predictable layouts of outbound paths on homing accuracy based on egocentric or allocentric reference frames. Whereas the standard encoding-error model of Fujita et al. (1993) proposes that all paths are encoded independently of each other, the extended configural model of Klatzky et al. (1999) assumes that the spatial representation also comprises distinct expectancies of ‘average’ pathways for each complexity level that determine the encoding process. Experiment 2 was designed to explore homing accuracy and latency of Turners and Nonturners when traversing pathways of reduced variability. Based on the encoding-error model, we supposed a regression to an overall mean, as well as a deskew of signed error scores (i.e., more pronounced over- and underestimations) due to uncertainty and memory loss when confronted with longer and more complex trajectories. The extended configural model, by contrast, should have resulted in linearly shifted regression patterns on each complexity level, emerging from representation-based expectancies of the interrelations between paths of varying complexity.

### 3.4.1 Methods

#### 3.4.1.1 Participants

Nineteen male students recruited from the Ludwig-Maximilians-University Munich, Germany, participated in Experiment 2 (age ( $M \pm SD$ ) =  $23.74 \pm 3.62$  years). Participants were either paid 8€ per hour or received course credit for taking part in the experiment. The experiment followed the American Psychological Association's (APA's) Ethical Principles of Psychologists and Code of Conduct (American Association of Psychology, 2002). Out of a pool of 20 subjects, ten subjects categorized as Turners and nine subjects categorized as Nonturners were selected. One Nonturner was excluded from the analyses due to miscomprehension of the instructions. All subjects had normal or corrected to normal vision and reported no history of neurological disorder. All Turners were right-handed, one of the remaining nine Nonturners was left-handed.

#### 3.4.1.2 Task, Materials, and Procedure

The experimental environment was the same as described for Experiment 1. Prior to the main experiment subjects underwent the categorization task (selection of reference frame specific responses for Turners  $M \pm SD = 98.3\% \pm 0.02\%$  and Nonturners:  $M \pm SD = 97.1\% \pm 0.05\%$ ; correlation between Preferred Strategy and strategy-specific arrow choice:  $r(19) = .995$ ,  $p < .00001$ ). After a training of approximately 12 minutes the main experiment started.

#### **Main Experiment**

The main experimental session included 20 blocks á 9 tunnels with minor in-between breaks. The experimental procedure was identical to Experiment 1. Tunnels with one turn had five segments, with the two initial and two final straight segments enclosing the turning segment of varying angles. Tunnels with two turns had a total of nine segments (turns located in segments 3 and 7). For all tunnels with two turns the direction of consecutive turns was identical, i.e., a right turn was always followed by a second right turn (or left-left turning segments). After the outbound path presentation, participants had to adjust the homing vector to point directly back to the starting point (no time limit for adjustment). Since subjects were categorized a priori, in 10% of the trials feedback on their adjustment accuracy was displayed dependent on the preferred reference frame.

### 3.4.2 Results

#### 3.4.2.1 Side Error

Overall, only few side errors (less than 0.95% for all subjects) were observed. A mixed-design ANOVA on percentage of side errors revealed no significant effect for Preferred Strategy [ $F(1, 17) = 0.003$ ,  $p = .957$ ], Number of Turns [ $F(1,$

$17) = 1.021, p = .325]$ , or Eccentricity of End Position [ $F(2.08, 51) = 0.982, p = .387$ ].

### 3.4.2.2 Other Incorrect Solutions

In contrast to the previous experiment, no arrowback responses were registered in Experiment 2. Further, for the whole study set, 2 reaction slips were detected (approx. 0.06%).

### 3.4.2.3 Angular Fit

Correlations of observed angular response with strategy-specific expected angular response revealed significant interrelationships for both Nonturners,  $r(144) = .956, p < .0001$ , and Turners,  $r(220) = .923, p < .0001$ . However, standardized correlation coefficients of Turners and Nonturners differed significantly ( $p < .01$ ). When angular fit was computed separately for tunnels with one turn and two turns Nonturners revealed significant lower correlations between adjusted and expected angular response for more complex tunnels as compared to tunnels with only one turn (one turn:  $r(72) = .976$ ; two turns:  $r(72) = .937; ps < .0001$ ; difference between tunnels with one and two turns:  $p < .004$ ). Although Turners displayed a comparable declining pattern (one turn:  $r(80) = .950$ ; two turns:  $r(140) = .924; ps < .0001$ ), no statistically significant difference was found between tunnels with one and two turns ( $p = .129$ ) for this strategy group. The significant difference in angular fit between Turners and Nonturners was caused by angular responses for tunnels with one turn ( $p < .02$ )<sup>9</sup>.

### 3.4.2.4 Response Time

Analysis of response times revealed a significant main effect of Number of Turns [ $F(1, 17) = 10.125, p < .005, \eta^2_G = .016$ ] and a significant interaction of the factors Preferred Strategy  $\times$  Number of Turns [ $F(1, 17) = 8.432, p < .01, \eta^2_G = .013$ ]. Multiple comparisons revealed response time of Turners to be significantly increased when confronted with two turns ( $p < .008$ ), whereas Nonturners' response time was unaffected by the number of turns. Despite the significant interaction of strategy and path complexity, the difference between Turners and Nonturners' response times at both complexity levels was found to be comparable (see Figure 3.8).

---

<sup>9</sup> In case of consecutive turns bending into the same direction, cognitive headings of Turners and Nonturners were misaligned, so that for paths of higher complexity allocentric and egocentric eccentricities did not correspond. The computation of angular fit took this into consideration, resulting in a higher amount of categorical egocentric end positions for Turners ( $N = 10$  participants  $\times$  14 categorical egocentric eccentricities = 140) as compared to Nonturners ( $N = 9$  participants  $\times$  8 categorical allocentric eccentricities = 72).

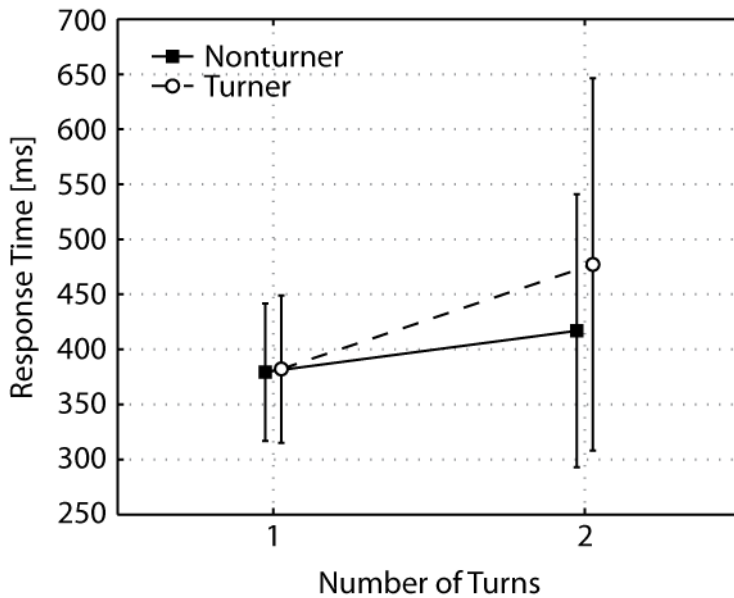


Figure 3.8: Experiment 2 – Mean RT ( $\pm 1$  SD, depicted by the error bars) of the adjusted homing vector for tunnels with one turn and two turns, separately for Nonturners (solid line) and Turners (dashed line).

### 3.4.2.5 Absolute Error

The analysis of absolute error revealed a significant main effect of Eccentricity of End Position [ $F(1.75, 51) = 34.486, p < .0001, \eta_G^2 = .246$ ], as well as a significant interaction Preferred Strategy  $\times$  Eccentricity of End Position [ $F(1.75, 51) = 4.907, p < .02, \eta_G^2 = .046$ ]. These effects were qualified by the interaction Preferred Strategy  $\times$  Number of Turns  $\times$  Eccentricity of End Position [ $F(1.70, 51) = 4.506, p < .023, \eta_G^2 = .060$ ] (see Figure 3.9). For tunnels with one turn, subsequent post-hoc tests revealed only for Nonturners significant differences in absolute error scores between end positions of  $15^\circ$  and  $30^\circ$ , as well as between  $15^\circ$  and  $45^\circ$  eccentricity ( $p < .001$ ). This strategy group also displayed differing absolute error scores for paths of higher complexity, between  $30^\circ$  and  $45^\circ$  eccentricity ( $p < .001$ ). However, Nonturners' absolute error scores did not differ between complexity levels. By contrast, absolute error scores of Turners were shown to be comparable both within as well as between complexity levels. Also, differences between absolute error scores of Turners and Nonturners were too weak to obtain statistical significance.

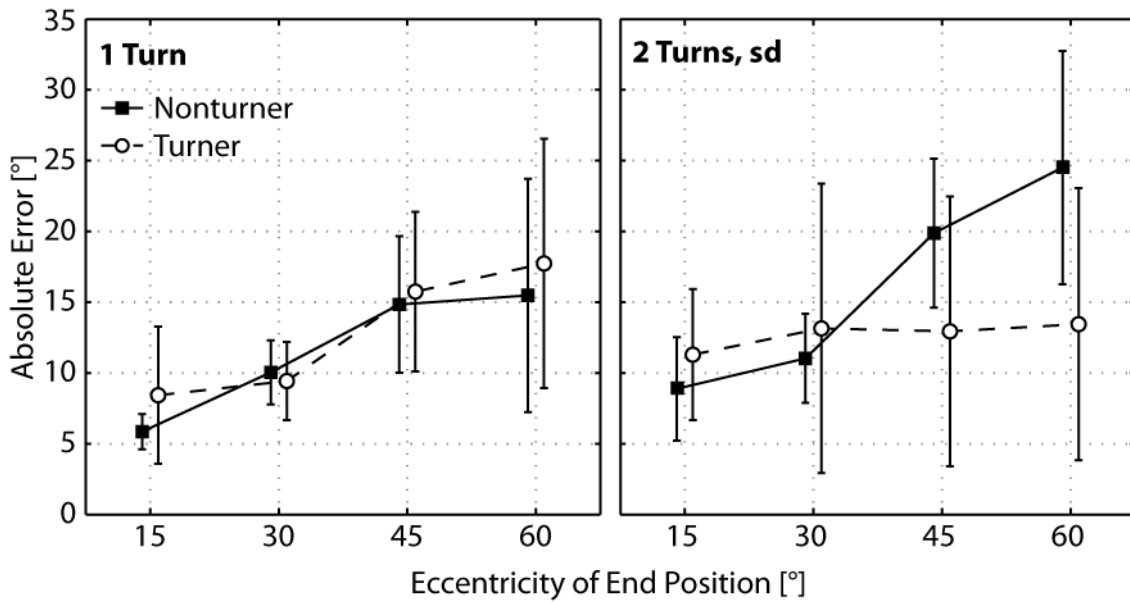


Figure 3.9: Experiment 2 – Mean absolute error ( $\pm 1$  SD, depicted by the error bars) of the adjusted homing vector for tunnels with one turn and two turns, dependent on the eccentricity of end position relative to the origin of the path (data from left and right turn values of equal eccentricities were pooled), separately for Nonturners (solid line) and Turners (dashed line).

### 3.4.2.6 Relative Error

The analysis of relative errors revealed a significant main effect of Strategy [ $F(1, 17) = 13.086, p < .002, \eta_G^2 = .224$ ], and Eccentricity of End Position [ $F(1.29, 51) = 27.629, p < .0001, \eta_G^2 = .175$ ]. Further, statistical significance was obtained for the interaction of Preferred Strategy  $\times$  Number of Turns [ $F(1, 17) = 5.290, p < .034, \eta_G^2 = .056$ ], as well as Preferred Strategy  $\times$  Eccentricity of End Position [ $F(1.29, 51) = 7.532, p < .008, \eta_G^2 = .058$ ]. These effects were qualified by the interaction of Preferred Strategy  $\times$  Number of Turns  $\times$  Eccentricity of End Position [ $F(2.14, 51) = 13.767, p < .0001, \eta_G^2 = .064$ ] (see Figure 3.10).

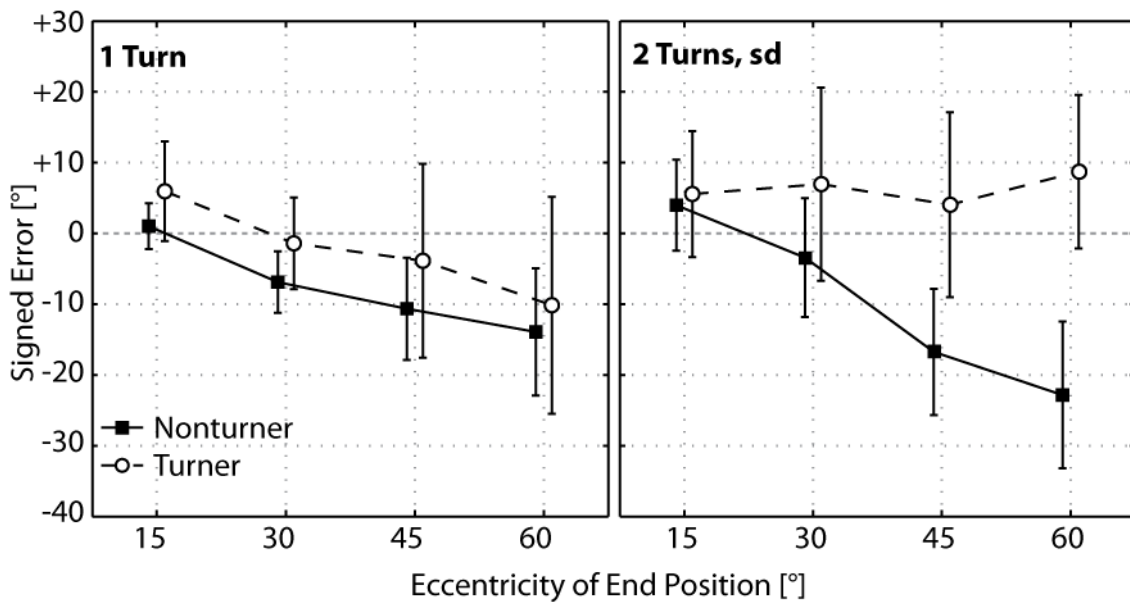


Figure 3.10: Experiment 2 – Mean signed error ( $\pm 1$  SD, depicted by the error bars) of the adjusted homing vector for tunnels with one turn and two turns, dependent on the eccentricity of end position relative to the origin of the path (turns of equal eccentricity to the left and right were pooled), separately for Nonturners (solid line) and Turners (dashed line).

Post-hoc tests found no significant differences between strategy groups traversing tunnels with one turn. Turners as well as Nonturners tended to underestimate the eccentricity of end position with increasing eccentricity. Nonturners' signed error rates for tunnels with one turn were found to differ significantly between eccentricities of 15° vs. 30°, as well as marginally between 15° vs. 60° eccentricity ( $p < .0001$ ). For Turners traversing tunnels with one turn, the difference between end positions of 45° vs. 60° eccentricity obtained statistical significance ( $p < .001$ ). When confronted with two turns, only Nonturners showed a more pronounced underestimation of end position at more lateral eccentricities, with signed error at the end position of 60° eccentricity differing significantly from the other end positions ( $p < .0006$ ). Further, signed error at 45° differed significantly from error rates at 15° and 30° eccentricity ( $p < .0002$ ). By contrast, Turners' relative error scores for tunnels with two turns were found to be comparable at all eccentricities. At the outmost eccentricities of 45° and 60°, Turners and Nonturners differed significantly in signed error scores ( $p < .0009$ ).

### 3.4.3 Discussion

The aim of Experiment 2 was to further elaborate findings of Experiment 1 regarding the influence of path complexity on the accuracy of the resultant spatial representation. Tunnels had either one turn or two turns bending into the same direction. Of particular interest was whether Turners' and Nonturners' responses were based on representations of the pathway that were updated continuously (history-free) or intermittent (configural).

The results of Experiment 2 indicated that Turners and Nonturners were generally able to solve the task by building up and utilizing a representation of the traversed outbound path. The existence of only few side errors at the tested complexity levels replicated findings of Experiment 1. Also, angular fit proved that subjects were not only able to coarsely distinguish between tunnels ending at the left or right side, but also to accurately adjust the homing vector according to the eccentricity of end position (Gramann et al., 2005). However, in contrast to Experiment 1, angular fit of Turners and Nonturners differed for tunnels with one turn, primarily attributable to the more pronounced within-group variations in angular adjustments for Turners at more lateral eccentricities.

For tunnels with one turn, both strategy groups resembled the findings of Experiment 1, with overestimations of inner and underestimations of more lateral eccentricities, suggesting configural updating of self-to-object relations along the outbound path (Fujita et al., 1993). The confrontation with more complex pathways resulted in strategy-specific error patterns. Mirroring the results of Experiment 1, updating of primitive parameters for Nonturners was accomplished in configural mode, as indicated by the regression tendencies. Turners, by contrast, were hardly affected by the increased pathway complexity.

However, there was pronounced within-group variation that could not be explained solely based on the assumptions of the encoding-error model. At this point it might be of importance that eccentricity of end position was defined within the allocentric reference system. Due to the symmetric layout of tunnels with one turn (2 straight segments, a curved segment, and another 2 straight segments) end positions could easily be transferred from allocentric to egocentric coordinates by simply changing of sign (due to the transformation rules depicted in Figure 1, a tunnel ending at  $30^\circ$  eccentricity in allocentric coordinates ended at  $-30^\circ$  eccentricity in egocentric coordinates; turning angle of  $60^\circ$ ). However, in the present experiment this straightforward transformation was not possible for tunnels with two turns, since the angular sum did not double the absolute eccentricity, and eccentricities were not symmetrical (In Experiment 1, they were symmetrical). Therefore, slight changes in the tunnel configurations resulted in pronounced changes of eccentricity within an egocentric reference frame, e.g., the allocentric eccentricity of  $30^\circ$  with two turns of  $34^\circ$  and  $14^\circ$  angle, respectively, corresponded to an *egocentric eccentricity* of  $30^\circ - (34^\circ + 14^\circ) = -18^\circ$ . Based on this computation, the virtual space covered by tunnels with two turns was seemingly reduced for Turners (absolute categorical end positions ranging from  $15^\circ$  to  $30^\circ$  eccentricity) as compared to Nonturners (ranging from  $15^\circ$  to  $60^\circ$ ). The pronounced variation in Turners' signed error scores might therefore be attributed to the fact that various tunnels of different angular constellations could end at the very same egocentric end position, whereas in allocentric coordinates these tunnels were clearly distinguishable.

Re-analysis of signed error scores for the ten Turner subjects with respect to the transformed egocentric eccentricities of tunnels with two turns was accomplished by means of a repeated-measures ANOVA with *Number of Turns* (1 turn vs. 2 turns), and *Eccentricity of End Position* ( $15^\circ$  vs.  $30^\circ$ ), as the within-subject factors. Analysis revealed a significant main effect of Eccentricity of End Position [ $F(1, 9) = 15.864$ ,  $p < .003$ ,  $\eta_G^2 = .638$ ].

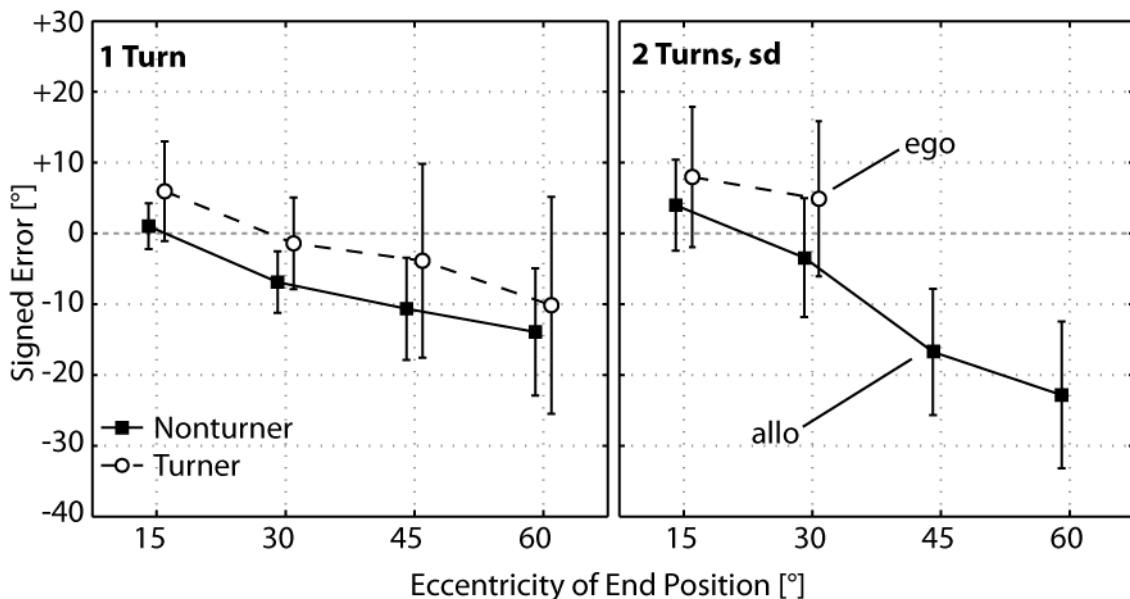


Figure 3.11: Experiment 2 – Mean signed error ( $\pm 1$  SD, depicted by the error bars) of the adjusted homing vector for tunnels with one turn and two turns. Due to the tunnel layout, allocentric and egocentric eccentricities for tunnels with two turns did not correspond. Therefore, tunnels with two turns ended at categorical egocentric end positions of  $15^\circ$  and  $30^\circ$ , respectively.

Although this re-analysis could be interpreted as evidence for a putative history-free spatial updating process for Turners traversing tunnels with two turns, their increasing response latencies for more complex tunnels disqualifies this assumption (Loomis et al., 1993; Loomis et al., 1999b). Additionally, signed error scores of tunnels with one and two turns corresponded at  $15^\circ$  and  $30^\circ$ , supporting the presence of a standard configural updating as proposed by Fujita et al. (1993), independent of the number of turns or overall length. Instead of building up different ‘average paths’ at each complexity level, Turners merged both configurations into a global representation, with eccentricities of end position being of higher impact on over- and underestimation tendencies as compared to the tunnel configuration itself.

This assumption might also have qualified for Nonturners. Although non-significant, the slightly amplified regression (more pronounced over- and underestimations) for paths of higher complexity corresponds to the assumptions of the standard encoding-error model of Fujita and colleagues (1993). In their model, errors during the encoding phase emerge from increased ambiguity

and memory loss, therefore the encoding is primarily based on expectancies instead of the actual stimulation values. However, if errors emerge solely based on encoding processes, they should appear to a comparable amount at all complexity levels. All values larger than the represented overall mean are underestimated, whereas smaller values are overestimated. Particularly at the outmost eccentricity, Nonturners were seemingly affected by the increase in complexity. In an egocentric reference frame, traversing tunnels with two turns resulted in less pronounced changes in the represented environment, i.e., an orientation change resulted in only gradual changes when updating the object array. For Nonturners, by contrast, the tunnel course of tunnels ending more laterally bent away from the allocentric reference direction. Therefore, an update of allocentric heading might have been cognitively more demanding (Klatzky, 1998). Avraamides and colleagues (2004a) suggested that interferences in triangle-completion tasks arise from modality incongruence during encoding and retrieval of spatial knowledge. Due to their account, spatial knowledge can be acquired based on passive viewing of virtual outbound trajectories, although the navigator is at all times located in a stationary position. Therefore, subjects update their cognitive heading whereas the perceptual heading remains identical throughout the passage. Since cognitive and perceptual headings spread apart with increasing rotation, larger turns resulted in increased cognitive load (e.g., Farrell & Robertson, 1998), becoming manifest in decreased homing accuracy (Presson & Montello, 1994; Rieser, 1989).

These results did not correspond to findings of Experiment 1, where subjects apparently based their homing response on a representation-based expectation of an average path for each complexity level. Instead, Turners and Nonturners merged both complexity levels on the representational level, and categorized the tunnels primarily based on their eccentricity instead of their layout, i.e., overall length or number of turns, resulting in an overall compression of the response range (Fujita et al., 1993; Loomis et al., 1993; Wiener & Mallot, 2006). This seems plausible, since curved segments of tunnels with two turns always bent into the same direction. Despite the straight inter-turn segments subjects might have interpreted the two curves as a single curve turning gradually, in order to reduce cognitive load. Since navigators in Experiment 1 were confronted with multiple, and unpredictably varying complexity levels, this strategy might not have been appropriate. However, the question was whether the findings of Experiment 2 could be replicated when participants traversed tunnels with one turn and two opposite turns of equal angularity.

### 3.5 Experiment 3 – Opposite Directions

The use of tunnels with two complementary turns of similar angularity results in parallel start- and end segments with identical return bearings for Turners and Nonturners. This configuration was supposed to be of higher complexity

as compared to Experiment 2, since with each change in heading direction egocentric return bearings as well as self-to-object bearings have to be rotated to opposing sides with respect to the navigator's intrinsic axis of orientation. For example, when Turners traverse a turn to the right side, the relative position of the starting point (and the direction of the homing arrow) changes to the right. An additional, consecutive turn to the left causes Turners' homing arrow to pass the sagittal axis of the navigator from the right to the left side. By contrast, Nonturners traversing the described tunnel configuration should maintain an allocentric bearing throughout the passage that always points to their left.

### 3.5.1 Methods

#### 3.5.1.1 Subjects

Eighteen male subjects recruited from the Ludwig-Maximilians-University Munich, Germany, took part in Experiment 3 (age ( $M \pm SD$ ) =  $25.60 \pm 3.42$  years). The experiment followed the American Psychological Association's (APA's) Ethical Principles of Psychologists and Code of Conduct (American Association of Psychology, 2002). Participants were either paid 8€ per hour or received course credit for taking part in the experiment. Ten subjects were categorized as Turners and eight subjects were categorized as Nonturners prior to the main experiment. All subjects had normal or corrected to normal vision and reported no history of neurological disorder. None of the Turners and three Nonturners were left-handed.

#### 3.5.1.2 Task, Materials, and Procedure

The experimental environment was the same as reported for Experiment 1. Prior to the main experiment subjects underwent the categorization task (strategy specific homing selection for Turners  $M \pm SD = 94.6\% \pm 0.05\%$  and Nonturners:  $M \pm SD = 96.3\% \pm 0.05\%$ ; correlation between Preferred Strategy and strategy-specific arrow choice:  $r(18) = .997$ ,  $p < .00001$ ). After a brief training the main experiment started.

#### **Main Experiment**

The main experimental session included 20 blocks á 9 tunnels with minor in-between breaks. The experimental procedure was identical to Experiment 1. Tunnels with one turn had five segments, with the two initial and two final straight segments enclosing the turning segment of varying angles. Tunnels with two turns had a total of nine segments (turns located in segments 3 and 7). After the outbound path presentation, participants had to adjust the homing vector to point directly back to the starting point (no time limit for adjustment). Since subjects were categorized a priori, in 10% of the trials feedback on their adjustment accuracy was displayed dependent on the preferred reference frame.

## 3.5.2 Results

### 3.5.2.1 Side Error

In Experiment 3, a total of 105 side errors were registered (approx. 4.86% of all trials) revealing a significant main effect of the layout of outbound paths [ $F(1,16) = 6.984$ ,  $p < .018$ ,  $\eta_G^2 = .138$ ]. Subjects committed side errors exclusively when traversing tunnels with two opposite turns ( $M \pm SD = 9.63\% \pm 14.83\%$ ), equally distributed over all end positions ( $15^\circ$  vs.  $30^\circ$  vs.  $45^\circ$ : 41 vs. 30 vs. 33 side errors, respectively). There were no main effects or interactions including the factor Strategy.

### 3.5.2.2 Other Incorrect Solutions

#### *Arrowback Responses*

For some of the tunnels with two opposite turns, four participants (3 Turners, 1 Nonturner) demonstrated arrow back responses adjusting the homing vector to point back more or less  $0^\circ$  (relative arrowback reactions for these 4 subjects: 1 turn: no arrowback responses; two turns:  $M \pm SD = 3.89\% \pm 3.06\%$ ; Range: 0.00% - 13.33%). Due to the small number of subjects displaying arrowback responses, no statistics could be applied.

### 3.5.2.3 Angular Fit

Angular responses correlated with strategy-specific expected angular responses significantly for both Nonturners,  $r(96) = .930$ ,  $p < .0001$ , and Turners,  $r(120) = .892$ ,  $p < .0001$ . In contrast to Experiment 2, correlations of Turners and Nonturners were found to be comparable. Taking the number of turns into account, both groups displayed significant interrelationships between expected and observed angular responses. For Nonturners, significantly decreasing correlations were obtained for tunnels with one and two turns ( $r_s(48) = .968$  and  $.895$ , respectively,  $p < .0001$ ; one vs. two turns:  $p < .003$ ). Turners displayed a comparable declining pattern with significant correlation for tunnels with one and two turns ( $r(60) = .951$  and  $r(60) = .899$ , respectively,  $p < .0001$ ; difference between the outbound paths:  $p < .04$ ).

### 3.5.2.4 Response Time

Response times were marginally affected by the Number of Turns [ $F(1, 16) = 4.386$ ,  $p = .053$ ,  $\eta_G^2 = .008$ ], with  $M \pm SD = 399.16 \text{ ms} \pm 98.98 \text{ ms}$  for tunnels with one turn vs.  $M \pm SD = 432.19 \text{ ms} \pm 136.72 \text{ ms}$  for tunnels with two turns, respectively. However, there were no main effects or interactions involving the factor Strategy [ $F(1, 16) = 1.626$ ,  $p = .220$ ], or Eccentricity of End Position [ $F(2, 32) = 1.260$ ,  $p = .297$ ].

### 3.5.2.5 Absolute Error

The absolute error showed a significant influence of Number of Turns [ $F(1, 16) = 22.273, p < .0001, \eta_G^2 = .161$ ]. Additionally, absolute errors were significantly influenced by Eccentricity of End Position [ $F(1.40, 32) = 41.594, p < .0001, \eta_G^2 = .402$ ], as well as an interaction of Number of Turns  $\times$  Eccentricity of End Position [ $F(1.40, 32) = 11.643, p < .001, \eta_G^2 = .153$ ], and an interaction of Preferred Strategy  $\times$  Eccentricity of End Position [ $F(1.40, 32) = 4.540, p < .033, \eta_G^2 = .073$ ]. Multiple comparisons revealed absolute error scores to be significantly higher at the outmost end position of  $45^\circ$  eccentricity as compared to eccentricities of  $15^\circ$  and  $30^\circ$ , respectively (all  $p < .005$ ) for tunnels with one turn. This difference between  $45^\circ$  and  $15^\circ/30^\circ$  eccentricity was even more pronounced for tunnels with two turns ( $p < .0001$ ). Therefore, absolute error scores of tunnels with one and two turns were comparable at the inner end positions, but differed at end position of  $45^\circ$  eccentricity ( $p < .0001$ ; see Figure 3.12).

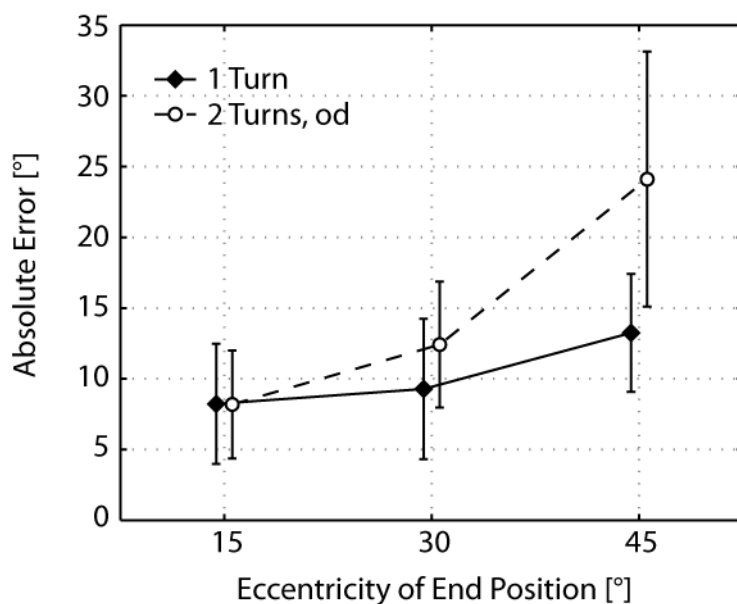


Figure 3.12: Experiment 3 – Mean absolute error ( $\pm 1$  SD, depicted by the error bars) of the adjusted homing vector for tunnels with one turn (solid line, closed diamonds) and two turns (dashed line, open circles), dependent on the eccentricity of end position relative to the origin of the path (sides were concatenated), averaged over Nonturners and Turners.

Nonturners' absolute error scores at  $45^\circ$  eccentricity differed significantly from  $15^\circ$  and  $30^\circ$ , respectively ( $p < .005$ ). For Turners, significant differences were found between all eccentricities ( $p < .004$ ). Although the interaction of Preferred Strategy and Eccentricity of End Position was found to be significant, post-hoc tests revealed no significant pairwise differences in mean absolute error scores between the strategy groups.

### 3.5.2.6 Relative Error

Signed error scores revealed significant main effects of Preferred Strategy [ $F(1, 16) = 4.877, p < .046, \eta^2_G = .082$ ], Number of Turns [ $F(1, 16) = 22.173, p < .0002, \eta^2_G = .290$ ], and Eccentricity of End Position [ $F(1.20, 32) = 83.456, p < .0001, \eta^2_G = .455$ ]. Additionally, the interaction of Number of Turns  $\times$  Eccentricity of End Position was found to be significant [ $F(1.42, 32) = 13.113, p < .0005, \eta^2_G = .102$ ]. Turners showed more pronounced underestimations of eccentricity of end position as compared to Nonturners ( $M \pm SD = -7.47^\circ \pm 3.56^\circ$  vs.  $M \pm SD = -2.89^\circ \pm 5.23^\circ$ , respectively). Additionally, multiple comparisons revealed declining errors at both complexity levels with higher eccentricity of end position ( $p < .002$ ), except for the comparison between  $15^\circ$  and  $30^\circ$  eccentricity for tunnels with one turn ( $p = .05$ ; see Figure 3.13). Finally, at all tested eccentricities errors for tunnels with two turns were significantly lower as compared to tunnels with one turn ( $15^\circ$ :  $p < .024$ ;  $30^\circ$  and  $45^\circ$ :  $p < .001$ ).

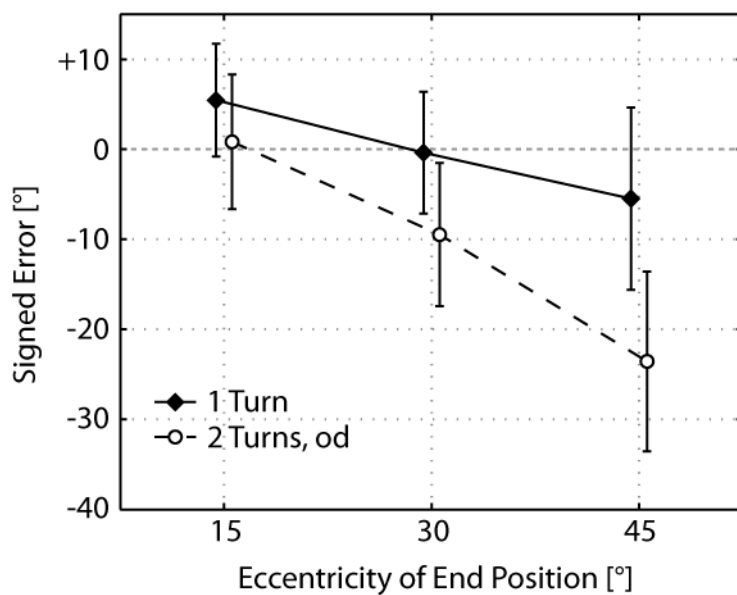


Figure 3.13: Experiment 3 – Mean signed error ( $\pm 1$  SD, depicted by the error bars) of the adjusted homing vector for tunnels with one turn (solid line) and two turns (dashed line), dependent on the eccentricity of end position relative to the origin of the path (sides were concatenated), averaged over Nonturner and Turner subjects.

### 3.5.3 Discussion

The results of Experiment 3 complemented and extended the results of the previous experiments, suggesting that paths with turns into opposite directions are more difficult to update as indicated by the increasing number of side errors. However, the reduction in complexity levels as compared to Experiment 1 might have accounted for less side errors.

In accordance with the extended encoding-error model of Klatzky et al. (1999), errors were not only caused by bottom-up encoding but also by representation-based expectations that biased the information uptake. Whereas tunnels with one turn, on average, were encoded more or less precisely (the mean of adjusted values corresponded to the mean of presented values), tunnels with two opposite turns were generally underestimated, as indicated by the complexity-related shift in signed error scores towards more pronounced underestimation. This result replicated the findings of Experiment 1. Turners and Non-turners might have resorted to a pathway model (Klatzky et al., 1999), preserving spatial relations that moderated the encoding of path segments and turns (Golledge, 1995). In contrast to Experiment 1, not only Turners but also Non-turners displayed an increase in response latencies as path complexity increased. This result seemingly contradicted findings of Loomis et al. (1993). However, overall effects were rather weak and might be attributed to differences in the participant population.

Taken together, when traversing tunnels with one turn and two opposite turns, primitive parameters of both Turners and Nonturners were updated in a configural fashion. Based on sensory experience, they might have built up distinct path models for less complex and more complex trajectories. Additionally, the data suggested that these representations were set in relation to each other, with end positions of tunnels with one turn serving as ‘standard’ for the calibration of more complex pathways (Klatzky et al., 1999). Comparable response latencies and error tendencies further suggest that egocentric and allocentric reference frames were applied in parallel, in accordance with conceptualizations of co-existing egocentric and allocentric spatial representations (Burgess, 2006; Gramann et al., 2005).

### 3.6 Behavioral Data – General Discussion

The present study investigated differences in homing accuracy based on egocentric or allocentric reference frames by systematically varying the complexity of virtual outbound paths. We asked whether visual path integration of the strategy groups was based on *history-free updating* (Müller & Wehner, 1988, 2007) or *configural updating* as initially proposed by the encoding-error model of Fujita and colleagues (1993). To the author’s knowledge, this was the first study on egocentric and allocentric path integration applying a virtual homing task with naturally bounding curves instead of on-spot rotations (Klatzky, 1998; Klatzky et al., 1990; Loomis et al., 1993; Riecke & Wiener, 2008; Wiener & Mallot, 2006). Additionally, this was the first study on complexity effects during visual path integration taking into consideration individual proclivities for coding space within a (body-centered) egocentric, or an (environment-centered) allocentric reference frame. Since configural updating implies that the path integration process is independent of path complexity, the homing task should

have been afflicted only with random error. In contrast, configural updating suggests that not only the configuration of the currently encoded path influences homing responses but also that expectations based on the history of previously traversed outbound paths impacts sensory integration during spatial updating. These experiences are assumed to reside in the representational system and are retrieved for encoding. Therefore, encoding would be context-dependent with the history of presented outbound paths influencing homing responses and latencies.

### 3.6.1 Configural Updating of Primitive Parameters

Based on the current findings, path integration is unlikely based on history-free updating processes, even when path complexity is unpredictably varying. Rather, path integration during outbound pathways of varying complexity seems to be based on configural updating processes including reference-frame specific primitive parameters (Klatzky, 1998). The history of traversed pathways serves as a basis for estimating the origin of the current passage (Peruch et al., 2005; von der Heyde, Riecke, Cunningham, & Bülthoff, 2000). Regarding the difference between the *standard* (Fujita et al., 1993) and the *extended configural model* (Klatzky et al., 1999), our results suggest that the different models explain behavioral performance to different degrees dependent on the reference frame used as well as the complexity of outbound paths.

The standard encoding-error model of Fujita and colleagues (1993) assumes errors to arise during sensory uptake and encoding of spatial information. Therefore, each outbound path is supposed to be encoded independently of other pathways in an ‘object-centered’ representation (Klatzky et al., 1999). By contrast, the extended configural model assumes that navigators build up a representation in which several pathways are interrelated, e.g., by assuming that all paths arise from a common starting point. In this case, encoding is mediated by the comparison of the current path’s configuration with respect to the distances and turning angles of the previously traversed trajectories. Based on previous experience the navigator might build up expectations regarding the layout of the traversed pathway (Cornell, Heth, & Skocylas, 1999). Navigators refer to these prototypical expectations whenever navigation may become too challenging, resulting in ambiguities regarding the layout of the traversed trajectory. Klatzky and colleagues (1999) assumed that in these cases the navigator resorts to an internal path model, a simplified ‘average path’.

In Experiment 1, where participants were confronted with multiple complexity levels, these ambiguities were associated with increasing side errors as well as inaccurate homing responses for paths with turns into opposite directions. This pattern supports the assumption that a more elaborated representation of pathways was computed comprising significant characteristics such as the number and direction of subsequent heading changes along different pathways. Fujita et al. (1993) suggested that participants’ angular responses might be characterized as compromise between presented and represented values

due to sensory noise, memory loss, and subjective awareness of lack of knowledge. In this case, the regression tendency should have been more pronounced the less effective information was encoded. However, signed error scores provided evidence for an *extended* configural updating. Tunnels were not encoded in a discrete manner, but were categorized due to the respective complexity levels (Klatzky et al., 1999). Turners and Nonturners built up representation-based expectancies incorporating a complexity-dependent ‘average path’, resulting in an overestimation of under-average pathways and an underestimation of over-average pathways (Lathrop & Kaiser, 2005).

When variability of complexity was reduced to tunnels with one and two turns bending into the same direction, Turners and Nonturners displayed distinctive regression patterns. Whereas Turners generally overestimated end positions for tunnels with two turns, Nonturners’ angular responses were primarily underestimations. However, based on the premises of models based on configural updating (Fujita et al., 1993; Klatzky et al., 1999), Turners and Nonturners did not apply separate average paths for each complexity level but rather encoded all tunnels with respect to their eccentricity of end position. Therefore, the response was primarily determined by the actual value of the end position (within an allocentric or an egocentric reference frame, respectively), and not by the number of turns. Interestingly, when turns bent into opposite directions, Turners and Nonturners again displayed comparable error patterns, resembling results of Experiment 1. Taken together, homing errors of both strategy groups were comparably affected by path complexity, mirroring and further extending results of previous tunnel studies (Gramann, 2002; Gramann et al., 2005; Gramann et al., 2006; Riccobon, 2007). Therefore, the present study accentuates the stability of the egocentric and allocentric reference frame even when confronted with multiple, unpredictably varying complexity levels.

### **3.6.2 Co-Existence of Egocentric and Allocentric Representations**

Turners’ response latencies grew linearly with increasing pathway complexity, bearing resemblance to triangle completion studies with blindfolded subjects (e.g., Loomis et al., 1993) and recent path integration studies in virtual environments (e.g., Riecke & Wiener, 2007). These differences might be linked to the updating of distinct primitive parameters within different reference frame. However, although the number of elements that have to be stored within an egocentric and an allocentric reference frame might be comparable, the representations might differ when the objects (i.e., the locations of turns along the pathway) have to be computed relative to the position (and orientation) of the navigator. Within an egocentric reference frame, these egocentric bearings have to be updated until the very end of the passage, whereas within an allocentric reference frame only the position (but not the orientation) of the navigator changes within stationary surroundings (Burgess, 2006; Klatzky, 1998; Klatzky & Wu, 2008). Therefore, Turners might have taken longer to initiate

the homing response, whereas Nonturners responded equally fast at all complexity levels.

Due to the first-person perspective of the incoming information path integration might be accomplished primarily based on an egocentric reference frame, with the primitive parameters of the egocentric locational representation subsequently transferred into an allocentric reference frame. Such a re-computation would be associated with increased response latencies as well as higher variability in homing responses. This was clearly not the case. Nonturners responded as fast as Turners and produced no additional errors or higher variance in homing responses. Rather, the data support the assumption that allocentric and egocentric reference frames co-exist in parallel as implied by neuropsychological investigations (Aguirre & D'Esposito, 1999; Burgess, 2006; Burgess et al., 2004; Byrne et al., 2007; Hartley et al., 2003; Mou et al., 2004; Redish, 1999; Sholl, 2001) and, more specifically, by recent neuropsychological investigations using the tunnel paradigm (Gramann et al., 2006; Gramann et al., submitted; Seubert et al., 2008).

### **3.6.3 Conclusions and Upcoming Steps**

The present results demonstrate that the complexity of an outbound path influences homing accuracy of subjects using distinct reference frames beyond the current outbound trajectory. Importantly, the use of distinct reference frames to build up a spatial representation and to maintain action-relevant information is influenced by path complexity to different extents. This demonstrates the necessity to incorporate individual strategies and the use of controlled paradigms to investigate the cognitive and neuropsychological basis of spatial navigation.

The following section will address if the comparable behavioral performance is also mirrored in terms of comparable cortical processes during encoding and retrieval of spatial information. Additionally, future research has to address how – additionally to directional estimations – distances are updated along the tested outbound pathways in order to gain further insights into mechanisms coding for the layout of the pathway. Also it would be of advantage if subjects were able to actively reproduce the traversed pathway, mirroring the retracing task of Loomis et al. (1993).

## Chapter 4

# Electroencephalographic Analyses

### 4.1 Abstract

Two experiments investigated the impact of path complexity on macroscopic brain dynamics of subjects preferring to use an egocentric (Turners) or an allocentric (Nonturners) reference frame during spatial navigation. Participants had to keep up orientation during visual presentation of 3D rendered desktop-simulated tunnel passages containing either one turn or two turns into the same direction (Experiment 1), or one turn or two turns of equal angularity bending into opposite directions (Experiment 2). At the end of a passage participants indicated their momentary position relative to the starting point ('point-to-origin'). High-density electroencephalographic (EEG) activity was recorded continuously during the passage as well as the homing vector adjustment phase and decomposed by Independent Component Analysis (ICA). Subsequently, generator sources of EEG activity were spatially localized within the cortical domain. Turners were found to encode spatial information primarily within occipito-parietal cortices subserving the egocentric reference frame, whereas Nonturners displayed more pronounced activation within the ventral pathway (allocentric reference frame), as well as in retrosplenial cortex, the transition zone between reference systems. With increasing path complexity, both Turners and Nonturners displayed increased frontal midline theta activity. Results suggest that human path integration is configural in nature, as reflected by differential brain dynamics during encoding of straight segments and curves, even in higher cortical areas. These findings extend and elaborate results of functional brain imaging studies on spatial navigation and highlight the need for considering individual proclivities when investigating physiological signatures of human navigation performance.

## 4.2 Introduction

Spatial navigation, constituting a sub-category of spatial cognition, denotes the capacity to plan and execute goal-directed paths (Gallistel, 1990) based on the computation, maintenance, and utilization of distinct but interacting internal representations of the environment. Following Klatzky (1998), these representations comprise the locations of threats, rewards, and other agents and their spatial relations, as well as one's own position with respect to the represented entities. However, representing the spatial structure of complex environments and self-to-object relations is impossible without establishing a reference frame, i.e., a mental coordinate system within which incoming spatial information is encoded and representational parameters are updated as the navigator moves (Grush, 2000; Klatzky, 1998; Miller & Allen, 2001; Mou & McNamara, 2002; Mou et al., 2004).

### 4.2.1 Path Integration

The methods utilized for integrating spatial cues vary with the richness of the environmental array. Whenever landmarks (i.e., distinct, stationary and salient objects or cues) are present, the navigator might resort to *piloting (position-based navigation)*, denoting the updating of one's position and orientation based on the calibration of the current view with an external or internally stored map of the surroundings (Etienne et al., 1999; Golledge, 1999b; Hunt & Waller, 1999). However, in absence of landmarks, e.g., during heavy fog or in darkness, this technique is not applicable. Interestingly, even in these situations, humans, like other mobile animals, are still able to infer information regarding their current position (and orientation). This is achieved by *path integration*, i.e., the continuous integration of local translations and rotations from movement cues without necessitating a map (Biegler, 2000; Etchamendy & Bohbot, 2007; Etienne et al., 1998; Loomis et al., 1999b; Mittelstaedt & Mittelstaedt, 1982; Tversky, 1993).

Under natural conditions, a wide range of external (*allothetic*) and internal (*ideothetic*) movement cues are available, with the former covering skylight polarization or geographical slant (Restat et al., 2004; Wehner, 2003), and the latter arising from various sensory modalities, including proprioceptive (Chance et al., 1998), kinesthetic (Waller & Greenauer, 2007), and vestibular systems (Glasauer et al., 2002; Peruch et al., 2005; Yardley & Higgins, 1998). In order to disentangle the specific contributions as well as interactive effects of internal and external movement cues on the accuracy of the path integration process, virtual environments (VE) have received increasing attention in the field of research on spatial navigation and orientation (Christou & Bühlhoff, 2000; Hettinger, 2002; Loomis et al., 1999a) due to the various advantages over real-world settings. Particularly, VE technology allows for precise definition of and control over experimental conditions, such as exclusion of specific

sensory modalities. Whereas in real-world settings navigators might resort to a piloting strategy whenever landmark information is present (Foo et al., 2007), the exclusion of landmark information in VE fosters participants to purely rely on their path integration system. In this context, visual flow has been proven to supply sufficient velocity and acceleration information for an appropriate update of position and orientation (Kearns et al., 2002; Lappe et al., 1999; Mossio et al., 2008; Warren et al., 2001). The visual flow field is a global visual stimulus comprising a set of elements that apparently ‘expand from a point in the direction of movement’ (Cutmore, Hine, Maberly, Langford, & Hawgood, 2000, p. 224). Navigators seemingly use the perceptive structure of a *changing* visual scene to derive the *invariant* layout of objects within the environment (Gibson, 1954; Tan, Czerwinski, & Robertson, 2003), which is stored on the representational level. Kirschen and colleagues (2000), investigating the efficiency of pure optic flow on navigation performance within a virtual environment (VE), found fluid optic flow to support faster learning of an environmental structure (less disorientation and backtracking) as compared to a choppier flow version. Further, in several recent VE path integration tasks based on the exclusive presentation of sparse visual flow participants have been shown to build up accurate internal representations of their surroundings (Gramann et al., 2005; Gramann et al., 2006; Riecke, 2003).

#### 4.2.2 Reference Frames in Spatial Navigation

The integration of sensory information during path integration takes place within distinct, but interacting spatial reference frames. Most generally, a distinction is made between a self-centered *egocentric* reference frame and an environment-centered *allocentric* reference frame (Brewer & Pears, 1999; Burgess, 2006; Klatzky, 1998; Klatzky et al., 1990; Klatzky & Wu, 2008; McNamara & Valiquette, 2004; Mou et al., 2004; Neggers et al., 2005; Sholl & Nolin, 1997; Wang & Spelke, 2002). Within the former, space is coded based on the three intrinsically defined axes of the navigator: front-back, right-left, and up-down (Bryant & Tversky, 1999; Franklin & Tversky, 1990). Distances and directions of entities in space are represented independent of each other, solely related to the navigator’s axis of orientation (Aguirre & D’Esposito, 1999; van Asselen et al., 2006). In other words, the world constantly changes around the spatially fixed navigator (Wang & Spelke, 2000). Since this *egocentric locational representation* (Klatzky, 1998) has to be updated with each translation and/or rotation, the resulting spatial representation, comprising *egocentric distances and bearings*, can be characterized as being highly dynamic and transient.

By contrast, an *allocentric reference frame* establishes a polar or Cartesian coordinate system with an origin external to the navigator and an external reference direction (Benhamou, 1997; Burgess, 2006; Mou et al., 2006; Wang & Spelke, 2002). Within the resulting *allocentric locational representation* inter-object relations are represented independent of the navigator’s current position and/or orientation, exclusively related to the external reference properties,

implying a map-like survey view of the surroundings with coordinate axes corresponding to the cardinal directions, or the global layout of the environment (Mou & McNamara, 2002; Mou et al., 2004; Shelton & McNamara, 2001; Shelton & McNamara, 2004). Also, the navigator himself is represented solely in terms of position, but without any orientation – comparable to a ‘you are here’-spot commonly encountered in man-made survey maps of indoor and outdoor spatial structures (Klippe et al., 2006). Therefore, applying an allocentric reference frame requires the moving navigator to constantly update positional but not orientation-related information, since all *allocentric object-to-object distances and bearings* remain stationary as the navigator proceeds.

Importantly, the subject’s choice for navigating within an egocentric or an allocentric reference frame has been shown to partly depend on the perspective which an environment is initially encountered and learned from (Shelton & Gabrieli, 2002; Shelton & Pippitt, 2007). Whereas exploratory ground-level encoding has been assumed to take place within an egocentric reference frame, the confrontation with a given environment from an aerial perspective has been linked to allocentric processing (Golledge, Dougherty, & Bell, 1995; Mellet, Briscogne, Tzourio-Mazoyer, Ghaem, Petit, Zago, Etard, Berthoz, Mazoyer, & Denis, 2000; Thorndyke & Hayes-Roth, 1982). However, several recent studies on homing accuracy during VE path integration have provided rich evidence for the existence of trait-like and intraindividually stable proclivities in applying either an egocentric or an allocentric frame for encoding visuo-spatial information (Gramann et al., 2005; Gramann et al., 2006; Riccobon, 2007; Schönebeck et al., 2001). That spatial encoding within the nonpreferred reference frame is generally possible, has been shown by Gramann (2005) and Riccobon (2007). However, results suggest that cognitive load is significantly reduced whenever the subject is able to encode and retrieve spatial information within the preferred reference frame.

Despite identical experimental stimulation with virtual turning tunnels and identical task instructions to keep oriented in order to adjust a simulated 3D-arrow to point directly back to the starting point of the trajectory (‘homing-task’), subjects were found to apply distinct strategies based on the reference frame chosen for updating the return bearing of the starting point. *Turners*, preferentially navigating within an egocentric reference frame, update the egocentric return bearing with successive rotations and translations. After a tunnel passage with a rightward turn, their homing arrow typically points to their right behind them. By contrast, *Nonturners*, using an allocentric reference frame, base their homing response on the allocentric return bearing. Since this group establishes a self-position independent, allocentric representation of the environment, and all orientation changes of the tunnel passage are set in relation to the reference direction, their final arrow adjustment after the very same rightward-turning tunnel passage points to the left behind them. In other words, the allocentric homing arrow overestimates the egocentric angular adjustment by the summed angles of rotations encountered along the outbound trajectory, also referred to as *allocentric heading* (see Figure 4.1).

Despite differing parameters, spatial processing within egocentric and allocentric reference frames has been shown to result in representations of comparable accuracy (Gramann et al., 2005).

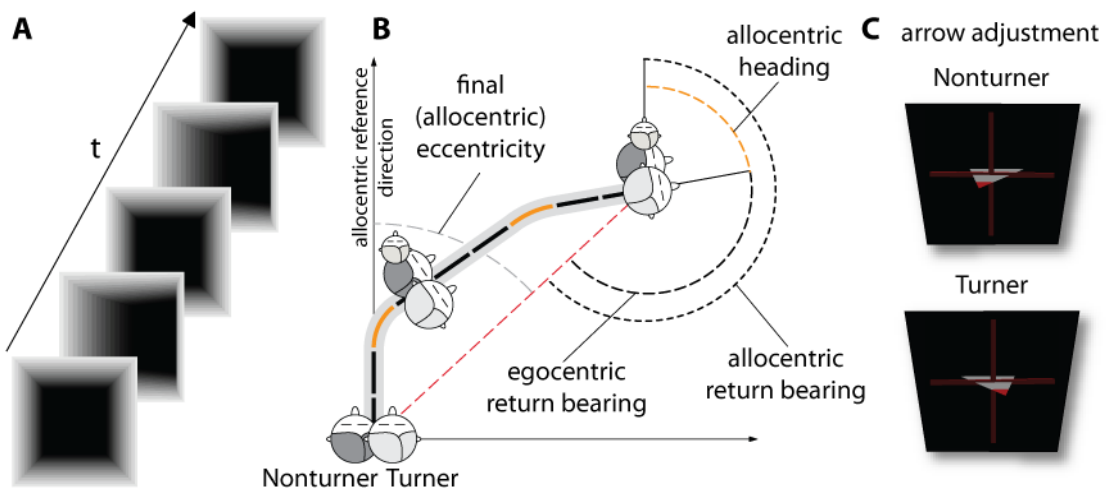


Figure 4.1: **(A)** Snapshot icons of the tunnel stimulation material providing continuous visual flow; **(B)** Return bearings of Turners and Nonturners are initially aligned, but diverge with orientation changes by the sum of rotational angles along the trajectory, also denoted as allocentric heading (orange); **(C)** Based on the return bearing of the respective reference frames, arrow adjustments of Nonturners and Turners differ. Whereas Nonturners adjust this arrow to point to the left side and back, for Turners the correct solution is an arrow pointing to their right side and back (adapted and modified from Gramann et al., 2005; Gramann et al., 2006).

#### 4.2.3 Cortical Differentiations between Egocentric and Allocentric Reference Frames

There is evidence for neurofunctional as well as neurostructural dissociations between egocentric and allocentric reference frames (Fink et al., 2003; Galati et al., 2000; Ota, Fujii, Suzuki, Fukatsu, & Yamadori, 2001; Shelton & Gabrieli, 2002, 2004; Vallar et al., 1999). Under natural conditions, both systems interact during encoding and retrieval of spatial knowledge, allowing the construction of an adaptive and coherent representation of the environment and one's position and orientation within it (Byrne & Becker, 2008; Byrne et al., 2007; Ekstrom et al., 2003; Harris, Egan, Sonkkila, Tochon-Danguy, Paxinos, & Watson, 2000). Based on incoming visual flow, information regarding one's own self-motion is extracted and further processed along the *dorsal pathway* within medial occipital and posterior parietal areas (Duffy & Wurtz, 1991a; Merriam et al., 2003), with the latter coordinating the transformations between various behaviorally relevant egocentric reference frames, e.g., eye-centered, body-centered, or head-centered reference frames, respectively (Cavanna & Trimble, 2006; Dean & Platt, 2006; Xing & Andersen, 2000). Firing patterns of these parietal cells are seemingly affected by various combinations of velocity, head direction, and visual stimuli, bearing resemblance to object tracking during

self-motion (Bremmer et al., 2002; Duhamel, Colby, & Goldberg, 1998), further corroborated by studies on navigation performance of patients suffering from parietal lesions (Aguirre & D'Esposito, 1999; Seubert et al., 2008). These subjects were not able to properly integrate heading information, a prerequisite for spatial updating.

Additional cells that respond selectively to head-direction irrespective of one's current position are located in cingulate and retrosplenial areas (Vann & Aggleton, 2004). Activity in these areas is associated with bidirectional exchange processes between egocentric (parietal) and allocentric (temporal) regions since neural firing of head-direction cells also affects activity of view-invariant place cells in medial temporal, particularly hippocampal structures. Place cells have been found to respond on an animal's location in space independent of its current orientation (O'Keefe, Burgess, Donnett, Jeffery, & Maguire, 1998; Redish, 1999). Interestingly, these place cells fire maximally whenever the animal is at a given distance and allocentric direction from an object or environmental landmark (Byrne et al., 2007), giving rise to the assumption that certain aspects of the allocentric reference frame are located in these areas (McNaughton, Battaglia, Jensen, Moser, & Moser, 2006). Additionally to object-based processing along the *ventral pathway*, hippocampal structures also receive context-independent efferent position information upstream from entorhinal grid cells. In contrast to place cells, these cells establish a map of the environment that is only initially anchored to external landmarks, but persists in their absence, which might contribute central elements for the long-term storage of spatial structures (Hafting, Fyhn, Molden, Moser, & Moser, 2005).

Finally, parietal as well as hippocampal structures possess interconnections to prefrontal regions that are associated with functions of spatial working memory comprising maintenance of encoded information as well as goal-directed and action-oriented planning (Barbas & Blatt, 1995; Lee & Kesner, 2003; Maguire et al., 1998a; Miller & D'Esposito, 2005).

#### **4.2.4 EEG Data Examination via Independent Component Analysis (ICA)**

Hemodynamic imaging studies have provided rich evidence for distinct brain areas activated during egocentric and allocentric processing. However, the high spatial resolution of these methodologies comes along with costs in temporal resolution. Analysis of spontaneous electroencephalographic (EEG) oscillations, by contrast, allows for an identification of sensory and cognitive processes on a subsecond time scale (Basar et al., 2000). In this context, alpha and theta frequency bands constitute the most extensively studied oscillations, since they have repeatedly been associated to correlate with mental states and strategies as well as stimulus characteristics, e.g., environmental complexity (von Stein & Sarnthein, 2000).

Activity in the (4 – 8 Hz) theta frequency band is directly related to memory maintenance and increases with task difficulty (Jensen & Tesche, 2002; Onton et al., 2005). Further, theta activity has been found to serve as gating mechanism at stages related to information encoding, as well as during memory storage and retrieval (Klimesch, 1999). Additionally, increased theta activity has been associated with increased environmental complexity, as registered in medial temporal, midline frontal, and parietal regions (Bischof & Boulanger, 2003; Caplan et al., 2001; Kahana et al., 1999). Particularly at critical time points, e.g., during upcoming heading changes, pronounced theta activity has been detected (Bischof & Boulanger, 2003), suggesting that this frequency band specifically correlates with memory retrieval and action-based pursuance of self-determined navigational goals (Caplan et al., 2003; Cornwell et al., 2008; de Araujo et al., 2002).

By contrast, activity in the (8 – 13 Hz) alpha frequency band has several different functional correlates reflecting sensory, motor, and memory functions (Basar & Schürmann, 1997; Lehmann & König, 1997). Alpha arises primarily from posterior sites, including occipital, parietal, and posterior temporal regions. Alpha is generally registered during mental and physical resting states with eyes closed, and is blocked or reduced during mental or bodily activity in terms of *event-related desynchronization* (ERD) (Klimesch et al., 1997a; Pfurtscheller & Lopez da Silva, 1999), suggesting that decreased alpha constitutes a valid signature of activation or cognitive preparedness of the cortical domain for processing of task-related information (Angelakis et al., 2004; Pfurtscheller, 2001; Pfurtscheller & Lopez da Silva, 1999). Recent studies differentiate between the (7 – 10 Hz) lower alpha and the (10 – 13 Hz) upper alpha band (Barutussek & Gräser, 1980). Whereas the upper alpha band has been found to be involved in semantic memory storage (Klimesch, 1997), the lower alpha band is closely linked to attentional encoding of spatial information, particularly structural features of the environment (de Araujo et al., 2002; Riccobon, 2007).

Importantly, the recorded signals do not arise on-site, e.g., directly located beneath a certain scalp electrode. Instead, they originate from partially synchronized local field potentials within distinct cortical patches, or source domains (Onton et al., 2006). As long as the local domain activity is non-synchronized, or cell activity spreads non-systematically in various directions, activities cancel each other out. Only in case of temporally synchronous extra-neuronal potentials activity spreads – in terms of summed ‘far-field’ potentials – further towards the scalp surface via volume conduction, gaining enough strength to be measured on the scalp surface. Most intriguingly, but following basic principles of electrical conductance, far-field potentials arising in spatially distinct cortical (and noncortical) domains emanate to and linearly sum at nearly every surface electrode. As a result, the retrieved EEG signal at each electrode is a *weighted linear mixture* of distinct, phase-independent, and spatially stationary cortical source signals, with the weights being determined by the distance between electrode and cortical source domain, their relative orientation, as well as the conduction properties of the intermediate structures

(cortex, intra-ventricular cerebro-spinal fluid, skull, and skin, respectively). In other words, it is possible to compose EEG scalp signals as a linear mixture of signals arising from cortical areas that – over sufficient time – act as single, distinct, and temporally independent neural compound generating locally synchronous EEG activity. To undo this mixing process, the registered scalp signals have to be spatially filtered in order to reveal the generator sources associated with distinct cortical processes. Based on the biologically plausible assumption of temporal independence, as well as spatial stationarity of EEG signals generated within distinct cortical domains (Makeig et al., 1996a; Makeig et al., 1996b), Independent Component Analysis (ICA) decomposition can learn spatial filters so that individual source signals can be reconstructed from high-density EEG mixtures obtained from the scalp surface.

#### 4.2.5 Aims of the Present Study

Based on the excellent temporal resolution of EEG recordings as well as seminal progress in utilizing scalp EEG recordings for intracortical source reconstruction, the current study aimed at the identification of generator sources of brain activity as well as macroscopic oscillatory dynamics during path integration at various complexity levels. Based on the assumptions of the history-free model (Hartmann & Wehner, 1995; Müller & Wehner, 1988), updating of representational primitives was supposed to be accomplished irrespective of path complexity, resulting in comparable brain activity patterns during turns and straight segments. Based on earlier results on spatial navigation in complex maze systems (Kahana et al., 2001; Kahana et al., 1999), this hypothesis was considered to be very unlikely. Rather, the human navigator builds up an internal representation of the path layout that is updated at certain anchor points, primarily during turns (Fujita et al., 1993; Klatzky et al., 1999). A canonical correlation analysis of Gramann and colleagues (2005) also suggested that participants' homing responses are primarily determined by the turning angles of curved segments rather than distances of straight segments along the outbound path. This configural updating was initially assumed to be independent of the learning history, solely related to bottom-up encoding of the currently traversed pathway (standard configural model, Fujita et al., 1993). However, errors in spatial encoding might also arise from top-down processes (Klatzky et al., 1999). Instead of solitarily processing incoming visual information the navigator might resort to an internal representation of the environment when mentally preparing the homing response, particularly when cognitive load is increased, and memory capacities are exhausted due to the increasing number of elements to be stored with increasing path length and complexity.

None of the previous studies investigating complexity effects on human path integration ability has taken into consideration individual proclivities for building up a spatial representation within egocentric or allocentric reference frames. Instead, in most of the cited studies environments have been pre-

sented from a certain perspective (e.g., ego-perspective vs. survey-view, Shelton & Gabrieli, 2002), so that subjects might have been triggered to apply a non-preferred navigation strategy. Since egocentric and allocentric primitives differ, it is likely that they are processed within distinct neural circuits (dorsal vs. ventral pathway). On the other hand, following the remarks of Burgess (2006) as well as initial results of Gramann and colleagues (2006), egocentric and allocentric systems might be activated in parallel during spatial tasks. However, there is, hitherto, no study on electrocortical dynamics on a sub-second time scale investigating the impact of complexity on spatial navigation within distinct referential systems. Even if egocentric and allocentric reference frames interact within comparable cortical networks, there might be differences with respect to the dynamics within certain areas responsible for coordinate transformation between reference frames.

In order to answer these questions, the tunnel paradigm was applied (Gramann, 2002; Schönebeck et al., 2001), providing the navigator with visual flow stimulation of 3D virtual turning tunnels with straight and curved segments (no vestibular input). After traversing the outbound trajectory participants had to adjust a virtual 3D-arrow to point directly back to the starting point of the passage (point to origin). Path complexity was operationalized as the number and directions of successive heading changes (of varying angularity) along an outbound trajectory. In *Experiment 1*, participants preferentially using an egocentric or an allocentric reference frame were confronted with tunnels with one and two turns bending into the same direction. Participants in *Experiment 2*, by contrast, traversed tunnels with one turn or tunnel with two turns with identical angles bending into opposite directions.

## 4.3 Experiment 1 – Same Direction

### 4.3.1 Methods

#### 4.3.1.1 Participants

Nineteen male students recruited from the Ludwig-Maximilians-University Munich, Germany, participated in Experiment 1 (age ( $M \pm SD$ ) =  $23.74 \pm 3.62$  years). Participants were either paid 8€ per hour or received course credit for taking part in the experiment. The experiment followed the American Psychological Association's (APA's) Ethical Principles of Psychologists and Code of Conduct (American Association of Psychology, 2002). Out of a pool of 20 subjects, ten subjects categorized as Turners and nine subjects categorized as Nonturners were selected. One Nonturner was excluded from the analyses due to miscomprehension of the instructions. All subjects had normal or corrected to normal vision and reported no history of neurological disorder. All Turners were right-handed, one of the remaining nine Nonturners was left-handed.

#### 4.3.1.2 Task, Materials, and Procedure

Passages through virtual tunnels with one turn and two turns were presented using the tunnel paradigm, a desktop-based virtual reality task. The simulation provided the navigator with sparse visual flow information on translational and rotational changes only through the rate of optic flow. Subjects had to keep up orientation during paths of straight and curved tunnel segments without landmarks. 160 experimental trials were generated. Out of these, 80 experimental trials consisted of five segments (with duration of approx. 1880 ms each) with the turn placed in the third segment [*1 turn*]. Additionally, tunnels with 9 segments were presented with turns (bending into the same direction) placed in segment 3 and segment 7 [*2 turns, sd*]. Therefore, subjects could not determine if traversing a tunnel with one or with two turns until either the end of the passage showed up or the tunnel continued with a second turn. Tunnels ended at categorical end positions of 15°, 30°, 45°, and 60° eccentricity ( $\pm 2^\circ$  deviation to avoid categorical reactions when adjusting the homing vector) to the left or the right with respect to the starting position. Each eccentricity to either side was repeated 10 times. At the end of each passage a 3D homing arrow cue was presented with the arrowhead pointing into the depth of the screen. The task of the subjects was to adjust this homing arrow to point as accurately as possible directly back to the starting point of the passage (pressing and holding left or right mouse button caused the arrow to rotate counter-clockwise or clockwise, respectively). When the participant adjusted the subjectively correct homing vector, the setting was confirmed by pressing the middle mouse button, and after a short interval the next trial was initiated.

In addition to the 160 experimental trials, 21 ‘filler’ trials with three straight segments were presented. Subjects were instructed to only watch the visual flow without orienting and to press the middle mouse button at the end of the passage when the reaction format was displayed (For further discussion see section 3.4.1). The main experimental session lasted approximately 70 minutes.

#### 4.3.1.3 Performance Measures

Mixed-design ANOVAs were conducted in order to reveal effects of the following factors on behavioral performance (homing accuracy and latency): ‘Number of Turns’ (one vs. two), ‘Eccentricity of End Position’ (15°, 30°, 45°, or 60°, respectively), ‘Side’ of the tunnel passage (right vs. left, relative to the starting point), as well as the between-subjects factor ‘Preferred Strategy’ (Turners vs. Nonturners). Analyses revealed no significant main effect or interaction of the factor ‘Side’ on error scores [absolute error:  $F(1, 17) = .359, p = .557$ ], therefore tunnels were collapsed in a final  $2 \times 4$  mixed-design analysis with repeated measures over the factors ‘Number of Turns’ (one vs. two) and ‘Eccentricity of End Position’ (15°, 30°, 45°, or 60°) with the subject’s preferred ‘Strategy’ as between-subject measure.

#### 4.3.1.4 EEG Recordings and Artifact Rejection

The electroencephalogram (EEG) was recorded continuously with an analog band pass from 0.016 Hz to 100 Hz with a sampling rate of 500 Hz, using 128 Ag/AgCl electrodes corresponding to the international 5%-system (Delorme & Makeig, 2004). Electrodes were placed in an elastic cap (*Falk Minow Services, Munich, Germany*) with electrode configuration as depicted in Figure 4.2. Impedance was kept below 7 kOhm. An additional electrode was placed on the infraorbital ridge of the left eye to record the vertical electrooculogram (EOG). Electrophysiological signals were amplified via BrainAmps (*Brain Products, Munich, Germany*) referenced to Cz. A digitizing system (*Zebris, CMS20S*) was used to individually determine the positions of the 128 channels.

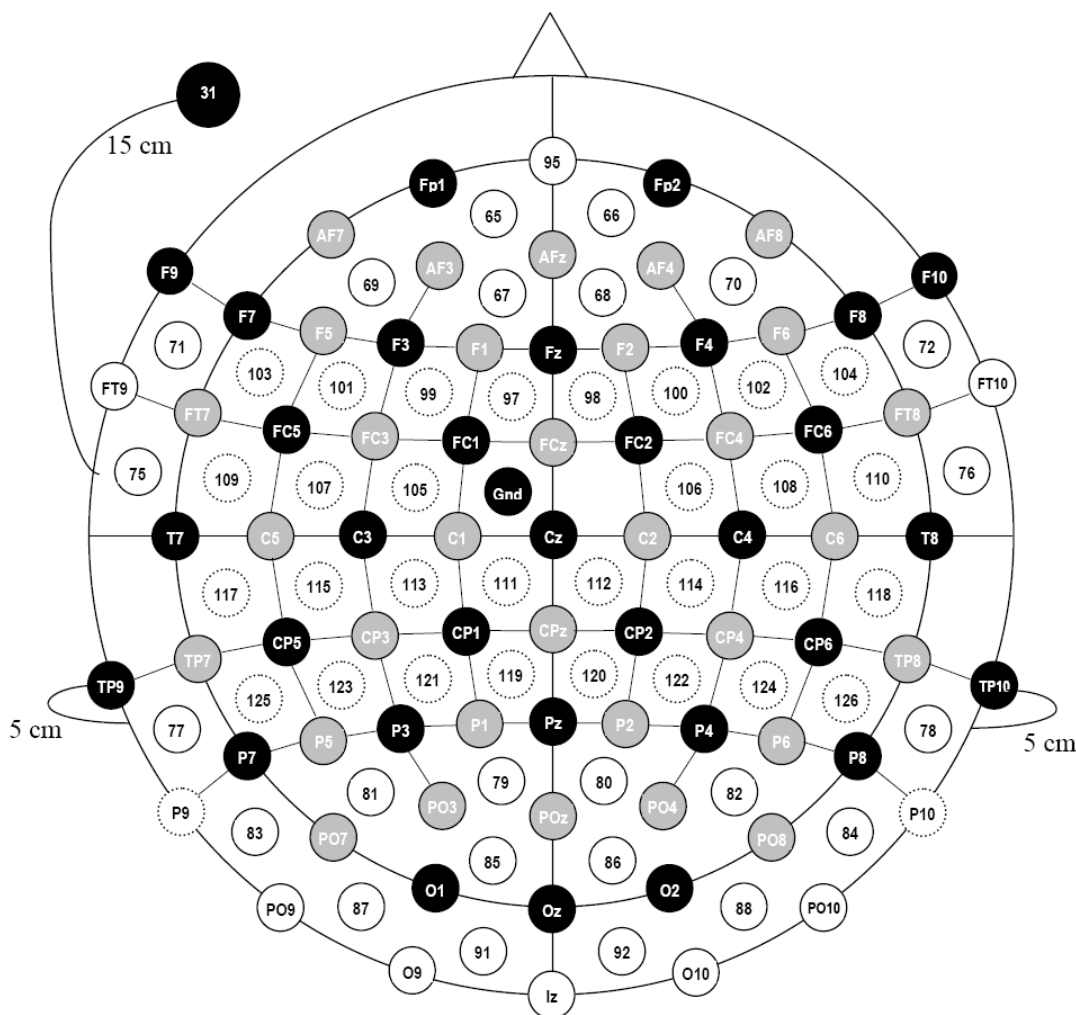


Figure 4.2: Experiment 1 – Configuration and designation of the 128-electrode-array (following the international 5%-system). Electrodes were arranged in four bundles with 32 electrodes per bundle for further signal processing to the amplifying system: (1) black filled circles [channels 1 – 32]; (2) grey filled circles [channels 33 – 64]; (3) white circles, solid lines [channels 65 – 96]; (4) white circles, dashed lines [channels 97 – 128]. Reference electrode (Ref/Cz) and ground electrode (Gnd) were connected through all amplifying bundles.

Data were analyzed by custom MATLAB scripts built on the open source EEG-LAB toolbox (Jung, Humphries, Lee, Makeig, McKeown, Iragui, & Sejnowski, 1998; Makeig et al., 1996a). EEG data were co-registered with behavioral trial-to-trial performance (absolute and signed error scores, response latencies), and re-referenced off-line to linked mastoids. Epochs containing artifacts were rejected by minute visual inspection. Criteria used for artifact rejection included extreme values (fixed thresholds), abnormal trends (linear drifts), and abnormally distributed data (high kurtosis). Following this rationale, intervals with excessive peak-to-peak deflections or bursts of electromyographic activity were excluded from further analyses. Eye movements were not defined as artifacts since these spatially stationary signals could be separated from other EEG processes applying subsequently applied ICA (Lee, Girolami, & Sejnowski, 1999).

#### 4.3.1.5 Independent Component Analysis and Component Selection

After downsampling to 250 Hz data were digitally filtered to remove frequencies above 50 Hz. Maximally independent EEG processes were obtained based on the extended infomax ICA (Makeig et al., 2004) using *binica* (Delorme & Makeig, 2004) from the EEGLAB toolbox. Default extended-mode *binica* training parameters were used (Delorme, Sejnowski, & Makeig, 2007; Jung et al., 1998; Onton & Makeig, 2006; Vigário, 1997) with an initial learning rate (a unitless scaling factor) of  $10^{-4}$ . Training was stopped when weight change was less than  $10^{-7}$ .

ICA is able to dissociate functional and non-brain artifactual ICs (e.g., eye blinks, electromyographic activity, cardiac pulse artifacts and electrical line noise), as has been shown by several studies (2006). These non-brain artifactual processes arising from (horizontal and vertical) eye movements, eye blinks, and muscle tensions have stereotyped scalp projections, but, however, irregular variations within a specific myographic pattern (e.g., blinking with a single eye) might result in more than one stereotyped scalp map pattern, therefore requiring more than one IC to be extracted from the data. Unfortunately, artifacts might also result from movements of the electrodes on the scalp due to large muscular movements or inadvertent shifts of the electrode cap and other external sources. In this case, artifacts concentrate dozens to hundreds of unique scalp projections, each requiring a separate IC. Since the number of reconstructed independent component sources is limited by the number of electrodes, even in case of high-density EEG recordings only a few ICs are left to cover the functional processes. Following Onton et al. (Akalin-Acar & Gencer, 2004; Oostenveld & Oostendorp, 2002), an iterative multi-step approach (consisting of several loops of data pruning and subsequent ICA decomposition) seems to be appropriate.

However, repeated visual inspection of each subject's ICA activations revealed no artifacts related to electrode cap movements. Therefore, we had reason to assume that the remaining dipole source locations of independent components

were spatially fixed regardless of tracking performance during each hour-long session. DIPFIT2 routines from EEGLAB were applied to fit single dipole source models to the remaining IC scalp topographies using a four-shell spherical head model (Anemüller, Sejnowski, & Makeig, 2003; Makeig et al., 2004). Default radii values for the four spheres (71, 72, 79, and 85 mm) and default conductance values (0.33, 1.0, 0.0042, and 0.33 S/m) were applied. In the DIPFIT2 software, the boundary element head model is co-registered with an anatomical average brain template constructed from 100 brain samples of subjects without neurological history (Montreal Neurological Institute), returning approximate Talairach coordinates for each IC equivalent dipole source. Components with bilaterally distributed scalp maps were fit with a dual dipole model using a symmetrical constraint. Components with more than 15% residual variance and components with equivalent dipole models located outside the sphere were not considered further.

#### **4.3.1.6 Component Power Spectra and Event-Related Spectral Perturbation (ERSP)**

After decomposition data were separated into overlapping epochs of 2875 ms (length of one tunnel segment plus 500 ms pre- and 500 ms post-stimulus time window). Each single-trial tunnel segment IC time series was transformed into a spectrographic image using 3-cycle Morlet wavelets in a frequency range between 3 Hz and 45 Hz. Component spectra were normalized for between subject comparison by subtracting mean log power from single-trial log power. This interval was chosen since ( $> 45$  Hz) gamma-band and near-DC dynamics appear to be less well modeled than activity in intermediate frequency bands (Makeig, 1993; Makeig et al., 2004). Each single-trial component activity time series was then transformed to a baseline-normalized spectrographic image.

The mean baseline spectrum for experimental *tunnel* passages was taken to be the average EEG spectrum of all trials, beginning with the second tunnel segment and ending with the penultimate segment of the tunnel passage (for tunnels with one turn: Segment 4; for tunnels with two turns: Segment 8). Mean ERSPs were created by subtracting the 2-D (frequency-by-latency) mean log power spectrum of the baseline from the mean log power at each time point of the experimental trials (Hartigan & Wong, 1979). By contrast, the mean baseline spectrum of the subsequent pre-response interval (500 ms) and the first 1300 ms of the arrow adjustment phase was taken to be the EEG spectrum during this time-window, again averaged over all trials. These images revealed event-related changes in spectral power in narrow-band frequency bins for the whole time course of the tunnel passage.

#### **4.3.1.7 IC (Pre-)Clustering**

In order to identify sets of similar components across all subjects, IC processes were clustered using a *K-means* cluster algorithm (Onton et al., 2006) implemented in the EEGLAB toolbox. For this purpose, an N-dimensional cluster

position vector for each IC was created to measure ‘distances’ between ICs in the defined cluster space based on particular IC characteristics such as IC log spectra, event-related potentials, equivalent dipole locations, ERSPs, and inter-trial coherence (Onton & Makeig, 2006). Since IC processes with comparable localization in 3-D Talairach space displaying coherent ERP and ERSP patterns might differ with respect to dipole orientation, different scalp projections and, followingly, scalp topographies might result (Delorme & Makeig, 2004). Therefore, IC scalp topography as used for the identification of functional IC source processes during component selection was excluded from pre-clustering. Information on component spectra, event-related potentials, ERSPs, and inter-trial coherence were each reduced to 10 principal dimensions in the cluster subspace by principle component analysis (PCA). The position measure for dipole models used 3 dimensions. For a comparison of location and activity measures, the data of all principle components was divided by the standard deviation of the first PCA component for this measure. In addition, information on dipole location was multiplicatively weighted with a factor of 15 and information on ERSP was weighted with a factor of 4 as compared to the standard weighting of 1 for all other measures (spectrum, ERP, and ITC). Parameters were chosen to emphasize 3-D location of sources and spectral perturbation which we expected to be most relevant given the present task. Only the onset of tunnel movement (first segment) and the onset of the response prompt included transient stimulation that could possibly lead to ITC or event-related potentials. Finally, dimensionality for all parameters was reduced to 10 final dimensions by means of PCA. Components that were located further than 3 standard deviations from any of the cluster centroids were removed from the cluster resulting in 22 final clusters (2 eye movement clusters and 20 functional clusters within the cortical domain).

#### 4.3.1.8 ERSP Statistics

Over the time course of the tunnel passages each component was checked for significant changes ( $p < 0.001$ , uncorrected for multiple comparisons) in mean log power from baseline. Time/frequency points with non-significantly varying mean ERSPs were masked with zero values. Significance of mean spectral differences from the baseline spectrum was computed using bootstrap resampling (Blair & Karniski, 1993; Delorme & Makeig, 2004). Grand means across subjects of these significance-masked ERSPs were consecutively masked for significance using nonparametric permutation-based statistical tests with  $p = .001$  at each time/frequency point. This procedure is a fairly conservative method for rejecting false positives arising from multiple comparisons, since it assigns the probability of any significant deviation from zero to be either non-significant or  $p < .001$ , no matter the actual probability. To further avoid false positives from multiple comparisons, effects in the grand mean ERSPs that were significant at only a few neighboring voxels (fluctuating activity with duration of significant deviation from baseline  $< 500$  ms) were not interpreted.

### 4.3.1.9 Strategy- and Complexity-Difference ERSP Computation

Permutation-based statistics for between-group ERSP differences were obtained by first computing surrogate-group means from sets of ERSPs drawn without substitution from ERSPs for the entire IC cluster in the same numbers in which Turners or Nonturners, respectively, contributed ICs to the cluster. Differences between such surrogate group-mean ERSPs formed a surrogate ERSP difference. At each time-frequency point, difference significance thresholds were taken to be .001 and .999 points in the distributions of surrogate group mean differences. Time-frequency points in the observed group-mean difference ERSPs were set to zero when their relative log power values did not differ significantly ( $p < .001$ ) from the expected power fluctuations at this frequency. Only IC clusters that revealed consecutive difference significance for a given time period ( $> 200$  ms) were considered to reliably represent group difference.

## 4.3.2 Results

### 4.3.2.1 Behavioral Performance

Behavioral results are depicted in detail in section 3.4.2. Subjects committed only few side errors (less than 0.95% for all trials) and displayed pronounced correlations between adjusted and expected homing responses (Nonturners vs. Turners:  $r_{NT}(144) = .956$ ,  $p < .0001$ , vs.  $r_T(220) = .923$ ,  $p < .0001$ ). Interestingly, overall correlation coefficients of Turners and Nonturners differed significantly ( $p < .01$ ), primarily caused by differences at the level of one-turn tunnels ( $p < .02$ ). Whereas for Nonturners correlation coefficients for tunnels with one turn were higher as compared to tunnels with two turns (Nonturners:  $r_{1\text{-turn}}(72) = .976$ ;  $r_{2\text{-turns}}(72) = .937$ ;  $p < .0001$ ; difference:  $p < .004$ ), correlation coefficients of Turners showed no statistically significant difference ( $r_{1\text{-turn}}(80) = .950$ ;  $r_{2\text{-turns}}(140) = .924$ ;  $p < .0001$ ).

Additionally, response latencies to initiate the homing arrow adjustment were found to be affected by the number of successive turns [main effect of Number of Turns;  $F(1, 17) = 10.125$ ,  $p < .005$ ,  $\eta_G^2 = .016$ ], replicating results of Loomis et al. (1993): The more complex a pathway was, the longer participants took to initiate the homing response. Interestingly, this pattern was primarily attributable to Turner subjects [interaction of Preferred Strategy  $\times$  Number of Turns;  $F(1, 17) = 8.432$ ,  $p < .01$ ,  $\eta_G^2 = .013$ ]. By contrast, Nonturners' responses after traversing tunnels with one turn and two turns were found to be comparable.

Analysis of signed error (over- and underestimations) revealed a significant main effect of Strategy [ $F(1, 17) = 13.086$ ,  $p < .002$ ,  $\eta_G^2 = .224$ ], and Eccentricity of End Position [ $F(1.29, 51) = 27.629$ ,  $p < .0001$ ,  $\eta_G^2 = .175$ ]. Further, statistical significance was obtained for the interaction of Preferred Strategy  $\times$  Number of Turns [ $F(1, 17) = 5.290$ ,  $p < .034$ ,  $\eta_G^2 = .056$ ], as well as Preferred Strategy  $\times$  Eccentricity of End Position [ $F(1.29, 51) = 7.532$ ,  $p < .008$ ,  $\eta_G^2 = .098$ ].

.058]. Additionally, the interaction of Preferred Strategy  $\times$  Number of Turns  $\times$  Eccentricity of End Position was found to take impact on signed error scores [ $F(2.14, 51) = 13.767, p < .0001, \eta^2_G = .064$ ]. Whereas Nonturners displayed a comparable pattern of overestimating inner and underestimating more lateral end positions for both tunnels with one turn and with two turns, Turners displayed this regression only for tunnels with one turn. When confronted with tunnels with two turns, their signed error scores were no longer determined by the allocentric eccentricities. Instead, they displayed a comparable level of overestimation at all tested eccentricities. This pattern was also obtained when error scores of Turners were computed in dependence of the *egocentric eccentricity of end position* (with categorical eccentricities of  $15^\circ$  and  $30^\circ$ , respectively, see Figure 4.3).

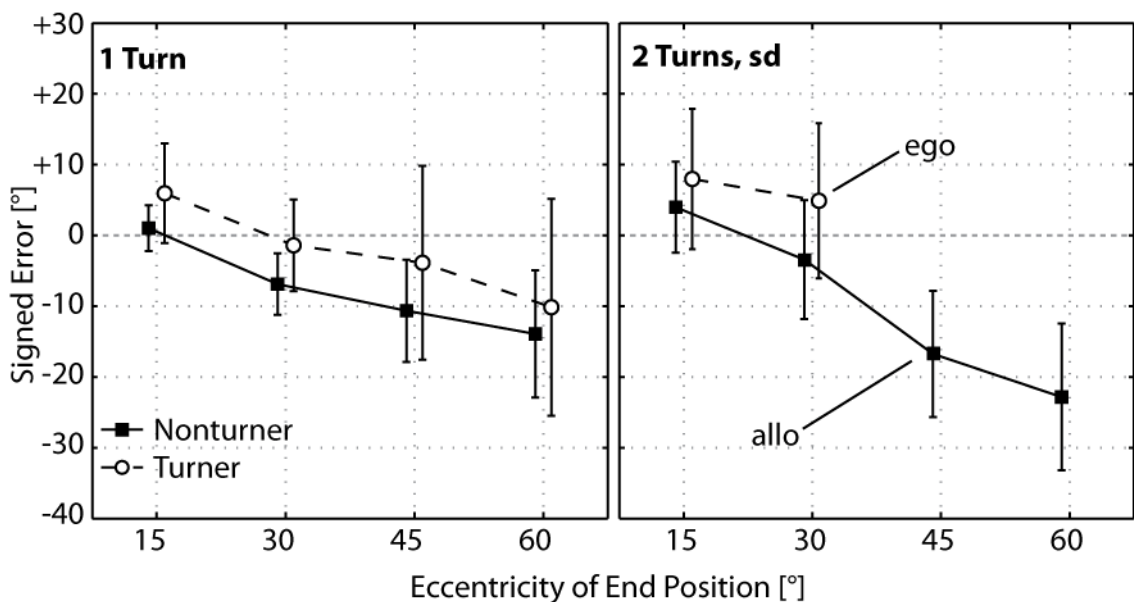


Figure 4.3: Experiment 1 – Mean signed error ( $\pm 1$  SD, depicted by the error bars) of the adjusted homing vector for tunnels with one turn and two turns, dependent on the eccentricity of end position relative to the origin of the path (turns of equal eccentricity to the left and right were pooled), separately for Nonturners (solid line) and Turners (dashed line). Due to dissociations in symmetry, allocentric and egocentric eccentricities for tunnels with two turns did not correspond. Therefore, tunnels with two turns ended at categorical allocentric eccentricities of  $15^\circ, 30^\circ, 45^\circ$ , and  $60^\circ$ , but within an *egocentric* reference frame laterality was reduced to end positions varying between  $10^\circ, 20^\circ$ , and  $30^\circ$ , respectively (see Appendix A for tunnel layouts).

#### 4.3.2.2 Source Reconstruction

22 clusters were obtained, with two clusters mirroring horizontal and vertical eye movement artifacts, as well as 20 clusters reflecting functional generator sources of maximally independent cortical processes. Stereotaxic Talairach coordinates (Lancaster, Woldorff, Parsons, Liotti, Freitas, Rainey, Kochunov, Nickerson, Mikiten, & Fox, 2000) as obtained via software-based reconstruction (<http://www.talairach.org/applet.html>, Lancaster et al., 2000), residual va-

riances, functional allocations within Brodmann Areas and the number of (Non-)Turner subjects and ICs within each cluster are summarized in Table 4.1. On average,  $M \pm SD = 16.32 \pm 4.31$  Independent Components per subject were obtained (range: 9 to 28). The number of localizable brain ICs in Non-turners and Turners (148 and 175) did not differ within the 20 non-artifactual clusters [ $F(1, 312) = 0.364, p = .547$ ].

| CI    | Talairach |     |     | RV<br>[%] | Brodmann Areas |                                   | $S_{NT}$ | $S_T$ | $IC_{NT}$ | $IC_T$ |
|-------|-----------|-----|-----|-----------|----------------|-----------------------------------|----------|-------|-----------|--------|
|       | x         | y   | z   |           |                |                                   |          |       |           |        |
| 1     |           |     |     |           |                | Parent Cluster                    | 9        | 10    | 175       | 197    |
| 2     |           |     |     |           |                | Outlier                           | 5        | 5     | 9         | 5      |
| 3     | -8        | -88 | -12 | 5.33      | BA 17/18       | L lingual gyrus                   | 6        | 7     | 9         | 7      |
| 4     | 25        | -80 | -1  | 3.25      | BA 18          | R (bilat.) lingual gyrus          | 7        | 8     | 13        | 16     |
| 5     | -27       | -73 | 17  | 3.70      | BA 19          | L (bilat.) middle occipital gyrus | 6        | 7     | 7         | 11     |
| 6     | 1         | -68 | 32  | 2.96      | BA 7/31        | midline precuneus                 | 8        | 8     | 10        | 12     |
| 7     | -46       | -59 | -3  | 3.83      | BA 19          | L occipito-temporal gyrus         | 6        | 5     | 6         | 6      |
| 8     | 12        | -50 | 12  | 5.37      | BA 29/30       | R posterior cingulate             | 5        | 5     | 8         | 9      |
| 9     | 31        | -41 | 36  | 3.30      | BA 40          | R inferior parietal lobule        | 6        | 5     | 10        | 7      |
| 10    | -32       | -40 | 39  | 4.33      | BA 40          | L inferior parietal lobule        | 7        | 5     | 9         | 9      |
| 11    | 0         | -37 | 38  | 3.70      | BA 7/31        | midline precuneus                 | 7        | 5     | 11        | 6      |
| 12    | -3        | -35 | -15 | 5.03      | -              | L cerebellar lingual              | 2        | 4     | 2         | 6      |
| 13    | 52        | -32 | -8  | 5.34      | BA 21          | R middle temporal gyrus           | 3        | 6     | 5         | 7      |
| 14    | -50       | -22 | -7  | 3.65      | BA 21          | L middle temporal gyrus           | 4        | 9     | 5         | 12     |
| 15    | 0         | -16 | 63  | 3.86      | BA 6           | midline medial frontal gyrus      | 6        | 4     | 7         | 6      |
| 16    | 40        | -12 | 53  | 1.61      | BA 4/6         | R precentral gyrus                | 6        | 8     | 9         | 14     |
| 17    | -38       | -8  | 49  | 2.01      | BA 4/6         | L precentral gyrus                | 6        | 6     | 7         | 9      |
| 18    | 3         | 0   | 39  | 5.94      | BA 32          | R (midline) medial frontal gyrus  | 6        | 5     | 7         | 8      |
| 19    | 35        | 3   | 21  | 4.50      | BA 13          | R insula                          | 4        | 4     | 5         | 5      |
| 20    | -27       | 17  | 15  | 3.24      | BA 13          | L insula                          | 3        | 4     | 3         | 4      |
| 21    | 1         | 20  | 47  | 3.08      | BA 8           | midline superior frontal gyrus    | 5        | 6     | 8         | 10     |
| 22    | 0         | 42  | 14  | 2.65      | BA 9/32        | midline anterior cingulate        | 5        | 5     | 6         | 5      |
| $e_h$ | 1         | 40  | -34 | 9.33      |                | horizontal EOG cluster            | 8        | 6     | 8         | 9      |
| $e_v$ | 3         | 51  | -27 | 7.51      |                | lateral EOG cluster               | 9        | 9     | 10        | 8      |

Table 4.1: Experiment 1 – Lateral and horizontal EOG clusters and 20 functional IC clusters, sorted from posterior to anterior IC cluster sites (along the y-axis). Columns provide information regarding (1) the location of the cluster centroids in Talairach space (x-y-z). All reconstructed clusters for each condition were anatomically specified within the stereotaxic coordinate system of Talairach and Tournoux using the Talairach demon software (Talairach & Tournoux, 1988), returning the coordinates of the nearest grey-matter point. Further, the table provides information regarding (2) the residual variance (RV, in %) of the reconstructed cluster centroids, and (3) their anatomical region defined in the Brodmann Area system (Brodmann, 1925). Finally, the table gives information regarding the number of Nonturner and Turner subjects ( $S_{NT}$ ,  $S_T$ ), as well as the amount of Nonturner and Turner Independent Components ( $IC_{NT}$ ,  $IC_T$ ) within each cluster.

### 4.3.2.3 Cluster Dynamics

#### *Occipital (BA 17/18), Occipito-Parietal (BA 18/31), and Occipito-Temporal (BA 19) IC Clusters*

A brief and partially phase-locked theta-band power increase marked the onset of the tunnel passage, accompanied by a desynchronization of the alpha frequency band (near 10 Hz). Additionally, an oscillatory power increase of the beta frequency band (near 13 – 15 Hz) was registered, which displayed a gradual downshift in peak frequency and merged with synchronized upper alpha band (10 – 13 Hz) until the first turn came into view. Upon intervisibility with the curved segment (first dashed red line), IC theta band power (near 4 – 8 Hz) was found to be increased relative to the baseline condition, prevailing until the actual onset of the turn. This theta complex was flanked by blocking of the alpha frequency band (near 10 Hz), most pronounced as participants approached the apex of the turn. However, approximately 100 ms after the onset of the turn upper alpha (near 13 Hz) frequency power was found to be increased, which persisted until participants had traversed the first turn. Subsequently, alpha band power (near 10 – 13 Hz) was synchronized throughout the straight segment following the first turn. The confrontation with the tunnel end (one turn condition, magenta line) or with an additional turn (two turn condition, third red dotted line) provoked another alpha desynchronization. Interestingly, approaching the second turn was associated with less pronounced and shortened desynchronization of the alpha frequency band (near 10 Hz), which ended already before subjects entered the turn segment. Encountering the tunnel end resulted in synchronization in the upper alpha band (near 10 – 13 Hz) and first harmonics (near 20 Hz), as well as increased theta power (near 4 – 8 Hz), persisting until the onset of the 3D arrow cue (final dashed red line). Here, another brief (and partially phase-locked) theta complex appeared, again accompanied by increased oscillatory alpha band power (near 10 – 13 Hz) and harmonics (see Figure 4.4).

Similar alpha blocking during turns also occurred in all IC clusters located in or near occipito-parietal cortex. However, in these IC clusters Turners and Nonturners displayed distinct ERSP patterns, primarily attributable to more pronounced blocking of the alpha frequency band (around 10 Hz) for Turners while approaching and entering the second turn (as can be seen from Figure 4.5 and Figure 4.6). Interestingly, the bilateral lingual IC cluster revealed a more pronounced synchronization of an alpha and beta complex at the end of the tunnel passage for Nonturners, which was even stronger for tunnels with two turns.

Spectral dynamics of occipito-temporal IC cluster 7 also resembled activation patterns of occipital clusters including synchronizations in the upper alpha-band (near 10 – 13 Hz) and in the beta-band (near 14 – 20 Hz) during straight segments, but less pronounced alpha desynchronizations when approaching and traversing curved segments. During both turns, but more markedly for the second turn, activations of Turners and Nonturners diverged, primarily caused

by more pronounced alpha desynchronization for Turners during these periods of travel (see Figure 4.7).

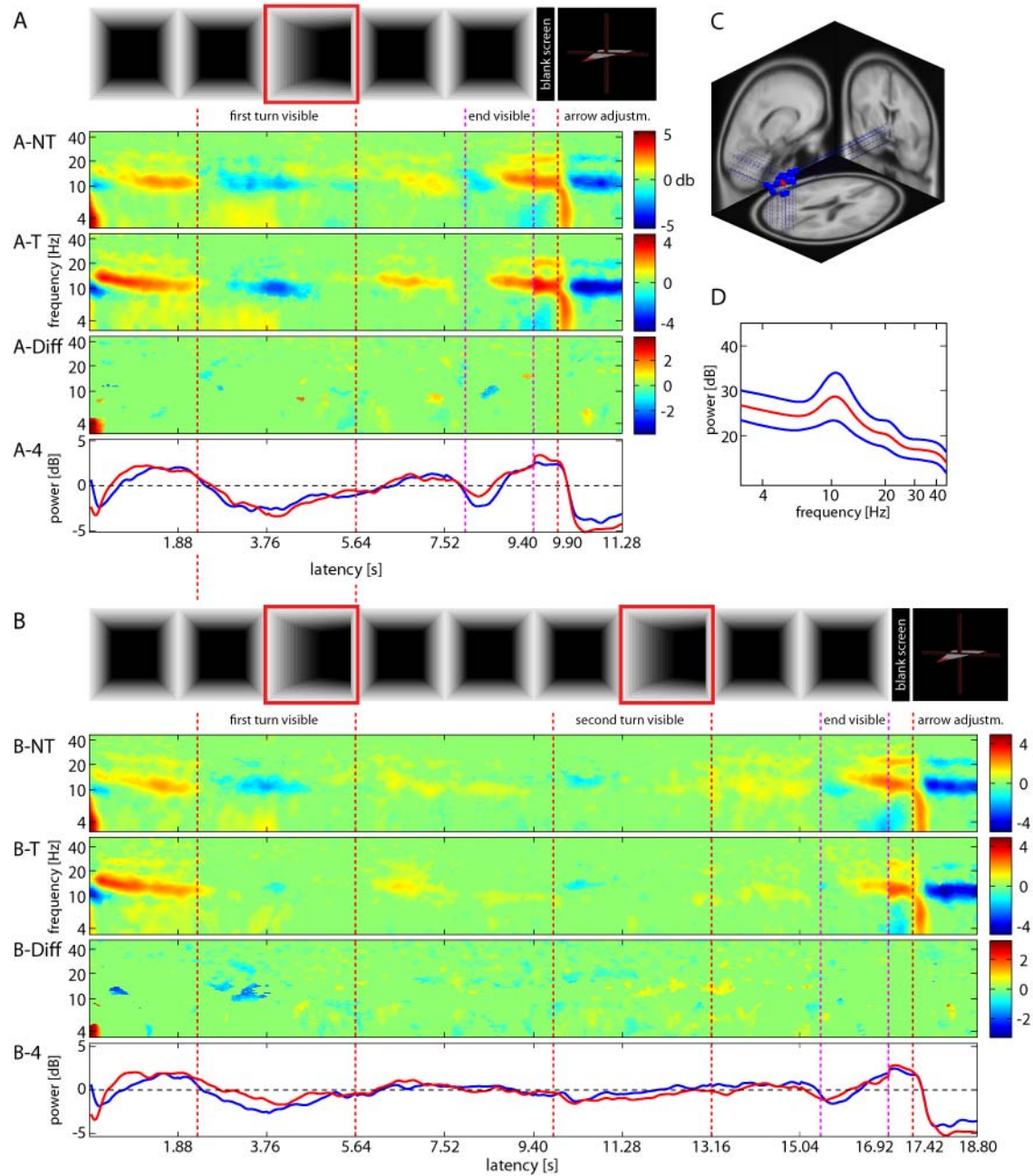


Figure 4.4: Mean event-related spectral perturbation (ERSP) images for an independent component cluster (ICC 3) located in or near left lingual gyrus (BA 17/18, panel C) revealing task-dependent changes in spectral power during spatial navigation through tunnel passages containing one turn (panel A) and two turns (panel B) and subsequent homing arrow adjustment. Cluster centroid mean ERSPs are plotted in log-spaced frequencies from 3 – 45 Hz for 11 IC processes of 8 Nonturner subjects (**A-NT**, **B-NT**), and 7 IC processes of 7 Turner subjects (**A-T**, **B-T**). ERSP difference between Nonturners and Turners is shown in panels **A-Diff** and **B-Diff** for tunnels with one turn and tunnels with 2 turns, respectively [see the following page for further explanation].

Green colors indicate no significant ( $p > 0.001$ ) difference in mean log power (dB) from baseline (mean activity of all tunnel passages; mean [ $\pm 1$  SD] baseline power depicted in **panel D**). Warm colors indicate significant increases in log power and cold colors indicate significant decreases in log power from baseline. Panels **A-4** and **B-4** depict dynamics in mean power (dB) over time for the (9 – 12 Hz) alpha band, separately for Nonturners (blue) and Turners (red). Important time points of the tunnel passage are marked with dashed lines: Red dashed lines indicate the period when participants perceived the approaching turn and the time period during the stimulus turn (from 3.76 s); magenta dashed lines indicate the time period during which the subjects were approaching the end of the tunnel. The final red dashed line indicates the time point when the virtual homing vector was displayed.

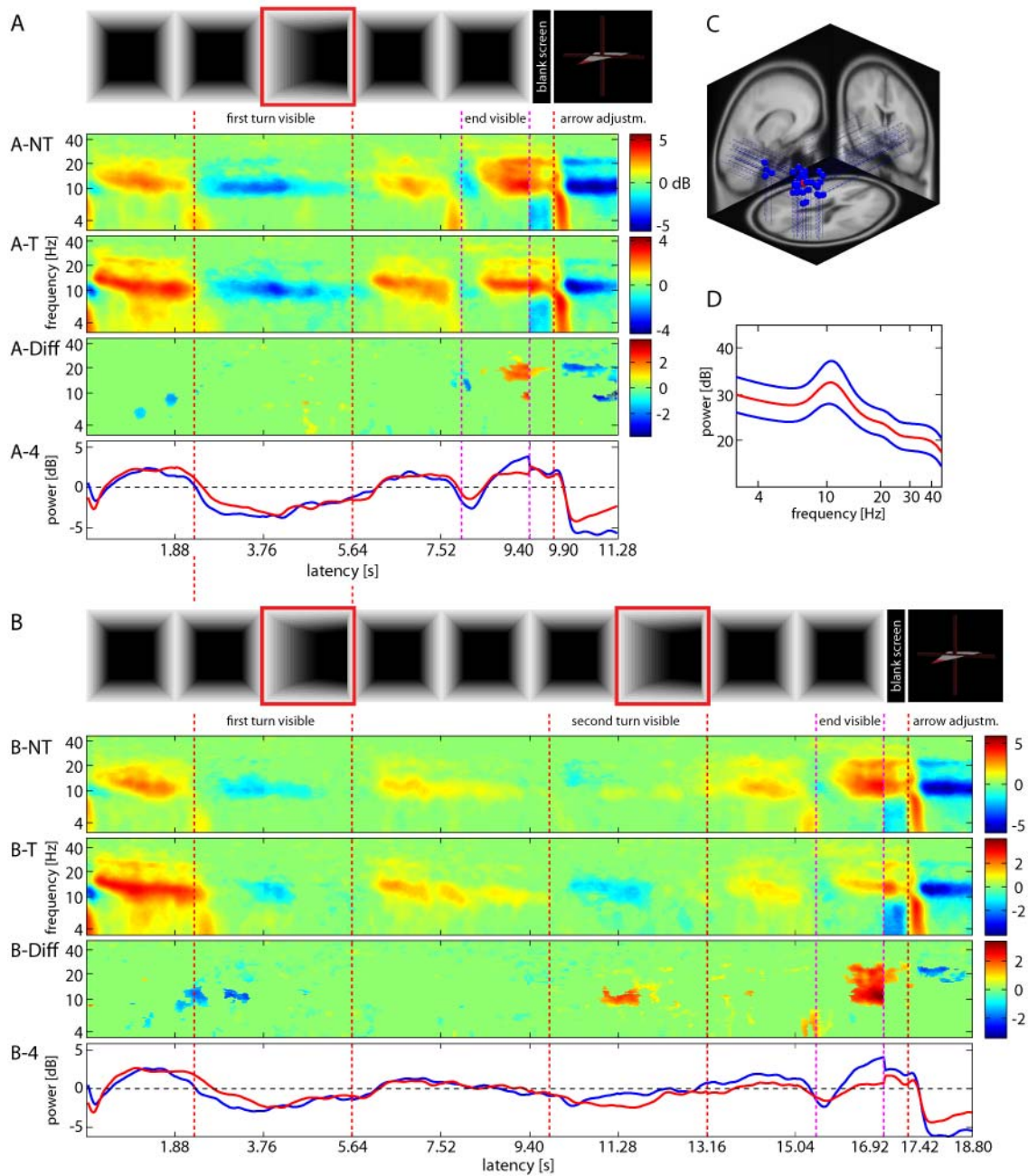


Figure 4.5: Mean event-related spectral perturbation (ERSP) images for an independent component cluster (ICC 4) located in or near right (bilateral) lingual gyrus (BA 17/18). For explanation see Figure 4.4 (page 96).

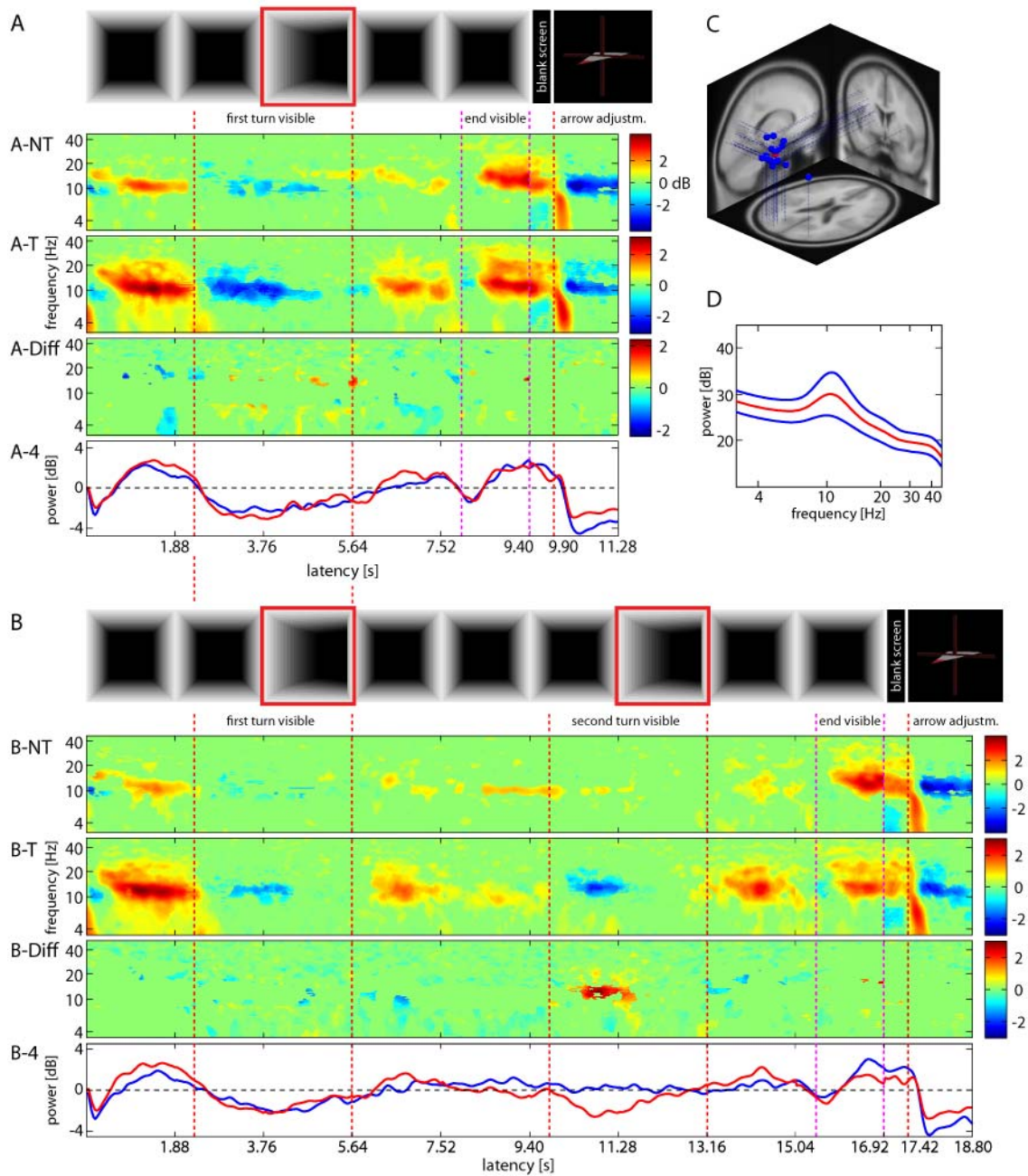


Figure 4.6: Mean event-related spectral perturbation (ERSP) images for an independent component cluster (ICC 5) located in or near middle occipital gyrus (BA 18/31). For explanation see Figure 4.4 (page 96).

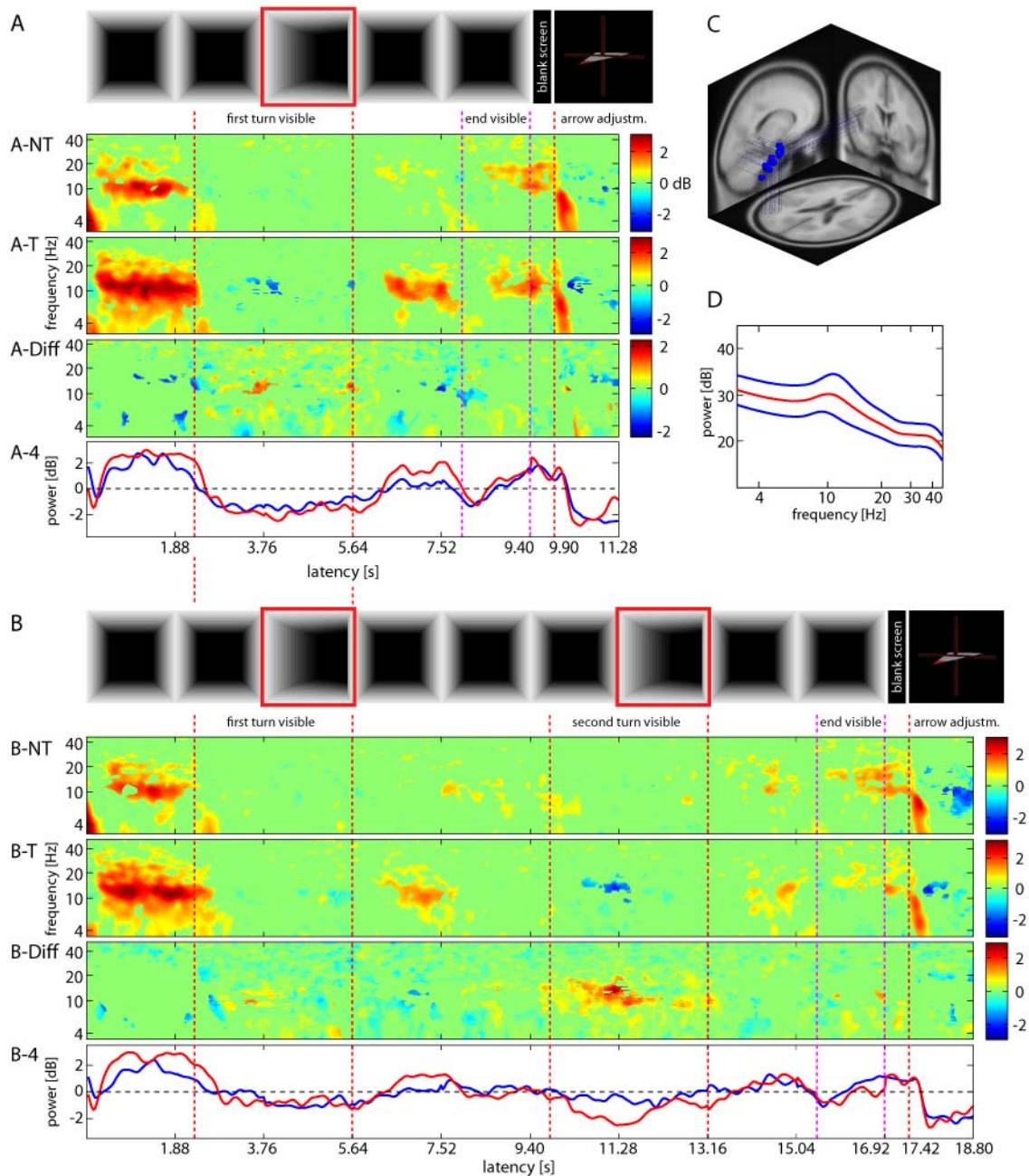


Figure 4.7: Mean event-related spectral perturbation (ERSP) images for an independent component cluster (ICC 7) located in or near left inferior temporal gyrus (BA 19/37). For explanation see Figure 4.4 (page 96).

***Superior (BA 7/31) and Inferior (BA 40) Parietal IC Clusters***

Activation patterns within parietal IC clusters resembled occipital IC cluster dynamics. However, alpha desynchronization during turns was found to be more pronounced in midline parietal clusters 6 and 11 as compared to inferior IC clusters 9 and 10.

In IC clusters located in or near midline superior parietal cortex (IC cluster 6), activation of Turners and Nonturners differed during the second turn, since Turners displayed more pronounced alpha blocking when approaching the curved segment (see Figure 4.8). Additionally, there was dissociation between strategy groups within the anterior IC cluster 11 (see Figure 4.9). Here, alpha desynchronization during turns as well as alpha synchronization during straight segments was significantly more pronounced for Turners as compared to Nonturners. Further, during the final segment of tunnels with two turns, Turners displayed an earlier increase in theta power as compared to Nonturners, which appeared already before the end of the passage came into view.

A massive synchronization of the alpha band in or near right inferior parietal cortex (IC cluster 10) marked the onset of the passage and sustained until the first turn came into view (see Figure 4.10). In the right hemisphere (IC cluster 9), by contrast, the tunnel onset was associated only with brief activation of a theta/alpha complex, followed by synchronization of the alpha band (near 10 Hz) and its first harmonic (near 20 Hz, see Figure 4.11). Importantly, both inferior parietal IC clusters revealed stronger alpha desynchronization during turns for Turners as compared to Nonturners, particularly when approaching and traversing the second turn. Additionally, Turners also displayed more pronounced alpha synchronization in straight segments following turns, resulting in significant differences between strategy groups.

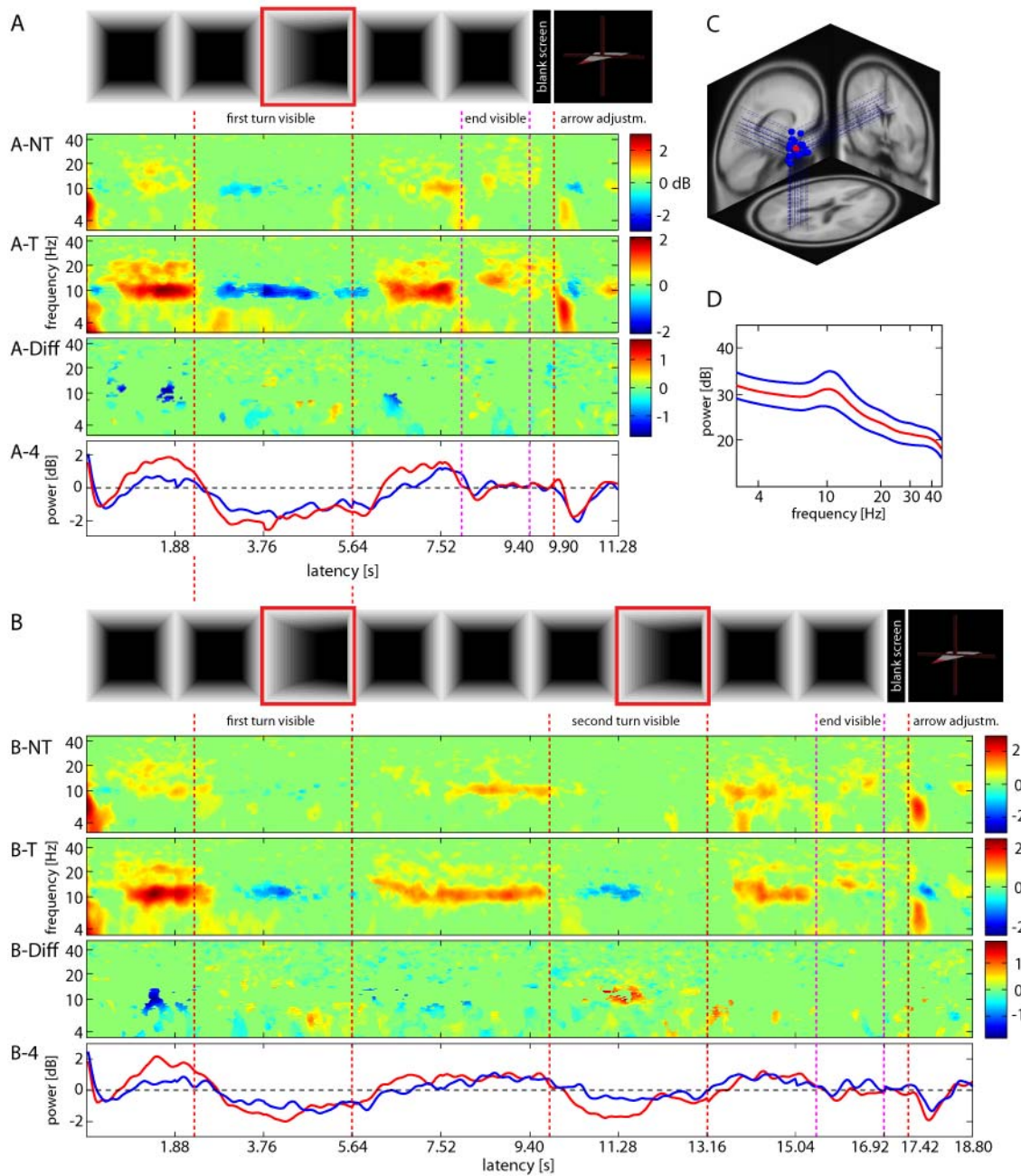


Figure 4.8: Mean event-related spectral perturbation (ERSP) images for an independent component cluster (ICC 6) located in or near midline precuneus (BA 7/31). For explanation see Figure 4.4 (page 96).

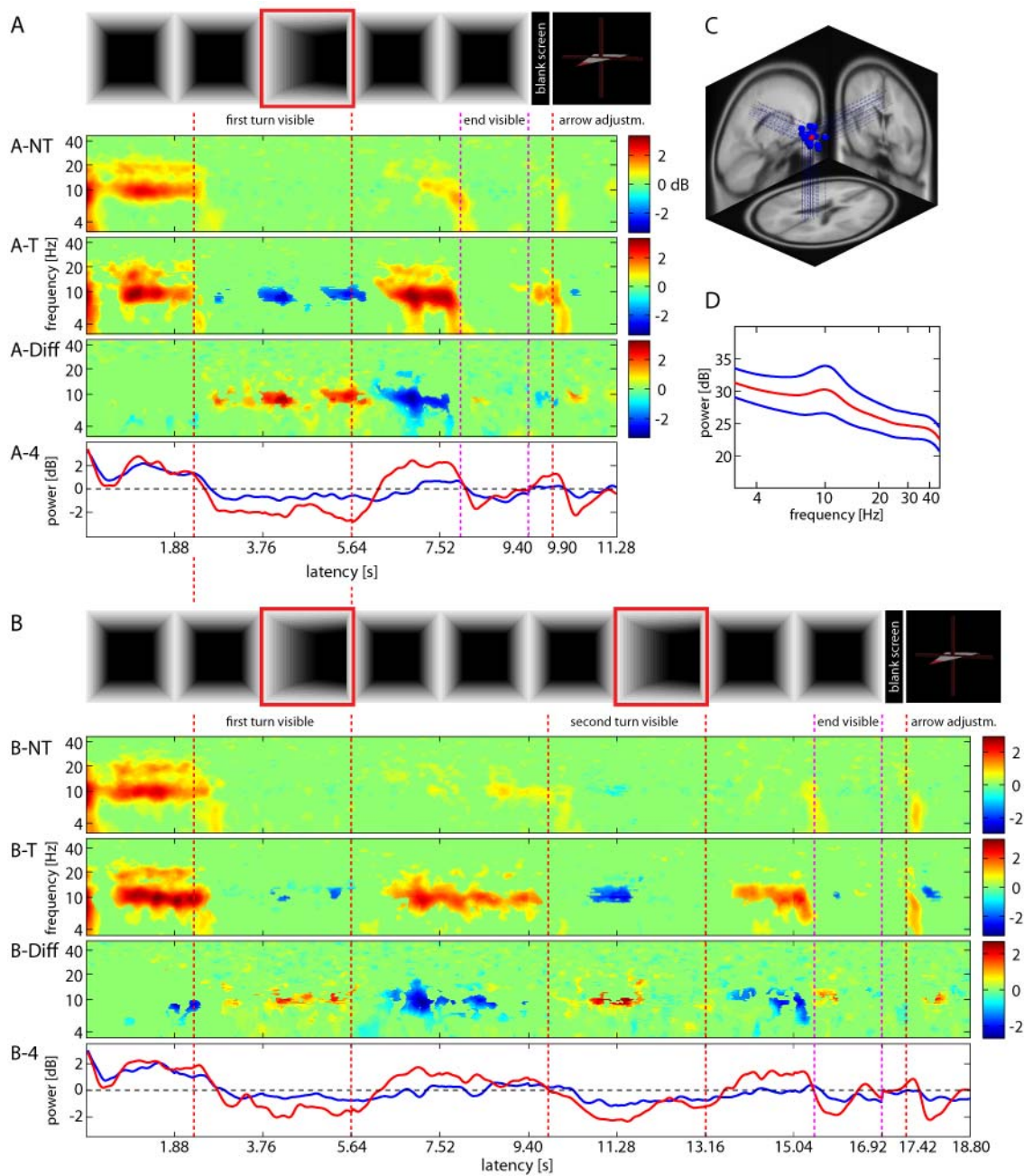


Figure 4.9: Mean event-related spectral perturbation (ERSP) images for an independent component cluster (ICC 11) located in or near midline precuneus (BA 7/31). For explanation see Figure 4.4 (page 96).

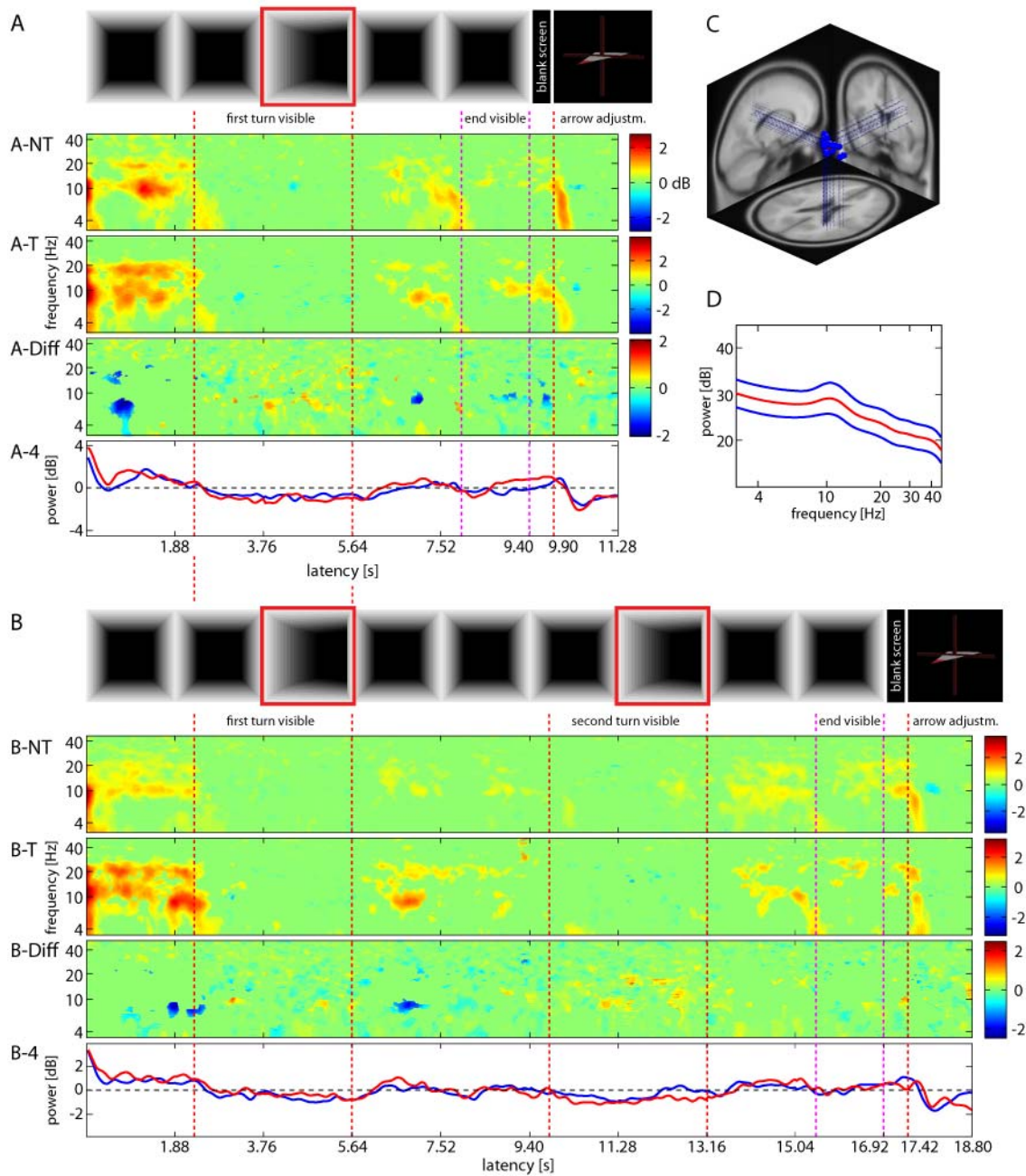


Figure 4.10: Mean event-related spectral perturbation (ERSP) images for an independent component cluster (ICC 9) located in or near right inferior parietal lobule (BA 40). For explanation see Figure 4.4 (page 96).

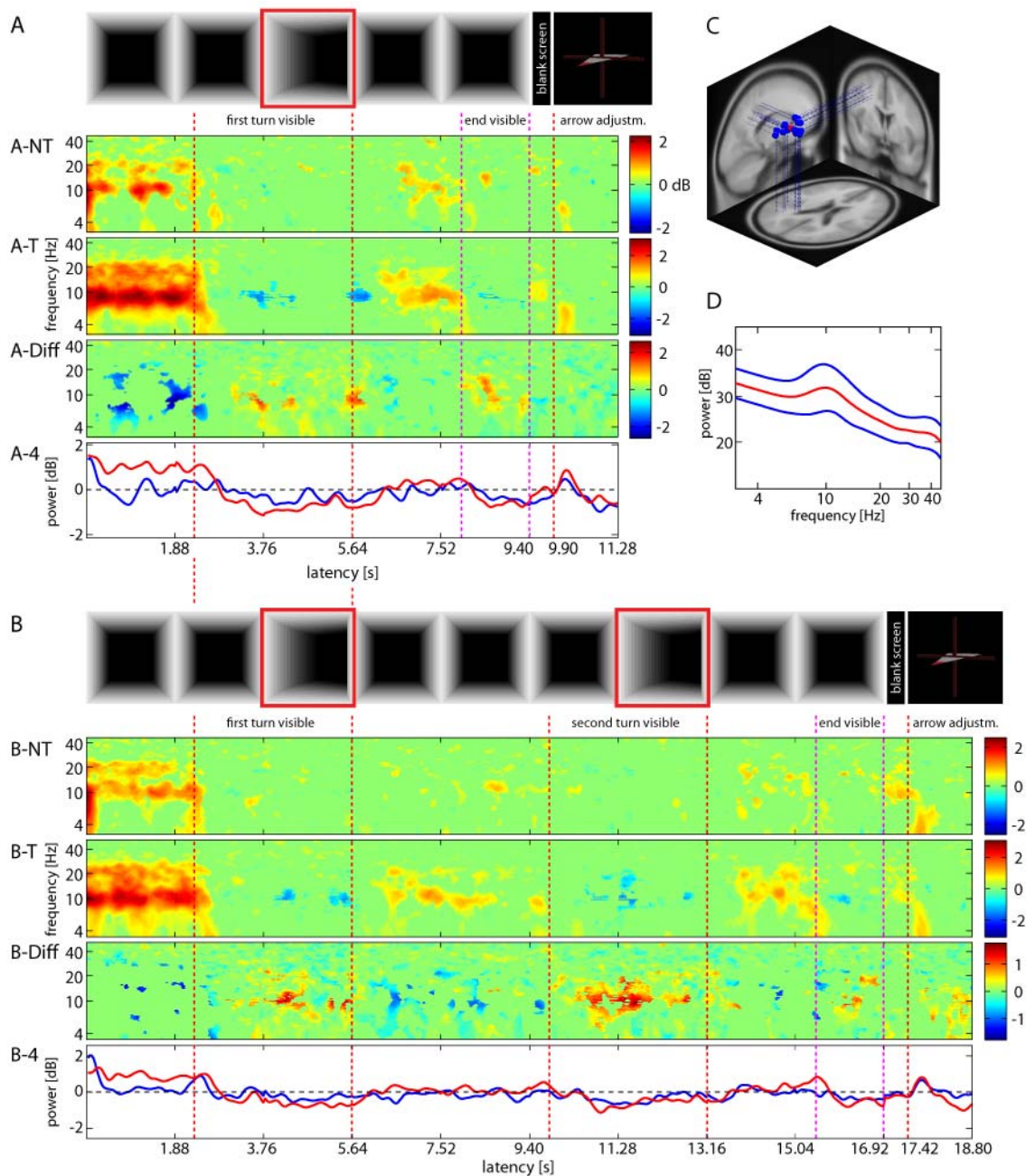


Figure 4.11: Mean event-related spectral perturbation (ERSP) images for an independent component cluster (ICC 10) located in or near left inferior parietal lobule (BA 40). For explanation see Figure 4.4 (page 96).

***Lateral Temporal (BA 21) and Cerebellar Lingual IC Clusters***

IC clusters 13 and 14 in or near right or left middle temporal cortex were found to exhibit comparable ERSP patterns for both strategy groups. Regarding theta band power, both IC clusters revealed a brief theta burst (near 4 – 8 Hz) upon entering the tunnel passage, followed by synchronization of the upper alpha frequency band (near 10 – 13 Hz), which persisted until the first turn came into view. Here, an augmented theta complex (near 4 – 8 Hz) of about 700 ms appeared. After the turn, alpha power was again found to be increased. As participants approached either the end of the tunnel or continued the outbound trajectory with a second turn, another theta burst appeared. In the right hemisphere, this final theta power increase was found at both complexity levels whereas in the left hemisphere increased theta activity at the tunnel end was predominantly found for tunnels with one turn. At both complexity levels, and more markedly in the right hemisphere, approaching the tunnel end was associated with increased oscillatory power of the alpha band (near 9 – 10 Hz) and its first harmonics (near 20 Hz, see Figure 4.12). The onset of the 3D arrow cue provoked another brief theta power increase, accompanied by decreased alpha power in the right hemisphere only.

IC cluster 12 located in or near midline cerebellar lingual cortex resembled comparable activation patterns at both complexity levels without resembling the final increase in alpha (10 – 13 Hz) and beta power (13 – 20 Hz) at the end of the passage.

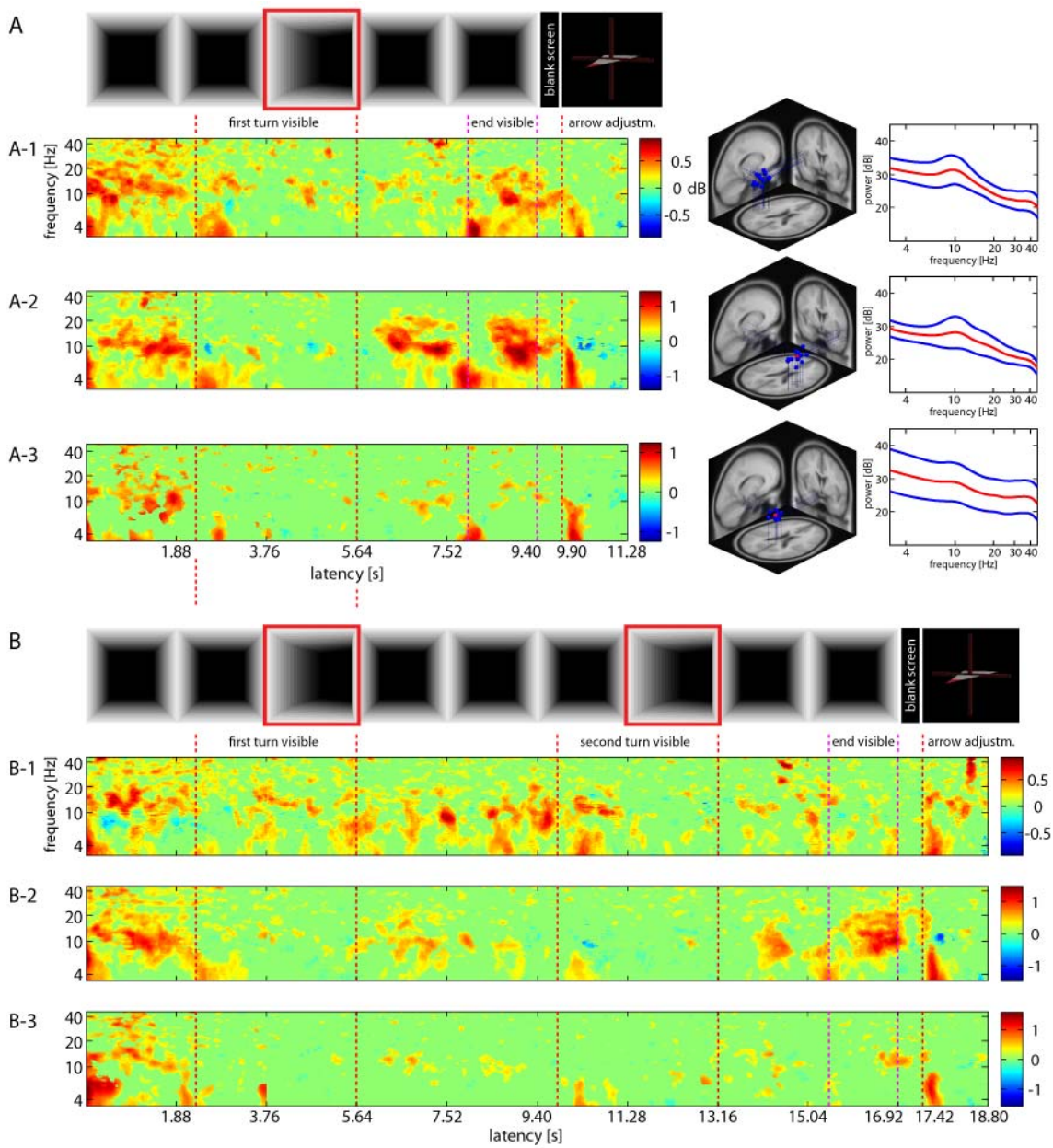


Figure 4.12: Mean event-related spectral perturbation (ERSP) images for three independent component clusters located in or near left (ICC 13, **A-1**, **B-1**) or right (ICC 14, **A-2**, **B-2**) middle temporal gyrus (BA 21), as well as cerebellar lingual gyrus (ICC 12, **A-3**, **B-3**) revealing task-dependent changes in spectral power during spatial navigation through tunnel passages containing one turn (panel A) and two turns (panel B) and subsequent homing arrow adjustment. Green colors indicate no significant ( $p > 0.001$ ) difference in mean log power (dB) from baseline. Warm colors indicate significant increases in log power and cold colors indicate significant decreases in log power from baseline. Important time points of the tunnel passage are marked with dashed lines: Red dashed lines indicate the period when participants perceived the approaching turn and the time period during the stimulus turn (from 3.76 s); magenta dashed lines indicate the time period during which the subjects were approaching the end of the tunnel. The final red dashed line indicates the time point when the virtual homing vector was displayed.

***Retrosplenial IC Cluster (BA 29/30)***

Activity of IC cluster 8 located in or near posterior cingulate/ retrosplenial cortex was found to share communalities particularly with posterior parietal clusters, e.g., the previously depicted theta bursts (near 4 – 8 Hz) at critical time-points of the passage, e.g., when turns or the tunnel end became visible. Another theta complex marked the onset of the 3D arrow cue. Importantly, Nonturners displayed more pronounced alpha blockage than Turners while approaching and entering the first turn, whereas approaching the second turn was associated with increased alpha desynchronization for Turners. Interestingly, Nonturners, but not Turners, displayed increased synchronization of the upper alpha band following the second turn (see Figure 4.13).

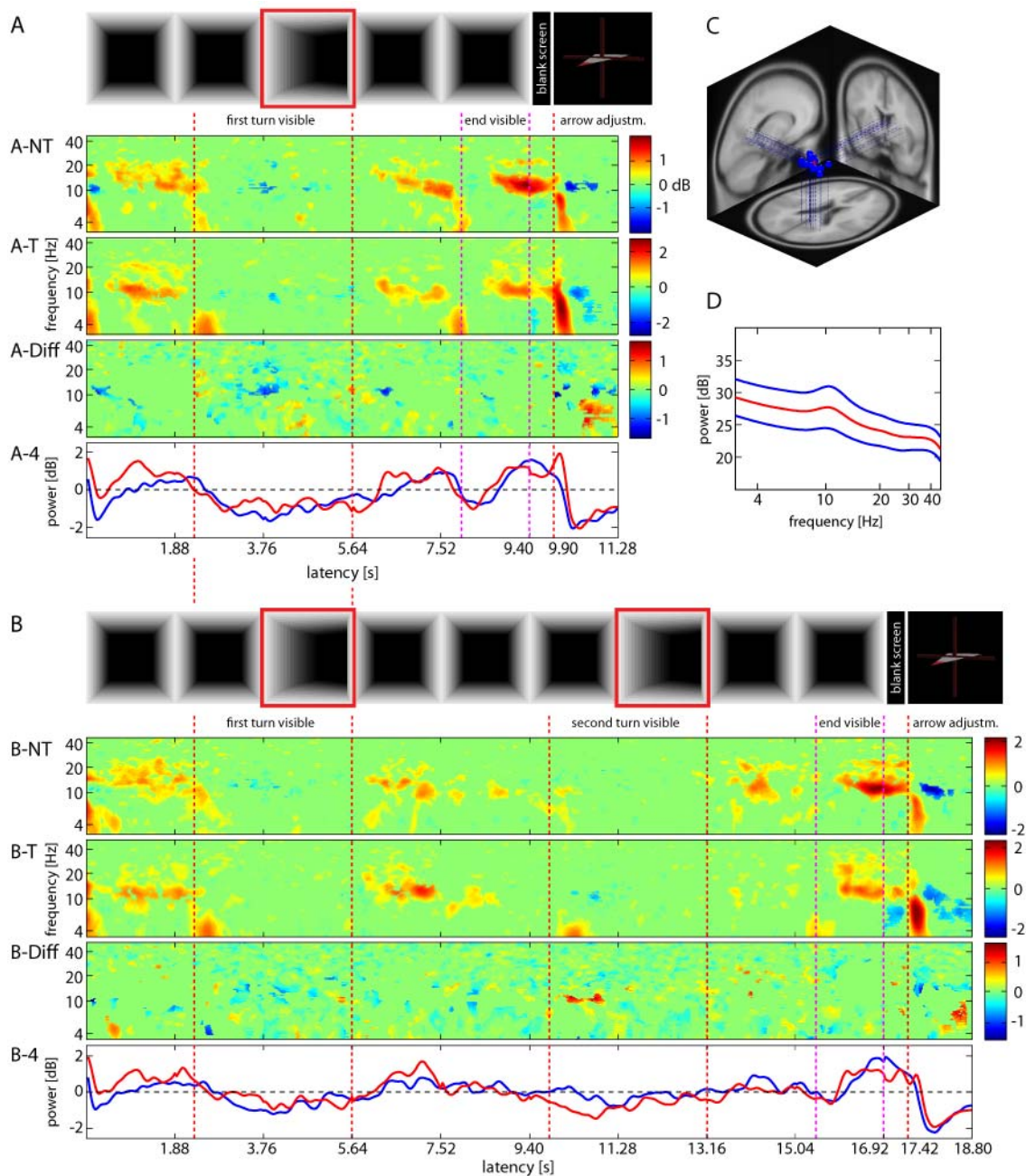


Figure 4.13: Mean event-related spectral perturbation (ERSP) images for an independent component cluster (ICC 8) located in or near right posterior cingulate/ retrosplenial cortex (BA 29/30). For explanation see Figure 4.4 (page 96).

***Precentral IC Clusters (BA 4/6)***

IC clusters 16 and 17 located in or near left or right precentral gyrus (BA 4/6) revealed dissociations in spectral dynamics between lower alpha (near 9 Hz and 18 Hz) and the upper alpha/mu frequency band (near 11 and 22 Hz). Within right prefrontal gyrus, upper alpha/mu activity decreased with movement onset and sustained until the participant entered the curved segment. This desynchronization was flanked by increased lower alpha activity. With onset of the turn, upper alpha/mu power increased, and persisted until approximately 500 ms after entering the straight post-turn segment. Interestingly, alpha desynchronization was only registered during the first, but not the second turn. Here, increased alpha power persisted until the end of the passage, more coherently for Nonturners as compared to Turners. For both tunnels with one turn and two turns, theta bursts marked significant time-points, e.g., the tunnel entrance, upcoming turns, as well as the tunnel end. Further, increased theta band activity was registered as the 3D arrow cue appeared (see Figure 4.14), initially followed by increased activity of the alpha/mu band (near 9 Hz and 18 Hz).

By contrast, in the left precentral IC cluster (contralateral to the response hand), activity within the upper alpha band was increased throughout the whole passage (peak baseline power near 11 Hz), whereas the flanking lower alpha/mu activity displayed significant deflections during the passage. E.g., the lower alpha frequency band and its first harmonic was initially increased, but as subjects approached the curved segment, synchronization was reduced to baseline level. During the first turn, only Turners displayed an additional increase in lower alpha/mu band power, whereas during the second turn both strategy groups showed this pattern. Approaching the end of the tunnel passage again provoked an alpha/mu desynchronization, followed by a relative increase in theta activity as the 3D arrow cue was presented (see Figure 4.15).

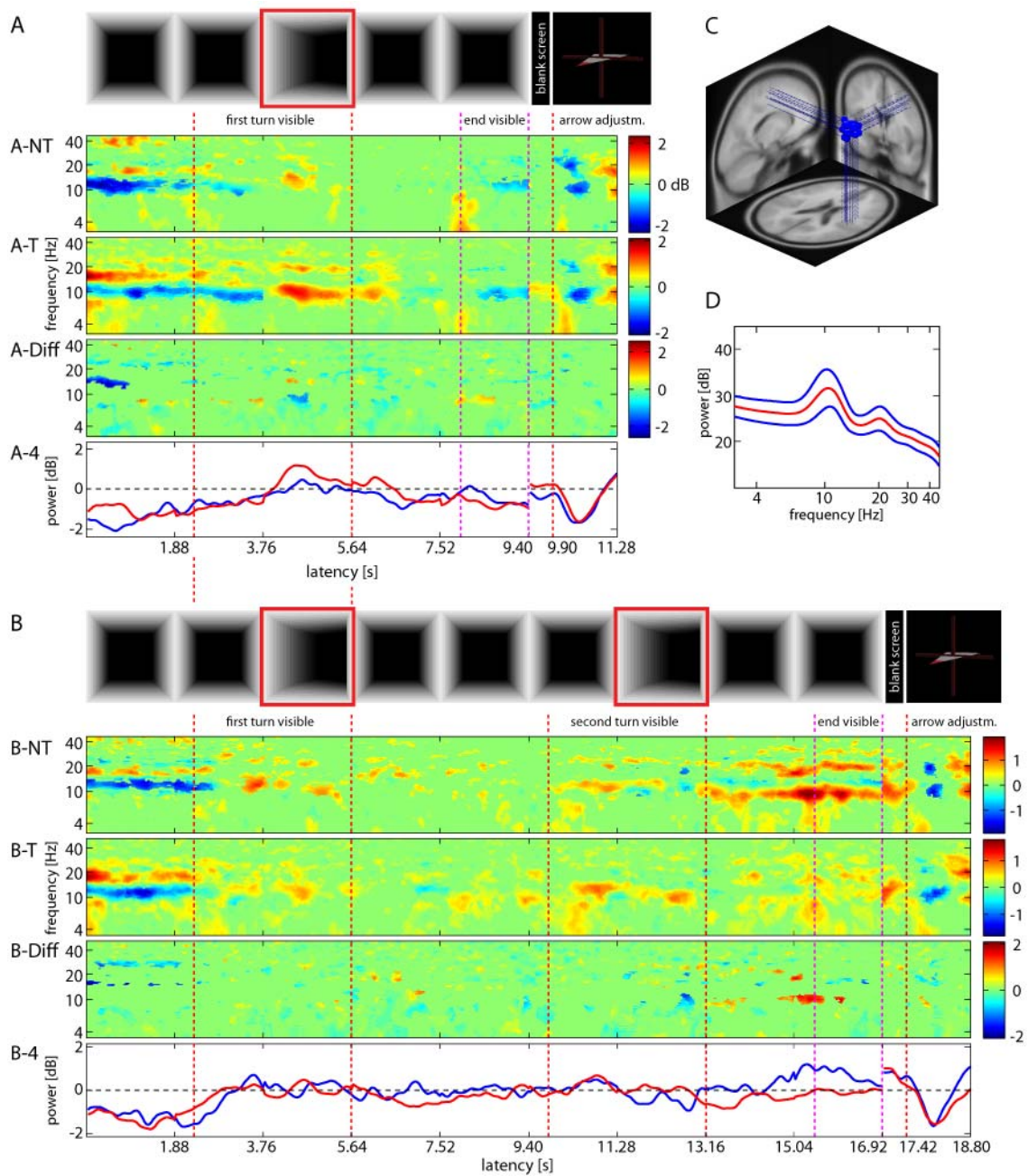


Figure 4.14: Mean event-related spectral perturbation (ERSP) images for an independent component cluster (ICC 16) located in or near right precentral gyrus (BA 4/6). For explanation see Figure 4.4 (page 96).

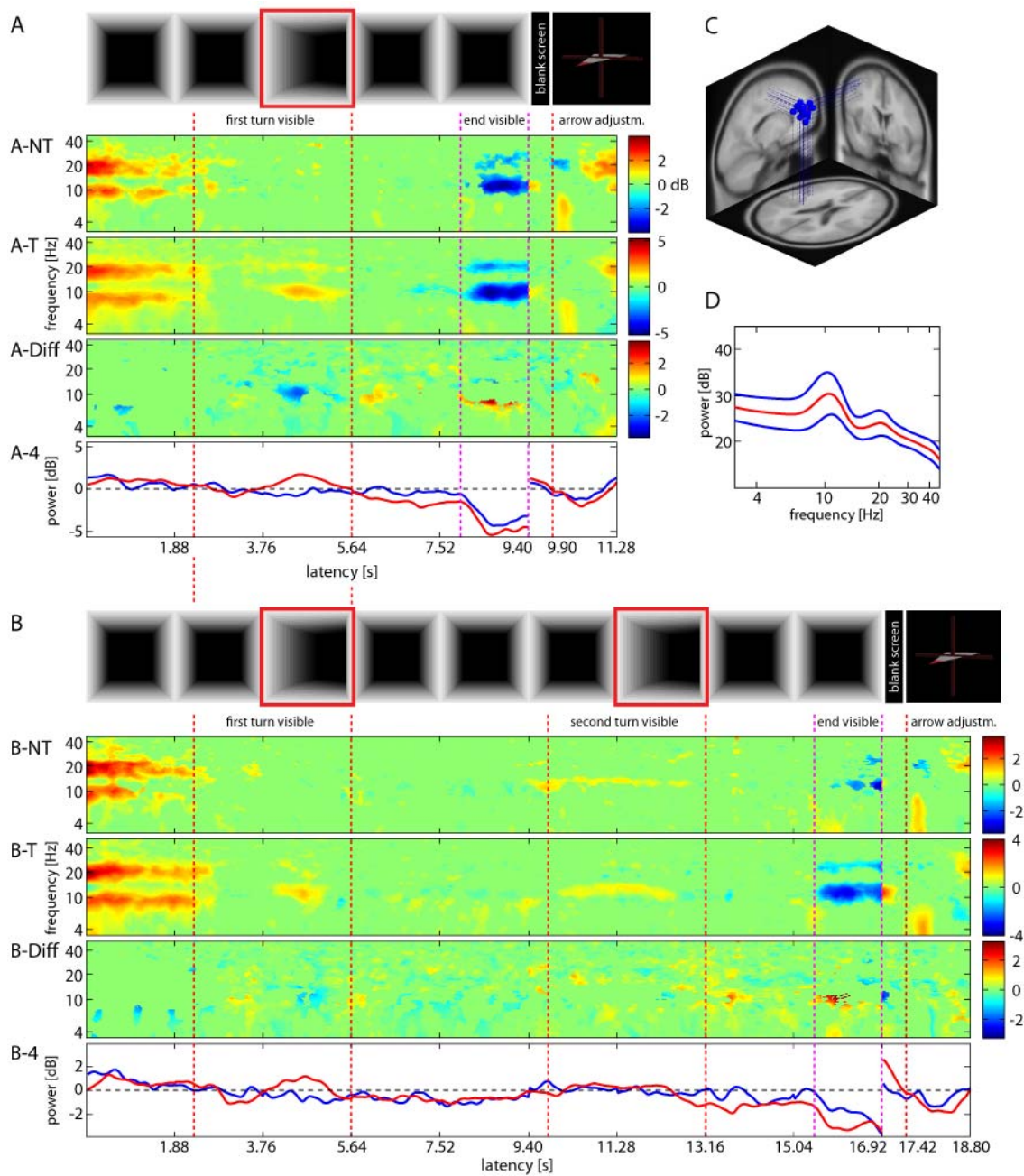


Figure 4.15: Mean event-related spectral perturbation (ERSP) images for an independent component cluster (ICC 17) located in or near left precentral gyrus (BA 4/6). For explanation see Figure 4.4 (page 96).

***Medial Frontal (BA 32) and Superior Frontal IC Clusters (BA 8)***

ERSP dynamics of IC cluster 18, located in or near midline medial frontal gyrus (BA 32), displayed increased theta activity (near 4 – 8 Hz) with movement onset, as the first turn came into view, as well as at the end of the turn (near 6 Hz). However, for tunnels with one turn another massive theta complex was located at the time-point of viewing the end of the passage, whereas for tunnels with two turns a comparable theta complex already appeared at the beginning of the second turn, preceded by several punctual theta bursts, see Figure 4.16).

In IC cluster 21, located in or near superior frontal gyrus (BA 8), movement onset was also associated with increased theta frequency band power (near 4 – 8 Hz). Additionally, initially increased oscillatory power of the lower alpha band (near 9 – 10 Hz) and its first harmonic (near 20 Hz) was registered, which persisted until onset of the turn. Approaching the apex of the turn provoked another power increase of the upper alpha frequency band (near 10 – 13 Hz), more markedly during the first turn of more complex tunnels. The previously depicted dislocation of the final theta burst at the end of tunnels with two turns was also registered in the current superior frontal cluster. Whereas for tunnels with one turn a final theta burst appeared upon viewing the tunnel end, for tunnels with two turns theta power already increased approximately 1000 ms before the second turn came into view. Punctual bursts of increased theta power accompanied the remaining passage, most pronounced approximately 500 ms after entering the final straight segment (At this time point, the end of the passage was still out of sight). Comparable activation patterns were also obtained for the remaining frontal IC clusters 15, 19, 20, and 22.

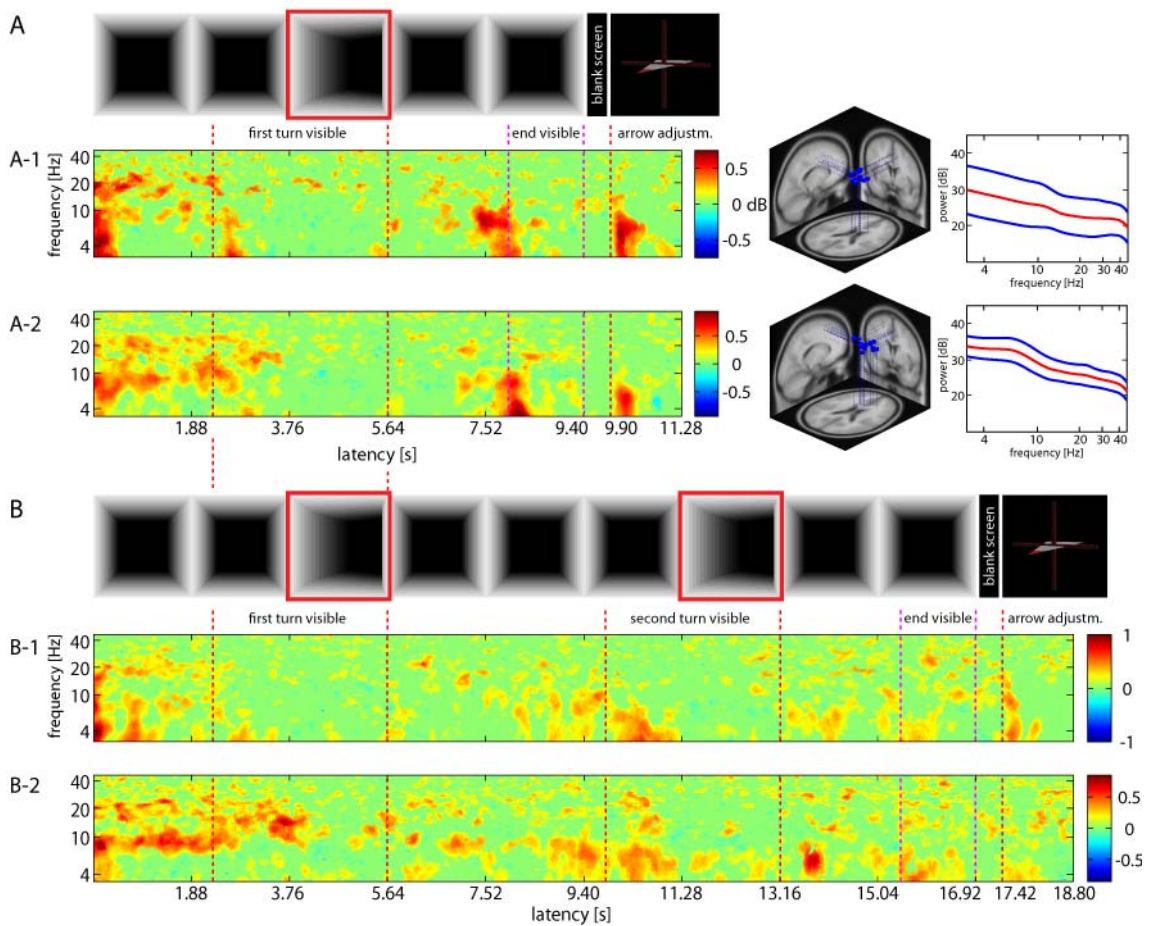


Figure 4.16: Mean event-related spectral perturbation (ERSP) images for two independent component clusters located in or near midline medial frontal gyrus (BA 32, ICC 18, **A-1**, **B-1**) and superior frontal gyrus (BA 8, ICC 21, **A-2**, **B-2**). For explanation see Figure 4.12 (page 107).

### 4.3.3 Discussion

Experiment 1 aimed at the identification of potential effects of pathway complexity in terms of overall length as well as number of consecutive turns along an outbound path on electrocortical dynamics of Nonturners and Turners, preferentially using an allocentric or an egocentric reference frame, respectively. Since each reference frame conveys distinct primitive parameters, which have to be updated during an outbound trajectory in order to keep up orientation, it was of particular interest whether spatial updating was accomplished continuously and irrespective of the pathway layout, or, by contrast, in a configural manner. Whereas continuous updating suggests oscillatory dynamics as well as behavioral responses to be unaffected by pathway layout and complexity, configural updating suggests that variations in pathway complexity significantly alter brain dynamics during spatial encoding as well as behavioral outcomes based on the retrieval of spatial knowledge (homing accuracy and latency).

Analysis of behavioral data provided evidence for participants being generally able to solve the task with high accuracy based on the acquisition, consolidation, and retrieval of spatial knowledge within distinct and individually preferred reference frames. Based on participants' performance the existence of a continuous or history-free updating mechanism could be rejected, since both Turners and Nonturners displayed systematic error and response time patterns that were significantly interlinked with features of the outbound path. Whereas for tunnels with one turn Turners and Nonturners displayed comparable errors in homing arrow adjustment, error patterns diverged during paths of higher complexity. However, after coordinate transformation of categorical end positions into the egocentric system, error patterns of Turners during tunnels with two turns bending into the same direction were found to resemble the regression tendencies of tunnels with one turn.

The existence of systematic regression tendencies in the present study suggested that the homing response was the result of a configural updating mechanism that allowed participants to not only update overall return bearing but also to store a more or less comprehensive record of the previously traversed pathway on the representational level (i.e., in spatial memory), which, in turn, affected the encoding of novel visuo-spatial information. In fact, the present behavioral results supported the conceptualizations of Klatzky et al. (1999). In their view, based on trial history, navigators build up route expectancies for each complexity level, so-called 'average pathways', that are retrieved from the representational level in a top-down manner whenever cognitive demands or memory-loss constrain a purely bottom-up encoding of incoming spatial information.

The question was, if this configural updating is also reflected in terms of oscillatory dynamics within distinct intracortical IC source locations reconstructed from continuous high-density scalp EEG recordings during the acquisition and retrieval of spatial knowledge. This procedure resembled for both strategy

groups a widespread cortical network compatible with results of recent functional imaging studies of spatial navigation and orientation (Committeri et al., 2004; Galati et al., 2000; Wolbers et al., 2007). Most generally, results replicated and extended findings of Gramann and colleagues (submitted) on spectral dynamics during spatial navigation on outbound paths containing a single turn.

Extraction of translational and rotational information from sparse visual flow was accompanied by specific variations in oscillatory power of several frequency bands within distinct cortical regions. E.g., cognitive processing in occipital and parietal cortices was primarily associated with activity of the alpha (near 10 Hz) frequency band, whereas in lateral prefrontal cortices mu (near 12 Hz), and in frontal cortex theta (near 6 Hz) activity dominated, bearing resemblance to findings of functional imaging studies on metabolic exchange rates accompanying the processing of spatial information from a first person perspective (Committeri et al., 2004; Hartley et al., 2003; Iaria et al., 2007; Maguire et al., 1998a; Wolbers & Büchel, 2005; Wolbers et al., 2007). Following, oscillatory dynamics will be discussed with special focus on the peak frequencies within the respective IC clusters.

### ***Primary Visual Cortex***

In or near primary visual cortex, processing of forward movement was associated with pronounced alpha band (near 10 Hz) synchronization, whereas upcoming and/or current heading changes were accompanied by alpha desynchronization, or alpha blockage as reported in experiments involving focused attention (Kaufman, Curtis, Wang, & Williamson, 1992; Makeig, 2002). With respect to the present navigation task, alpha blockage during upcoming tunnel curves most likely reflected increased cognitive load due to the processing of the relevant visual flow information in order to extract rotational and translational information (Maguire et al., 1998b). By contrast, the final increase in alpha power (near 10 – 12 Hz) most likely reflected a relative inhibition of visuo-spatial encoding in favor of memory retrieval in order to respond on the subsequent homing task (Klimesch, Sauseng, & Hanslmayr, 2007; Klimesch et al., 1993; Krause, Sillanmäki, Koivisto, Saarela, Häggqvist, Laine, & Hämäläinen, 2000; Stipacek, Grabner, Neuper, Fink, & Neubauer, 2003).

Importantly, alpha desynchronization during the first turn of more complex tunnels was less pronounced as compared to the one-turn condition, which was initially surprising since participants could not determine whether traversing a one-turn or a two-turn tunnel until either the end showed up or the passage continued with a second turn. However, due to the layout of the constructed tunnels, the first turn of more complex tunnels was generally smaller ( $10^\circ$  -  $76^\circ$ ) as compared to turns of tunnel configurations with only one turn ( $30^\circ$  -  $120^\circ$ ). Therefore, the rotational changes as provided by the visual flow were on average smaller than during larger turns of less complex tunnels, resulting in less pronounced desynchronization for both groups.

### **Secondary and Associative Visual Cortices**

Although the general pattern of alpha synchronizations and desynchronizations was also registered in secondary and associative visual areas (V3 and MT+, respectively), ERSP patterns of Turners and Nonturners markedly diverged as path complexity was increased. Here, Turners displayed more pronounced alpha desynchronization during the second turn as compared to Nonturners, suggesting increased visual processing of this strategy group (Foxe, Simpson, & Ahlfors, 1998; Pfurtscheller, Stancak, & Neuper, 1996; Vanni, Revonsuo, & Hari, 1997), which might be linked to the cognitively more demanding update of egocentric self-to-object bearings during the second rotation. Whereas area MT+ has been shown to be involved in scene processing (Ray & Cole, 1985), as well as heading estimation from certain components of optic flow, such as circular and radial motion (Fetsch et al., 2007; Morrone et al., 2000; Peuskens et al., 2001; Wall & Smith, 2008), dorsal area V3 codes spatial information within a retino-centered egocentric reference frame (Merriam et al., 2003; Morland et al., 2001). Interestingly, as the end of the passage came into view, Nonturners displayed increased alpha band power in or near right-hemispheric associative visual cortex (area V3, BA 19), suggesting event-related decreases in cortical processing of stimuli presented in the peripheral visual field (Galletti et al., 1995), including attention-related decoupling of visual processing along the dorsal pathway (Worden, Foxe, Wang, & Simpson, 2000) in order to facilitate allocentric processing along the ventral pathway.

### **Anterior and Posterior Parietal Cortex**

Indeed, during the confrontation with more complex tunnels, strategy-specific oscillatory activation patterns emerged within higher-order brain areas, primarily in midline posterior and anterior parietal cortex, resembling its functional role in coordinate transformation within multiple reference frames (Cavanna & Trimble, 2006). In posterior parietal IC sources, spectral dynamics of the alpha frequency band (near 10 – 13 Hz) largely corresponded to activity patterns obtained in occipital and occipito-parietal regions, with synchronized activity of the alpha band and its first harmonic (near 11 Hz and 20 Hz) during straight segments and alpha blocking during upcoming and current heading changes, replicating and extending results of Gramann et al. (2006; submitted). Again, the difference in activation patterns between Turners and Nonturners was more pronounced during the second turn, with Turners displaying significantly decreased alpha band activity, primarily upon entering the second turn, whereas Nonturners' alpha activity did not differ from baseline. As recently suggested by Cavanna & Trimble (2006), *posterior* parietal cortex is primarily involved in episodic memory retrieval. Therefore, the present results might suggest that in posterior parietal regions only Turners accomplished a self-centered processing of visuo-spatial information in order to update future heading during all turns (Field, Wilkie, & Wann, 2007), whereas Nonturners did not process heading changes when encountering the second turn. The different activation patterns between strategy groups were further embossed as activity spread towards anterior parietal cortex cluster locations. At both com-

plexity levels, Turners displayed more pronounced alpha band (near 10 Hz) desynchronizations during turns as well as alpha synchronizations during straight segments following the turning segments. Since *anterior* precuneus has been found to subserve self-centered mental imagery strategies (Cavanna & Trimble, 2006; Meltzer, Zaveri, Goncharova, Distasio, Papademetris, Spencer, Spencer, & Constable, 2007), the dynamics of the alpha frequency band might be linked to increased processing of self-to-object relations for Turners (see Calton & Taube, 2009). Results on spectral dynamics in or near inferior parietal clusters corresponded to findings of Gramann and colleagues (2006), who reported increased activity within this region exclusively for Turners, who seemingly coordinate spatial parameters such as self-to-object bearings within multiple reference frames, in collaboration with lateral parietal as well as posterior cingulate/ retrosplenial cortex (Cavanna & Trimble, 2006; Maguire, 2001).

### ***Retrosplenial Cortex***

Replicating and elaborating results of Gramann et al. (submitted), Nonturners displayed increased alpha band desynchronization and therefore stronger retrosplenial activation only during the first turn, irrespective of path complexity. By contrast, encountering the second turn resulted in more pronounced alpha desynchronization for Turners. Retrosplenial cortex possesses dense interconnections to medial temporal regions, dorsolateral prefrontal as well as posterior parietal cortex, and has been shown to serve as platform for exchange of egocentric and allocentric spatial information (Burgess et al., 2001; Ino et al., 2002; Maguire, 2001; Vann & Aggleton, 2004). Several studies on spatial navigation have provided evidence that increased activity within this region can be associated with transformation of reference-frame-specific spatial parameters into the alternative referential system (Byrne et al., 2007; Wolbers et al., 2007). The present findings suggest that for Nonturners these ego-to-allo transformations are accomplished by default. However, following the second turn, Nonturners again had to disrupt the exchange between referential systems, as evident from increased upper alpha band (near 11 Hz) synchronization (Klimesch, Doppelmayr, Schwaiger, Auinger, & Winkler, 1999), in order to reliably update spatial parameters within the preferred reference frame without further interference from the alternative referential system (Gramann et al., submitted). Turners, by contrast, seemingly resorted to the processing of combined egocentric and allocentric spatial information only when task difficulty in terms of pathway complexity became cognitively too demanding for solely relying on egocentric updating of position and orientation in space.

### ***Lateral Temporal Cortex and Cerebellar Lingual Structures***

Both strategy groups displayed comparable activity patterns within right- and left-hemispheric lateral temporal structures, which have been considered to support the construction of object representations that remain stable as the observing subject moves through the environment (Milner & Goodale, 1996). Theta (near 4 Hz) and alpha (near 10 Hz) deflections marked critical time

points of the passage (e.g., upcoming turns or the end of the passage), suggesting that these areas were involved in the encoding of spatial information into a coherent representation of the tunnel trajectory, irrespective of the navigator's current position and heading. Moreover, during paths of higher complexity theta also synchronized during the straight segment between turns. Although no rotational information was present in this interval, subjects seemingly coordinated the integration of information about the previous turn with translational information of the current straight segments (Riccobon, 2007).

Additionally, medial structures (cerebellar lingual/ claustrum) were found to display systematic deflections of the theta frequency band (near 4 Hz). Although no hippocampal activity was found in the current experiment, there is evidence for pronounced interactions between the claustrum and the lateral hippocampus, as well as retrosplenial cortex and visual cortices (LeVay & Sherk, 1981), supporting the interaction of several reference-frame specific areas in order to facilitate spatial navigation.

### **Premotor Cortex**

In left and right IC clusters in or near BA 4/6 (sensorimotor cortex and/ or frontal eye fields), different alpha sub-bands (lower alpha near 9 Hz vs. upper alpha/mu near 11 Hz and harmonics) were registered. In left premotor cortex (contralateral to the response hand), upon tunnel entrance the lower alpha band displayed increased power, which was reduced to baseline level as subjects approached the first turn. Upon entering the turn segment, power of the lower alpha band again increased. Importantly, approaching the second turn resulted in less synchronized alpha activity as compared to the first turn. However, alpha synchronization prevailed more consistently until the end of the turning segment. At the end of the passage, lower alpha power decreased, suggesting motor-related movement planning and –execution over Rolandic regions in order to accomplish the upcoming homing task (Pfurtscheller & Aranibar, 1979), thus replicating results of Gramann et al. (submitted).

Importantly, the increased activity during tunnel turns could only partially be explained by controlling of eye movements such as saccades as well as pursuit and optokinetic eye movements during visual flow stimulation (Field et al., 2007; Paus, 1996; Petit & Haxby, 1999). Analysis of ERSP dynamics associated with horizontal and vertical eye movements provided evidence for activity in premotor cortices to only partially overlap with oscillatory dynamics of eye movement clusters (e.g., right premotor cortex: vertical eye movements upon viewing the end of tunnels with two turns). Therefore, it seems to be reasonable to assume that premotor regions are also involved in processing of imaginary body rotations (de Vega & Rodrigo, 2001).

### **Medial Frontal Cortex**

In medial frontal IC clusters, theta band (near 4 – 8 Hz) power was found to be punctually increased at distinct time points of the passage, which has been associated with increased workload during the attention-based processing of

spatial information (Bischof & Boulanger, 2003; Caplan et al., 2000; Gramann et al., submitted; Kahana et al., 1999). The present results replicated and further extended previous findings on increased theta band power to emerge at critical time points of travel, e.g., during upcoming heading changes at decision points, reflecting frontal-executive control over spatial working memory processes (Gramann, 2002). However, the length as well as the position of these theta bursts was found to be affected by pathway complexity. During tunnels with one turn, theta appeared at the beginning of the virtual passage, upon viewing the first turn and the tunnel end. Whenever the tunnel continued with a second turn, single theta bursts already appeared approximately 1500 ms before viewing the second turn, culminating in a pronounced theta complex as participants were approaching and entering the turning segment. Additionally, in anterior frontal IC cluster sites, both groups were found to display a pronounced theta burst within the last straight segment of an outbound passage, although the end was still not visible. Therefore, this theta burst most likely reflected the impact of executive processes on spatial information processing in a top-down manner, bearing resemblance to the conceptualizations of Klatzky et al. (1999) on the role of internal expectancies on spatial encoding. As subjects had passed the final turn, they might have resorted to an internal ‘average path’, derived from the representational level, instead of further encoding the incoming visuo-spatial information, which was inevitably identical for all tunnels (therefore mirroring the finding of alpha blockage in premotor cortex at the end of the passage). However, solely based on the present data this conclusion remains putative and requires further examination.

### **Conclusion**

Taken together, the present experiment provided evidence for egocentric and allocentric reference frames to encode visuo-spatial information from sparse visual flow in a configural manner, i.e., by updating spatial parameters not continuously but at certain time-points of the passage, e.g., as turns or the end of the passage came into view. Translational and (upcoming and current) rotational information was accompanied by specific oscillatory deflections. Importantly, when confronted with increased path complexity, both strategy groups were found to display comparable oscillatory dynamics in anterior clusters, e.g., midline medial frontal cortex, suggesting that allocentric and egocentric spatial encoding was moderated by executive top-down attentional control, corroborating the assumptions of the extended encoding-error model of Klatzky et al. (1999). However, the increase in complexity also had differential effects on spectral dynamics of Turners and Nonturners, particularly during the extended straight segment between turns as well as during the upcoming and current second turn. Most pronounced differences between Turners and Nonturners were found within IC source locations located in posterior cortical regions, e.g., occipital, occipito-parietal and parietal regions. For Nonturners, confrontation with more complex pathways resulted in less pronounced egocentric information processing of body rotations during and after the second

turn, as evident from blocking of occipito-parietal, as well as retrosplenial regions. Turners, by contrast, displayed pronounced oscillatory deflections in parietal regions, which were additionally enriched by increased retrosplenial activation during the second turn. Turners, confronted with increased complexity-related ambiguities in egocentric spatial updating, might have therefore resorted to the additional integration of allocentric information in order to reliably update spatial parameters.

## 4.4 Experiment 2 – Opposite Directions

The question was, if these patterns could be replicated when participants traversed tunnels with one turn and two opposite turns of equal angularity, resulting in identical egocentric and allocentric eccentricities of end position. The use of tunnels with two complementary turns of similar angularity results in parallel start- and end segments with identical return bearings for Turners and Nonturners. This configuration was supposed to be of higher complexity as compared to Experiment 1, since within an egocentric reference frame far more spatial parameters have to be updated as compared to the allocentric reference frame. For example, when Turners traverse a turn to the right side, the relative position of the starting point, and therefore their internal ‘homing vector’, changes to the right. An additional, consecutive turn to the left causes Turners’ homing vector to pass the sagittal axis of the navigator from the right to the left side. By contrast, Nonturners traversing the described tunnel configuration should maintain an allocentric bearing throughout the passage that always points to their left.

### 4.4.1 Methods

#### 4.4.1.1 Participants

Eighteen male subjects recruited from the Ludwig-Maximilians-University Munich, Germany, took part in Experiment 2 (age ( $M \pm SD$ ) =  $25.60 \pm 3.42$  years). The experiment followed the American Psychological Association's (APA's) Ethical Principles of Psychologists and Code of Conduct (American Association of Psychology, 2002). Participants were either paid 8€ per hour or received course credit for taking part in the experiment. Ten subjects were categorized as Turners and eight subjects were categorized as Nonturners prior to the main experiment. All subjects had normal or corrected to normal vision and reported no history of neurological disorder. None of the Turners and three Nonturners were left-handed.

#### 4.4.1.2 Task, Materials, and Procedure

The experimental environment was the same as reported for Experiment 1. Prior to the main experiment subjects underwent the categorization task. After a brief training the main experiment started, including 20 blocks á 9 tunnels with minor in-between breaks. The experimental procedure was identical to Experiment 1. Tunnels with one turn had five segments, with the two initial and two final straight segments enclosing the turning segment of varying angles. Tunnels with two opposite turns of equal angularity had a total of nine segments (turns located in segments 3 and 7). Tunnels ended at categorical end positions of 15°, 30°, and 45° eccentricity to the left and right relative to the starting point. After the outbound path presentation, participants had to adjust the homing vector to point directly back to the starting point (no time limit for adjustment). Since subjects were categorized a priori, in 10% of the trials feedback on their adjustment accuracy was displayed dependent on the preferred reference frame.

#### 4.4.1.3 Performance Measures, EEG Recordings and Statistical Analyses

Mixed-design ANOVAs were conducted in order to reveal effects of the following factors on behavioral performance (homing accuracy and latency): 'Number of Turns' (one vs. two), 'Eccentricity of End Position' (15°, 30°, or 45°, respectively), 'Side' of the tunnel passage (right vs. left, relative to the starting point), as well as the between-subjects factor 'Preferred Strategy' (Turners vs. Nonturners). Analyses revealed no significant main effect or interaction of the factor 'Side' on error scores [absolute error:  $F(1, 16) = 1.908, p = .186$ ], therefore tunnels were collapsed in a final  $2 \times 3$  mixed-design analysis with repeated measures over the factors 'Number of Turns' (one vs. two) and 'Eccentricity of End Position' (15°, 30°, or 45°) with the subject's preferred 'Strategy' as between-subject measure.

EEG data recording and analysis resembled the procedure of Experiment 1 (section 4.3.1, pages 85ff.).

### 4.4.2 Results

#### 4.4.2.1 Behavioral Performance

Behavioral results are depicted in detail in 3.5.2. In contrast to Experiment 1, side errors were found to be increased for tunnels with two turns ( $M \pm SD = 9.63\% \pm 14.83\%$ ). However, expected and adjusted angular responses correlated significantly for both Nonturners,  $r(96) = .930, p < .0001$ , and Turners,  $r(120) = .892, p < .0001$ . Both strategy groups displayed a decreasing pattern in correlation coefficients for tunnels with one and two turns (Nonturners:  $r_{1\text{-turn}}(48) = .968$  and  $r_{2\text{-turns}}(48) = .895$ ; Turners:  $r_{1\text{-turn}}(60) = .951$  and  $r_{2\text{-turns}}(60) = .899$ ;  $p < .0001$ ; one vs. two turns:  $p < .04$ ).

Response time was marginally affected by the Number of Turns [ $F(1, 16) = 4.386, p = .053, \eta_G^2 = .008$ ]. Other factors did not take impact on response latencies [Strategy:  $F(1, 16) = 1.626, p = .220$ ; Eccentricity:  $F(2, 32) = 1.260, p = .297$ ]. Absolute error scores showed a significant influence of Number of Turns [ $F(1, 16) = 22.273, p < .0001, \eta_G^2 = .161$ ]. Additionally, absolute errors were significantly affected by Eccentricity of End Position [ $F(1.40, 32) = 41.594, p < .0001, \eta_G^2 = .402$ ], as well as an interaction of Number of Turns  $\times$  Eccentricity of End Position [ $F(1.40, 32) = 11.643, p < .001, \eta_G^2 = .153$ ]. Both strategy groups displayed decreasing homing accuracy for tunnels ending at 45° eccentricity, even more pronounced for tunnels with two turns.

With respect to the direction of error, significant main effects of Preferred Strategy [ $F(1, 16) = 4.877, p < .046, \eta_G^2 = .082$ ], Eccentricity of End Position were obtained [ $F(1.20, 32) = 83.456, p < .0001, \eta_G^2 = .455$ ], and Number of Turns [ $F(1, 16) = 22.173, p < .0002, \eta_G^2 = .290$ ], with more pronounced underestimation of eccentricity for more complex tunnels. Additionally, the interaction of Number of Turns  $\times$  Eccentricity of End Position was found to take impact on signed error scores [ $F(1.42, 32) = 13.113, p < .0005, \eta_G^2 = .102$ ]. With increasing laterality of end position, subjects displayed stronger underestimation of eccentricity. This tendency was additionally intensified for tunnels with two opposite turns (see Figure 3.13).

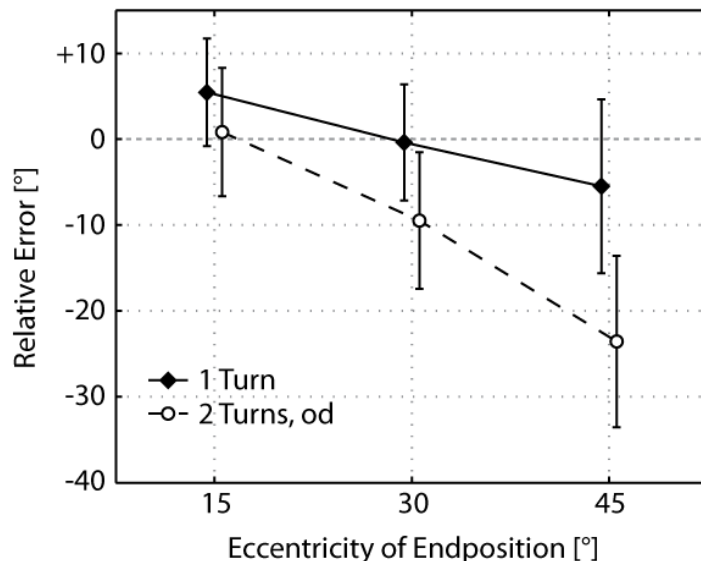


Figure 4.17: Experiment 2 – Mean signed error ( $\pm 1$  SD, depicted by the error bars) of the adjusted homing vector for tunnels with one turn (solid line) and two turns (dashed line), dependent on the eccentricity of end position relative to the origin of the path (sides were concatenated), averaged over Nonturner and Turner subjects.

#### 4.4.2.2 Source Reconstruction

22 clusters were obtained, with two clusters mirroring horizontal and vertical eye movement artifacts, as well as 20 clusters reflecting functional generator sources of maximally independent cortical processes. Stereotaxic Talairach coordinates (Lancaster et al., 2000) as obtained via software-based reconstruction (<http://www.talairach.org/applet.html>, Lancaster et al., 2000), residual variances, functional allocations within Brodmann Areas and the number of (Non-)Turner subjects and ICs within each cluster are summarized in Table 4.2. On average,  $M \pm SD = 16.83 \pm 2.18$  Independent Components per subject were obtained (range: 13 to 22). The relative number of localizable brain ICs in Nonturners and Turners (127 and 149) did not differ within the 20 non-artifactual clusters [ $F(1, 274) = .323, p = .570$ ].

| CI    | Talairach |     |     | RV<br>[%] | Brodmann Areas |                                     | $S_{NT}$ | $S_T$ | $IC_{NT}$ | $IC_T$ |
|-------|-----------|-----|-----|-----------|----------------|-------------------------------------|----------|-------|-----------|--------|
|       | x         | y   | z   |           |                |                                     |          |       |           |        |
| 1     |           |     |     |           |                | Parent Cluster                      | 8        | 10    | 151       | 177    |
| 2     |           |     |     |           |                | Outlier                             |          |       | 5         | 5      |
| 3     | 5         | -80 | -10 | 3.27      | BA 18          | R lingual gyrus                     | 2        | 6     | 2         | 9      |
| 4     | -22       | -80 | 12  | 3.37      | BA 17/18       | L (bilat.) middle occipital gyrus   | 4        | 6     | 5         | 6      |
| 5     | 32        | -78 | -1  | 3.57      | BA 18/19       | R (bilat.) inferior occipital gyrus | 6        | 9     | 9         | 17     |
| 6     | -35       | -71 | -13 | 2.58      | BA 18/19       | L (bilat.) middle occipital gyrus   | 5        | 4     | 6         | 5      |
| 7     | 7         | -69 | 27  | 2.34      | BA 7/31        | R (pre-)cuneus                      | 5        | 7     | 6         | 11     |
| 8     | -32       | -48 | 10  | 4.23      | -              | L superior temporal gyrus           | 3        | 6     | 4         | 7      |
| 9     | -2        | -48 | 9   |           | BA 29/30       | L (midline) posterior cingulate     | 4        | 4     | 8         | 8      |
| 10    | 30        | -45 | 29  | 3.83      | BA 40          | R supramarginal gyrus               | 5        | 10    | 6         | 14     |
| 11    | -6        | -45 | 43  | 2.31      | BA 7/31        | L precuneus                         | 6        | 8     | 9         | 10     |
| 12    | -37       | -31 | 44  | 3.09      | BA 40          | L inferior parietal lobule          | 3        | 6     | 4         | 11     |
| 13    | 26        | -29 | 45  | 3.14      | BA 4           | R precentral gyrus                  | 4        | 6     | 5         | 7      |
| 14    | 43        | -24 | -1  | 5.96      | BA 13          | R superior temporal gyrus           | 4        | 4     | 7         | 4      |
| 15    | -51       | -21 | -18 | 4.32      | BA 20          | L inferior temporal gyrus           | 5        | 5     | 6         | 5      |
| 16    | -38       | -20 | 60  | 1.87      | BA 4/6         | L precentral gyrus                  | 6        | 3     | 9         | 6      |
| 17    | 41        | -13 | 56  | 2.47      | BA 4/6         | R precentral gyrus                  | 7        | 10    | 12        | 15     |
| 18    | 4         | -11 | 63  | 2.70      | BA 6           | R medial frontal gyrus              | 3        | 1     | 5         | 1      |
| 19    | -33       | -6  | 46  | 4.93      | BA 6           | L middle frontal gyrus              | 4        | 1     | 5         | 1      |
| 20    | 12        | 6   | 29  | 4.04      | BA 32          | R cingulate gyrus                   | 7        | 4     | 12        | 4      |
| 21    | -24       | 20  | 17  | 5.15      | -              | L claustrum                         | 4        | 3     | 4         | 3      |
| 22    | 3         | 37  | 27  | 2.23      | BA 9/32        | R medial frontal gyrus              | 3        | 5     | 3         | 5      |
| $e_h$ | -1        | 48  | -30 | 10.12     |                | horizontal EOG cluster              | 8        | 10    | 8         | 10     |
| $e_v$ | -1        | 50  | -29 | 6.20      |                | lateral EOG cluster                 | 8        | 10    | 11        | 13     |

Table 4.2: Experiment 2 – Lateral and horizontal EOG and 20 functional clusters, sorted from posterior to anterior IC cluster sites (along the y-axis). Columns provide information regarding (1) the location of the cluster centroids in Talairach coordinates (x-y-z). All reconstructed clusters for each condition were anatomically specified within the stereotaxic coordinate system of Talairach and Tournoux using the Talairach demon software, returning the coordinates of the nearest grey-matter point. Further, the table provides information regarding (2) the residual variance (RV, in %) of the reconstructed cluster centroids, and (3) their anatomical region defined in the Brodmann Area system (BA, Brodmann, 1925). Finally, the table gives information regarding the number of Nonturner and Turner subjects ( $S_{NT}$ ,  $S_T$ ), as well as the amount of Nonturner and Turner Independent Components ( $IC_{NT}$ ,  $IC_T$ ) within each cluster.

#### 4.4.2.3 Cluster Dynamics

##### ***Occipital (BA 17/18) and Occipito-Parietal (BA 19) IC Clusters***

IC cluster dynamics in or near occipital and occipito-parietal regions replicated and extended results of Experiment 1. Spectral dynamics of the peak alpha frequency band (near 11 Hz) were closely linked to the visual flow stimulation, with synchronizations being present during straight segments as well as upon encountering the end of the passage, and desynchronizations accompanying rotations. However, the preferred utilization of an egocentric or an allocentric reference frame moderated the amount of deviation from baseline. In all occipital and occipito-parietal areas except IC cluster 4 in or near bilateral cuneus, Turners displayed decreased alpha band power during the first turn, most pronounced as they entered the turning segment (see Figure 4.18 and Figure 4.19). By contrast, during the second turn desynchronization comprised an increased frequency range (near 9 – 13 Hz), and persisted longer, i.e., until the end of the curved segment. Nonturners, by contrast, showing comparable alpha synchronization during straight segments, revealed decreased alpha band power during upcoming heading changes only in IC clusters in or near inferior occipital cortex, more markedly in the left hemisphere (see Figure 4.20). Here, alpha blocking during the second turn was even more pronounced as compared to Turners.

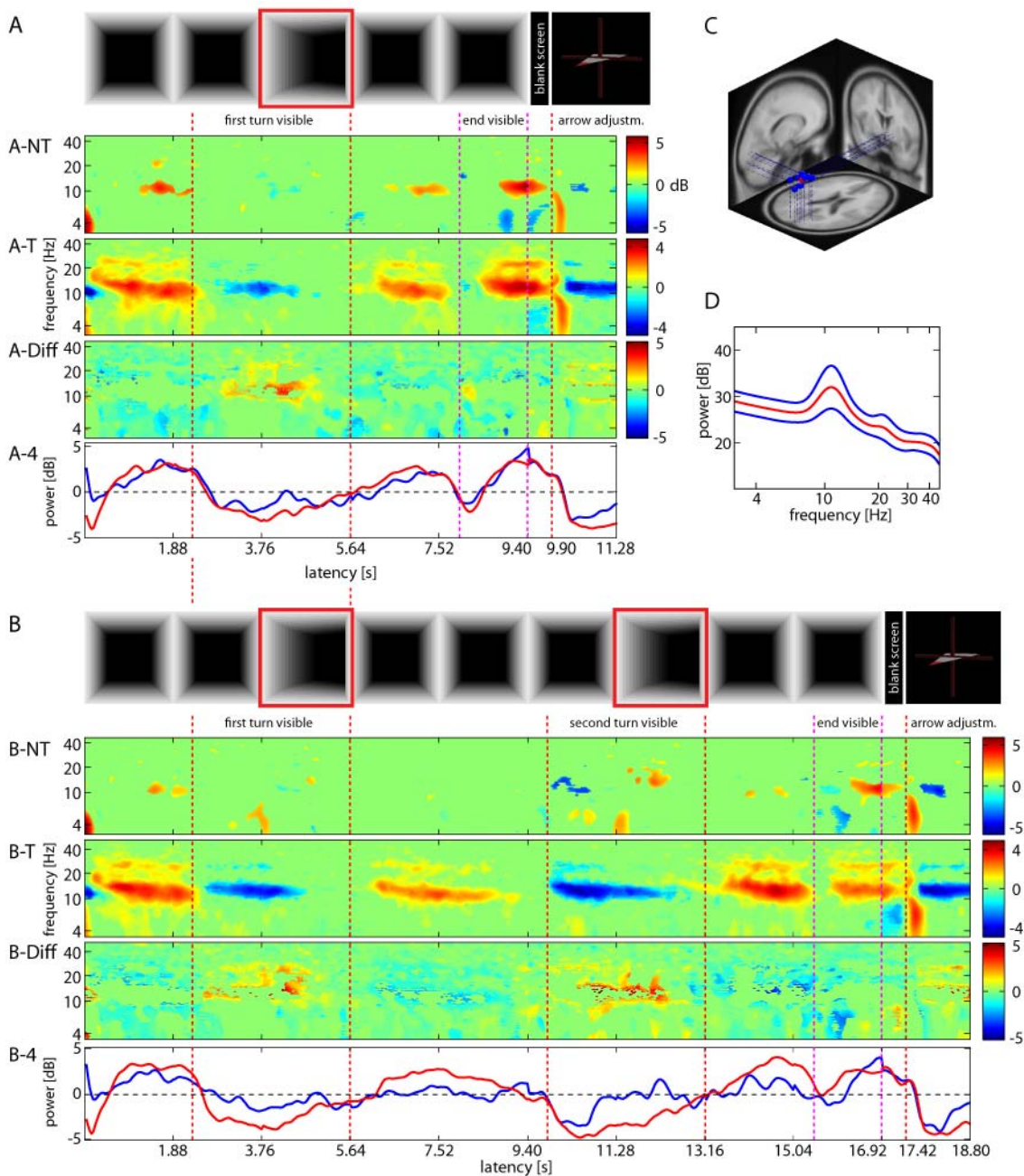


Figure 4.18: Mean event-related spectral perturbation (ERSP) images for an independent component cluster (ICC 3) located in or near right lingual gyrus (BA 18, panel C) revealing task-dependent changes in spectral power during spatial navigation through tunnel passages containing one turn (panel A) and two turns (panel B) and subsequent homing arrow adjustment. Cluster centroid mean ERSPs are plotted in log-spaced frequencies from 3 – 45 Hz for 2 IC processes of 2 Nonturner subjects (**A-NT**, **B-NT**), and 9 IC processes of 6 Turner subjects (**A-T**, **B-T**). ERSP difference between Nonturners and Turners is shown in panels **A-Diff** and **B-Diff** for tunnels with one turn and tunnels with 2 turns, respectively [see the following page for further explanation].

Green colors indicate no significant ( $p > 0.001$ ) difference in mean log power (dB) from baseline (mean activity of all tunnel passages; mean [ $\pm 1$  SD] baseline power depicted in **panel D**). Warm colors indicate significant increases in log power and cold colors indicate significant decreases in log power from baseline. Panels **A-4** and **B-4** depict dynamics in mean power (dB) over time for the (9 – 12 Hz) alpha band, separately for Nonturners (blue) and Turners (red). Important time points of the tunnel passage are marked with dashed lines: Red dashed lines indicate the period when participants perceived the approaching turn and the time period during the stimulus turn (from 3.76 s); magenta dashed lines indicate the time period during which the subjects were approaching the end of the tunnel. The final red dashed line indicates the time point when the virtual homing vector was displayed.

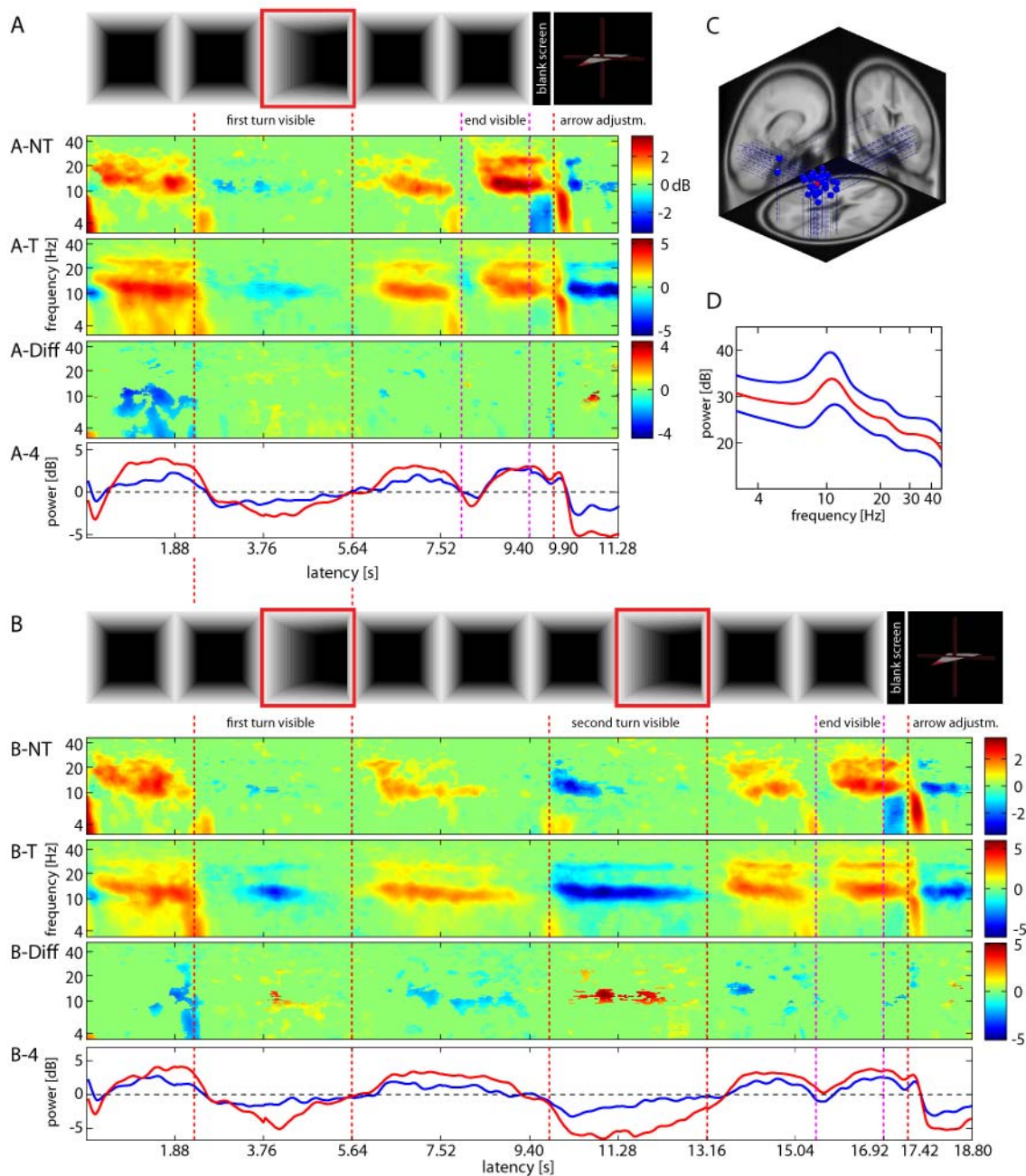


Figure 4.19: Mean event-related spectral perturbation (ERSP) images for an independent component cluster (ICC 5) located in or near right (bilateral) inferior occipital gyrus (BA 18/19). For explanation see Figure 4.18 (page 127).

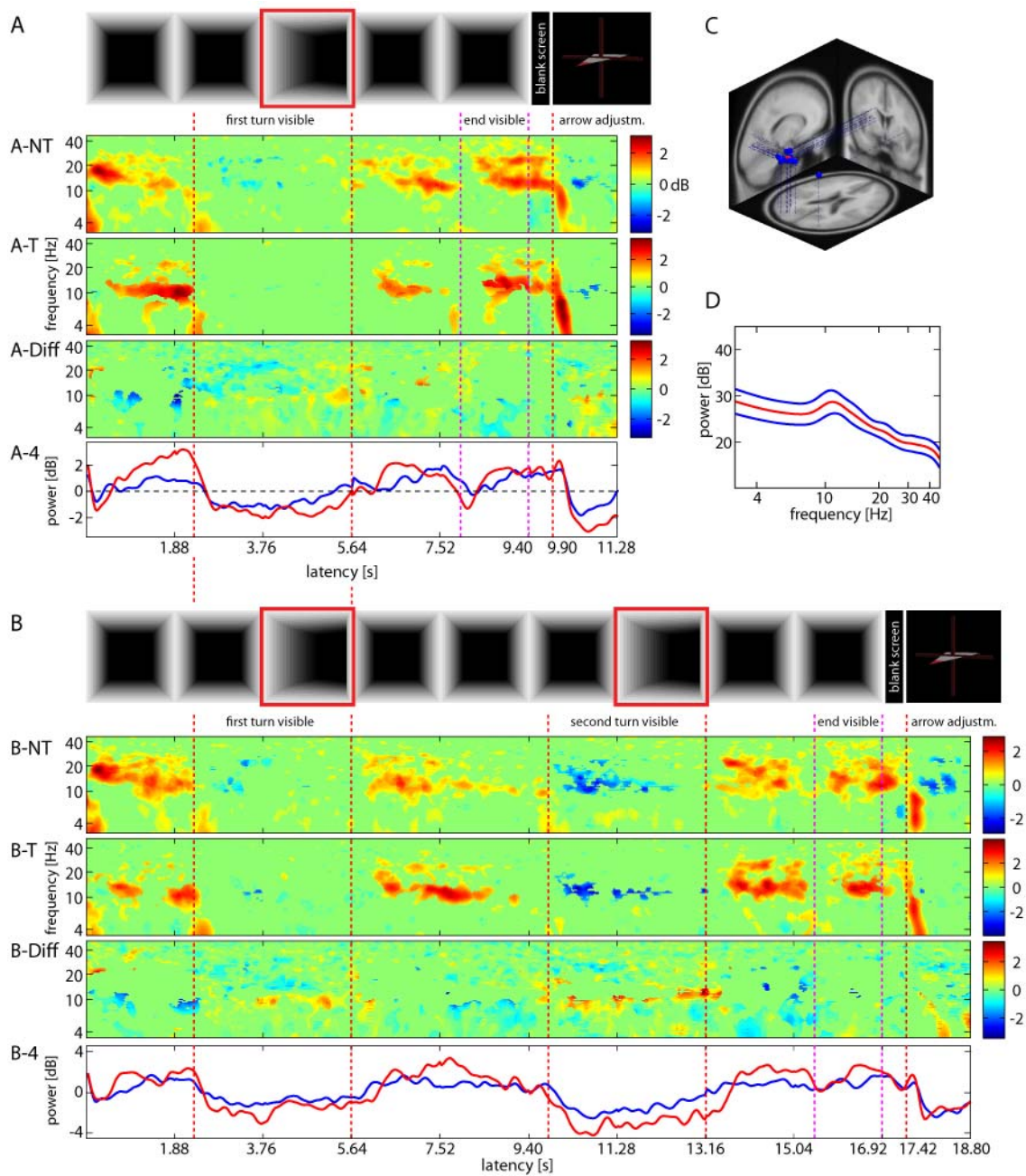


Figure 4.20: Mean event-related spectral perturbation (ERSP) images for an independent component cluster (ICC 4) located in or near left (bilateral) cuneus (BA 19). For explanation see Figure 4.18 (page 127).

***Superior (BA 7/31) and Inferior (BA 40) Parietal IC Clusters***

Alpha band activity in IC clusters 7 and 11 in or near superior parietal cortex was found to resemble patterns in dorsolateral associative visual cortex. For Turners, entering and traversing the curved segment was associated with increased desynchronization of the alpha band (near 10 Hz). This desynchronization was even stronger during the second turn. Here, the decrease in alpha power occurred already upon viewing the second turn and persisted until leaving the turning segment. For Nonturners traversing more complex tunnels, this alpha desynchronization in superior parietal IC cluster 7 was less pronounced as for Turners, since it already decreased to baseline upon entering the second turn (see Figure 4.21). Within the anterior IC cluster 11, activation patterns of the alpha band (near 10 Hz) were slightly different from posterior sites, particularly for Nonturners. Upon viewing the second turn, the initial alpha synchronization during the pre-turn segments deteriorated to baseline level as participants were approaching the turn. Entering the second turn was followingly associated with alpha desynchronization, which persisted until the end of the turning segment (see Figure 4.22).

As can be seen from Figure 4.23, IC clusters in or near inferior parietal cortex largely resembled the oscillatory pattern of superior IC clusters. Again, a strategy-specific effect of environmental complexity was found during the second turn. Here, Turners displayed more consistent alpha desynchronization while approaching and traversing the curved segment, whereas alpha desynchronization of Nonturners only comprised a narrow central alpha frequency band (near 10 Hz), deteriorating to baseline level upon entering the turn.

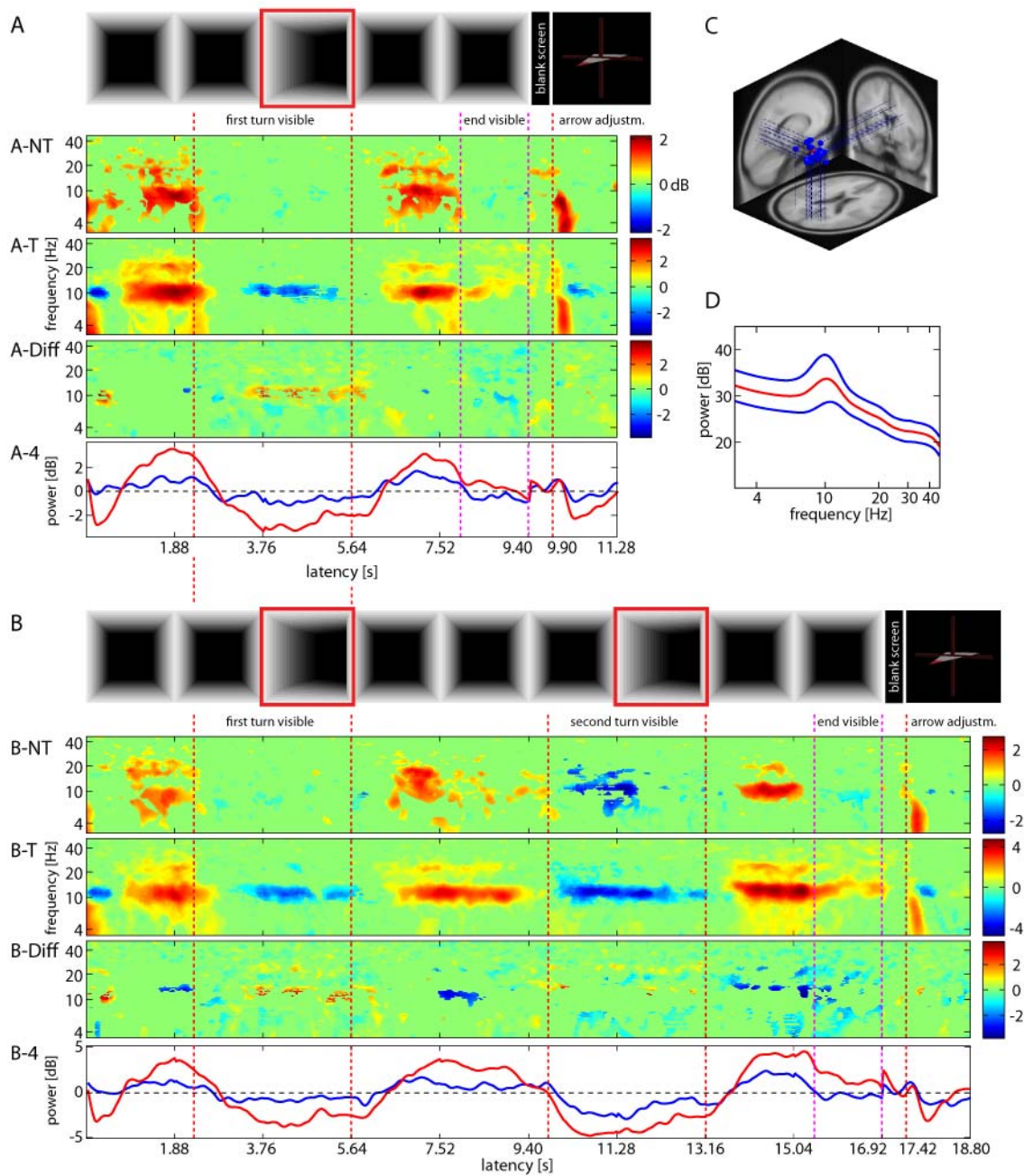


Figure 4.21: Mean event-related spectral perturbation (ERSP) images for an independent component cluster (ICC 7) located in or near right precuneus (BA 7/31). For explanation see Figure 4.18 (page 127).

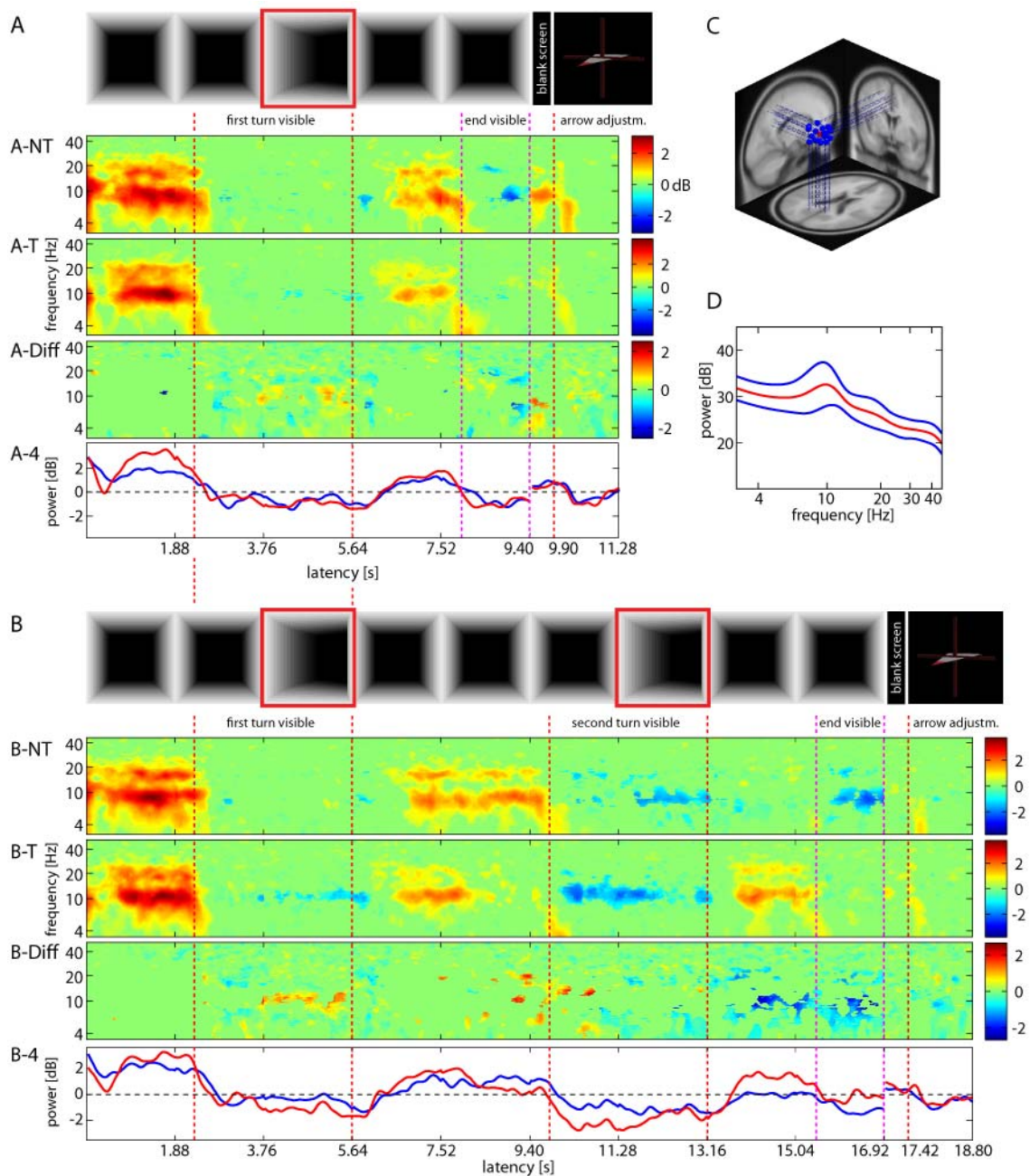


Figure 4.22: Mean event-related spectral perturbation (ERSP) images for an independent component cluster (ICC 11) located in or near left precuneus (BA 7/31). For explanation see Figure 4.18 (page 127).

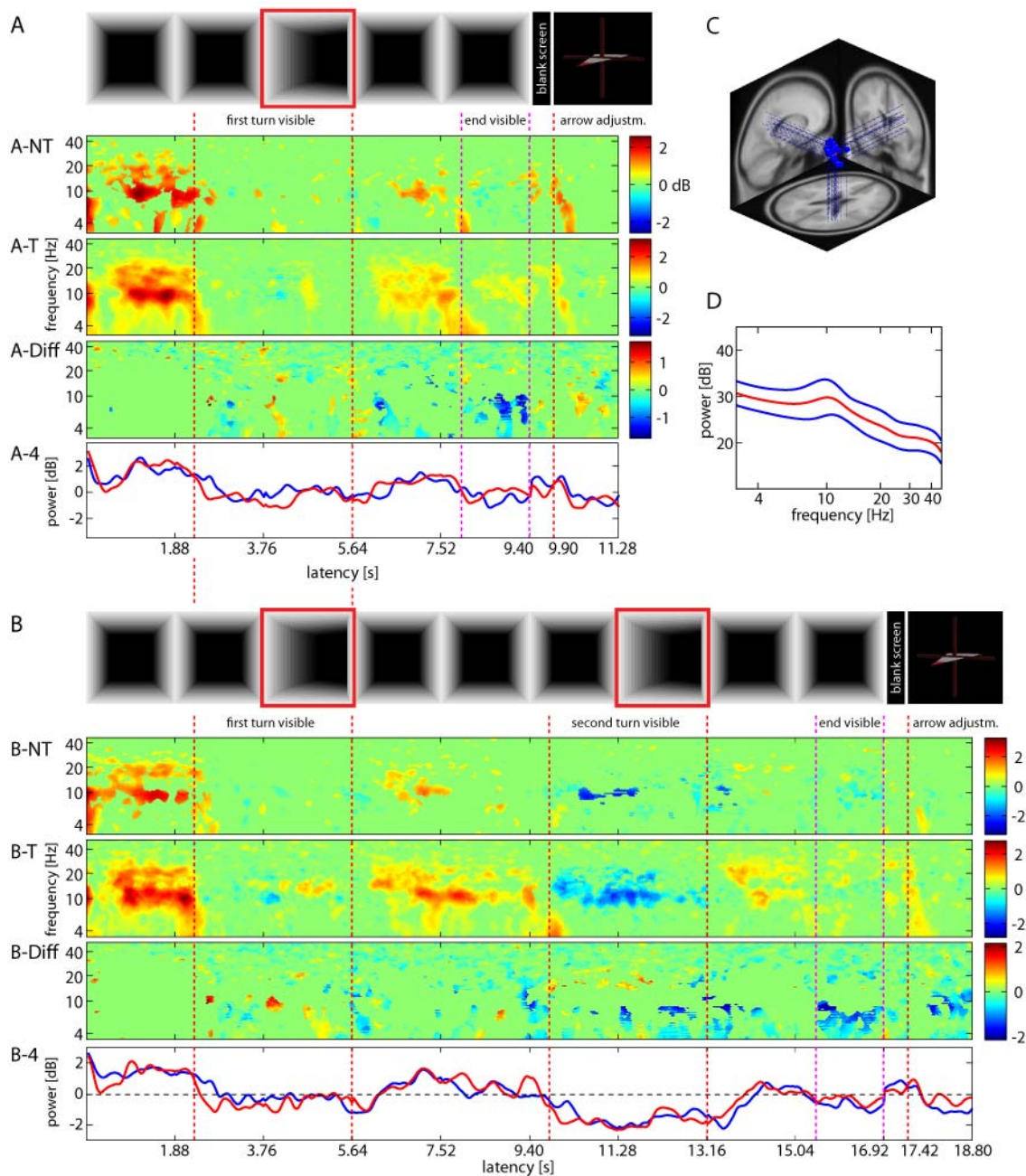


Figure 4.23: Mean event-related spectral perturbation (ERSP) images for an independent component cluster (ICC 10) located in or near right supramarginal gyrus (BA 40). For explanation see Figure 4.18 (page 127).

***Lateral Temporal IC Clusters (BA 13/20)***

Activity in IC clusters in or near lateral temporal cortex resembled findings of Experiment 1, particularly in superior temporal IC clusters (see Figure 4.24, panel A). Turners and Nonturners displayed comparable ERSP patterns that were identically affected by pathway complexity. Increased theta (near 4 – 8 Hz) power marked significant time points of the trajectory, e.g., upcoming heading changes. Interestingly, in the right-hemispheric IC cluster a final theta burst occurred as the end of the passage came into view. However, for more complex paths this burst was shifted towards the time-point of initially encountering the second turn. At the end of tunnels with two turns, no additional theta complex was registered. An identical though weaker pattern was also registered for the IC cluster in the left hemisphere (see Figure 4.24, panel B).

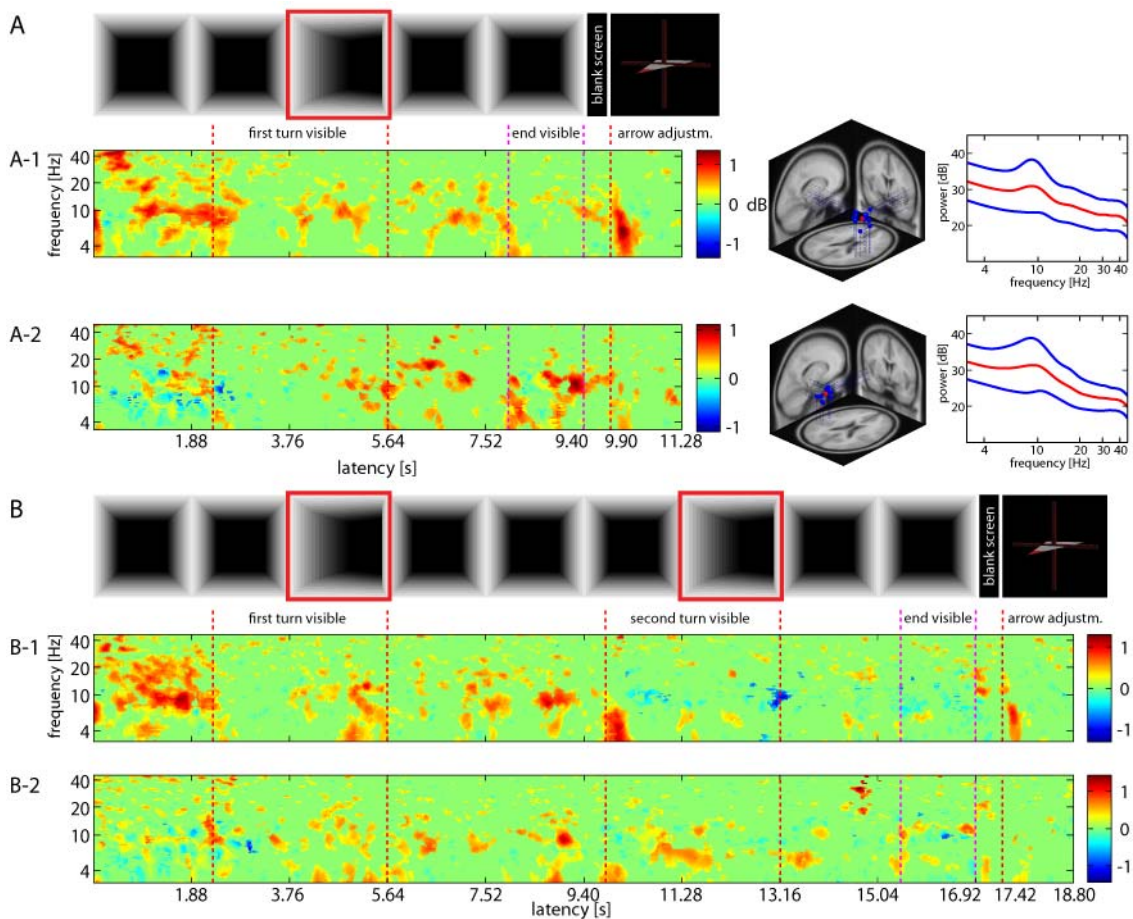


Figure 4.24: Mean event-related spectral perturbation (ERSP) images for two independent component clusters located in or near right superior temporal gyrus (BA 13, ICC 14, **A-1, B-1**) and left inferior temporal gyrus (BA 20, ICC 15, **A-2, B-2**) revealing task-dependent changes in spectral power during spatial navigation through tunnel passages containing one turn (panel A) and two turns (panel B) and subsequent homing arrow adjustment. Green colors indicate no significant ( $p > 0.001$ ) difference in mean log power (dB) from baseline. Warm colors indicate significant increases in log power and cold colors indicate significant decreases in log power from baseline. Important time points of the tunnel passage are marked with dashed lines: Red dashed lines indicate the period when participants perceived the approaching turn and the time period during the stimulus turn (from 3.76 s); magenta dashed lines indicate the time period during which the subjects were approaching the end of the tunnel. The final red dashed line indicates the time point when the virtual homing vector was displayed.

***Retrosplenial IC Cluster (BA 29/30)***

Retrosplenial IC cluster 9 revealed an effect of preferred navigation strategy on oscillatory dynamics during the passage. Generally, Nonturners displayed increased alpha (near 10 Hz) desynchronization when encountering and entering turns, as well as augmented synchronization of the upper alpha (near 12 Hz) frequency band when approaching the end of the passage. Importantly, blocking of alpha was more pronounced during the second turn. Additionally, at the end of more complex tunnels synchronization of the upper alpha band was accompanied by lower alpha desynchronization, as can be seen from Figure 4.25.

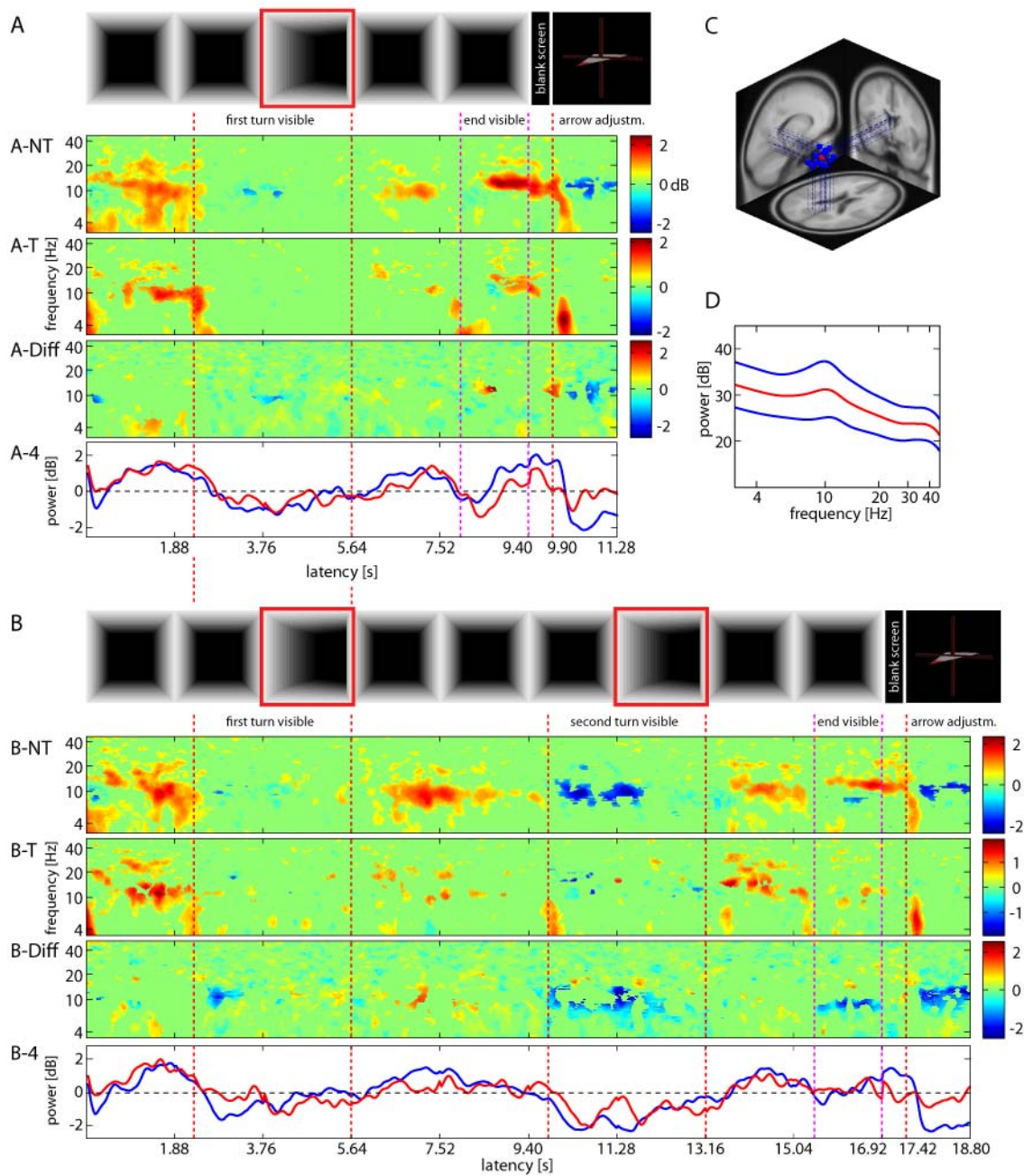


Figure 4.25: Mean event-related spectral perturbation (ERSP) images for an independent component cluster (ICC 9) located in or near left (midline) posterior cingulate/ retrosplenial cortex (BA 29/30). For explanation see Figure 4.18 (page 127).

### Precentral IC Clusters (BA 4/6)

Activity in IC clusters 16 and 17 in or near bilateral premotor cortices was found to be comparable for Turners and Nonturners. Lower and upper alpha/mu (near 9 Hz and 18 Hz, vs. 11 and 22 Hz, respectively) displayed distinctive patterns of (de-)synchronization following the visual stimulation. Interestingly, an effect of pathway complexity was found in the right-hemispheric IC cluster. Whereas during the first turn, alpha/mu power increased with onset of the rotation, visual contact with the second turn on its own provoked an augmented theta burst (near 4 – 8 Hz), followed by increased synchronization of the lower alpha/mu band (and its harmonics) until approximately 300 ms after leaving the turning segment (see Figure 4.26).

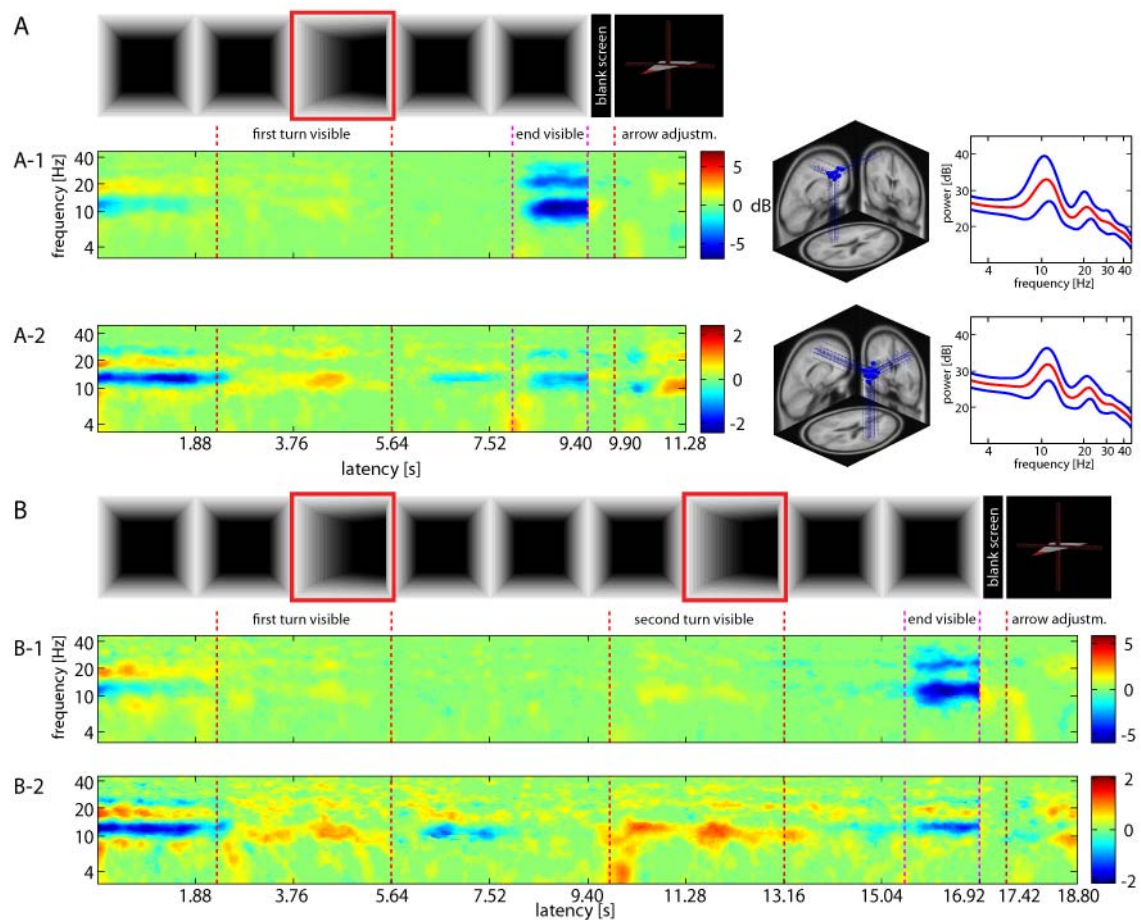


Figure 4.26: Mean event-related spectral perturbation (ERSP) images for two independent component clusters located in or near left precentral gyrus (BA 4/6, ICC 16, **A-1**, **B-1**) and right precentral gyrus (BA 4/6, ICC 17, **A-2**, **B-2**). For explanation see Figure 4.24 (page 136).

### Medial Frontal IC Clusters (BA 6/32)

ERSP dynamics of IC cluster 20 in or near right cingulate gyrus (BA 32) were seemingly affected by outbound path complexity. Whereas during tunnels with one turn, increases in theta power (near 4 – 8 Hz) marked the first turn as well as the end of the passage, the confrontation with a second turn provoked an augmented theta complex, which was followed by only punctual burst until the end came into view (see Figure 4.27). This dislocation of the final theta complex during paths of higher complexity was present in all frontal IC clusters (clusters 21, 22).

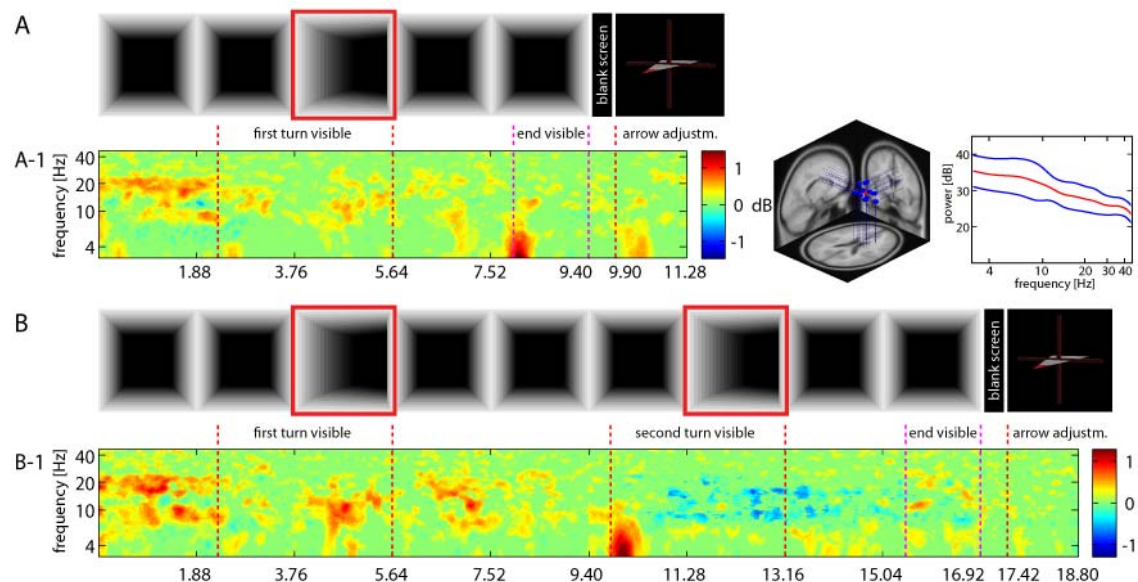


Figure 4.27: Mean event-related spectral perturbation (ERSP) images for an independent component cluster located in or near right cingulate gyrus (BA 32, ICC 20). For explanation see Figure 4.24 (page 136).

#### 4.4.2.4 Discussion

The results of Experiment 2 complemented and extended findings of Experiment 1. Participants, preferentially using an egocentric (Turners) or an allocentric (Nonturners) reference frame, traversed tunnels with one turn and two opposite turns of equal angularity, with the latter resulting in aligned egocentric and allocentric coordinates at the end of the passage. Behavioral data implied that participants were able to solve the task, although side error scores were found to be increased for tunnels with two opposite turns. Turners and Nonturners displayed comparable error patterns, e.g. overestimation of inner end positions and underestimation of more lateral end positions, further increased for more complex pathways. Results suggested that participants most likely encoded spatial information in a configural (and not history-free) manner, additionally moderated by representation-based expectancies regarding the layout of the upcoming pathway (Fujita et al., 1993; Klatzky et al., 1999). Since Turners and Nonturners displayed comparable error scores, but the ‘primitive parameters’ (Klatzky, 1998, p. 2) of egocentric and allocentric reference frames differ, the question was whether these errors emerge from stages of information processing common to both strategy groups, or if each reference system independently accumulates errors, nonetheless resulting in qualitatively equivalent spatial representations and behavior.

Analysis of spectral dynamics within reconstructed cortical source locations most generally suggested that for both Turners and Nonturners a widespread cortical network was activated during navigation that revealed task-dependent spectral power modulations in theta, lower alpha and upper alpha/mu frequency bands (Klimesch, 1999). Both strategy groups differentially processed translational and rotational information, as evident from deflections of the alpha band in occipital, occipito-parietal, as well as parietal regions. Whereas alpha was increased during translations, it was found to be blocked during turns, in line with studies on decreased alpha activity during sensory processing in dorsal regions (Klimesch et al., 1997b; Klimesch et al., 1993). However, in the current experiment, this effect was more pronounced for Turners as compared to Nonturners, particularly during the processing of the second, opposite turn. Whereas for Nonturners alpha blocking only prevailed during upcoming heading changes, Turners displayed alpha blocking while approaching and, additionally, actually traversing the turn. This prolonged processing of rotational information might constitute the prerequisite for an accurate, though cognitively highly demanding spatial updating of egocentric self-to-object relations (including the return bearing) during the second turn in order to keep up orientation (Loomis et al., 1999b). In fact, results suggested that for Turners a network along the dorsal pathway was active, in line with several recent studies demonstrating parietal involvement in egocentric spatial processing (Aguirre & D'Esposito, 1997; Colby & Goldberg, 1999; Galati et al., 2001; Gramann et al., 2006; Hartley et al., 2003; Maguire et al., 1998a; Shelton & Gabrielelli, 2002; Vallar et al., 1999; Wolbers & Büchel, 2005).

By contrast, Nonturners displayed increased processing in associative visual cortex (BA 19), posterior parietal regions, as well as in retrosplenial cortex, where information transfer between egocentric and allocentric reference frames is accomplished (Iaria et al., 2007; Maguire, 2001). With respect to the current task, this seems plausible, since Nonturners had to constantly transfer the visual flow information, provided from a first-person-perspective, into allocentric coordinates. But whereas Turners seemingly processed both upcoming and current heading changes from visual flow, Nonturners only processed *upcoming* heading changes, particularly of the second turn. Within an allocentric reference frame, all object-to-object relations remain stationary while the navigator is moving. Therefore, Nonturners only had to update their own position within stable global structures. In contrast to Experiment 1, for tunnels with two turns this ‘global structure’ might have become clear upon viewing the direction of the second turn<sup>10</sup>. In this case, it should not have been necessary to further encode visuo-spatial/rotational information since first and second turn corresponded to each other, and an internal representation of the pathway might have already been stored during the remaining passage. In favor of this assumption, the spectral dynamics in temporal and medial frontal cortices have to be considered. For tunnels with one turn a final theta burst was located upon viewing the tunnel end, whereas during more complex tunnels, the final theta (4 – 8 Hz) complex was found to be shifted towards the time point of encountering the second turn, replicating earlier findings on frontal midline theta demarking critical time points of travel, as heading information became available (Bischof & Boulanger, 2003; Caplan et al., 2003; Kahana et al., 2001; Onton et al., 2005). Most importantly, this theta shift was registered for both strategy groups, suggesting that encoding of visuo-spatial information within egocentric and allocentric reference frames was coordinated in a top-down manner by executive processes residing in frontal areas (Posner, 1975; 1995). In the General Discussion, this notion will be further elaborated.

## 4.5 EEG Analyses – General Discussion

The present study investigated the impact of path complexity on macroscopic EEG brain dynamics subserving the acquisition and retrieval of spatial knowledge during visual path integration within a (body-centered) egocentric or an (environment-centered) allocentric reference frame. Previous studies on spatial navigation have provided rich evidence for effects of either the applied strate-

---

<sup>10</sup> Experimental stimulation also contained tunnels with two turns bending into the same direction, which ended at categorical end positions of  $\pm 60^\circ$ , serving as filler trials. Until segment 6, their layout was identical to tunnels with two opposite turns ending at categorical end positions of  $\pm 30^\circ$  (see Appendix A).

gy (e.g., Committeri et al., 2004; Galati et al., 2000; Gramann et al., 2006) or environmental complexity (e.g., Bischof & Boulanger, 2003; Kahana et al., 1999) on brain dynamics during spatial navigation, but there was lacking knowledge about interactive effects of both factors. This question gains additional relevance when considering the existence of distinct spatial strategies based on intraindividually stable proclivities for encoding spatial information either within an egocentric (*Turners*) or an allocentric (*Nonturners*) reference frame, as recently suggested by Gramann and colleagues (2005; 2006) as well as Riccobon (2007).

By applying information-based spatial filtering of high-density EEG recordings into maximally independent component (IC) processes, the current study aimed at the identification of specific effects of pathway complexity on spectral dynamics of Turners, applying an egocentric reference frame, and Nonturners, applying an allocentric reference frame during path integration. In this context, complexity was conceptualized as the overall length as well as the number and relative direction of successive heading changes along the outbound trajectory. In *Experiment 1*, participants were traversing tunnels with one and two turns that always bent into the same direction, whereas in *Experiment 2*, tunnels with one turn and two opposite turns of equal angularity were presented, resulting in parallel start-end segments. However, participants could not determine whether traversing a short tunnel with one turn or a longer tunnel with two turns until either the end of the passage showed up or the tunnel continued with a second turn.

Analysis of behavioral data suggested the presence of an extended configural updating mechanism as proposed by Klatzky and colleagues (1999) that integrated more than just a homing vector comprising only overall distance and direction. Navigators built up more or less coherent representations of the traversed pathways, resulting in an internal expectation of an ‘average-pathway’ that was utilized as standard of comparison for pathways traversed later on (Fujita et al., 1993; Klatzky et al., 1999). Navigators refer to these prototypical expectations whenever navigation may become too challenging, resulting in ambiguities regarding the layout of the currently traversed trajectory. The existence of regression to the mean in over- and underestimations of eccentricity of end position could be interpreted as behavioral outcome of this expectancy-based encoding of novel spatial information.

The question was, if and to what extent configural updating is also reflected in oscillatory dynamics within distinct intracortical IC source locations reconstructed from continuous high-density scalp EEG recordings. This procedure resembled for both strategy groups a widespread cortical network with regionalized task-dependent oscillatory deflections in frontal midline theta (near 4 – 8 Hz), occipital and parietal alpha (near 10 Hz) and prefrontal lateral upper alpha/mu (near 12 Hz) frequency bands compatible with results of recent functional imaging studies on metabolic exchange rates during spatial navigation and orientation (Committeri et al., 2004; Galati et al., 2000; Wolbers et al.,

2007). Most generally, results replicated and further extended findings of Gramann and colleagues (submitted) on EEG spectral dynamics of Turners and Nonturners traversing outbound paths containing a single turn.

However, the present results suggested that even rather small variations in the visual stimulation, i.e., changing the relative direction of successive heading changes, resulted in pronounced differences in cortical activation patterns of both Turners and Nonturners during more complex paths. These differences were most prominent in spectral dynamics of the alpha frequency band (near 10 Hz) in posterior cortical sites, e.g., occipital, occipito-parietal and parietal cortices, whereas prefrontal upper alpha/mu activity (near 12 Hz) and frontal midline theta (near 4 – 8 Hz) activation patterns were found to be more or less identical for both strategy groups. In the following section, these differences will be discussed in detail.

#### **4.5.1 Interaction of Environmental Complexity and Preferred Strategy in Occipito-Parietal and Parietal Cortices**

Turners as well as Nonturners had to process incoming visual flow from a first-person perspective, resulting in comparable activation of primary and secondary visual cortices. Whereas purely translational information was associated with synchronization of the alpha frequency band (near 10 Hz), the combined translational/ rotational information during curved segments resulted in alpha desynchronizations, that have been associated with increased cognitive processing during relevant time-points of a given task (de Araujo et al., 2002; Gevins et al., 1997; Klimesch, 1999). Areas along the dorsal pathway have been repeatedly proven to be involved in egocentric processing of space, with posterior parietal regions undertaking the coordination of multiple (eye-, head-, trunk-centered) reference frames which can then be used by motor structures to code appropriate movements (Foster et al., 1989; Harris et al., 2000; Meltzer et al., 2007). Additionally, posterior parietal cortex has been associated with heading processing (Maguire et al., 1998a; Morrone et al., 2000), accomplished in concert with posterior cingulate/retrosplenial cortex, suggesting that posterior parietal cortex also conveys allocentric aspects (see Calton & Taube, 2009).

Increased pathway complexity had differential effects on egocentric and allocentric processing within these areas. In Experiment 1, where tunnels with two turns bent into the same direction, cognitive processing of the second turn was limited to the interval when participants approached the turn, as suggested by increased alpha desynchronization, corroborating the central role of posterior parietal cortex for the processing of upcoming heading changes (Field et al., 2007). However, Nonturners did not display significantly increased alpha blockage during confrontation with the second turn, suggesting that they disrupted the processing of translational/ rotational information along the dorsal pathway in order to facilitate direct allocentric processing along the ventral

pathway, further supported by increased alpha activity in associative visual cortex (V3) for Nonturners at the end of the passage, that is closely interlinked with lateral temporal structures (Worden et al., 2000).

In Experiment 2, by contrast, tunnels with two turns of equal angularity were always bending into opposite directions. Here, Nonturners and Turners displayed increased processing of the second turn as compared to the first turn, as evident from pronounced alpha desynchronization in occipital and parietal regions while approaching and traversing the second turn. Again, Turners and Nonturners displayed differential patterns in alpha desynchronization. For Turners, alpha desynchronization in all parietal IC cluster sites persisted from viewing the turn until the end of the curve, providing evidence for configural updating of egocentric self-to-object relations to heavily rely on accurate processing of incoming visuo-spatial information, that was supposed to be cognitively more demanding when confronted with opposite turns as compared to successive turns into the same direction. Within an egocentric reference frame, opposite turns necessitate the whole environmental array to be shifted with respect to the intrinsic axis of the navigator. Current results confirmed that this shift of relative object location is accomplished in posterior parietal cortex (Andersen, 1995). For Nonturners, by contrast, alpha in posterior parietal regions as well as in retrosplenial cortex was blocked only as they approached the second turn, suggesting increased coordination of egocentric and allocentric information during the processing of upcoming heading changes (Byrne et al., 2007; Maguire, 2001), in line with findings of Gramann et al. (submitted).

#### 4.5.2 Activity in Common to Turners and Nonturners

Additional to the strategy-specific spectral dynamics of the alpha frequency band (near 10 Hz) in occipital and parietal cortices, Turners and Nonturners displayed comparable upper alpha/mu activity (near 12 Hz) in precentral areas, as well as theta activation (near 4 – 8 Hz) in lateral temporal and medial frontal cortices.

Bilateral activation of the sensorimotor cortex displayed specific spectral dynamics during the tunnel passages. In sensorimotor areas, desynchronizations of the lower alpha and beta frequency band are associated with movement preparation and execution (Pfurtscheller & Aranibar, 1979; Pfurtscheller et al., 1996). Also, processing of optokinetic stimulation has been found to significantly affect activity in precentral areas (Dieterich, Bense, Stephan, Yousry, & Brandt, 2003; Petit & Haxby, 1999). Since both IC clusters were closely linked to areas of the frontal eye fields (FEF) region (Petit & Haxby, 1999), precentral activity might be associated to saccades, pursuit, and optokinetic eye movements. Therefore, the time course of alpha synchronization during the tunnel passage might closely resemble patterns observed for eye movements during tunnel navigation (Gramann, El Sharkawy, & Deubel, in press), whereas at the

end of the tunnel alpha might desynchronize in order to facilitate the upcoming manual response.

Spectral dynamics of the theta band (4 – 8 Hz) in or near bilateral temporal cortex revealed increased activity at certain time points of the trajectory, e.g., as turns or the end of the passage showed up, confirming the role of theta activity to index cognitive effort during spatial encoding and memory retrieval (Caplan et al., 2003; Doppelmayr, Klimesch, Pachinger, & Ripper, 1998; Kahneman et al., 1999; Klimesch et al., 1997b). With respect to the question if path integration is accomplished in history-free or configurational mode, these theta deflections most likely suggested the presence of the latter. With upcoming turns as well as at the end of the passage, cognitive processing was increased in order to supply resources for the updating of spatial parameters.

Comparably, in medial frontal IC clusters, theta bursts reflected increased cognitive demands during critical stages of the passage related to upcoming heading changes. Activity of the anterior cingulate cortex has been recently linked to task-related theta activity related to memory processing (Onton et al., 2005), and has been shown in several virtual navigation studies (Maguire et al., 1998a; Shelton & Gabrieli, 2002; Wolbers & Büchel, 2005). Theta bursts were located at the time point of encountering the upcoming turn as well as the end of the passage (Gramann et al., 2006; Gramann et al., submitted). However, when confronted with increasing pathway complexity, participants displayed a final theta burst either after the final turn (same direction) or already before entering the turn (opposite direction). This dissociation most likely was related to specific variations of the stimulus material. Whereas turns of more complex tunnels in Experiment 2 were of identical angularity and always bent into opposite directions, participants could easily determine the angle of the upcoming second turn. This might have prevented the occurrence of a final theta burst anteceding the final turning segment. By contrast, in Experiment 1 turns of more complex tunnels bent into the same direction but due to stimulus variety several path layouts could end on a certain eccentricity. Therefore, participants had to first process the rotational information during the second turn before reliably updating their heading by means of a final theta burst following the second turn.

### 4.5.3 Conclusion

Taken together, individual preferences for applying an egocentric or an allocentric reference frame was accompanied by dissociable brain dynamics in distinct cortical networks that became even more apparent as environmental complexity was increased. Turners and Nonturners displayed differential spectral activation patterns of the alpha frequency band (near 9 – 13 Hz) within several IC clusters in posterior regions such as occipital, occipito-parietal, and parietal cortices, as well as in retrosplenial cortex. These differences might be closely linked to differences in the updating of representational primitives such as self-to-object or inter-object bearings and distances from integration of ro-

tational and/ or translational information. However, both strategy groups displayed comparable activation patterns in precentral, medial frontal, and lateral temporal cortices. Within the latter areas, spectral dynamics of the theta frequency band (near 4 – 8 Hz) most likely mirrored cognitive effort during the tunnel passage.

Referring to the initial question if visual path integration within an egocentric or an allocentric reference frame is accomplished in configural or history-free manner, analysis of EEG spectral dynamics during confrontation with outbound paths of varying complexity provided rich evidence for the existence of a configural updating of representational primitives at distinct sections of the outbound trajectory, e.g., during upcoming heading changes or during straight passages following turns. Fujita et al. (1993) suggested that the navigation process might be described as a result of several sub-routines, i.e., (1) sensing the outbound path, (2) forming a representation, either of the path or of current position and orientation, (3) computing a return path, and (4) executing that path. The authors assumed errors to solely arise at levels (1) and (2), subsumed as ‘encoding’. However, the current results showed that rotations (and translations) are not encoded equivalently, but that expectations based on the history of previously traversed outbound paths impacts sensory integration during spatial updating (Posner, 1975, 1995). Particularly spectral dynamics of theta activity might mirror the retrieval of these expectations from the respective representational systems subserving egocentric and allocentric reference frames. Therefore, individual proclivities for coding space within distinct reference frames should be considered in research on effects of path complexity on spectral dynamics as well as behavioral responses during spatial navigation.

## Chapter 6

# Deutsche Zusammenfassung

### 5.1 Theoretischer Hintergrund

Orientierung und Navigation im Raum stellen grundlegende Voraussetzungen für eine adäquate Interaktion mit unserer Umwelt dar und sind damit überlebensnotwendig. Über die Aufnahme, Integration und Weiterverarbeitung multimodaler Information innerhalb verschiedener Referenzsysteme können wir im Navigationsprozess Auskünfte zu unserer momentanen Position und Ausrichtung erhalten. Höhere kognitive Prozesse, wie z.B. zielgerichtetes Verhalten, sind ohne die Erzeugung einer räumlichen Repräsentation der Umwelt (und der eigenen Orientierung innerhalb dieser Umwelt) kaum vorstellbar.

Der Aufbau einer räumlichen Repräsentation kann als komplexe kognitive Fähigkeit angesehen werden, da sensorischer Input aus unterschiedlichen Modalitäten (visuell, vestibulär, kinästhetisch und propriozeptiv), Informationen zur aktuellen Position des Navigierenden sowie Handlungspläne aus dem Langzeitgedächtnis fortlaufend konsolidiert, abgeglichen und integriert werden müssen (Gramann et al., 2005). Bei der Navigation innerhalb der Umwelt greifen wir auf verschiedene Mechanismen zurück: Während *positionsbasierter Navigation* bzw. „Pilotierung“ wird die Position des Navigierenden ausschließlich durch Außenreize aktualisiert. In diesem Fall dienen signifikante Landmarken in Kombination mit einer Karte als Referenzpunkte zur Bestimmung der aktuellen Position der Person. Im Gegensatz dazu bezieht sich Wegintegration („path integration“) auf die Aktualisierung von Position und Ausrichtung innerhalb der Umgebung auf Grundlage internaler (*ideothetischer*) und externaler (*allothetic*) Informationen (Klatzky, 1998 (Klatzky, 1998); Loomis, Klatzky, Golledge, & Philbeck, 1999; Mittelstaed & Mittelstaed, 1982).

Die perzeptive Vielfalt der Umwelt beeinflusst dabei, ob die Person beim Durchschreiten einer Trajektorie auf Landmarken zurückgreifen kann (sog. ‚piloting‘, oder Landmarken-basierte Navigation), oder ob – bei der Abwesenheit von Landmarken - der Navigationsprozess ausschließlich auf Wegintegration (sog. ‚path integration‘), d.h. der kontinuierlichen Integration von Bewegungssignalen (z.B. propriozeptiv registrierter Rotationen oder visuellen Flusses) basiert. Während positionsbasierte Navigation ausschließlich visuellen Input verarbeitet, verknüpft Wegintegration visuelle, vestibuläre, motorische und kinästhetische Informationen. Dass Wegintegration auf Grundlage rein visueller Information möglich ist, wurde in mehreren Studien nachgewiesen (Gramann, Müller, Eick, & Schönebeck, 2005; Riecke, van Veen, & Bühlhoff, 2002). Bei Abwesenheit signifikanter Landmarken kommt der Wegintegration damit eine zentrale Rolle zu (Gramann, Müller, Schönebeck, & Debus, 2006).

Während Pilotierung generell mit der Nutzung eines allozentrischen Referenzrahmens assoziiert wird, besteht in Bezug auf Wegintegration weniger Klarheit. Generell kann Wegintegration auf Grundlage eines allozentrischen oder eines egozentrischen Referenzrahmens (oder einer Kombination beider Systeme) erfolgen (Burgess, 2006; Wang & Spelke, 2000). Bisherige Forschungsergebnisse bestätigten die Existenz trait-ähnlicher individueller Präferenzen bei der Konstruktion einer räumlichen Repräsentation innerhalb eines egozentrischen bzw. allozentrischen Referenzsystems (Gramann et al., 2005; Gramann et al., 2006). Diese Präferenzen kommen jedoch nur unter geeigneten experimentellen Bedingungen zum Tragen. In einer virtuellen Navigationsaufgabe wird über die Präsentation visuellen Flusses eine passive Fahrt durch Tunnel simuliert, in deren Anschluss die Versuchsperson einen simulierten Pfeil (sog. ‚homing arrow‘) vom Ende des Tunnels auf den Startpunkt der Passage einstellen sollten.

Bei der Pfeileinstellung kommt es zu einer Dissoziation der Probanden in zwei nahezu gleich große Gruppen. Die sog. ‚Turner‘ benutzen zur Orientierung während der Tunnelfahrt einen egozentrischen Referenzrahmen. Alle Informationen werden dabei in Bezug auf die Körperachsen (posterior-anterior / rechts- bzw. linkslateral) des Navigierenden verarbeitet. Die Adjustierung des Pfeils erfolgt daher auf Grundlage des während der Tunnelfahrt aktualisierten *egozentrischen bearings* des Startpunktes relativ zur finalen Ausrichtung der Person am Ende der Tunnelfahrt – ein Tunnel mit zwei Rechtskurven resultiert in einer Pfeileinstellung nach hinten rechts. Im Gegensatz dazu erhalten die sog. ‚Nonturner‘, welche die Benutzung eines allozentrischen Referenzrahmens präferieren, ihre initiale, durch das erste gerade Segment der Tunnelpassage determinierte kognitive Orientierung aufrecht und aktualisieren das *allozentrische bearing* des Startpunktes. Der allozentrische Raum wird demzufolge durch ein Koordinatensystem mit externem Ursprung und externer Referenzrichtung aufgespannt. Im Anschluss an die oben beschriebene Tunnelfahrt mit zwei Rechtskurven weist der Pfeil für einen Nonturner erwartungsgemäß nach hinten links, und überschätzt die Exzentrizität der Endposition dabei um

die Winkelsumme der während der Fahrt durchquerten Kurvensegmente (Gramann et al., 2005; Gramann, Müller, Schönebeck, & Debus, 2006).

Die Nutzung des jeweiligen Referenzsystems führt zur Enkodierung unterschiedlicher ‚primitiver Parameter‘ (Klatzky, 1998), welche in die mentale Repräsentation einfließen. Diese primitiven Parameter müssen während der Bewegung des Navigierenden aktualisiert werden – entweder kontinuierlich oder intermittierend. Wegintegrations-Modelle, die einen kontinuierlichen Aktualisierungsprozess postulieren (Müller & Wehner, 1988), nehmen an, dass der Navigierende lediglich die Gesamtdistanz und -Richtung des Startpunktes, nicht aber das Layout des zurückgelegten Weges repräsentiert. Demzufolge sollte die Aktualisierung der primitiven Parameter (und damit verbunden auch Navigationsfehler) unabhängig von Charakteristika des Weges erfolgen. Navigierende sind jedoch durchaus in der Lage, unterschiedliche Wegkonfigurationen anhand ihres Layouts zu unterscheiden oder einen Weg zurückzuverfolgen (Cornell & Greidanus, 2006; Cornell & Heth, 2004; Loomis et al., 1993). Demzufolge wird im Laufe des Weges mehr als nur die Gesamtrichtung und – Entfernung aktualisiert. Das ‚encoding-error‘-Modell (Fujita et al., 1993) nimmt an, dass die Aktualisierung primitiver Parameter nur zu bestimmten Zeitpunkten, insbesondere während Richtungsänderungen, erfolgt und damit signifikant durch die Wegkonfiguration determiniert wird.

## 5.2 Zusammenfassung der durchgeführten Untersuchung

Ausgehend von den dargestellten Konzeptualisierungen zielten die vorliegenden Experimente auf die Beantwortung der Frage, inwiefern behaviorale, neuroanatomische und elektrokortikale Korrelate ego- bzw. allozentrischer Wegintegration (Turner vs. Nonturner) durch die Komplexität der Umwelt beeinflusst werden. Zusätzlich galt es herauszufinden, ob die Aktualisierung innerhalb der Referenzrahmen grundsätzlich konfigural oder kontinuierlich erfolgt. Zur Untersuchung dieser Fragestellungen kamen behaviorale (Reaktionszeiten, absolute Fehler, relative Fehler) und elektrophysiologische Verfahren zum Einsatz. Die informationsbasierte Filterung hochauflösender elektroenzephalographischer (EEG) Aufzeichnungen in (möglichst) unabhängige Komponenten („Independent Components“, IC’s) gestattete die Untersuchung von Strategieunterschieden in der durchschnittlichen spektralen Dynamik während visueller Wegintegration.

### 5.2.1 Zusammenfassung Kapitel 3

Initiale behaviorale Ergebnisse von Gramann et al. (2005) und Riccobon (2007) belegen zwar den starken Einfluss der Kurvenzahl während einer Tunnelfahrt auf die Genauigkeit der Heimfindungs-Leistung („homing“) von Turnern und

Nonturnern, jedoch wurde die Gesamtlänge der Trajektorien über alle Komplexitätsebenen konstant gehalten (Innerhalb einer bestimmten Strecke wurde eine variable Anzahl von Kurven positioniert). Demnach konnten die Studienteilnehmer bereits bei der Annäherung an die erste Kurve das Gesamtlayout des Weges extrahieren, was möglicherweise zu materialbedingten Verzerrungen in den Verhaltensdaten geführt haben könnte. Ebenfalls wurden zur Analyse der Leistungsdaten Tunnel mit zwei Kurven ohne Berücksichtigung der relativen Richtung der zweiten Kurve (gleichläufig vs. gegenläufig) aggregiert, wodurch evtl. strategiebedingte Fehler in der Winkeleinstellung verdeckt wurden.

Für die vorliegende Untersuchung wurden daher ausschließlich Tunnelkonfigurationen gewählt, welche eine systematische Analyse von Komplexitätseffekten auf die jeweiligen Referenzsysteme erlaubte. In Experiment 1 wurden Tunnel mit entweder einer einzigen Kurve, zwei gleichläufigen oder zwei entgegen-gesetzten Kurven präsentiert. In Experiment 2 wurde die perzeptive Vielfalt reduziert und nur Tunnel mit einer bzw. zwei gleichläufigen Kurven simuliert. In Experiment 3 durchfuhren die Probanden letztlich nur einkurvige und gegenläufige zweikurvige Tunnel. Komplexere Tunnel waren länger, so dass die Teilnehmer die Gesamtconfiguration eines Tunnels nicht extrahieren konnten, bevor sie sich entweder dem Ende des Tunnels näherten oder sich die Fahrt mit einem zweiten Tunnel fortsetzte. Am Ende der Passage adjustierten die Teilnehmer einen virtuellen ‚Homing‘-Pfeil.

Die experimentellen Befunde vergleichbarer Fehlermuster von Turnern und Nonturnern bei der Adjustierung des Homing-Pfeils (Regression zur Mitte) belegten für beide Strategiegruppen die Präsenz eines *erweiterten* konfiguralen Aktualisierungsprozesses bei der Integration rotationaler und translationaler Informationen (Klatzky et al., 1999). Aufgrund von Speicherfehlern und Unsicherheit beim Durchqueren komplexerer Tunnel konstruieren Turner und Nonturner repräsentationsbasierte ‚Durchschnitts-Pfade‘, welche als Vergleichsmaßstab bei der Enkodierung des jeweils aktuellen Durchgangs benutzt werden. Dieses Vorgehen resultiert in systematischen Verschiebungen der Regressionstendenzen für komplexere Wege. Die Ergebnisse bestätigen und erweitern bestehende Befunde (Gramann et al., 2005), und legen die Berücksichtigung individueller Strategien während räumlicher Navigation nahe.

## 5.2.2 Zusammenfassung Kapitel 4

In der Folge galt es herauszufinden, ob die Vergleichbarkeit der Leistungsparameter von Turnern und Nonturnern ihre Entsprechung auf elektrokortikaler und neuroanatomischer Ebene fand. Dazu wurden die hochauflösenden (128-Kanal-) EEG-Aufzeichnungen aus den Experimenten 2 (gleichläufige zweikurvige Tunnel) und 3 (gegenläufige Richtungen, identischer Winkel) mittels Independent Component Analysis (ICA, Makeig et al., 2004) ausgewertet. Auf Grundlage der Aktivität unabhängiger Komponenten (IC's) erfolgte die modellbasierte Lokalisierung intrakortikaler Generatorquellen, bezeichnet als

,equivalent current dipole modeling (Anemüller, Sejnowski, & Makeig, 2003; Makeig et al., 2004). Im Gegensatz zu klassischen ERP-Ansätzen zu induzierter elektrokortikaler Aktivität einzelner Frequenzbänder (z.B. Alpha bzw. Theta) innerhalb weniger Millisekunden gestattet die Analyse ereigniskorrelierter spektraler Dynamik Einsicht in kontinuierliche Gehirnaktivität im Frequenzbereich von 3 – 45 Hz (da in der vorliegenden Untersuchung Frequenzen jenseits von 45 Hz keine Berücksichtigung fanden, wurde der Frequenzbereich > 45 Hz gefiltert).

In Korrespondenz mit aktuellen bildgebenden Studien zu räumlicher Navigation (Committeri et al., 2004; Galati et al., 2000; Maguire et al., 1998a; Wolbers et al., 2007) sowie zur Verarbeitung visuellen Flusses (Culham et al., 2001; Sunaert et al., 1999) konnten die vorliegenden Experimente ein komplexes und weitreichendes kortikales Netzwerk von IC Ursprungsorten identifizieren, deren spektrale Dynamik teilweise eng an die Verarbeitung translationaler und rotationaler Informationen während der Konfrontation mit Kurvensegmenten gekoppelt war. Turner enkodierten räumliche Information hauptsächlich in okzipito-parietalen bzw. parietalen Kortexarealen, welche mit der Konstruktion eines egozentrischen Referenzrahmens in Verbindung gebracht werden (Calton & Taube, 2009). Für Nonturner konnte dagegen eine vermehrte Aktivierung ventraler Kortexareale registriert werden (allozentrischer Referenzrahmen), ergänzt durch Aktivierung des retrosplenialen Kortex' (Maguire, 2001), einem Areal, welches den Austausch zwischen egozentrischem und allozentrischem Referenzrahmen koordiniert. Zusätzlich zu diesen strategiespezifischen Aktivierungsmustern wiesen Turner und Nonturner bei der Konfrontation mit komplexeren Pfadkonfigurationen vermehrte Theta-Aktivität in ‚frontal midline‘-Arealen auf. Aktivität in diesen Arealen steht in Verbindung mit der Enkodierung bzw. dem Abruf episodischer Erinnerungen (Bischof & Boulanger, 2003).

### 5.3 Schlussfolgerungen

Die Ergebnisse der in Kapitel 3 und 4 vorgestellten Experimente belegen eindrücklich das Vorliegen eines *erweiterten* konfiguralen Aktualisierungsprozesses während egozentrischer und allozentrischer Wegintegration (Klatzky et al., 1999), d.h. die Aktualisierung strategiespezifischer primitiver Parameter während kritischer Zeitpunkte entlang des Weges, z.B. bei der Annäherung bzw. Durchquerung von Kurven. Basierend auf konfiguraler Aktualisierung wird eine Trajektorie aus zwei geraden Segmenten, welche durch eine 90° Drehung miteinander verbunden sind, als L-förmig repräsentiert. Bei komplexeren Trajektorien entstehen beim navigierenden Subjekt jedoch zunehmend Unsicherheit und Speicherlimitationen, verursacht durch die Zunahme an translationaler und rotationaler Information, die enkodiert werden muss. Die Ergebnisse der Leistungsdaten legen nahe, dass räumliche Enkodierung nicht ausschließ-

lich objektbasiert erfolgt, sondern zusätzlich durch repräsentationsbasierte Erwartungen bzgl. des zukünftigen Weglayouts moderiert wird. Die Enkodierung der beschriebenen Wegkonfiguration resultiert demnach nicht immer in einer L-förmigen Repräsentation, sondern variiert in Abhängigkeit der zuvor durchquerten Wegkonfigurationen, welche zu einem ‚Durchschnittspfad‘ aggregiert wurden. Bei Unsicherheit greift der Navigierende auf diese grobe Schätzung zurück, um zumindest die ungefähre Richtung und Entfernung des Startpunktes eines Weges zu erhalten. Die vorliegenden Befunde sprechen eindeutig dafür, dass Turner und Nonturner bei Konfrontation mit multiplen Tunnelkonfigurationen komplexitäts-spezifische ‚Durchschnittspfade‘ aufbauen (Experiment 1). Bei reduzierter Variabilität (Experimente 2 und 3) determinierte die Konfiguration der durchquerten Pfade, ob beide Komplexitätsebenen in einem generellen ‚Durchschnittspfad‘ münden (eine Kurve und zwei gleichgerichtete Kurven), oder ob jeweils komplexitäts-spezifische ‚Durchschnittspfade‘ erstellt werden (eine Kurve und zwei gegenläufige Kurven).

Die Analyse der ereigniskorrelierten spektralen Dynamik (ERSPs) legte nahe, dass egozentrische und allozentrische Verarbeitung Gemeinsamkeiten hinsichtlich der Verarbeitung translationaler und rotationaler Information aufweisen. Bei Konfrontation mit komplexeren Wegen erfolgt jedoch eine Aktivierung strategiespezifischer Areale, innerhalb derer egozentrische bzw. allozentrische primitive Parameter (Klatzky, 1998) verarbeitet werden, z.B. von ‚heading‘ in retrosplenialen bzw. posterior-parietalen Arealen (Calton & Taube, 2009; Nitz, 2009). Zusätzlich belegen die vorliegenden Befunde einen moderierenden Effekt frontal-exekutiver Prozesse auf räumliche Enkodierung von Translationen und Rotationen. Basierend auf Studienergebnissen zum Zusammenhang von Theta-Aktivität mit der Enkodierung und dem Abruf episodischer Erinnerungen an kritischen Punkten entlang eines Weges (Kahana et al., 2001), markieren die Theta-Perturbationen der vorliegenden Experimente Zeitpunkte, zu denen die repräsentationalen primitiven Parameter aktualisiert wurden. Theta-Aktivierung koordinierte dabei wahrscheinlich den dargestellten Abruf von ‚Durchschnittspfaden‘ zur Enkodierung des aktuell durchquerten Weges. Die Befunde legen somit nahe, dass strategiespezifische Verarbeitung eingehender Information durch Prozesse moderiert wird, die ihrerseits unabhängig von der präferentiellen Nutzung spezifischer Referenzsysteme sind. Abschließend können die Ergebnisse der vorliegenden Dissertation dahingehend interpretiert werden, dass allozentrische und egozentrische Referenzsysteme koexistieren (Aguirre & D'Esposito, 1999; Burgess, 2006; Burgess et al., 2004; Byrne et al., 2007; Hartley et al., 2003; Mou et al., 2004; Redish, 1999; Sholl, 2001).

Zukünftige Studien werden der Frage nachzugehen haben, inwiefern die aktuellen Ergebnisse auf realistischere Navigationsaufgaben übertragbar sind, z.B. wenn der Navigierende zusätzlich zur visuellen Stimulation ideothetische (vestibuläre) Information zur Aktualisierung primitiver Parameter nutzen kann. Ebenfalls dürfte von Interesse sein, wie sich allothetische Stimuli (Landmarken) auf die Navigationsleistung von Turnern und Nonturnern auswirken. Er-

gebnisse von Foo et al. (2007) legen nahe, dass räumliche Enkodierung dadurch wesentlich beeinflusst werden sollte. Diese realistischeren Navigationsaufgaben erfordern jedoch die präzise experimentelle Kontrolle. Immersive Virtuelle Realitäten (VR) in Kombination mit Technologien des ‚mobile brain imaging‘ (Makeig, Gramann, Jung, Sejnowski, & Poizner, *in press*; Makeig et al., 2007) stellen eine viel versprechende Basis für die weiterführende Analyse von Komplexitätseffekten auf behaviorale, neuroanatomische und elektrokortikale Korrelate ego- und allozentrischer Navigation in realitätsnahen Umwelten dar.

# Bibliography

- Aguirre, G. K., & D'Esposito, M. (1997). Environmental knowledge is subserved by separable dorsal/ventral neural areas. *Journal of Neuroscience*, 17(7), 2512-2518.
- Aguirre, G. K., & D'Esposito, M. (1999). Topographical disorientation: A synthesis and taxonomy. *Brain*, 122(9), 1613-1628.
- Aguirre, G. K., Zarahn, E., & D'Esposito, M. (1998). Neural components of topographical representation. *Proceedings of the Proceedings of the National Academy of Sciences of the United States of America*, 95(3), 839-846.
- Akalin-Acar, Z., & Gencer, N. G. (2004). An advanced boundary element method (BEM) implementation for the forward problem of electromagnetic source imaging. *Physics in Medicine and Biology*, 49(21), 5011-5028.
- Alyan, S., & McNaughton, B. L. (1999). Hippocampectomized rats are capable of homing by path integration. *Behavioral Neuroscience*, 113(1), 19-31.
- American Association of Psychology. (2002). Ethical principles of psychologists and code of conduct. Retrieved 10-01-2009: <http://www.apa.org/ethics/code2002.pdf>
- Andersen, R. A. (1995). Encoding of intention and spatial location in the posterior parietal cortex. *Cerebral Cortex*, 5(5), 457-469.
- Andersen, R. A., Snyder, L. H., Bradley, D. C., & Xing, J. (1997). Multimodal representation of space in the posterior parietal cortex and its use in planning movements. *Annual Review of Neuroscience*, 20, 303-330.

- Anemüller, J., Sejnowski, T. J., & Makeig, S. (2003). Complex independent component analysis of frequency-domain electroencephalographic data. *Neural Networks, 16*(9), 1311-1323.
- Angelakis, E., Lubar, J. F., Stathopoulou, S., & Kounios, J. (2004). Peak alpha frequency: an electroencephalographic measure of cognitive preparedness. *Clinical Neurophysiology, 115*(4), 887-897.
- Asada, H., Fukuda, Y., Tsunoda, S., Yamaguchi, M., & Tonoike, M. (1999). Frontal midline theta rhythms reflect alternative activation of prefrontal cortex and anterior cingulate cortex in humans. *Neuroscience Letters, 274*(1), 29-32.
- Astafiev, S. V., Shulman, G. L., Stanley, C. M., Snyder, A. Z., Van Essen, D. C., & Corbetta, M. (2003). Functional organization of human intraparietal and frontal cortex for attending, looking, and pointing. *Journal of Neuroscience, 23*(11), 4689-4699.
- Avraamides, M. N., Klatzky, R. L., Loomis, J. M., & Golledge, R. G. (2004a). Use of cognitive versus perceptual heading during imagined locomotion depends on the response mode. *Psychological Science, 15*(6), 403-408.
- Avraamides, M. N., Loomis, J. M., Klatzky, R. L., & Golledge, R. G. (2004b). Functional equivalence of spatial representations derived from vision and language: evidence from allocentric judgments. *Journal of Experimental Psychology - Learning Memory and Cognition, 30*(4), 804-814.
- Avraamides, M. N., & Sofroniou, S. G. (2006). Spatial frameworks in imagined navigation. *Psychonomic Bulletin & Review, 13*(3), 510-515.
- Bakeman, R. (2005). Recommended effect size statistics for repeated measures designs. *Behavior Research Methods, 37*(3), 379-384.
- Bakker, N. H., Werkhoven, P. J., & Passenier, P. O. (1999). The effects of proprioceptive and visual feedback on geographical orientation in virtual environments. *Presence - Teleoperators and Virtual Environments, 8*(1), 36-53.
- Barbas, H., & Blatt, G. J. (1995). Topographically specific hippocampal projections target functionally distinct prefrontal areas in the rhesus monkey. *Hippocampus, 5*(6), 511-533.
- Bartussek, D., & Gräser, H. (1980). Ergebnisse dreimodaler Faktorenanalysen von EEG-Frequenzspektren. In S. Kubicki, W. M. Herrmann & G. Laudahn (Eds.), *Faktorenanalyse und Variablenbildung aus dem Electroenzephalogramm* (pp. 79-87). Stuttgart: Fischer.
- Basar, E., Basar-Eroglu, C., Karakas, S., & Schürmann, M. (2000). Brain oscillations in perception and memory. *International Journal of Psychophysiology, 35*(2-3), 95-124.

- Basar, E., & Schürmann, M. (1997). Functional correlates of alphas. Panel discussion of the conference 'Alpha Processes in the Brain'. *International Journal of Psychophysiology*, 26(1-3), 455-474.
- Begall, S., Cervený, J., Neef, J., Vojtech, O., & Burda, H. (2008). Magnetic alignment in grazing and resting cattle and deer. *Proceedings of the National Academy of Sciences of the United States of America*, 105(36), 13451.
- Bell, A. J., & Sejnowski, T. J. (1995a). Blind Separation and Blind Deconvolution - an Information-Theoretic Approach. *1995 International Conference on Acoustics, Speech, and Signal Processing - Conference Proceedings, Vols 1-5*, 3415-3418.
- Bell, A. J., & Sejnowski, T. J. (1995b). An information-maximization approach to blind separation and blind deconvolution. *Neural Computation*, 7(6), 1129-1159.
- Benhamou, S. (1997). On systems of reference involved in spatial memory. *Behavioural Processes*, 40(2), 149-163.
- Benhamou, S., Sauve, J. P., & Bovet, P. (1990). Spatial memory in large-scale movements - Efficiency and limitation of the egocentric coding process. *Journal of Theoretical Biology*, 145(1), 1-12.
- Benhamou, S., & Seguinot, V. (1995). How to find one's way in the labyrinth of path integration models. *Journal of Theoretical Biology*, 174, 352-355.
- Berger, H. (1929). Über das Elektrenkephalogramm des Menschen. *Archiv für Psychiatrie und Nervenkrankheiten*, 87, 527-570.
- Biegler, R. (2000). Possible uses of path integration in animal navigation. *Animal Learning & Behavior*, 28(3), 257-277.
- Bischof, W. F., & Boulanger, P. (2003). Spatial navigation in virtual reality environments: An EEG analysis. *CyberPsychology & Behavior*, 6(5), 487-495.
- Bisetzky, A. R. (1957). Die Tänze der Bienen nach einem Fussweg zum Futterplatz. *Journal of Comparative Physiology A: Sensory, Neural, and Behavioral Physiology*, 40(3), 264-288.
- Blair, R. C., & Karniski, W. (1993). An alternative method for significance testing of waveform difference potentials. *Psychophysiology*, 30, 518-524.
- Bohbot, V. D., Iaria, G., & Petrides, M. (2004). Hippocampal function and spatial memory: evidence from functional neuroimaging in healthy participants and performance of patients with medial temporal lobe resections. *Neuropsychology*, 18(3), 418-425.
- Bohbot, V. D., Kalina, M., Stepankova, K., Spackova, N., Petrides, M., & Nadel, L. (1998). Spatial memory deficits in patients with lesions to the right hip-

- pocampus and to the right parahippocampal cortex. *Neuropsychologia*, 36(11), 1217-1238.
- Boston, M., & Charlestown, M. (2001). Medial Temporal and Prefrontal Contributions to Working Memory Tasks With Novel and Familiar Stimuli. *Hippocampus*, 11, 337-346.
- Boussaoud, D. (1995). Primate premotor cortex: modulation of preparatory neuronal activity by gaze angle. *Journal of Neurophysiology*, 73(2), 886-890.
- Boussaoud, D. (2001). Attention versus intention in the primate premotor cortex. *Neuroimage*, 14(1), 40-45.
- Bowman, D. A., & McMahan, R. P. (2007). Virtual reality: How much immersion is enough? *Computer*, 40(7), 36-43.
- Brandt, T., Schautzer, F., Hamilton, D. A., Bruning, R., Markowitsch, H. J., Kalla, R., Darlington, C., Smith, P., & Strupp, M. (2005). Vestibular loss causes hippocampal atrophy and impaired spatial memory in humans. *Brain*, 128(11), 2732-2741.
- Bremmer, F., Duhamel, J. R., Ben Hamed, S., & Graf, W. (2002). Heading encoding in the macaque ventral intraparietal area (VIP). *European Journal of Neuroscience*, 16(8), 1554-1568.
- Bremmer, F., Schlack, A., Duhamel, J. R., Graf, W., & Fink, G. R. (2001). Space coding in primate posterior parietal cortex. *Neuroimage*, 14(1), S46-S51.
- Bremmer, F., Schlack, A., Shah, N. J., Zafiris, O., Kubischik, M., Hoffmann, K. P., Zilles, K., & Fink, G. R. (2001). Polymodal motion processing in posterior parietal and premotor cortex: A human fMRI study strongly implies equivalencies between humans and monkeys. *Neuron*, 29(1), 287-296.
- Brett, M., Anton, J. L., Valabregue, R., & Poline, J. B. (2002). Region of interest analysis using an SPM toolbox. *Neuroimage*, 16(2), 1140-1141.
- Brewer, B., & Pears, J. (1999). Introduction: Spatial representations. In N. Eilan, R. McCarthy & B. Brewer (Eds.), *Spatial Representation: Problems in Philosophy and Psychology* (2. ed., pp. 31-42). New York: Oxford University Press.
- Britten, K. H., & van Wezel, R. J. A. (1998). Electrical microstimulation of cortical area MST biases heading perception in monkeys. *Nature Neuroscience*, 1, 59-63.
- Britten, K. H., & van Wezel, R. J. A. (2002). Area MST and heading perception in macaque monkeys. *Cerebral Cortex*, 12(7), 692-701.
- Brodmann, K. (1925). *Vergleichende Lokalisationslehre der Grosshirnrinde: In ihren Principien dargestellt auf Grund des Zellenbaues* (2. ed.). Leipzig: Johann Ambrosius Barth Verlag.

- Brotchie, P. R., Andersen, R. A., Snyder, L. H., & Goodman, S. J. (1995). Head position signals used by parietal neurons to encode locations of visual stimuli. *Nature*, 375(6528), 232-235.
- Bryant, D. J. (1992). A spatial representation system in humans [Electronic Version]. *Psychology, 3* from <http://www.cogsci.ecs.soton.ac.uk/cgi/psyc/newpsy?3.16>.
- Bryant, D. J., & Tversky, B. (1999). Mental representations of perspective and spatial relations from diagrams and models. *Journal of Experimental Psychology - Learning Memory and Cognition*, 25(1), 137-156.
- Buckwalter, J. A., Schumann, C. M., & Van Hoesen, G. W. (2008). Evidence for direct projections from the basal nucleus of the amygdala to retrosplenial cortex in the Macaque monkey. *Experimental Brain Research*, 186(1), 47-57.
- Bullock, T. H. (1992). Introduction to induced rhythms: A widespread, heterogeneous class of oscillations. In E. Basar & T. H. Bullock (Eds.), *Induced rhythms in the brain* (pp. 1-26). Boston: Birkhäuser.
- Burgess, N. (2006). Spatial memory: How egocentric and allocentric combine. *Trends in Cognitive Sciences*, 10(12), 551-557.
- Burgess, N. (2008). Spatial cognition and the brain. *Annals of the New York Academy of Sciences*, 1124, 77-96.
- Burgess, N., Maguire, E. A., & O'Keefe, J. (2002). The human hippocampus and spatial and episodic memory. *Neuron*, 35(4), 625-641.
- Burgess, N., Maguire, E. A., Spiers, H. J., & O'Keefe, J. (2001). A temporoparietal and prefrontal network for retrieving the spatial context of lifelike events. *Neuroimage*, 14(2), 439-453.
- Burgess, N., Spiers, H. J., & Paleologou, E. (2004). Orientational manoeuvres in the dark: dissociating allocentric and egocentric influences on spatial memory. *Cognition*, 94(2), 149-166.
- Byrne, P., & Becker, S. (2008). A principle for learning egocentric-allocentric transformation. *Neural Computation*, 20(3), 709-737.
- Byrne, P., Becker, S., & Burgess, N. (2007). Remembering the past and imagining the future: A neural model of spatial memory and imagery. *Psychological Review*, 114(2), 340-377.
- Calton, J. L., & Taube, J. S. (2009). Where am I and how will I get there from here? A role for posterior parietal cortex in the integration of spatial information and route planning. *Neurobiology of Learning and Memory*, 91(2), 186-196.

- Caplan, J. B., Kahana, M. J., Sekuler, R., Kirschen, M., & Madsen, J. R. (2000). Task dependence of human theta: The case for multiple cognitive functions. *Neurocomputing*, 32(33), 659-665.
- Caplan, J. B., Madsen, J. R., Raghavachari, S., & Kahana, M. J. (2001). Distinct patterns of brain oscillations underlie two basic parameters of human maze learning. *Journal of Neurophysiology*, 86(1), 368-380.
- Caplan, J. B., Madsen, J. R., Schulze-Bonhage, A., Aschenbrenner-Scheibe, R., Newman, E. L., & Kahana, M. J. (2003). Human theta oscillations related to sensorimotor integration and spatial learning. *Journal of Neuroscience*, 23(11), 4726-4736.
- Cavada, C., & Goldman-Rakic, P. S. (1989a). Posterior parietal cortex in rhesus monkey: I. Parcellation of areas based on distinctive limbic and sensory corticocortical connections. *Journal of Comparative Neurology*, 287(4), 393-421.
- Cavada, C., & Goldman-Rakic, P. S. (1989b). Posterior parietal cortex in rhesus monkey: II. Evidence for segregated corticocortical networks linking sensory and limbic areas with the frontal lobe. *Journal of Comparative Neurology*, 287(4), 422-445.
- Cavanna, A. E., & Trimble, M. R. (2006). The precuneus: a review of its functional anatomy and behavioural correlates. *Brain*, 129, 564-583.
- Chance, S. S., Gaunet, F., Beall, A., & Loomis, J. M. (1998). Locomotion mode affects the updating of objects encountered during travel: The contribution of vestibular and proprioceptive inputs to path integration. *Presence - Teleoperators and Virtual Environments*, 7(2), 168-178.
- Chen, L. L., Lin, L., Green, E. J., Barnes, C. A., & McNaughton, B. L. (1994). Head-direction cells in the rat posterior cortex. I. Anatomical distribution and behavioral modulation. *Experimental Brain Research*, 101(1), 8-23.
- Chen, L. L., Lin, L. H., Barnes, C. A., & McNaughton, B. L. (1994). Head-direction cells in the rat posterior cortex. II. Contributions of visual and ideothetic information to the directional firing. *Experimental Brain Research*, 101(1), 24-34.
- Christou, C., & Bühlhoff, H. H. (2000). Using realistic virtual environments in the study of spatial encoding. In C. Freksa, W. Brauer, C. Habel & K. F. Wender (Eds.), *Lecture Notes in Artificial Intelligence, Spatial Cognition II* (Vol. 1849, pp. 317-332). New York: Springer.
- Cisek, P., & Kalaska, J. F. (2005). Neural correlates of reaching decisions in dorsal premotor cortex: Specification of multiple direction choices and final selection of action. *Neuron*, 45(5), 801-814.
- Colby, C. L., & Goldberg, M. E. (1999). Space and attention in parietal cortex. *Annual Review of Neuroscience*, 22, 319-349.

- Collett, M., & Collett, T. S. (1982). Do geese use path integration for walking? In F. Papi & P. Wallraff (Eds.), *Avian Navigation* (pp. 198-307). Berlin: Springer.
- Collett, M., & Collett, T. S. (2000). How do insects use path integration for their navigation? *Biological Cybernetics*, 83, 245–259.
- Coluccia, E., & Louse, G. (2004). Gender differences in spatial orientation: A review. *Journal of Environmental Psychology*, 24, 329-340.
- Committeri, G., Galati, G., Paradis, A. L., Pizzamiglio, L., Berthoz, A., & LeBihan, D. (2004). Reference frames for spatial cognition: Different brain areas are involved in viewer-, object-, and landmark-centered judgments about object location. *Journal of Cognitive Neuroscience*, 16(9), 1517-1535.
- Cooper, B. G., Manka, T. F., & Mizumori, S. J. Y. (2001). Finding your way in the dark: The retrosplenial cortex contributes to spatial memory and navigation without visual cues. *Behavioral Neuroscience*, 115(5), 1012-1028.
- Cornell, E. H., & Bourassa, C. M. (2007). Human non-visual discrimination of gradual turning is poor. *Psychological Research*, 71(3), 314-321.
- Cornell, E. H., & Greidanus, E. (2006). Path integration during a neighborhood walk *Spatial Cognition & Computation*, 6(3), 203 - 234.
- Cornell, E. H., & Heth, C. D. (2004). Memories of travel: Dead reckoning within the cognitive map. In G. L. Allen (Ed.), *Human Spatial Memory: Remembering Where* (pp. 191-216). Mahwah: Lawrence Erlbaum Associates.
- Cornell, E. H., Heth, C. D., & Skoczyłas, M. J. (1999). The nature and use of route expectancies following incidental learning. *Journal of Environmental Psychology*, 19(3), 209-229.
- Cornetz, V. (1912). Über den Gebrauch des Ausdruckes „tropisch“ und über den Charakter der Richtungskraft bei Ameisen [Concerning the usage of term "tropic" and concerning the character of sense of direction in ants]. *Pflügers Archiv für die gesamte Physiologie des Menschen und der Tiere*, 147(3/5), 215-233.
- Cornwell, B. R., Johnson, L. L., Holroyd, T., Carver, F. W., & Grillon, C. (2008). Human hippocampal and parahippocampal theta during goal-directed spatial navigation predicts performance on a virtual Morris water maze. *Journal of Neuroscience*, 28(23), 5983-5990.
- Cousins, J. H., Siegel, A. W., & Maxwell, S. E. (1983). Way finding and cognitive mapping in large-scale environments: a test of a developmental model. *Journal of Experimental Child Psychology*, 35(1), 1-20.
- Culham, J., He, S., Dukelow, S., & Verstraten, F. A. J. (2001). Visual motion and the human brain: What has neuroimaging told us? *Acta Psychologica*, 107(1-3), 69-94.

- Cutmore, T. R. H., Hine, T. J., Maberly, K. J., Langford, N. M., & Hawgood, G. (2000). Cognitive and gender factors influencing navigation in a virtual environment. *International Journal of Human computer studies*, 53(2), 223-250.
- Cutting, J. E., & Vishton, P. M. (1995). Perceiving layout and knowing distances: The integration, relative potency, and contextual use of different information about depth. In W. Epstein & S. Rogers (Eds.), *Handbook of perception and cognition, Vol 5; Perception of space and motion*. San Diego, CA: Academic Press.
- Darwin, C. (1873). Origin of certain instincts. *Nature*, 7, 417-418.
- de Araujo, D. B., Baffa, O., & Wakai, R. T. (2002). Theta oscillations and human navigation: A magnetoencephalography study. *Journal of Cognitive Neuroscience*, 14(1), 70-78.
- de Jong, B. M., Shipp, S., Skidmore, B., Frackowiak, R. S. J., & Zeki, S. (1994). The cerebral activity related to the visual perception of forward motion in depth. *Brain*, 117(5), 1039.
- de Vega, M., & Rodrigo, M. J. (2001). Updating spatial layouts mediated by pointing and labelling under physical and imaginary rotation. *European Journal of Cognitive Psychology*, 13(3), 369 - 393.
- Dean, H. L., & Platt, M. L. (2006). Allocentric spatial referencing of neuronal activity in macaque posterior cingulate cortex. *Journal of Neuroscience*, 26(4), 1117-1127.
- Debener, S., Ullsperger, M., Siegel, M., Fiehler, K., von Cramon, D. Y., & Engel, A. K. (2005). Trial-by-trial coupling of concurrent electroencephalogram and functional magnetic resonance imaging Identifies the dynamics of performance monitoring. *Journal of Neuroscience*, 25(50), 11730.
- Delorme, A., & Makeig, S. (2003). EEG changes accompanying learned regulation of 12-Hz EEG activity. *Neural Systems and Rehabilitation Engineering, IEEE Transactions on [see also IEEE Trans. on Rehabilitation Engineering]*, 11(2), 133-137.
- Delorme, A., & Makeig, S. (2004). EEGLAB: An open source toolbox for analysis of single-trial EEG dynamics including independent component analysis. *Journal of Neuroscience Methods*, 134, 9-21.
- Delorme, A., Sejnowski, T., & Makeig, S. (2007). Enhanced detection of artifacts in EEG data using higher-order statistics and independent component analysis. *Neuroimage*, 34(4), 1443-1449.
- Denis, M., & Loomis, J. M. (2007). Perspectives on human spatial cognition: Memory, navigation, and environmental learning. *Psychological Research*, 71(3), 235-239.

- Denis, M., Pazzaglia, F., & Cornoldi, C. (1999). Spatial discourse and navigation: An analysis of route directions in the city of Venice. *Applied Cognitive Psychology, 13*, 145-174.
- Desimone, R., Albright, T. D., Gross, C. G., & Bruce, C. (1984). Stimulus-selective properties of inferior temporal neurons in the macaque. *Journal of Neuroscience, 4*(8), 2051-2062.
- Dichgans, J., & Brandt, T. (1978). Visual vestibular interaction: Effects on self-motion perception and postural control. In R. Held, H. W. Leibowitz & H. L. Teuber (Eds.), *Perception* (pp. 756-804). Berlin: Springer.
- Dieterich, M., Bense, S., Stephan, T., Yousry, T. A., & Brandt, T. (2003). fMRI signal increases and decreases in cortical areas during small-field optokinetic stimulation and central fixation. *Experimental Brain Research, 148*(1), 117-127.
- Diwadkar, V. A., Carpenter, P. A., & Just, M. A. (2000). Collaborative activity between parietal and dorso-lateral prefrontal cortex in dynamic spatial working memory revealed by fMRI. *Neuroimage, 12*(1), 85-99.
- Doppelmayr, M. M., Klimesch, W., Pachinger, T., & Ripper, B. (1998). The functional significance of absolute power with respect to event-related desynchronization. *Brain Topography, 11*(2), 133-140.
- Duffy, C. J., Page, W. K., & Froehler, M. T. (2005). Posterior cortical processing of self-movement cues: MSTd's role in Papez's circuit for navigation and orientation. In J. M. Wiener & J. S. Taube (Eds.), *Head Direction Cells and the Neural Mechanisms of Spatial Orientation* (pp. 319-345). Cambridge: MIT Press.
- Duffy, C. J., & Wurtz, R. H. (1991a). Sensitivity of MST neurons to optic flow stimuli. I. A continuum of response selectivity to large-field stimuli. *Journal of Neurophysiology, 65*(6), 1329-1345.
- Duffy, C. J., & Wurtz, R. H. (1991b). Sensitivity of MST neurons to optic flow stimuli. II. Mechanisms of response selectivity revealed by small-field stimuli. *Journal of Neurophysiology, 65*(6), 1346-1359.
- Duhamel, J. R., Colby, C. L., & Goldberg, M. E. (1998). Ventral intraparietal area of the macaque: congruent visual and somatic response properties. *Journal of Neurophysiology, 79*(1), 126-136.
- Dupont, P., Orban, G. A., De Bruyn, B., Verbruggen, A., & Mortelmans, L. (1994). Many areas in the human brain respond to visual motion. *Journal of Neurophysiology, 72*(3), 1420-1424.
- Dyer, F. (1998). Cognitive ecology of navigation. In R. Dukas (Ed.), *Cognitive Ecology* (pp. 201-260). Chicago: University of Chicago Press.

- Ekstrom, A. D., Kahana, M. J., Caplan, J. B., Fields, T. A., Isham, E. A., Newman, E. L., & Fried, I. (2003). Cellular networks underlying human spatial navigation. *Nature*, 425(6954), 184-188.
- Enright, J. T. (1998). On the 'cyclopean eye': Saccadic asymmetry and the reliability of perceived straight-ahead. *Vision Research*, 38(3), 459-469.
- Epstein, R. A., Parker, W. E., & Feiler, A. M. (2007). Where am I now? Distinct roles for parahippocampal and retrosplenial cortices in place recognition. *Journal of Neuroscience*, 27(23), 6141-6149.
- Etchamendy, N., & Bohbot, V. D. (2007). Spontaneous navigational strategies and performance in the virtual town. *Hippocampus*, 17(8), 595-599.
- Etienne, A. S., & Jeffery, K. J. (2004). Path integration in mammals. *Hippocampus*, 14(2), 180-192.
- Etienne, A. S., Maurer, R., Berlie, J., Reverdin, B., Rowe, T., Georgakopoulos, J., & Seguinot, V. (1998). Navigation through vector addition. *Nature*, 396(6707), 161-164.
- Etienne, A. S., Maurer, R., & Georgakopoulos, J. (1999). Dead reckoning (path integration), landmarks, and representation of space in a comparative perspective. In R. G. Golledge (Ed.), *Wayfinding Behavior: Cognitive Mapping and Other Spatial Processes* (pp. 197-128). Baltimore: Johns Hopkins University Press.
- Etienne, A. S., Maurer, R., & Seguinot, V. (1996). Path integration in mammals and its interaction with visual landmarks. *Journal of Experimental Biology*, 199(Pt 1), 201-209.
- Farrell, M. J., & Robertson, I. H. (1998). Mental rotation and the automatic updating of body-centered spatial relationships. *Journal of Experimental Psychology - Learning Memory and Cognition*, 24(1), 227-233.
- Farrell, M. J., & Robertson, I. H. (2000). The automatic updating of egocentric spatial relationships and its impairment due to right posterior cortical lesions. *Neuropsychologia*, 38(5), 585-595.
- Farrer, C., & Frith, C. D. (2002). Experiencing oneself vs another person as being the cause of an action: The neural correlates of the experience of agency. *Neuroimage*, 15(3), 596-603.
- Fernandez, C., & Goldberg, J. M. (197). Physiology of peripheral neurons innervating otolith organs of the squirrel monkey. II. Directional selectivity and force-response relations. *Journal of Neurophysiology*, 39, 985-995.
- Fetsch, C. R., Wang, S., Gu, Y., Deangelis, G. C., & Angelaki, D. E. (2007). Spatial reference frames of visual, vestibular, and multimodal heading signals in the dorsal subdivision of the medial superior temporal area. *Journal of Neuroscience*, 27(3), 700-712.

- Field, D. T., Wilkie, R. M., & Wann, J. P. (2007). Neural systems in the visual control of steering. *Journal of Neuroscience*, 27(30), 8002-8010.
- Fink, G. R., Marshall, J. C., Shah, N. J., Weiss, P. H., Halligan, P. W., Grosse-Ruyken, M., Ziemons, K., Zilles, K., & Freund, H. J. (2000). Line bisection judgments implicate right parietal cortex and cerebellum as assessed by fMRI. *Neurology*, 54(6), 1324-1331.
- Fink, G. R., Marshall, J. C., Weiss, P. H., Stephan, T., Grefkes, C., Shah, N. J., Zilles, K., & Dieterich, M. (2003). Performing allocentric visuospatial judgments with induced distortion of the egocentric reference frame: an fMRI study with clinical implications. *Neuroimage*, 20(3), 1505-1517.
- Fletcher, P. C., Shallice, T., Frith, C. D., Frackowiak, R. S. J., & Dolan, R. J. (1996). Brain activity during memory retrieval. The influence of imagery and semantic cuing. *Brain*, 119, 1587-1596.
- Foo, P., Duchon, A., Warren, W. H., Jr., & Tarr, M. J. (2007). Humans do not switch between path knowledge and landmarks when learning a new environment. *Psychological Research*, 71(3), 240-251.
- Foo, P., Warren, W. H., Duchon, A., & Tarr, M. J. (2005). Do humans integrate routes into a cognitive map? Map- versus landmark-based navigation of novel shortcuts. *Journal of Experimental Psychology - Learning Memory and Cognition*, 31(2), 195-215.
- Foster, T. C., Castro, C. A., & McNaughton, B. L. (1989). Spatial selectivity of rat hippocampal neurons: Dependence on preparedness for movement. *Science*, 244(4912), 1580-1582.
- Fowler, K. S., Saling, M. M., Conway, E. L., Semple, J. M., & Louis, W. J. (2002). Paired associate performance in the early detection of DAT. *Journal of the International Neuropsychological Society*, 8(01), 58-71.
- Foxe, J. J., & Simpson, G. V. (2002). Flow of activation from V1 to frontal cortex in humans. *Experimental Brain Research*, 142(1), 139-150.
- Foxe, J. J., Simpson, G. V., & Ahlfors, S. P. (1998). Parieto-occipital ~10 Hz activity reflects anticipatory state of visual attention mechanisms. *NeuroReport*, 9(17), 3929.
- Franklin, N., & Tversky, B. (1990). Searching imagined environments. *Journal of Experimental Psychology - General*, 119, 63-76.
- Frenz, H., & Lappe, M. (2005). Absolute travel distance from optic flow. *Vision Research*, 45(13), 1679-1692.
- Froehler, M. T., & Duffy, C. J. (2006). Neurons in cortical area MST integrate heading and landmark cues for spatial orientation. *Annals of Neurology*, 60, S32-S32.

- Fujii, N., Mushiake, H., & Tanji, J. (2000). Rostrocaudal distinction of the dorsal premotor area based on oculomotor involvement. *Journal of Neurophysiology*, 83(3), 1764-1769.
- Fujita, N., Klatzky, R. L., Loomis, J. M., & Golledge, R. G. (1993). The encoding-error model of pathway completion without vision. *Geographical Analysis*, 25(4), 295-314.
- Fuster, J. M. (2008). *The prefrontal cortex* (4. ed.). London: Elsevier Science & Technology.
- Gaffan, E. A., Gaffan, D., & Harrison, S. (1988). Disconnection of the amygdala from visual association cortex impairs visual reward-association learning in monkeys. *Journal of Neuroscience*, 8(9), 3144-3150.
- Galati, G., Committeri, G., Sanes, J. N., & Pizzamiglio, L. (2001). Spatial coding of visual and somatic sensory information in body-centred coordinates. *European Journal of Neuroscience*, 14(4), 737-746.
- Galati, G., Lobel, E., Vallar, G., Berthoz, A., Pizzamiglio, L., & Le Bihan, D. (2000). The neural basis of egocentric and allocentric coding of space in humans: a functional magnetic resonance study. *Experimental Brain Research*, 133(2), 156-164.
- Galletti, C., Battaglini, P. P., & Fattori, P. (1995). Eye position influence on the parieto-occipital area PO (V6) of the macaque monkey. *European Journal of Neuroscience*, 7(12), 2486-2501.
- Gallistel, C. R. (1990). *The organization of learning*. Cambridge: MIT Press.
- Gallistel, C. R. (1993). *The organization of learning* (2. ed.). Cambridge: MIT Press.
- Georges-Francois, P., Rolls, E. T., & Robertson, R. G. (1999). Spatial view cells in the primate hippocampus: Allocentric view not head direction or eye position or place. *Cerebral Cortex*, 9(3), 197-212.
- Gevins, A., & Smith, M. E. (2000). Neurophysiological measures of working memory and individual differences in cognitive ability and cognitive style. *Cerebral Cortex*, 10(9), 829-839.
- Gevins, A., Smith, M. E., McEvoy, L., & Yu, D. (1997). High-resolution EEG mapping of cortical activation related to working memory: Effects of task difficulty, type of processing, and practice. *Cerebral Cortex*, 7(4), 374-385.
- Ghaem, O., Mellet, E., Crivello, F., Tzourio, N., Mazoyer, B., Berthoz, A., & Denis, M. (1997). Mental navigation along memorized routes activates the hippocampus, precuneus, and insula. *Neuroreport*, 8(3), 739.
- Ghosh, S., & Gattera, R. (1995). A comparison of the ipsilateral cortical projections to the dorsal and ventral subdivisions of the macaque premotor cortex. *Somatosensory and Motor Research*, 12(3), 359-378.

- Gibson, J. J. (1954). The visual perception of objective motion and subjective movement. *Psychological Review*, 61(5), 304-314.
- Gillner, S., & Mallot, H. A. (1998). Navigation and acquisition of spatial knowledge in a virtual maze. *Journal of Cognitive Neuroscience*, 10(4), 445-463.
- Glasauer, S., Amorim, M.-A., & Viaud-Delmon, I. (2002). Differential effects of labyrinthine dysfunction on distance and direction during blindfolded walking of a triangular path. *Experimental Brain Research*, 145, 489-497.
- Goldman-Rakic, P. S., Selemon, L. D., & Schwartz, M. L. (1984). Dual pathways connecting the dorsolateral prefrontal cortex with the hippocampal formation and parahippocampal cortex in the rhesus monkey. *Neuroscience*, 12(3), 719-743.
- Goldstein, B. (2007). Sensation and perception. London: Wadsworth-Thomson Learning.
- Golledge, R. G. (1995). Primitives of spatial knowledge. In T. L. Nyerges, R. Laurini, M. J. Egenhofer & D. M. Mark (Eds.), *Cognitive aspects of human-computer interaction for geographic information systems* (pp. 29-44). Norwell, MA: Kluwer Academic Publishers.
- Golledge, R. G. (1997). Path selection and route preference in human navigation: A progress report. In S. Hirtle & A. U. Frank (Eds.), *Spatial information theory: A theoretical basis for GIS : International International Conference COSIT '97* (pp. 207-222). Heidelberg: Springer.
- Golledge, R. G. (1999a). Human wayfinding and cognitive maps. In R. G. Golledge (Ed.), *Wayfinding behavior. Cognitive mapping and other spatial processes* (pp. 5-45). Baltimore: Johns Hopkins University Press.
- Golledge, R. G. (Ed.). (1999b). *Wayfinding behavior. Cognitive mapping and other spatial processes*. Baltimore: Johns Hopkins University Press.
- Golledge, R. G., Dougherty, V., & Bell, S. (1995). Acquiring spatial knowledge - Survey versus route-based knowledge in unfamiliar environments. *Annals of the Association of American Geographers*, 85(1), 134-158.
- Görner, P. (1958). Die optische und kinästhetische Orientierung der Trichterpinne *Agelena Labyrinthica* (Cl.). *Journal of Comparative Physiology A: Neuroethology, Sensory, Neural, and Behavioral Physiology*, 41(2), 111-153.
- Gramann, K. (2002). *Arbeitsgedächtnis und elektrokortikale Aktivität. Eine experimentelle Untersuchung zur Differenzierung von Subsystemen des Arbeitsgedächtnisses*. Rheinisch-Westfälische Technische Hochschule, Aachen.
- Gramann, K., El Sharkawy, J., & Deubel, H. (in press). Eye-movements during navigation in a virtual tunnel. *International Journal of Neuroscience*.

- Gramann, K., Müller, H. J., Eick, E. M., & Schönebeck, B. (2005). Evidence of separable spatial representations in a virtual navigation task. *Journal of Experimental Psychology - Human Perception and Performance*, 31(6), 1199-1223.
- Gramann, K., Müller, H. J., Schönebeck, B., & Debus, G. (2006). The neural basis of ego- and allocentric reference frames in spatial navigation: evidence from spatio-temporal coupled current density reconstruction. *Brain Research*, 1118(1), 116-129.
- Gramann, K., Onton, J., Riccobon, D., Müller, H. J., Bardins, S., & Makeig, S. (submitted). Human brain dynamics accompanying the use of egocentric and allocentric reference frames during spatial navigation.
- Graziano, M. S., Yap, G. S., & Gross, C. G. (1994). Coding of visual space by premotor neurons. *Science*, 266(5187), 1054-1057.
- Green, J. D., & Arduini, A. A. (1954). Hippocampal electrical activity in arousal. *Journal of Neurophysiology*, 17(6), 533-557.
- Grön, G., Wunderlich, A. P., Spitzer, M., Tomczak, R., & Riepe, M. W. (2000). Brain activation during human navigation: Gender-different neural networks as substrate of performance. *Nature Neuroscience*, 3(4), 404-408.
- Grush, R. (2000). Self, world and space: The meaning and mechanisms of ego- and allocentric spatial representation. *Brain and Mind*, 1, 59-92.
- Haalman, I., & Vaadia, E. (1997). Dynamics of neuronal interactions: Relation to behavior, firing rates, and distance between neurons. *Human Brain Mapping*, 5(4), 249-253.
- Hafting, T., Fyhn, M., Molden, S., Moser, M. B., & Moser, E. I. (2005). Microstructure of a spatial map in the entorhinal cortex. *Nature*, 436(7052), 801-806.
- Haggard, P., Newman, C., Blundell, J., & Andrew, H. (2000). The perceived position of the hand in space. *Perception & Psychophysics*, 68(2), 363-377.
- Harris, I. M., Egan, G. F., Sonkkila, C., Tochon-Danguy, H. J., Paxinos, G., & Watson, J. D. G. (2000). Selective right parietal lobe activation during mental rotation - A parametric PET study. *Brain*, 123, 65-73.
- Hartigan, J. A., & Wong, M. A. (1979). Algorithm AS 136: A k-means clustering algorithm. *Applied Statistics*, 28(1), 100-108.
- Hartley, T., Maguire, E. A., Spiers, H. J., & Burgess, N. (2003). The well-worn route and the path less traveled: Distinct neural bases of route following and wayfinding in humans. *Neuron*, 37(5), 877-888.
- Hartmann, G., & Wehner, R. (1995). The ant's path integration system - a neural architecture. *Biological Cybernetics*, 73(6), 483-497.

- Haxby, J. V., Grady, C. L., Horwitz, B., Ungerleider, L. G., Mishkin, M., Carson, R. E., Herscovitch, P., Schapiro, M. B., & Rapoport, S. I. (1991). Dissociation of object and spatial visual processing pathways in human extrastriate cortex. *Proceedings of the Proceedings of the National Academy of Sciences of the United States of America*, 88(5), 1621-1625.
- Heft, H. (1979). The role of environmental features in route-learning: Two exploratory studies of way-finding. *Environmental Psychology and Nonverbal Behavior*, 3, 172-185.
- Herrmann, W. M., Fichte, K., & Kubicki, S. (1980). Definition von EEG-Frequenzbändern aufgrund strukturanalytischer Betrachtungen. In S. Kubicki, W. M. Herrmann & G. Laudahn (Eds.), *Faktorenanalyse und Variablenbildung aus dem Electroencephalogramm* (pp. 61-74). Stuttgart: Fischer.
- Hettinger, L. J. (2002). Illusory self-motion in virtual environments. In K. M. Stanney (Ed.), *Handbook of virtual environments* (pp. 471-492). Hillsdale: Lawrence Erlbaum.
- Hunt, E., & Waller, D. (1999). Orientation and wayfinding: A review [Electronic Version]  
<http://www.cs.umu.se/kurser/TDBD12/HT02/papers/hunt99orientation.pdf>.
- Hyvärinen, A. (1999). Survey on independent component analysis. *Neural Computing Surveys*, 2(4), 94-128.
- Hyvärinen, A., & Oja, E. (2000). Independent component analysis: Algorithms and applications. *Neural Networks*, 13(4-5), 411-430.
- Iaria, G., Chen, J. K., Guariglia, C., Ptito, A., & Petrides, M. (2007). Retrosplenial and hippocampal brain regions in human navigation: Complementary functional contributions to the formation and use of cognitive maps. *European Journal of Neuroscience*, 25(3), 890-899.
- Iaria, G., Petrides, M., Dagher, A., Pike, B., & Bohbot, V. D. (2003). Cognitive strategies dependent on the hippocampus and caudate nucleus in human navigation: Variability and change with practice. *Journal of Neuroscience*, 23(13), 5945-5952.
- Ino, T., Inoue, Y., Kage, M., Hirose, S., Kimura, T., & Fukuyama, H. (2002). Mental navigation in humans is processed in the anterior bank of the parieto-occipital sulcus. *Neuroscience Letters*, 322(3), 182-186.
- Ivanenko, Y., Grasso, R., Israel, I., & Berthoz, A. (1997). Spatial orientation in humans: Perception of angular whole-body displacements in two-dimensional trajectories. *Experimental Brain Research*, 117(3), 419-427.
- Jansen-Osmann, P., & Berendt, B. (2002). Investigating distance knowledge using virtual environments. *Environment and Behavior*, 34(2), 178-193.

- Jansen-Osmann, P., & Wiedenbauer, G. (2006). Distance cognition in virtual environmental space: Further investigations to clarify the route-angularity effect. *Psychological Research*, 70(1), 43-51.
- Jasper, H. H., & Andrews, H. L. (1938). Electro-encephalography. III. Normal differentiation of occipital and precentral regions in man. *Swiss Archives of Neurology and Psychiatry*, 39, 96-115.
- Jensen, O., & Tesche, C. D. (2002). Frontal theta activity in humans increases with memory load in a working memory task. *European Journal of Neuroscience*, 15(8), 1395-1399.
- Johnsrude, I., Owen, A., Crane, J., Milner, B., & Evans, A. (1999). A cognitive activation study of memory for spatial relationships. *Neuropsychologia*, 37(7), 829-841.
- Jonsson, E. (2002). *Inner navigation: Why we get lost and how we find our way*. New York: Scribner.
- Jung, T. P., Humphries, C., Lee, T. W., Makeig, S., McKeown, M. J., Iragui, V., & Sejnowski, T. J. (1998). Extended ICA removes artifacts from electroencephalographic recordings. *Advances in Neural Information Processing Systems 10*, 10, 894-900.
- Kahana, M. J., Seelig, D., & Madsen, J. R. (2001). Theta returns. *Current Opinion in Neurobiology*, 11(6), 739-744.
- Kahana, M. J., Sekuler, R., Caplan, J. B., Kirschen, M., & Madsen, J. R. (1999). Human theta oscillations exhibit task dependence during virtual maze navigation. *Nature*, 399(6738), 781-784.
- Kalaska, J. F., & Crammond, D. J. (1992). Cerebral cortical mechanisms of reaching movements. *Science*, 255(5051), 1517-1523.
- Kanwisher, N., McDermott, J., & Chun, M. M. (1997). The fusiform face area: A module in human extrastriate cortex specialized for face perception. *Journal of Neuroscience*, 17(11), 4302-4311.
- Kaufman, L., Curtis, S., Wang, J. Z., & Williamson, S. J. (1992). Changes in cortical activity when subjects scan memory for tones. *Electroencephalography and Clinical Neurophysiology*, 82(4), 266.
- Kearns, M. J., Warren, W. H., Duchon, A. P., & Tarr, M. J. (2002). Path integration from optic flow and body senses in a homing task. *Perception*, 31(3), 349-374.
- Kerkhoff, G. (2000). Räumlich-perzeptive, räumlich-kognitive, räumlich-konstruktive und räumlich topographische Störungen. In W. Sturm, M. Herrmann & C.-W. Wallesch (Eds.), *Lehrbuch der Klinischen Neuropsychologie* (pp. 411-429). Lisse, NL: Swets & Zeitlinger.

- Kimichi, T., Etienne, A. S., & Terkel, J. (2004). A subterranean mammal uses the magnetic compass for path integration. *Proceedings of the National Academy of Sciences of the United States of America*, 101, 1105-1109.
- King, J. A., Trinkler, I., Hartley, T., Vargha-Khadem, F., & Burgess, N. (2004). The hippocampal role in spatial memory and the familiarity-recollection distinction: A case study. *Neuropsychology*, 18(3), 405-417.
- Kirschen, M. P., Kahana, M. J., Sekuler, R., & Burack, B. (2000). Optic flow helps humans learn to navigate through synthetic environments. *Perception*, 29(7), 801-818.
- Klatzky, R. L. (1998). Allocentric and egocentric spatial representations: Definitions, distinctions, and interconnections. In C. Freksa, C. Habel & K. F. Wender (Eds.), *Lecture Notes in Artificial Intelligence, Spatial Cognition I* (pp. 1-17). Heidelberg: Springer.
- Klatzky, R. L., Beall, A., Loomis, J. M., Golledge, R. G., & Philbeck, J. W. (1999). Human navigation ability: Tests of the encoding-error model of path integration. *Spatial Cognition & Computation*, 1(1), 31-65.
- Klatzky, R. L., Loomis, J. M., Beall, A., Chance, S. S., & Golledge, R. G. (1998). Spatial updating of self-position and orientation during real, imagined, and virtual locomotion. *Psychological Science*, 9, 293-298.
- Klatzky, R. L., Loomis, J. M., Golledge, R. G., Cicinelli, J. G., Doherty, S., & Peligrino, J. W. (1990). Acquisition of route and survey knowledge in the absence of vision. *Journal of Motor Behavior*, 22(1), 19-43.
- Klatzky, R. L., & Wu, B. (2008). The embodied actor in multiple frames of reference. In R. Klatzky, M. Behrmann & B. MacWhinney (Eds.), *Embodiment, ego-space and action* (pp. 145-176). Mahwah: Erlbaum.
- Klimesch, W. (1996). Memory processes, brain oscillations and EEG synchronization. *International Journal of Psychophysiology*, 24(1-2), 61-100.
- Klimesch, W. (1997). EEG-alpha rhythms and memory processes. *International Journal of Psychophysiology*, 26(1-3), 319-340.
- Klimesch, W. (1999). EEG alpha and theta oscillations reflect cognitive and memory performance: A review and analysis. *Brain Research Reviews*, 29(2-3), 169-195.
- Klimesch, W., Doppelmayr, M., Pachinger, T., & Ripper, B. (1997a). Brain oscillations and human memory: EEG correlates in the upper alpha and theta band. *Neuroscience Letters*, 238(1-2), 9-12.
- Klimesch, W., Doppelmayr, M., Russegger, H., Pachinger, T., & Schwaiger, J. (1998). Induced alpha band power changes in the human EEG and attention. *Neuroscience Letters*, 244(2), 73-76.

- Klimesch, W., Doppelmayr, M., Schimke, H., & Ripper, B. (1997b). Theta synchronization and alpha desynchronization in a memory task. *Psychophysiology*, 34(2), 169-176.
- Klimesch, W., Doppelmayr, M., Schwaiger, J., Auinger, P., & Winkler, T. (1999). 'Paradoxical' alpha synchronization in a memory task. *Cognitive Brain Research*, 7(4), 493-501.
- Klimesch, W., Sauseng, P., & Hanslmayr, S. (2007). EEG alpha oscillations: The inhibition-timing hypothesis. *Brain Research Reviews*, 53(1), 63-88.
- Klimesch, W., Schimke, H., & Pfurtscheller, G. (1993). Alpha frequency, cognitive load and memory performance. *Brain Topography*, 5(3), 241-251.
- Klippel, A., Freksa, C., & Winter, S. (2006). You-are-here maps in emergencies. The danger of getting lost. *Journal of Spatial Science*, 51(1), 117-131.
- Kobatake, E., & Tanaka, K. (1994). Neuronal selectivities to complex object features in the ventral visual pathway of the macaque cerebral cortex. *Journal of Neurophysiology*, 71(3), 856-867.
- Kobayashi, Y., & Amaral, D. G. (2000). Macaque monkey retrosplenial cortex: I. Three-dimensional and cytoarchitectonic organization. *The Journal of Comparative Neurology*, 426(3), 339-365.
- Kobayashi, Y., & Amaral, D. G. (2003). Macaque monkey retrosplenial cortex: II. Cortical afferents. *The Journal of Comparative Neurology*, 466(1), 48-79.
- Kobayashi, Y., & Amaral, D. G. (2007). Macaque monkey retrosplenial cortex: III. Cortical efferents. *The Journal of Comparative Neurology*, 502(5), 810-833.
- Koshino, Y., & Niedermeyer, E. (1975). Enhancement of rolandic mu-rhythm by pattern vision. *Electroencephalography and Clinical Neurophysiology*, 38(5), 535-538.
- Krause, C. M., Sillanmäki, L., Koivisto, M., Saarela, C., Häggqvist, A., Laine, M., & Hämäläinen, H. (2000). The effects of memory load on event-related EEG desynchronization and synchronization. *Clinical Neurophysiology*, 111(11), 2071-2078.
- Krauth, J., & Lienert, G. A. (1973). *Die Konfigurationsfrequenzanalyse und ihre Anwendung in Psychologie und Medizin*. München: Verlag K. Alber.
- Lambrey, S., Amorim, M. A., Samson, S., Noulhiane, M., Hasboun, D., Dupont, S., Baulac, M., & Berthoz, A. (2008). Distinct visual perspective-taking strategies involve the left and right medial temporal lobe structures differently. *Brain*, 131, 523-534.
- Lamm, C., Windischberger, C., Leodolter, U., Moser, E., & Bauer, H. (2001). Evidence for premotor cortex activity during dynamic visuospatial imagery

- from single-trial functional magnetic resonance imaging and event-related slow cortical potentials. *Neuroimage*, 14(2), 268-283.
- Lancaster, J. L., Woldorff, M. G., Parsons, L. M., Liotti, M., Freitas, C. S., Rainey, L., Kochunov, P. V., Nickerson, D., Mikiten, S. A., & Fox, P. T. (2000). Automated Talairach atlas labels for functional brain mapping. *Human Brain Mapping*, 10, 120-131.
- Landau, B., & Jackendoff, R. (1993). Spatial cognition. *Behavioral and Brain Sciences*, 16, 217-265.
- Lappe, M., Bremmer, F., & van den Berg, A. V. (1999). Perception of self-motion from visual flow. *Trends in Cognitive Sciences*, 3(9), 329-336.
- Lathrop, W. B., & Kaiser, M. K. (2005). Acquiring spatial knowledge while traveling simple and complex paths with immersive and nonimmersive interfaces. *Presence - Teleoperators and Virtual Environments*, 14(3), 249-263.
- Lawton, C. A. (1996). Strategies for indoor wayfinding: The role of orientation. *Journal of Environmental Psychology*, 16(2), 137-145.
- Lawton, C. A., & Morrin, K. A. (1999). Gender differences in pointing accuracy in computer-simulated 3D mazes. *Sex Roles*, 40(1-2), 73-92.
- Lee, I., & Kesner, R. P. (2003). Time-dependent relationship between the dorsal hippocampus and the prefrontal cortex in spatial memory. *Journal of Neuroscience*, 23(4), 1517-1523.
- Lee, T. W., Girolami, M., Bell, A. J., & Sejnowski, T. J. (2000). A unifying information-theoretic framework for independent component analysis. *Computers & Mathematics with Applications*, 39(11), 1-21.
- Lee, T. W., Girolami, M., & Sejnowski, T. J. (1999). Independent component analysis using an extended infomax algorithm for mixed subgaussian and supergaussian sources. *Neural Computation*, 11(2), 417-441.
- Leeb, R., Scherer, R., Keinrath, C., Guger, C., & Pfurtscheller, G. (2005). Exploring virtual environments with an EEG-based BCI through motor imagery. *Biomedical Engineering*, 50(4), 86-91.
- Lehmann, D., & König, T. (1997). Spatio-temporal dynamics of alpha brain electric fields, and cognitive modes. *International Journal of Psychophysiology*, 26(1-3), 99-112.
- LeVay, S., & Sherk, H. (1981). The visual claustrum of the cat. I. Structure and connections. *Journal of Neuroscience*, 1(9), 956-980.
- Linsker, R. (1992). Local synaptic learning rules suffice to maximize mutual information in a linear-network. *Neural Computation*, 4(5), 691-702.

- Loomis, J. M., & Beall, A. (1998). Visually controlled locomotion: Its dependence on optic flow, three-dimensional space perception, and cognition. *Ecological Psychology, 10*(3-4), 71–285.
- Loomis, J. M., Blascovich, J. J., & Beall, A. C. (1999a). Immersive virtual environment technology as a basic research tool in psychology. *Behavior Research Methods, Instruments, & Computers, 31*(4), 557-564.
- Loomis, J. M., Klatzky, R. L., Golledge, R. G., Cicinelli, J. G., Pellegrino, J. W., & Fry, P. A. (1993). Nonvisual navigation by blind and sighted: Assessment of path integration ability. *Journal of Experimental Psychology - General, 122*(1), 73-91.
- Loomis, J. M., Klatzky, R. L., Golledge, R. G., & Philbeck, J. W. (1999b). Human navigation by path integration. In R. G. Golledge (Ed.), *Wayfinding behavior: Cognitive mapping and spatial processes* (pp. 125-151). Baltimore: John Hopkins Univ. Press.
- Lui, L. L., Bourne, J. A., & Rosa, M. G. P. (2006). Functional response properties of neurons in the dorsomedial visual area of new world monkeys (*calithrix jacchus*). *Cerebral Cortex, 16*(2), 162-177.
- Maaswinkel, H., Jarrard, L. E., & Whishaw, I. Q. (1999). Hippocampectomized rats are impaired in homing by path integration. *Hippocampus, 9*(5), 553-561.
- Maguire, E. A. (2001). The retrosplenial contribution to human navigation: A review of lesion and neuroimaging findings. *Scandinavian Journal of Psychology, 42*(3), 225-238.
- Maguire, E. A., Burgess, N., Donnett, J. G., Frackowiak, R. S., Frith, C. D., & O'Keefe, J. (1998a). Knowing where and getting there: A human navigation network. *Science, 280*(5365), 921-924.
- Maguire, E. A., Burgess, N., & O'Keefe, J. (1999). Human spatial navigation: Cognitive maps, sexual dimorphism, and neural substrates. *Current Opinion in Neurobiology, 9*(2), 171-177.
- Maguire, E. A., Burke, T., Phillips, J., & Staunton, H. (1996). Topographical disorientation following unilateral temporal lobe lesions in humans. *Neuropsychologia, 34*(10), 993-1000.
- Maguire, E. A., Frackowiak, R. S. J., & Frith, C. D. (1997). Recalling routes around London: Activation of the right hippocampus in taxi drivers. *Journal of Neuroscience, 17*(18), 7103-7110.
- Maguire, E. A., Frith, C. D., Burgess, N., Donnett, J. G., & O'Keefe, J. (1998b). Knowing where things are: Parahippocampal involvement in encoding object locations in virtual large-scale space. *Journal of Cognitive Neuroscience, 10*(1), 61-76.

- Maguire, E. A., Gadian, D. G., Johnsrude, I. S., Good, C. D., Ashburner, J., Frackowiak, R. S., & Frith, C. D. (2000). Navigation-related structural change in the hippocampi of taxi drivers. *Proceedings of the National Academy of Sciences of the United States of America*, 97(8), 4398-4403.
- Maguire, E. A., Mummery, C. J., & Büchel, C. (2000). Patterns of hippocampal-cortical interaction dissociate temporal lobe memory subsystems. *Hippocampus*, 10(4), 475-482.
- Makeig, S. (1993). Auditory event-related dynamics of the EEG spectrum and effects of exposure to tones. *Electroencephalography and Clinical Neurophysiology*, 86(4), 283-293.
- Makeig, S. (2002). Response: Event-related brain dynamics-unifying brain electrophysiology. *Trends in Neurosciences*, 25(8), 390.
- Makeig, S., Bell, A. J., Jung, T. P., & Sejnowski, T. J. (1996a). Independent component analysis of electroencephalographic data. *Advances in Neural Information Processing Systems* 8, 8, 145-151.
- Makeig, S., Debener, S., Onton, J., & Delorme, A. (2004). Mining event-related brain dynamics. *Trends in Cognitive Sciences*, 8(5), 204-210.
- Makeig, S., Gramann, K., Jung, T.-P., Sejnowski, T. J., & Poizner, H. (accepted). Linking brain, mind and behavior. *International Journal of Psychophysiology*.
- Makeig, S., Gramann, K., Jung, T.-P., Sejnowski, T. J., & Poizner, H. (in press). Linking brain, mind and behavior. *International Journal of Psychophysiology*.
- Makeig, S., Jung, T. P., Bell, A. J., Ghahremani, D., & Sejnowski, T. J. (1997). Blind separation of auditory event-related brain responses into independent components. *Proceedings of the National Academy of Sciences of the United States of America*, 94(20), 10979-10984.
- Makeig, S., Jung, T. P., & Sejnowski, T. J. (1996b). Using feedforward neural networks to monitor alertness from changes in EEG correlation and coherence. *Advances in Neural Information Processing Systems* 8, 8, 931-937.
- Makeig, S., Onton, J., Sejnowski, T., & Poizner, H. (2007). Prospects for mobile, high-definition brain imaging: EEG spectral modulations during 3-D reaching. *Neuroimage*, V1, S40.
- Makeig, S., Westerfield, M., Jung, T. P., Enghoff, S., Townsend, J., Courchesne, E., & Sejnowski, T. J. (2002). Dynamic brain sources of visual evoked responses. *Science*, 295(5555), 690-694.
- Malach, R., Reppas, J. B., Benson, R. R., Kwong, K. K., Jiang, H., Kennedy, W. A., Ledden, P. J., Brady, T. J., Rosen, B. R., & Tootell, R. B. H. (1995). Object-related activity revealed by functional magnetic resonance imaging in

- human occipital cortex. *Proceedings of the Proceedings of the National Academy of Sciences of the United States of America*, 92(18), 8135-8139.
- Manzey, D. (1998). Psychophysiologie mentaler Beanspruchung. In H. Rösler (Ed.), *Enzyklopädie der Psychologie, Vol. 5: Ergebnisse und Anwendungen der Psychophysiologie*. (pp. 799-864). Göttingen: Hogrefe.
- Masuo, O., Maeshima, S., Kubo, K., Terada, T., Nakai, K., Itakura, T., & Komai, N. (1999). A case of amnestic syndrome caused by a subcortical haematoma in the right occipital lobe. *Brain Injury*, 13(3), 213-216.
- Matelli, M., Govoni, P., Galletti, C., Kutz, D. F., & Luppino, G. (1998). Superior area 6 afferents from the superior parietal lobule in the macaque monkey. *The Journal of Comparative Neurology*, 402, 327-352.
- Matsumura, N., Nishijo, H., Tamura, R., Eifuku, S., Endo, S., & Ono, T. (1999). Spatial-and task-dependent neuronal responses during real and virtual translocation in the monkey hippocampal formation. *Journal of Neuroscience*, 19(6), 2381-2393.
- Maunsell, J. H., & van Essen, D. C. (1983). The connections of the middle temporal visual area (MT) and their relationship to a cortical hierarchy in the macaque monkey. *Journal of Neuroscience*, 3(12), 2563-2586.
- Maurer, A. P., & Seguinot, V. (1995). What is modelling for? A critical review of the models of path integration. *Journal of Theoretical Biology*, 175, 346-364.
- May, M. (1996). Cognitive and embodied modes of spatial imagery. *Psychologische Beiträge*, 38(418-434).
- May, M. (2004). Imaginal perspective switches in remembered environments: Transformation versus interference accounts. *Cognitive Psychology*, 48(2), 163-206.
- May, M., & Klatzky, R. L. (2000). Path integration while ignoring irrelevant movement. *Journal of Experimental Psychology - Learning Memory and Cognition*, 26(1), 169-186.
- May, M., Wartenberg, F., & Peruch, P. (1997). Raumorientierung in virtuellen Umgebungen. In R. H. Kluwe (Ed.), *Kognitionswissenschaften: Strukturen und Prozesse intelligenter Systeme* (pp. 15-40). Wiesbaden: Deutscher Universitätsverlag.
- Mayes, A. R., Montaldi, D., Spencer, T. J., & Roberts, N. (2004). Recalling spatial information as a component of recently and remotely acquired episodic or semantic memories: an fMRI study. *Neuropsychology*, 18(3), 426-441.
- McCarthy, R. A., Evans, J. J., & Hodges, J. R. (1996). Topographic amnesia: Spatial memory disorder, perceptual dysfunction, or category specific semantic memory impairment? *Journal of Neurology, Neurosurgery & Psychiatry*, 60(3), 318-325.

- McIntosh, A. R., Grady, C. L., Ungerleider, L. G., Haxby, J. V., Rapoport, S. I., & Horwitz, B. (1994). Network analysis of cortical visual pathways mapped with PET. *Journal of Neuroscience*, 14(2), 655-666.
- McNamara, T. P., Rump, B., & Werner, S. (2003). Egocentric and geocentric frames of reference in memory of large-scale space. *Psychonomic Bulletin & Review*, 10(3), 589-595.
- McNamara, T. P., & Valiquette, C. M. (2004). Remembering where things are. In G. L. Allen (Ed.), *Human spatial memory: Remembering where* (pp. 251-285). Mahwah: Lawrence Erlbaum Associates
- McNaughton, B. L., Barnes, C. A., Gerrard, J. L., Gothard, K., Jung, M. W., Knierim, J. J., Kudrimoti, H., Qin, Y., Skaggs, W. E., Suster, M., & Weaver, K. L. (1996). Deciphering the hippocampal polyglot: The hippocampus as a path integration system. *Journal of Experimental Biology*, 199(1), 173-185.
- McNaughton, B. L., Battaglia, F. P., Jensen, O., Moser, E. I., & Moser, M. B. (2006). Path integration and the neural basis of the 'cognitive map'. *Nature Reviews Neuroscience*, 7(8), 663-678.
- Mecklinger, A., Kramer, A. F., & Strayer, D. L. (1992). Event related potentials and EEG components in a semantic memory search task. *Psychophysiology*, 29(1), 104-119.
- Mellet, E., Briscogne, S., Tzourio-Mazoyer, N., Ghaem, O., Petit, L., Zago, L., Etard, O., Berthoz, A., Mazoyer, B., & Denis, M. (2000). Neural correlates of topographic mental exploration: The impact of route versus survey perspective learning. *Neuroimage*, 12(5), 588-600.
- Meltzer, J., Zaveri, H. P., Goncharova, I., Distasio, M. M., Papademetris, X., Spencer, S. S., Spencer, D. D., & Constable, R. T. (2007). Effects of working memory load on oscillatory power in human intracranial EEG. *Cerebral Cortex, Advance Access, published December 5, 2007*.
- Merkle, T., Rost, M., & Alt, W. (2006). Egocentric path integration models and their application to desert arthropods. *Journal of Theoretical Biology*, 240(3), 385-399.
- Merriam, E. P., Genovese, C. R., & Colby, C. L. (2003). Spatial updating in human parietal cortex. *Neuron*, 39(2), 361-373.
- Miller, B. T., & D'Esposito, M. (2005). Searching for "the top" in top-down control. *Neuron*, 48(4), 535-538.
- Miller, C. R., & Allen, G. L. (2001). Spatial frames of reference used in identifying direction of movement: An unexpected turn. In D. R. Montello (Ed.), *Lecture Notes in Computer Science* (pp. 206-216). Berlin: Springer.
- Miller, E. K., Li, L., & Desimone, R. (1993). Activity of neurons in anterior inferior temporal cortex during a short-term memory task. *Journal of Neuroscience*, 13(4), 1460-1478.

- Milner, A. D., & Goodale, M. A. (1996). *The visual brain in action*. Oxford: Oxford University Press.
- Mishkin, M., Ungerleider, L. G., & Macko, K. A. (2001). Object vision and spatial vision: Two cortical pathways. In W. Bechtel, P. Mandik, J. Mundale & R. Stufflebeam (Eds.), *Philosophy and the Neurosciences: A Reader*. London: Blackwell Publishing.
- Mittelstaedt, H. (1985). Analytical cybernetics of spider navigation. In F. Barth (Ed.), *Neurobiology of Arachnids* (pp. 298-316). Berlin: Springer.
- Mittelstaedt, H. (2000). Triple-loop model of path control by head direction and place cells. *Biological Cybernetics*, 83(3), 261-270.
- Mittelstaedt, H., & Mittelstaedt, M.-L. (1982). Homing by path integration. In F. Papi & H. G. Walrapp (Eds.), *Avian Navigation* (pp. 290-297). New York: Springer.
- Mittelstaedt, M.-L., & Glasauer, S. (1991). Idiothetic navigation in gerbils and humans. *Zoologisches Jahrbuch, Allgemeine Zoologie u. Physiologie*, 95, 427-435.
- Miyashita, Y. (1993). Inferior temporal cortex: Where visual perception meets memory. *Annual Reviews in Neuroscience*, 16(1), 245-263.
- Mizuhara, H., Wang, L. Q., Kobayashi, K., & Yamaguchi, Y. (2004). A long-range cortical network emerging with theta oscillation in a mental task. *Neuroreport*, 15(8), 1233.
- Montello, D. R. (1993). Scale and multiple psychologies of space. *Lecture Notes in Computer Science*, 312-312.
- Montello, D. R., Waller, D., Hegarty, M., & Richardson, A. E. (2004). Spatial memory of real environments, virtual environments, and maps. In G. L. Allen (Ed.), *Human spatial memory: Remembering where* (pp. 251-285). Mahwah: Lawrence Erlbaum Associates.
- Morland, A. B., Baseler, H. A., Hoffmann, M. B., Sharpe, L. T., & Wandell, B. A. (2001). Abnormal retinotopic representations in human visual cortex revealed by fMRI. *Acta Psychologica*, 107(1-3), 229-247.
- Morris, R., Paxinos, G., & Petrides, M. (2000). Architectonic analysis of the human retrosplenial cortex. *The Journal of Comparative Neurology*, 421(1), 14-28.
- Morris, R., Petrides, M., & Pandya, D. N. (1999). Architecture and connections of retrosplenial area 30 in the rhesus monkey (macaca mulatta). *European Journal of Neuroscience*, 11(7), 2506-2518.
- Morrone, M. C., Tosetti, M., Montanaro, D., Fiorentini, A., Cioni, G., & Burr, D. C. (2000). A cortical area that responds specifically to optic flow, revealed by fMRI. *Nature Neuroscience*, 3, 1322-1328.

- Mossio, M., Vidal, M., & Berthoz, A. (2008). Traveled distances: New insights into the role of optic flow. *Vision Research, in press*.
- Mou, W., & McNamara, T. P. (2002). Intrinsic frames of reference in spatial memory. *Journal of Experimental Psychology - Learning Memory and Cognition, 28*(1), 162-170.
- Mou, W., McNamara, T. P., Rump, B., & Xiao, C. (2006). Roles of egocentric and allocentric spatial representations in locomotion and reorientation. *Journal of Experimental Psychology - Learning Memory and Cognition, 32*(6), 1274-1290.
- Mou, W., McNamara, T. P., Valiquette, C. M., & Rump, B. (2004). Allocentric and egocentric updating of spatial memories. *Journal of Experimental Psychology - Learning Memory and Cognition, 30*(1), 142-157.
- Müller, M., & Gramann, K. (2007). The influence of path's complexity on allocentric and egocentric spatial navigation. In K. F. Wender, S. Mecklenbräuker, G. D. Rey & T. Wehr (Eds.), *Beiträge zur 49. Tagung experimentell arbeitender Psychologen. 26. bis 28. März 2007 in Trier*. Lengerich: Pabst Science Publishers.
- Müller, M., & Wehner, R. (1988). Path integration in desert ants, *Cataglyphis fortis*. *Proceedings of the National Academy of Sciences of the United States of America, 85*(14), 5287-5290.
- Müller, M., & Wehner, R. (1994). The hidden spiral - Systematic search and path integration in desert ants, *Cataglyphis-Fortis*. *Journal of Comparative Physiology A - Sensory, Neural, and Behavioral Physiology, 175*(5), 525-530.
- Müller, M., & Wehner, R. (2007). Wind and sky as compass cues in desert ant navigation. *Naturwissenschaften, 94*(7), 589-594.
- Muller, R. (1996). A quarter of a century of place cells. *Neuron, 17*, 979-990.
- Murphy, J. J. (1873). Instinct: A mechanical analogy. *Nature, 7*(182), 483.
- Nadal, J. P., & Parga, N. (1994). Nonlinear neurons in the low-noise limit - A factorial code maximizes information-transfer. *Network-Computation in Neural Systems, 5*(4), 565-581.
- Neggers, S. F., Schölvinck, M. L., van der Lubbe, R. H., & Postma, A. (2005). Quantifying the interactions between allo- and egocentric representations of space. *Acta Psychologica, 118*(1-2), 25-45.
- Niedermeyer, E., & da Silva, F. L. (2005). *Electroencephalography: Basic principles, clinical applications, and related fields*: Lippincott Williams & Wilkins.

- Nitz, D. A. (2009). Parietal cortex, navigation, and the construction of arbitrary reference frames for spatial information. *Neurobiology of Learning and Memory*, 21(2), 179-185.
- O'Keefe, J., & Burgess, N. (1999). Theta activity, virtual navigation and the human hippocampus. *Trends in Cognitive Sciences*, 3(11), 403-406.
- O'Keefe, J., Burgess, N., Donnett, J. G., Jeffery, K. J., & Maguire, E. A. (1998). Place cells, navigational accuracy, and the human hippocampus. *Philosophical Transactions of the Royal Society of London (B): Biological Sciences*, 353(1373), 1333-1340.
- O'Keefe, J., & Nadel, L. (1978). *The hippocampus as a cognitive map*. Oxford: Oxford University Press.
- Ohnishi, T., Matsuda, H., Hirakata, M., & Ugawa, Y. (2006). Navigation ability dependent neural activation in the human brain: An fMRI study. *Neuroscience Research*, 55(4), 361-369.
- Olejnik, S., & Algina, J. (2003). Generalized eta and omega squared statistics: Measures of effect size for some common research designs. *Psychological Methods*, 8(4), 434-447.
- Ono, H., Mapp, A. P., & Howard, I. P. (2002). The cyclopean eye in vision: The new and old data continue to hit you right between the eyes. *Vision Research*, 42(10), 1307-1324.
- Onton, J., Delorme, A., & Makeig, S. (2005). Frontal midline EEG dynamics during working memory. *Neuroimage*, 27(2), 341-356.
- Onton, J., & Makeig, S. (2006). Information-based modeling of event-related brain dynamics. In C. Neuper & E. Klimesch (Eds.), *Progress in Brain Research* (Vol. 159, pp. 99-120).
- Onton, J., Westerfield, M., Townsend, J., & Makeig, S. (2006). Imaging human EEG dynamics using independent component analysis. *Neuroscience and Biobehavioral Reviews*, 30(6), 808-822.
- Oostenveld, R., & Oostendorp, T. F. (2002). Validating the boundary element method for forward and inverse EEG computations in the presence of a hole in the skull. *Human Brain Mapping*, 17(3), 179-192.
- Ota, H., Fujii, T., Suzuki, K., Fukatsu, R., & Yamadori, A. (2001). Dissociation of body-centered and stimulus-centered representations in unilateral neglect. *Neurology*, 57(11), 2064-2069.
- Pandya, D. N., Hoesen, G. W., & Mesulam, M. M. (1981). Efferent connections of the cingulate gyrus in the rhesus monkey. *Experimental Brain Research*, 42(3), 319-330.

- Parslow, D. M., Morris, R. G., Fleminger, S., Rahman, Q., Abrahams, S., & Recce, M. (2005). Allocentric spatial memory in humans with hippocampal lesions. *Acta Psychologica*, 118(1-2), 123-147.
- Parslow, D. M., Rose, D., Brooks, B., Fleminger, S., Gray, J. A., Giampietro, V., Brammer, M. J., Williams, S., Gasston, D., Andrew, C., Vythelingum, G. N., Loannou, G., Simmons, A., & Morris, R. G. (2004). Allocentric spatial memory activation of the hippocampal formation measured with fMRI. *Neuropsychology*, 18(3), 450-461.
- Parvizi, J., Van Hoesen, G. W., Buckwalter, J., & Damasio, A. (2006). Neural connections of the posteromedial cortex in the macaque. *Proceedings of the National Academy of Sciences of the United States of America*, 103(5), 1563-1568.
- Paus, T. (1996). Location and function of the human frontal eye-field: A selective review. *Neuropsychologia*, 34(6), 475-483.
- Pazzaglia, F., & de Beni, R. (2001). Strategies of processing spatial information in survey and landmark-centred individuals. *European Journal of Cognitive Psychology*, 13(4), 493-508.
- Pazzaglia, F., & Taylor, H. A. (2007). Perspective, instruction, and cognitive style in spatial representation of a virtual environment. *Spatial Cognition & Computation*, 7(4), 349-364.
- Perenin, M. T., & Vighetto, A. (1988). Optic ataxia: A specific disruption in visuo-motor mechanisms: I. Different aspects of the deficit in reaching for objects. *Brain*, 111(3), 643-674.
- Perrett, D. I., Smith, P. A. J., Potter, D. D., Mistlin, A. J., Head, A. S., Milner, A. D., & Jeeves, M. A. (1984). Neurones responsive to faces in the temporal cortex: Studies of functional organization, sensitivity to identity and relation to perception. *Human Neurobiology*, 3(4), 197-208.
- Perrett, D. I., Smith, P. A. J., Potter, D. D., Mistlin, A. J., Head, A. S., Milner, A. D., & Jeeves, M. A. (1985). Visual cells in the temporal cortex sensitive to face view and gaze direction. *Proceedings of the Royal Society of London. Series B, Biological Sciences* (1934-1990), 223(1232), 293-317.
- Peruch, P., Borel, L., Magnan, J., & Lacour, M. (2005). Direction and distance deficits in path integration after unilateral vestibular loss depend on task complexity. *Cognitive Brain Research*, 25(3), 862-872.
- Peruch, P., Gaunet, F., Thinus-Blanc, C., & Loomis, J. M. (2000). Understanding and learning virtual spaces. In R. M. Kitchin & S. Freundschuh (Eds.), *Cognitive Mapping: Past, Present and Future* (pp. 108-124). London: Routledge.
- Peruch, P., May, M., & Wartenberg, F. (1997). Homing in virtual environments: effects of field of view and path layout. *Perception*, 26(3), 301-311.

- Petit, L., & Haxby, J. V. (1999). Functional anatomy of pursuit eye movements in humans as revealed by fMRI. *Journal of Neurophysiology*, 82(1), 463-471.
- Peuskens, H., Sunaert, S., Dupont, P., Van Hecke, P., & Orban, G. A. (2001). Human brain regions involved in heading estimation. *Journal of Neuroscience*, 21(7), 2451.
- Pfurtscheller, G. (1992). Event-related synchronization (ERS): An electrophysiological correlate of cortical areas at rest. *Electroencephalography and Clinical Neurophysiology*, 83(1), 62-69.
- Pfurtscheller, G. (2001). Functional brain imaging based on ERD/ERS. *Vision Research*, 41(10-11), 1257-1260.
- Pfurtscheller, G., & Aranibar, A. (1977). Event-related cortical desynchronization detected by power measurements of scalp EEG. *Electroencephalography and Clinical Neurophysiology*, 42(6), 817-826.
- Pfurtscheller, G., & Aranibar, A. (1979). Evaluation of event-related desynchronization (ERD) preceding and following voluntary self-paced movement. *Electroencephalography and Clinical Neurophysiology*, 46(2), 138-146.
- Pfurtscheller, G., Leeb, R., Keinrath, C., Friedman, D., Neuper, C., Guger, C., & Slater, M. (2006). Walking from thought. *Brain Research*, 1071(1), 145-152.
- Pfurtscheller, G., & Lopez da Silva, F. H. (1999). Event-related EEG/MEG synchronization and desynchronization: Basic principles. *Clinical Neurophysiology*, 110(11), 1842-1857.
- Pfurtscheller, G., Neuper, C., Andrew, C., & Edlinger, G. (1997). Foot and hand area mu rhythms. *International Journal of Psychophysiology*, 26(1-3), 121-135.
- Pfurtscheller, G., Stancak, A., & Neuper, C. (1996). Event-related synchronization (ERS) in the alpha band - An electrophysiological correlate of cortical idling: A review. *International Journal of Psychophysiology*, 24(1-2), 39-46.
- Pick, H. L., Jr. (1999). Organization of spatial knowledge in children. In N. Elilan, R. McCarthy & B. Brewer (Eds.), *Spatial Representation. Problems in Philosophy and Psychology* (2 ed., pp. 31-42). New York: Oxford University Press.
- Pizzamiglio, L., Committeri, G., Galati, G., & Patria, F. (2000). Psychophysical properties of line bisection and body midline perception in unilateral neglect. *Cortex*, 36(4), 469-484.
- Posner, M. I. (1975). Psychobiology of attention. In M. Gazzaniga & C. Blakemore (Eds.), *Handbook of Psychobiology* (pp. 441-480). New York: Academic Press.

- Posner, M. I. (1995). Attention in cognitive neuroscience: An overview. In M. Gazzaniga (Ed.), *The Cognitive Neurosciences* (pp. 615-624). Cambridge, MA: MIT Press.
- Presson, C. C., & Montello, D. R. (1994). Updating after rotational and translational body movements: Coordinate structure of perspective space. *Perception*, 23(12), 1447-1455.
- Rajapakse, J. C., Cichocki, A., & Sanchez, V. D. (2002). Independent component analysis and beyond in brain imaging: EEG, MEG, fMRI, and PET. *Icnnip'02: Proceedings of the 9th International Conference on Neural Information Processing*, 404-412.
- Ranganath, C., Cohen, M. X., Dam, C., & D'Esposito, M. (2004). Inferior temporal, prefrontal, and hippocampal contributions to visual working memory maintenance and associative memory retrieval. *Journal of Neuroscience*, 24(16), 3917-3925.
- Ray, W. J., & Cole, H. W. (1985). EEG alpha activity reflects attentional demands, and beta activity reflects emotional and cognitive processes. *Science*, 228(4700), 750-752.
- Redish, A. D. (1999). *Beyond the cognitive map: From place cells to episodic memory*. Cambridge: The MIT Press.
- Regolin, L., Vallortigara, G., & Zanforlin, M. (1994). Object and spatial representations in detour problems by chicks. *Animal Behavior*, 49, 195-199.
- Restat, J., Steck, S. D., Mochnatzki, H. F., & Mallot, H. A. (2004). Geographical slant facilitates navigation and orientation in virtual environments. *Perception*, 33, 667-687.
- Riccobon, D. (2007). *Behavioral and electrocortical evidence of distinct reference frames supporting path integration*. Ludwig-Maximilians-University, Munich, Germany.
- Riecke, B. E. (2003). *How far can we get with just visual information? Path integration and spatial updating studies in Virtual Reality*. Unpublished PhD thesis, Eberhard-Karls-Universität, Tübingen.
- Riecke, B. E., Cunningham, D. W., & Bülthoff, H. H. (2007). Spatial updating in virtual reality: the sufficiency of visual information. *Psychological Research*, 71(3), 298-313.
- Riecke, B. E., & Schulte-Pelkum, J. (2006). Using the perceptually oriented approach to optimize spatial presence & ego-motion simulation. Technical report No. 153  
[http://www.kyb.mpg.de/publications/attachments/RieckeSchulte-Pelkum\\_06\\_MPIK-TR-153\\_4186%5B0%5D.pdf](http://www.kyb.mpg.de/publications/attachments/RieckeSchulte-Pelkum_06_MPIK-TR-153_4186%5B0%5D.pdf)

- Riecke, B. E., van Veen, H. A., & Bülthoff, H. H. (2002). Visual homing is possible without landmarks: A path integration study in virtual reality. *Presence - Teleoperators and Virtual Environments*, 11(5), 443-473.
- Riecke, B. E., & Wiener, J. M. (2007). Can people not tell left from right in VR? Point-to-origin studies revealed qualitative errors in visual path integration. *Proceedings of IEEE Virtual Reality 2007 (VR '07)*, 3-10.
- Riecke, B. E., & Wiener, J. M. (2008). Can people not tell left from right in VR? point-to-origin studies revealed qualitative errors in visual path integration. *Psychological Bulletin*.
- Rieser, J. J., Guth, D. A., & Hill, E. W. (1982). Mental processes mediating independent travel: Implications for orientation and mobility. *Journal of Visual Impairment and Blindness*, 76, 213-218.
- Rieser, J. T. (1989). Access to knowledge of spatial structure at novel points of observation. *Journal of Experimental Psychology - Learning Memory and Cognition*, 15(6), 1157-1165.
- Rizzolatti, G., Riggio, L., & Sheliga, B. M. (1994). Space and selective attention. In C. Umiltà & M. Moscovitch (Eds.), *Attention and performance XV: Conscious and nonconscious information processing*. Cambridge: MIT Press.
- Rolls, E. T. (1999). Spatial view cells and the representation of place in the primate hippocampus. *Hippocampus*, 9(4), 467-480.
- Rossetti, Y., Pisella, L., & Vighetto, A. (2003). Optic ataxia revisited. *Experimental Brain Research*, 153(2), 171-179.
- Ruddle, R. A., Payne, S. J., & Jones, D. M. (1998). Navigating large-scale "desktop" virtual buildings: Effects of orientation aids and familiarity. *Presence - Teleoperators and Virtual Environments*, 7(2), 179-192.
- Sakthivel, M., Patterson, P. E., & Cruz-Neira, C. (1999). Gender differences in navigating virtual worlds. *Biomedical Sciences Instrumentation*, 35, 353-359.
- Salmelin, R., & Hari, R. (1994). Spatiotemporal characteristics of sensorimotor neuromagnetic rhythms related to thumb movement. *Neuroscience*, 60(2), 537-550.
- Sanchez-Vives, M. V., & Slater, M. (2005). From presence to consciousness through virtual reality. *Nature Reviews Neuroscience*, 6(332-339).
- Sandstrom, N. J., Kaufman, J., & Huettel, S. A. (1998). Males and females use different distal cues in a virtual environment navigation task. *Cognitive Brain Research*, 6(4), 351-360.
- Sarnthein, J., Petsche, H., Rappelsberger, P., Shaw, G. L., & von Stein, A. (1998). Synchronization between prefrontal and posterior association cor-

- tex during human working memory (Vol. 95, pp. 7092-7096): National Acad Sciences.
- Sauseng, P., Klimesch, W., Schabus, M., & Doppelmayr, M. (2005). Fronto-parietal EEG coherence in theta and upper alpha reflect central executive functions of working memory. *International Journal of Psychophysiology*, 57(2), 97-103.
- Schack, B., Klimesch, W., & Sauseng, P. (2005). Phase synchronization between theta and upper alpha oscillations in a working memory task. *International Journal of Psychophysiology*, 57(2), 105-114.
- Schnitzler, A., Salenius, S., Salmelin, R., Jousmäki, V., & Hari, R. (1997). Involvement of primary motor cortex in motor imagery: A neuromagnetic study. *Neuroimage*, 6(3), 201-208.
- Schönebeck, B., Thanhäuser, J., & Debus, G. (2001). Die Tunnelaufgabe: Eine Methode zur Untersuchung kognitiver Teilprozesse räumlicher Orientierungsleistungen. *Zeitschrift für Experimentelle Psychologie*, 48(4), 339-364.
- Schwartz, B. J., Salustri, C., Kaufman, L., & Williamson, S. J. (1989). *Alpha suppression related to a cognitive task*. New York: Plenum Press.
- Seguinot, V., Cattet, J., & Benhamou, S. (1998). Path integration in dogs. *Animal Behaviour*, 55, 787-797.
- Seguinot, V., Maurer, R., & Etienne, A. S. (1993). Dead reckoning in a small mammal: The evaluation of distance. *Journal of Comparative Physiology*, 173(1), 103-113.
- Seubert, J., Humphreys, G. W., Müller, H. J., & Gramann, K. (2008). Straight after the turn: The role of the parietal lobes in egocentric space processing. *Neurocase*, 14(2), 204-219.
- Shallice, T., Fletcher, P., Frith, C. D., Grasby, P., Frackowiak, R. S. J., & Dolan, R. J. (1994). Brain regions associated with acquisition and retrieval of verbal episodic memory. *Nature*, 368(6472), 633-635.
- Shelton, A. L., & Gabrieli, J. D. (2002). Neural correlates of encoding space from route and survey perspectives. *Journal of Neuroscience*, 22(7), 2711-2717.
- Shelton, A. L., & Gabrieli, J. D. (2004). Neural correlates of individual differences in spatial learning strategies. *Neuropsychology*, 18(3), 442-449.
- Shelton, A. L., & McNamara, T. P. (2001). Systems of spatial reference in human memory. *Cognitive Psychology*, 43, 274-310.
- Shelton, A. L., & McNamara, T. P. (2004). Spatial memory and perspective taking. *Memory & Cognition*, 32(3), 416-426.

- Shelton, A. L., & Pippitt, H. A. (2007). Fixed versus dynamic orientations in environmental learning from ground-level and aerial perspectives. *Psychological Research*, 71(3), 333-346.
- Shibata, H., Kondo, S., & Naito, J. (2004). Organization of retrosplenial cortical projections to the anterior cingulate, motor, and prefrontal cortices in the rat. *Neuroscience Research*, 49(1), 1-11.
- Sholl, J. (Ed.). (2001). *The role of a self-reference system in spatial navigation* (Vol. 2205). Berlin: Springer.
- Sholl, M. J., & Nolin, T. L. (1997). Orientation specificity in representations of place. *Journal of Experimental Psychology - Learning Memory and Cognition*, 23(6), 1494-1507.
- Siegel, A. W., & White, A. M. (1975). The development of spatial representations of large-scale environments. In H. W. Reese (Ed.), *Advances in child development and behavior* (Vol. 10, pp. 9-55). New York: Academic Press.
- Smith, D. M., & Mizumori, S. J. (2006). Hippocampal place cells, context, and episodic memory. *Hippocampus*, 16(9), 716-729.
- Soechting, J. F., & Flanders, M. (1992). Moving in three-dimensional space: Frames of reference, vectors, and coordinate systems. *Annual Reviews in Neuroscience*, 15(1), 167-191.
- Squire, L. R., Stark, C. E. L., & Clark, R. E. (2004). The medial temporal lobe. *Annual Review of Neuroscience*, 27, 279-306.
- Stankiewicz, B. J., Legge, G. E., Mansfield, J. S., & Schlicht, E. J. (2006). Lost in virtual space: Studies in human and ideal spatial navigation. *Journal of Experimental Psychology - Human Perception and Performance*, 32(3), 688-704.
- Steck, S., Mochnatzki, H. F., & Mallot, H. A. (2004). The role of geographical slant in virtual environment navigation. In C. Freksa, W. Brauer, C. Habel & K. F. Wender (Eds.), *Lecture Notes in Artificial Intelligence, Spatial Cognition III* (pp. 62-76). Heidelberg: Springer.
- Stiles, J. (2001). Spatial cognitive development. In C. A. Nelson & M. Luciana (Eds.), *Handbook of Developmental Cognitive Neuroscience* (pp. 399-414). Cambridge, MA: Collins.
- Stipacek, A., Grabner, R. H., Neuper, C., Fink, A., & Neubauer, A. C. (2003). Sensitivity of human EEG alpha band desynchronization to different working memory components and increasing levels of memory load. *Neuroscience Letters*, 353(3), 193-196.
- Stone, J. V. (2004). *Independent Component Analysis: A tutorial introduction*. Bradford: MIT Press.

- Stricanne, B., Andersen, R. A., & Mazzoni, P. (1996). Eye-centered, head-centered, and intermediate coding of remembered sound locations in area LIP. *Journal of Neurophysiology*, 76(3), 2071-2076.
- Sun, H. J., Campos, J. L., Young, M., Chan, G. S. W., & Ellard, C. G. (2004). The contributions of static visual cues, nonvisual cues, and optic flow in distance estimation. *Perception*, 33(1), 49-65.
- Sunaert, S., Van Hecke, P., Marchal, G., & Orban, G. A. (1999). Motion-responsive regions of the human brain. *Experimental Brain Research*, 127(4), 355-370.
- Suzuki, W. A., & Amaral, D. G. (1994). Perirhinal and parahippocampal cortices of the macaque monkey: Cortical afferents. *The Journal of Comparative Neurology*, 350(4), 497-533.
- Talairach, J., & Tournoux, P. (1988). *Co-planar stereotaxic atlas of the human brain*: Thieme Medical Publishers New York.
- Tan, D. S., Czerwinski, M., & Robertson, G. (2003). *Women go with the (optical) flow*. Poster presented at the conference Human Factors in Computing Systems, New York, NY, USA.
- Tanaka, K., Saito, H., Fukada, Y., & Moriya, M. (1991). Coding visual images of objects in the inferotemporal cortex of the macaque monkey. *Journal of Neurophysiology*, 66(1), 170-189.
- Tanaka, K., Sugita, Y., Moriya, M., & Saito, H. (1993). Analysis of object motion in the ventral part of the medial superior temporal area of the macaque visual cortex. *Journal of Neurophysiology*, 69(1), 128-142.
- Tarr, M. J., & Warren, W. H. (2002). Virtual reality in behavioral neuroscience and beyond. *Nature Neuroscience Supplement*, 5, 1089-1092.
- Thier, P., & Erickson, R. G. (1992). Responses of visual-tracking neurons from cortical area MST-I to visual, eye and head motion. *European Journal of Neuroscience*, 4(6), 539-553.
- Thinus-Blanc, C., & Gaunet, F. (1997). Representation of space in blind persons: Vision as a spatial sense? *Psychological Bulletin*, 121(1), 20-42.
- Thorndyke, P. W., & Hayes-Roth, B. (1982). Differences in spatial knowledge acquired from maps and navigation. *Cognitive Psychology*, 14(4), 560-589.
- Tootell, R. B. H., Mendola, J. D., Hadjikhani, N. K., Ledden, P. J., Liu, A. K., Reppas, J. B., Sereno, M. I., & Dale, A. M. (1997). Functional analysis of V3A and related areas in human visual cortex. *Journal of Neuroscience*, 17(18), 7060-7078.
- Touretzky, D. S., & Redish, A. D. (1996). Theory of rodent navigation based on interacting representations of space. *Hippocampus*, 6(3), 247-270.

- Trowbridge, C. C. (1913). On fundamental methods of orientation and 'imaginary maps'. *Science*, 38(990), 888-897.
- Turriziani, P., Carlesimo, G. A., Perri, R., Tomaiuolo, F., & Caltagirone, C. (2003). Loss of spatial learning in a patient with topographical disorientation in new environments. *Journal of Neurology, Neurosurgery & Psychiatry*, 74(1), 61-69.
- Tversky, B. (1993). Cognitive maps, cognitive collages, and spatial mental models. In A. U. Frank & I. Campari (Eds.), *Spatial Information Theory*. Heidelberg: Springer.
- Tye, M. (1991). *The imagery debate*. Cambridge: MIT Press.
- Ungerleider, L. G., & Mishkin, M. (1982). Two cortical visual systems. In D. J. Ingle, M. A. Goodale & R. J. W. Mansfield (Eds.), *Analysis of Visual Behavior* (pp. 549-586). Cambridge: MIT Press.
- Vallar, G. (1998). Spatial hemineglect in humans. *Trends in Cognitive Sciences*, 2(3), 87-97.
- Vallar, G., Lobel, E., Galati, G., Berthoz, A., Pizzamiglio, L., & Le Bihan, D. (1999). A fronto-parietal system for computing the egocentric spatial frame of reference in humans. *Experimental Brain Research*, 124(3), 281-286.
- van Asselen, M., Kessels, R. P., Kappelle, L. J., Neggers, S. F., Frijns, C. J., & Postma, A. (2006). Neural correlates of human wayfinding in stroke patients. *Brain Research Bulletin*, 1067, 229-238.
- van Wezel, R. J. A., & Britten, K. H. (2002). Motion adaptation in area MT. *Journal of Neurophysiology*, 88(6), 3469-3476.
- Vann, S. D., & Aggleton, J. P. (2004). Testing the importance of the retrosplenial guidance system: effects of different sized retrosplenial cortex lesions on heading direction and spatial working memory. *Behavioural Brain Research*, 155(1), 97-108.
- Vanni, S., Portin, K., Virsu, V., & Hari, R. (1999). Mu rhythm modulation during changes of visual percepts. *Neuroscience*, 91(1), 21-31.
- Vanni, S., Revonsuo, A., & Hari, R. (1997). Modulation of the parieto-occipital alpha rhythm during object detection. *Journal of Neuroscience*, 17(18), 7141-7147.
- Vigário, R. N. (1997). Extraction of ocular artefacts from EEG using independent component analysis. *Electroencephalography and Clinical Neurophysiology*, 103(3), 395-404.
- Vogeley, K., & Fink, G. R. (2003). Neural correlates of the first-person-perspective. *Trends in Cognitive Sciences*, 7(1), 38-42.

- Vogeley, K., May, M., Ritzl, A., Falkai, P., Zilles, K., & Fink, G. R. (2004). Neural correlates of first-person perspective as one constituent of human self-consciousness. *Journal of Cognitive Neuroscience*, 16(5), 817-827.
- Vogt, B. A., Absher, J. R., & Bush, G. (2000). Human retrosplenial cortex: Where is it and is it involved in emotion? *Trends in Neurosciences*, 23(5), 195-196.
- von der Heyde, M., Riecke, B. E., Cunningham, D. W., & Bülthoff, H. H. (2000). Humans can extract distance and velocity from vestibular perceived acceleration. *Journal of Cognitive Neuroscience*, 63C(Abstract 77).
- von Stein, A., & Sarnthein, J. (2000). Different frequencies for different scales of cortical integration: from local gamma to long range alpha/theta synchronization. *International Journal of Psychophysiology*, 38(3), 301-313.
- Wade, N. J. (1992). The representation of orientation in vision. *Australian Journal of Psychology*, 44(3), 139-145.
- Wall, M. B., & Smith, A. T. (2008). The representation of egomotion in the human brain. *Current Biology*.
- Waller, D., & Greenauer, N. (2007). The role of body-based sensory information in the acquisition of enduring spatial representations. *Psychological Research*, 71(3), 322-332.
- Waller, D., & Hodgson, E. (2006). Transient and enduring spatial representations under disorientation and self-rotation. *Journal of Experimental Psychology - Learning Memory and Cognition*, 32(4), 867-882.
- Walter, W. G. (1953). *The living brain*. New York: Norton.
- Wang, R. F., & Spelke, E. (2000). Updating egocentric representations in human navigation. *Cognition*, 77(3), 215-250.
- Wang, R. F., & Spelke, E. (2002). Human spatial representation: Insights from animals. *Trends in Cognitive Sciences*, 6(9), 376.
- Warren, W. H., Jr., Kay, B. A., Zosh, W. D., Duchon, A. P., & Sahuc, S. (2001). Optic flow is used to control human walking. *Nature Neuroscience*, 4(2), 213-216.
- Wartenberg, F., May, M., & Peruch, P. (1998). Spatial orientation in virtual environments: Background consideration and experiments. In C. Freksa, C. Habel & K. F. Wender (Eds.), *Lecture Notes in Artificial Intelligence, Spatial Cognition I* (pp. 469-489). Heidelberg: Springer.
- Waxman, S. G. (2002). *Clinical Neuroanatomy* (25. ed.). Chicago: McGraw-Hill Professional.
- Wehner, R. (2003). Desert ant navigation: How miniature brains solve complex tasks. *Journal of Comparative Physiology*, 189, 579–588.

- Wehner, R., Bleuler, S., Nievergelt, C., & Shah, D. (1990). Bees Navigate by Using Vectors and Routes Rather Than Maps. *Naturwissenschaften*, 77(10), 479-482.
- Wehner, R., & Wehner, S. (1986). Path integration in desert ants - Approaching a long-standing puzzle in insect navigation. *Monitore Zoologico Italiano*, 20(3), 309-331.
- Wehner, R., & Wehner, S. (1990). Insect Navigation - Use of Maps or Ariadne's Thread. *Ethology Ecology & Evolution*, 2(1), 27-48.
- White, N. M., & McDonald, R. J. (2002). Multiple parallel memory systems in the brain of the rat. *Neurobiology of Learning and Memory*, 77(2), 125-184.
- Wiener, J. M., & Mallot, H. A. (2006). Path complexity does not impair visual path integration. *Spatial Cognition and Computation*, 6(4), 333-346.
- Wiener, J. M., Schnee, A., & Mallot, H. A. (2004). Use and interaction of navigation strategies in regionalized environments. *Journal of Environmental Psychology*, 24(4), 475-493.
- Wilson, F. A., Scalaidhe, S. P., & Goldman-Rakic, P. S. (1993). Dissociation of object and spatial processing domains in primate prefrontal cortex. *Science*, 260(5116), 1955.
- Wilson, K. D., Woldorff, M. G., & Mangun, G. R. (2005). Control networks and hemispheric asymmetries in parietal cortex during attentional orienting in different spatial reference frames. *Neuroimage*, 25(3), 668-683.
- Wilson, M. A., & McNaughton, B. L. (1993). Dynamics of the hippocampal ensemble code for space. *Science*, 261(5124), 1055-1058.
- Windischberger, C., Lamm, C., Bauer, H., & Moser, E. (2003). Human motor cortex activity during mental rotation. *Neuroimage*, 20(1), 225-232.
- Winship, I. R., Pakan, J. M. P., Todd, K. G., & Wong-Wylie, D. R. (2006). A comparison of ventral tegmental neurons projecting to optic flow regions of the inferior olive vs. the hippocampal formation. *Neuroscience*, 141(1), 463-473.
- Wolbers, T., & Büchel, C. (2005). Dissociable retrosplenial and hippocampal contributions to successful formation of survey representations. *Journal of Neuroscience*, 25(13), 3333-3340.
- Wolbers, T., Wiener, J. M., Mallot, H. A., & Büchel, C. (2007). Differential recruitment of the hippocampus, medial prefrontal cortex, and the human motion complex during path integration in humans. *Journal of Neuroscience*, 27(35), 9408-9416.
- Worden, M. S., Foxe, J. J., Wang, N., & Simpson, G. V. (2000). Anticipatory biasing of visuospatial attention indexed by retinotopically specific  $\alpha$ -bank

- electroencephalography increases over occipital cortex. *Journal of Neuroscience*, 20(6), 63-63.
- Wraga, M. (2003). Thinking outside the body: An advantage for spatial updating during imagined versus physical self-rotation. *Journal of Experimental Psychology - Learning Memory and Cognition*, 29(5), 993-1005.
- Wraga, M., Creem-Regehr, S. H., & Proffitt, D. R. (2004). Spatial updating of virtual displays during self- and display rotation. *Memory & Cognition*, 32(3), 399-415.
- Wylie, D. R. W., Glover, R. G., & Aitchison, J. D. (1999). Optic flow input to the hippocampal formation from the accessory optic system. *Journal of Neuroscience*, 19(13), 5514-5527.
- Xing, J., & Andersen, R. A. (2000). Models of the Posterior Parietal Cortex Which Perform Multimodal Integration and Represent Space in Several Coordinate Frames. *Journal of Cognitive Neuroscience*, 12(4), 601-614.
- Yardley, L., & Higgins, M. (1998). Spatial updating during rotation: The role of vestibular information and mental activity. *Journal of Vestibular Research*, 8(6), 435-442.
- Zeki, S., Watson, J. D., Lueck, C. J., Friston, K. J., Kennard, C., & Frackowiak, R. S. (1991). A direct demonstration of functional specialization in human visual cortex. *Journal of Neuroscience*, 11(3), 641-649.

# Index of Figures and Tables

|   |    |
|---|----|
| Figure 1.1: Path integration – Examples of systematic errors over species during homing after following L-shaped outbound trajectories (redrawn with permission from Maurer & Seguinot, 1995, p. 459). Circles indicate starting positions. The homing vector (solid black arrowhead) typically displays an inward-error, therefore crossing the previously traversed path. ....  | 5  |
| Figure 1.2: Path integration, polar coordinates – The navigator might estimate his position and angular orientation based on <b>(A)</b> ideothetic input, or <b>(B)</b> allocentric information (adapted and modified from Mittelstaedt, 2000, and Benhamou & Seguinot, 1995). ....   | 7  |
| Figure 1.3: Egocentric (left) and allocentric (right) reference frames – Ego's intrinsic axis of orientation defines angles in a polar coordinate system, and Ego's egocenter establishes the origin of a vector that connects Ego with an object in the environment. Object-to-object relations (distances and directions) may also be defined with respect to an allocentric reference frame as established by the reference direction of the environment and an extrinsically defined origin (adapted from Klatzky & Wu, 2008). .... | 13 |
| Figure 1.4: Tunnel-task (Gramann et al., 2005; 2006) – <b>(A)</b> Visual flow stimulation of virtual turning tunnels; right-turning segment; <b>(B)</b> Proposed model of spatial encoding within an allocentric reference frame ('Nonturners', dark grey heads) and an egocentric reference frame ('Turners', light grey head), respectively (see text for explanation). Detailed sketches will be provided in section 3. ....   | 17 |

Figure 1.5: Brain areas involved in spatial processing – **(A)** Lateral view of the left cerebral hemisphere and **(B)** medial view of the right cerebral hemisphere showing major sulci and fissures e.g., precentral sulcus (PreCS), central sulcus (CS), postcentral sulcus (PostCS), superior (STS) and inferior temporal sulci (ITS), intraparietal sulcus (IPS), and, lateral occipital sulcus (LOS), respectively. Additionally, in medial view are depicted the corpus callosum (CC), as well as parieto-occipital (POF) and calcarine fissures (CF). Colored numbers represent approximative centroids of areas involved in processing of spatial information: (1) Primary/secondary visual cortices (V1/V2, BAs 17/18); (2) associative visual cortex V3, subarea V3A within dorsal V3 (2a) and ventral aspects (2b); (3) MT+ cluster, at the junction of the ITS and LOS; (4) posterior parietal cortex, precuneus (BA 7); (5) premotor cortex (BA 6); (6) frontal eye fields (BA 8); (7) dorsolateral prefrontal cortex (BA 9/46); (8) superior temporal gyrus (BA 22); (9) inferior temporal gyrus (BA 20); (10) (para-)hippocampal gyrus; (11) retrosplenial cortex (BA 29/30) (adapted and modified from Culham, He, Dukelow, & Verstraten, 2001; Sunaert, Van Hecke, Marchal, & Orban, 1999; Waxman, 2002)..... 20

Figure 1.6: Mixing process – The EEG outputs of two electrodes  $x_1$  and  $x_2$  can be conceptualized as linear mixtures of (at most) two IC source signals  $s_1$  and  $s_2$ . The relative proportions of each source signal in the signal mixtures depend on the distance from the electrodes to the sources..... 33

Figure 1.7: Unmixing process – The goal of ICA consists of the identification of *unmixing coefficients* in order to convert the signal mixtures  $x_1$  and  $x_2$  to form the two estimated source signals  $s_1$  and  $s_2$ . ..... 33

Figure 3.1: **(A)** Configural updating within an egocentric reference frame. As the subject moves along the outbound trajectory, egocentric distances and bearing are updated at significant time points of travel, e.g., during rotations. Thus, the path is partitioned into straight segments separated by turns. During the initial translation from S to  $P_1$ , only the return distance has to be updated while the bearing remains identical. However, during the curve, bearing as well as distance change. As a result, S moves to the right side with respect to the navigator's intrinsic axis of orientation. Between turns, distances and bearings have to be updated accordingly. During the curve at  $P_2$ , the starting point again moves from the right to the left side. **(B)** By contrast, within an allocentric reference frame, traversing the outbound trajectory based on configural updating denotes the updating of allocentric distance and bearing with respect to the reference direction. In order to process rotational information, the navigator has to update the allocentric heading, i.e., the relative direction of travel with respect to the reference direction. Since within an allocentric reference frame the navigator moves within the array of stationary objects, the return bearing does not change sides. If the allocentric bearing after the first turn is to the left, it is still on left as the path continues with an opposing turn..... 46

Figure 3.2: Cognitive headings of Turners and Nonturners differ with respect to the tunnel configuration. **(A)** Tunnels with one and two turns bending into the same direction result in distinct cognitive headings at the end of the passage. **(B)** By contrast, tunnels with two opposite turns of equal angularity result in identical final cognitive headings for Turners and Nonturners..... 49

Figure 3.3: Experiment 1 – Time line of a single trial without feedback. After 500 ms presentation of a fixation cross, a static image of the tunnel entrance was displayed (200 ms). Thereafter, the tunnel passage was presented, lasting either 9400 ms for tunnels with one turns or 16920 ms for tunnels with two turns. A snapshot of the tunnel end was presented for another 500 ms, followed by a 500 ms blank screen pre-response interval. The arrow appeared, pointing into the depth of the screen, which could be adjusted without time limit. Upon response confirmation, feedback could be provided (2000 ms). A consecutive 500 – 1500 ms blank screen announced the next trial..... 50

Figure 3.4: Experiment 1 – Percentaged mean side errors ( $\pm 1$  SD, depicted by black boxes;  $N = 20$ ), and percentaged mean arrowback reactions ( $\pm 1$  SD, depicted by grey boxes;  $N = 10$ ), for tunnels with one turn, two turns bending into the same direction (sd), and two opposite turns (od). ..... 54

Figure 3.5: Experiment 1 – Mean RT ( $\pm 1$  SD, depicted by the error bars) of the adjusted homing vector for tunnels with one turn, two turns bending into the same direction (sd), and two opposite turns (od), separately for Nonturners (solid line, boxes) and Turners (dashed line, circles). ..... 56

Figure 3.6: Experiment 1 – Mean absolute error ( $\pm 1$  SD, depicted by the error bars; solid line) of the adjusted homing vector at different eccentricities (sides were concatenated), separately for tunnels with one turn (solid line), two turns bending into the same direction (dashed line, open circles), and two opposite turns (dashed line, filled circles). ..... 57

Figure 3.7: Experiment 1 – Mean signed error ( $\pm 1$  SD, depicted by the error bars) of the adjusted homing vector at different eccentricities (sides were concatenated), separately for tunnels with one turn (solid line), two turns bending into the same direction (dashed line, open circles), and two opposite turns (dashed line, filled circles). ..... 58

Figure 3.8: Experiment 2 – Mean RT ( $\pm 1$  SD, depicted by the error bars) of the adjusted homing vector for tunnels with one turn and two turns, separately for Nonturners (solid line) and Turners (dashed line). ..... 63

Figure 3.9: Experiment 2 – Mean absolute error ( $\pm 1$  SD, depicted by the error bars) of the adjusted homing vector for tunnels with one turn and two turns, dependent on the eccentricity of end position relative to the origin of the path (data from left and right turn values of equal eccentricities were pooled), separately for Nonturners (solid line) and Turners (dashed line). ..... 64

- Figure 3.10: Experiment 2 – Mean signed error ( $\pm 1$  SD, depicted by the error bars) of the adjusted homing vector for tunnels with one turn and two turns, dependent on the eccentricity of end position relative to the origin of the path (turns of equal eccentricity to the left and right were pooled), separately for Nonturners (solid line) and Turners (dashed line)..... 65
- Figure 3.11: Experiment 2 – Mean signed error ( $\pm 1$  SD, depicted by the error bars) of the adjusted homing vector for tunnels with one turn and two turns. Due to the tunnel layout, allocentric and egocentric eccentricities for tunnels with two turns did not correspond. Therefore, tunnels with two turns ended at categorical egocentric end positions of 15° and 30°, respectively. .... 67
- Figure 3.12: Experiment 3 – Mean absolute error ( $\pm 1$  SD, depicted by the error bars) of the adjusted homing vector for tunnels with one turn (solid line, closed diamonds) and two turns (dashed line, open circles), dependent on the eccentricity of end position relative to the origin of the path (sides were concatenated), averaged over Nonturners and Turners. .... 71
- Figure 3.13: Experiment 3 – Mean signed error ( $\pm 1$  SD, depicted by the error bars) of the adjusted homing vector for tunnels with one turn (solid line) and two turns (dashed line), dependent on the eccentricity of end position relative to the origin of the path (sides were concatenated), averaged over Nonturner and Turner subjects. .... 72
- Figure 4.1: **(A)** Snapshot icons of the tunnel stimulation material providing continuous visual flow; **(B)** Return bearings of Turners and Nonturners are initially aligned, but diverge with orientation changes by the sum of rotational angles along the trajectory, also denoted as allocentric heading (orange); **(C)** Based on the return bearing of the respective reference frames, arrow adjustments of Nonturners and Turners differ. Whereas Nonturners adjust this arrow to point to the left side and back, for Turners the correct solution is an arrow pointing to their right side and back (adapted and modified from Gramann et al., 2005; Gramann et al., 2006). .... 81
- Figure 4.2: Experiment 1 – Configuration and designation of the 128-electrode-array (following the international 5%-system). Electrodes were arranged in four bundles with 32 electrodes per bundle for further signal processing to the amplifying system: (1) black filled circles [channels 1 – 32]; (2) grey filled circles [channels 33 – 64]; (3) white circles, solid lines [channels 65 – 96]; (4) white circles, dashed lines [channels 97 – 128]. Reference electrode (Ref/Cz) and ground electrode (Gnd) were connected through all amplifying bundles. .... 87
- Figure 4.3: Experiment 1 – Mean signed error ( $\pm 1$  SD, depicted by the error bars) of the adjusted homing vector for tunnels with one turn and two turns, dependent on the eccentricity of end position relative to the origin of the path (turns of equal eccentricity to the left and right were pooled), separately for

Nonturners (solid line) and Turners (dashed line). Due to dissociations in symmetry, allocentric and egocentric eccentricities for tunnels with two turns did not correspond. Therefore, tunnels with two turns ended at categorical allocentric eccentricities of 15°, 30°, 45°, and 60°, but within an *egocentric* reference frame laterality was reduced to end positions varying between 10°, 20°, and 30°, respectively (see Appendix A for tunnel layouts)..... 92

Figure 4.4: Mean event-related spectral perturbation (ERSP) images for an independent component cluster (ICC 3) located in or near left lingual gyrus (BA 17/18, panel C) revealing task-dependent changes in spectral power during spatial navigation through tunnel passages containing one turn (panel A) and two turns (panel B) and subsequent homing arrow adjustment. Cluster centroid mean ERSPs are plotted in log-spaced frequencies from 3 – 45 Hz for 11 IC processes of 8 Nonturner subjects (**A-NT**, **B-NT**), and 7 IC processes of 7 Turner subjects (**A-T**, **B-T**). ERSP difference between Nonturners and Turners is shown in panels **A-Diff** and **B-Diff** for tunnels with one turn and tunnels with 2 turns, respectively [see the following page for further explanation]. ..... 96

Figure 4.5: Mean event-related spectral perturbation (ERSP) images for an independent component cluster (ICC 4) located in or near right (bilateral) lingual gyrus (BA 17/18). For explanation see Figure 4.4 (page 96). ..... 98

Figure 4.6: Mean event-related spectral perturbation (ERSP) images for an independent component cluster (ICC 5) located in or near middle occipital gyrus (BA 18/31). For explanation see Figure 4.4 (page 96). ..... 99

Figure 4.7: Mean event-related spectral perturbation (ERSP) images for an independent component cluster (ICC 7) located in or near left inferior temporal gyrus (BA 19/37). For explanation see Figure 4.4 (page 96). ..... 100

Figure 4.8: Mean event-related spectral perturbation (ERSP) images for an independent component cluster (ICC 6) located in or near midline precuneus (BA 7/31). For explanation see Figure 4.4 (page 96). ..... 102

Figure 4.9: Mean event-related spectral perturbation (ERSP) images for an independent component cluster (ICC 11) located in or near midline precuneus (BA 7/31). For explanation see Figure 4.4 (page 96). ..... 103

Figure 4.10: Mean event-related spectral perturbation (ERSP) images for an independent component cluster (ICC 9) located in or near right inferior parietal lobule (BA 40). For explanation see Figure 4.4 (page 96). ..... 104

Figure 4.11: Mean event-related spectral perturbation (ERSP) images for an independent component cluster (ICC 10) located in or near left inferior parietal lobule (BA 40). For explanation see Figure 4.4 (page 96). ..... 105

Figure 4.12: Mean event-related spectral perturbation (ERSP) images for three independent component clusters located in or near left (ICC 13, **A-1**, **B-1**) or

|   |     |
|---|-----|
| right (ICC 14, <b>A-2</b> , <b>B-2</b> ) middle temporal gyrus (BA 21), as well as cerebellar lingual gyrus (ICC 12, <b>A-3</b> , <b>B-3</b> ) revealing task-dependent changes in spectral power during spatial navigation through tunnel passages containing one turn (panel A) and two turns (panel B) and subsequent homing arrow adjustment. Green colors indicate no significant ( $p > 0.001$ ) difference in mean log power (dB) from baseline. Warm colors indicate significant increases in log power and cold colors indicate significant decreases in log power from baseline. Important time points of the tunnel passage are marked with dashed lines: Red dashed lines indicate the period when participants perceived the approaching turn and the time period during the stimulus turn (from 3.76 s); magenta dashed lines indicate the time period during which the subjects were approaching the end of the tunnel. The final red dashed line indicates the time point when the virtual homing vector was displayed..... | 107 |
| Figure 4.13: Mean event-related spectral perturbation (ERSP) images for an independent component cluster (ICC 8) located in or near right posterior cingulate/ retrosplenial cortex (BA 29/30). For explanation see Figure 4.4 (page 96). .....   | 109 |
| Figure 4.14: Mean event-related spectral perturbation (ERSP) images for an independent component cluster (ICC 16) located in or near right precentral gyrus (BA 4/6). For explanation see Figure 4.4 (page 96). .....   | 111 |
| Figure 4.15: Mean event-related spectral perturbation (ERSP) images for an independent component cluster (ICC 17) located in or near left precentral gyrus (BA 4/6). For explanation see Figure 4.4 (page 96). .....  | 112 |
| Figure 4.16: Mean event-related spectral perturbation (ERSP) images for two independent component clusters located in or near midline medial frontal gyrus (BA 32, ICC 18, <b>A-1</b> , <b>B-1</b> ) and superior frontal gyrus (BA 8, ICC 21, <b>A-2</b> , <b>B-2</b> ). For explanation see Figure 4.12 (page 107). .....   | 114 |
| Figure 4.17: Experiment 2 – Mean signed error ( $\pm 1$ SD, depicted by the error bars) of the adjusted homing vector for tunnels with one turn (solid line) and two turns (dashed line), dependent on the eccentricity of end position relative to the origin of the path (sides were concatenated), averaged over Nonturner and Turner subjects. ....   | 123 |
| Figure 4.18: Mean event-related spectral perturbation (ERSP) images for an independent component cluster (ICC 3) located in or near right lingual gyrus (BA 18, panel C) revealing task-dependent changes in spectral power during spatial navigation through tunnel passages containing one turn (panel A) and two turns (panel B) and subsequent homing arrow adjustment. Cluster centroid mean ERSPs are plotted in log-spaced frequencies from 3 – 45 Hz for 2 IC processes of 2 Nonturner subjects ( <b>A-NT</b> , <b>B-NT</b> ), and 9 IC processes of 6 Turner subjects ( <b>A-T</b> , <b>B-T</b> ). ERSP difference between Nonturners and Turners  |     |

|  |     |
|--|-----|
| is shown in panels <b>A-Diff</b> and <b>B-Diff</b> for tunnels with one turn and tunnels with 2 turns, respectively [see the following page for further explanation]. .....  | 127 |
| Figure 4.19: Mean event-related spectral perturbation (ERSP) images for an independent component cluster (ICC 5) located in or near right (bilateral) inferior occipital gyrus (BA 18/19). For explanation see Figure 4.18 (page 127). ....  | 129 |
| Figure 4.20: Mean event-related spectral perturbation (ERSP) images for an independent component cluster (ICC 4) located in or near left (bilateral) cuneus (BA 19). For explanation see Figure 4.18 (page 127).....   | 130 |
| Figure 4.21: Mean event-related spectral perturbation (ERSP) images for an independent component cluster (ICC 7) located in or near right precuneus (BA 7/31). For explanation see Figure 4.18 (page 127).....   | 132 |
| Figure 4.22: Mean event-related spectral perturbation (ERSP) images for an independent component cluster (ICC 11) located in or near left precuneus (BA 7/31). For explanation see Figure 4.18 (page 127).....   | 133 |
| Figure 4.23: Mean event-related spectral perturbation (ERSP) images for an independent component cluster (ICC 10) located in or near right supramarginal gyrus (BA 40). For explanation see Figure 4.18 (page 127).134   |     |
| Figure 4.24: Mean event-related spectral perturbation (ERSP) images for two independent component clusters located in or near right superior temporal gyrus (BA 13, ICC 14, <b>A-1, B-1</b> ) and left inferior temporal gyrus (BA 20, ICC 15, <b>A-2, B-2</b> ) revealing task-dependent changes in spectral power during spatial navigation through tunnel passages containing one turn (panel A) and two turns (panel B) and subsequent homing arrow adjustment. Green colors indicate no significant ( $p > 0.001$ ) difference in mean log power (dB) from baseline. Warm colors indicate significant increases in log power and cold colors indicate significant decreases in log power from baseline. Important time points of the tunnel passage are marked with dashed lines: Red dashed lines indicate the period when participants perceived the approaching turn and the time period during the stimulus turn (from 3.76 s); magenta dashed lines indicate the time period during which the subjects were approaching the end of the tunnel. The final red dashed line indicates the time point when the virtual homing vector was displayed. .... | 136 |
| Figure 4.25: Mean event-related spectral perturbation (ERSP) images for an independent component cluster (ICC 9) located in or near left (midline) posterior cingulate/ retrosplenial cortex (BA 29/30). For explanation see Figure 4.18 (page 127). ....  | 138 |
| Figure 4.26: Mean event-related spectral perturbation (ERSP) images for two independent component clusters located in or near left precentral gyrus (BA  |     |

4/6, ICC 16, **A-1, B-1**) and right precentral gyrus (BA 4/6, ICC 17, **A-2, B-2**).  
For explanation see Figure 4.24 (page 136). ..... 139

Figure 4.27: Mean event-related spectral perturbation (ERSP) images for an independent component cluster located in or near right cingulate gyrus (BA 32, ICC 20). For explanation see Figure 4.24 (page 136). ..... 140

---

|  |     |
|--|-----|
| Table 4.1: Experiment 1 – Lateral and horizontal EOG clusters and 20 functional IC clusters, sorted from posterior to anterior IC cluster sites (along the y-axis). Columns provide information regarding (1) the location of the cluster centroids in Talairach space (x-y-z). All reconstructed clusters for each condition were anatomically specified within the stereotaxic coordinate system of Talairach and Tournoux using the Talairach demon software (Talairach & Tournoux, 1988), returning the coordinates of the nearest grey-matter point. Further, the table provides information regarding (2) the residual variance (RV, in %) of the reconstructed cluster centroids, and (3) their anatomical region defined in the Brodmann Area system (Brodmann, 1925). Finally, the table gives information regarding the number of Nonturner and Turner subjects ( $S_{NT}$ , $S_T$ ), as well as the amount of Nonturner and Turner Independent Components ( $IC_{NT}$ , $IC_T$ ) within each cluster..... | 94  |
| Table 4.2: Experiment 2 – Lateral and horizontal EOG and 20 functional clusters, sorted from posterior to anterior IC cluster sites (along the y-axis). Columns provide information regarding (1) the location of the cluster centroids in Talairach coordinates (x-y-z). All reconstructed clusters for each condition were anatomically specified within the stereotaxic coordinate system of Talairach and Tournoux using the Talairach demon software, returning the coordinates of the nearest grey-matter point. Further, the table provides information regarding (2) the residual variance (RV, in %) of the reconstructed cluster centroids, and (3) their anatomical region defined in the Brodmann Area system (BA, Brodmann, 1925). Finally, the table gives information regarding the number of Nonturner and Turner subjects ( $S_{NT}$ , $S_T$ ), as well as the amount of Nonturner and Turner Independent Components ( $IC_{NT}$ , $IC_T$ ) within each cluster.....                                | 125 |

# Appendix A

# Tunnel Material

## A.1 Instructions

### A.1.1 Instruction of the Categorization Phase

Thank you for participating in our study. We hope that you will enjoy it. The experiment is concerned with how humans orient in space. If you are interested in the background of the experiment, please feel free to ask the investigator after the experiment.

The task on each trial comprises a virtual journey through simulated tunnels with straight and curved segments. At the end of the journey, your task is to point back to the tunnel entrance, that is, the starting point of your journey. To solve this task, it is crucial that you keep up orientation during the journey.

A single trial will look like this: Each tunnel starts with a straight segment and ends with a straight segment. After each curve, a straight segment follows. During this simulation, you are “moving” forward into the depth of the simulated space through straight and curved segments bending either to the right or to the left. Prior to each trial, a fixation cross will appear which you should focus on.

After the tunnel passages (and some additional time) two arrows will appear, pointing directly towards the starting point of the tunnel, the tunnel entrance. Your task is to intuitively decide which one of the two arrows represents the correct direction toward the tunnel entrance. If it is the right arrow, please press the right mouse button; if it is the left arrow, please press the left button. Take your time for the decision to avoid premature answers. If you lost orienta-

tion during the passage, choose the arrow that you feel most likely represents the correct answer. After that, the experiment will continue with the next trial.

If you have any questions concerning the task or the experiment, feel free to ask the investigator now. Thank you very much.

### A.1.2 Instruction of the Training Phase

Thank you for still participating in our study. You will now encounter the Training Phase. During training trials, you are “moving” forward into the depth of the simulated space through straight and curved segments. At the end of the tunnel passage, your task is to point back to the tunnel entrance, that is, the starting point of your journey. To solve this task, it is crucial that you keep up orientation.

Each tunnel starts with a straight segment and ends with a straight segment. After each curve, a straight segment follows. During this simulation, you are “moving” forward into the depth of the simulated space through straight and curved segments bending either to the right or to the left. Prior to each trial, a fixation cross will appear which you should focus on.

After each trial, an arrow will appear pointing straight ahead into the depth of the virtual space. Your task now is to adjust this arrow by using the left and right mouse buttons to point directly back to the starting point of the traversed passage. If you want to rotate the arrow counter-clockwise, keep the left mouse button pressed. Use the right mouse button to rotate the arrow clockwise. Please try to adjust the arrow as accurate as possible, and press the middle mouse button (mouse wheel) to confirm your adjustment. Afterwards you will see the adjusted arrow on the left side of the screen. On the right side, a feedback arrow will be presented, showing the correct angular adjustment.

If you lost orientation during the passage, adjust the arrow to most likely point directly back to the starting point. After that, the experiment will continue with the next trial.

If you have any questions concerning the task or the experiment, feel free to ask the investigator now. Thank you very much.

### A.1.3 Instruction of the Main Experiments

Thank you for still participating in our study. You will now encounter the Main Experiment. During each trial, you are “moving” forward into the depth of the simulated space through straight and curved segments. At the end of the tunnel passage, your task is to point back to the tunnel entrance, that is, the starting point of your journey. To solve this task, it is crucial that you keep up orientation.

In the upcoming experimental phase you will encounter two different tunnel categories: One group of tunnels will comprise one or two turns, another group will have no turns. Each tunnel starts with a straight segment and ends with a straight segment. After each curve, a straight segment follows. During this simulation, you are “moving” forward into the depth of the simulated space through straight and curved segments bending either to the right or to the left. Prior to each trial, a fixation cross will appear which you should focus on.

After each trial, an arrow will appear pointing straight ahead into the depth of the virtual space. Your task now is to adjust this arrow by using the left and right mouse buttons to point directly back to the starting point of the traversed passage. If you want to rotate the arrow counter-clockwise, keep the left mouse button pressed. Use the right mouse button to rotate the arrow clockwise. Please try to adjust the arrow as accurate as possible, and press the middle mouse button (mouse wheel) to confirm your adjustment. In contrast to the Training Phase, feedback will be provided just once in a while.

If you lost orientation during the passage, adjust the arrow to most likely point directly back to the starting point. After that, the experiment will continue with the next trial.

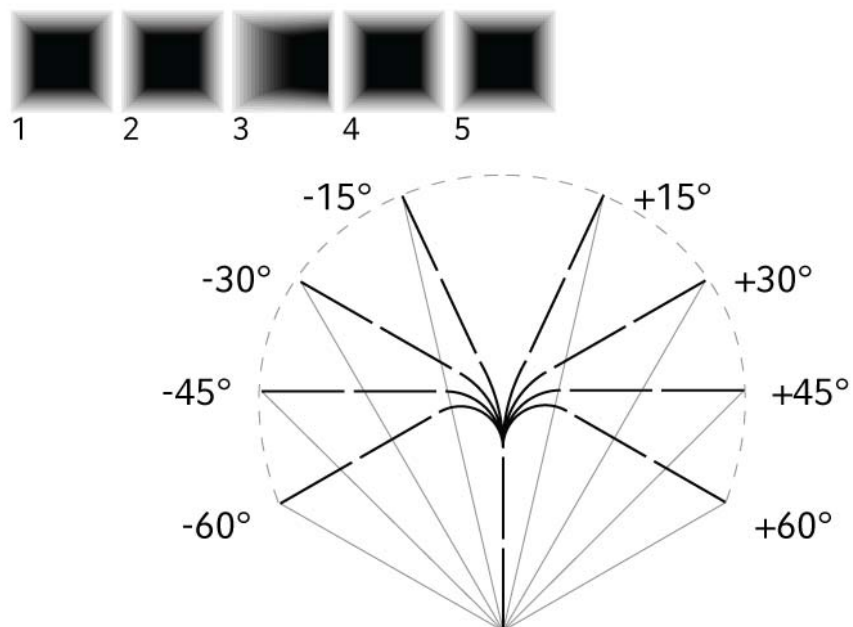
If you have any questions concerning the task or the experiment, feel free to ask the investigator now. Thank you very much.

## A.2 Tunnel Configurations

The following tables contain information regarding the experimental material of the virtual tunnel passages: (1) Angles of the consecutive segments [ $^{\circ}$ ], (2) the angular sum of the entire trajectory [ $^{\circ}$ ], (3) the length of the tunnel passage [virtual standard units; 25 virtual standard units = 1 subsegment; 14 sub-segments = 1 main segment], (4) the final exact eccentricity of end position [ $^{\circ}$ ], and (5) the final categorical eccentricity of end position [ $^{\circ}$ ], respectively. Participants were at no point of the experiment provided neither with information regarding the precise (metric) structure nor map-like sketches of the passages.

### A.2.1 Tunnels with 1 Turn (5 Segments)

#### Tunnel Layout



## Tunnel Segments

| S1 | S2 | S3   | S4 | S5 | Angle Sum | Length | Eccentricity | Categorical Eccentricity |
|----|----|------|----|----|-----------|--------|--------------|--------------------------|
| 0  | 0  | -121 | 0  | 0  | -121      | 279.40 | -60.50       | -60                      |
| 0  | 0  | -118 | 0  | 0  | -118      | 289.26 | -59.00       | -60                      |
| 0  | 0  | -91  | 0  | 0  | -91       | 370.18 | -45.50       | -45                      |
| 0  | 0  | -88  | 0  | 0  | -88       | 378.19 | -44.00       | -45                      |
| 0  | 0  | -62  | 0  | 0  | -62       | 438.06 | -31.00       | -30                      |
| 0  | 0  | -58  | 0  | 0  | -58       | 445.63 | -29.00       | -30                      |
| 0  | 0  | -32  | 0  | 0  | -32       | 483.21 | -16.00       | -15                      |
| 0  | 0  | -28  | 0  | 0  | -28       | 487.13 | -14.00       | -15                      |
| 0  | 0  | 28   | 0  | 0  | 28        | 487.13 | 14.00        | 15                       |
| 0  | 0  | 32   | 0  | 0  | 32        | 483.21 | 16.00        | 15                       |
| 0  | 0  | 58   | 0  | 0  | 58        | 445.63 | 29.00        | 30                       |
| 0  | 0  | 62   | 0  | 0  | 62        | 438.06 | 31.00        | 30                       |
| 0  | 0  | 88   | 0  | 0  | 88        | 378.19 | 44.00        | 45                       |
| 0  | 0  | 91   | 0  | 0  | 91        | 370.18 | 45.50        | 45                       |
| 0  | 0  | 118  | 0  | 0  | 118       | 289.26 | 59.00        | 60                       |
| 0  | 0  | 121  | 0  | 0  | 121       | 279.40 | 60.50        | 60                       |

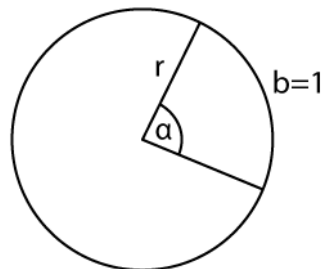
## Angular Specifications

Based on the radian equation

$$b = \pi \cdot r \cdot \frac{\alpha}{180^\circ} \quad (\text{A.1})$$

with  $b = 14$  [standard virtual units] equation (A.2) can be solved for  $r$ :

$$r = \frac{b}{\pi} \cdot \frac{180^\circ}{\alpha} = \frac{14}{\pi} \cdot \frac{180^\circ}{\alpha}. \quad (\text{A.2})$$

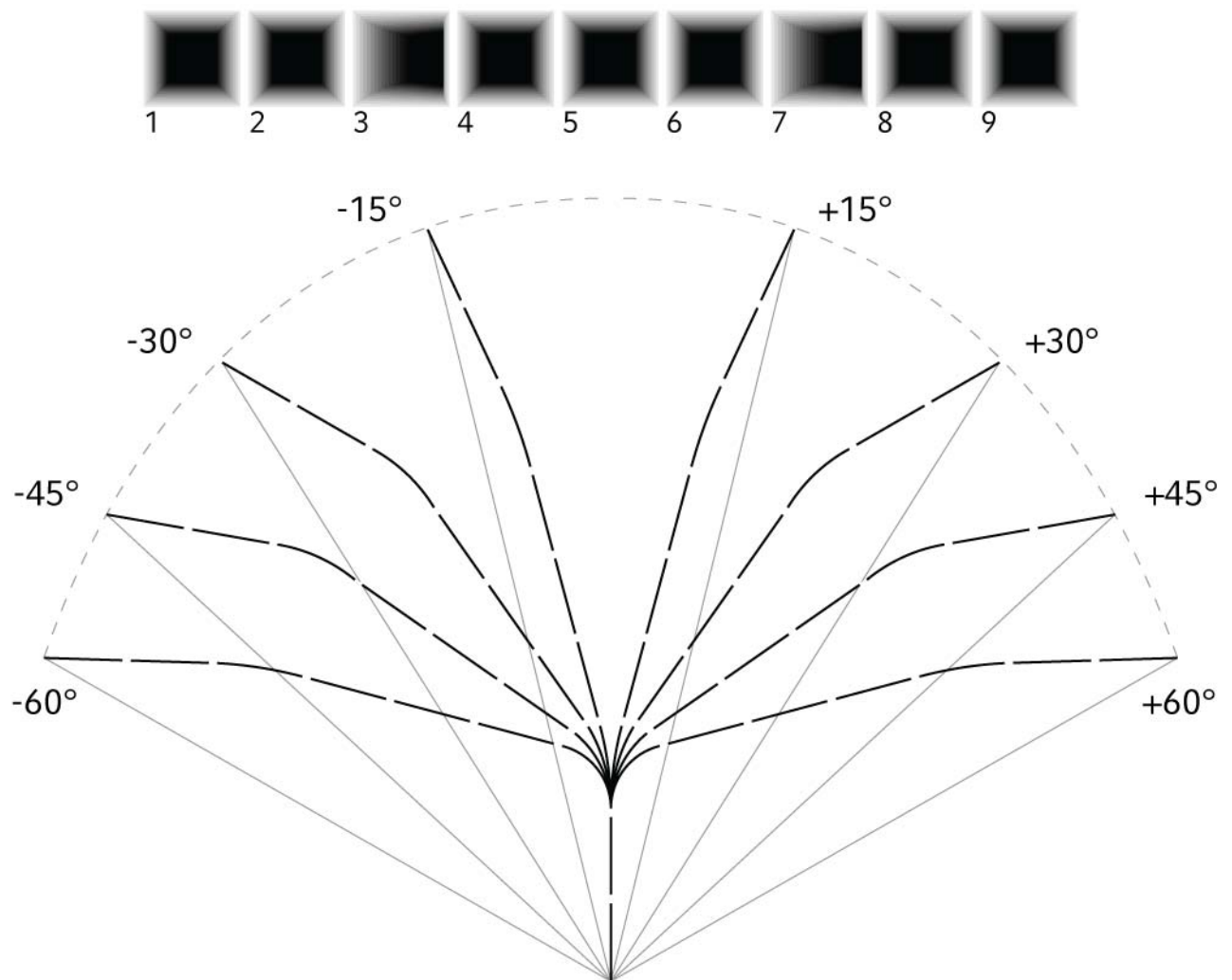


Radii of the turns [in standard virtual units; 1 unit = 1 sub-segment]

| Absolute Turning Angle | Radius |
|------------------------|--------|
| 28                     | 28.644 |
| 32                     | 26.740 |
| 58                     | 13.832 |
| 62                     | 12.936 |
| 88                     | 9.114  |
| 91                     | 8.820  |
| 118                    | 6.804  |
| 121                    | 6.636  |

### A.2.2 Tunnels with 2 Turns, Same Direction (9 Segments)

Tunnel Layout



## Tunnel Segments

| S1 | S2 | S3  | S4 | S5 | S6 | S7  | S8 | S9 | Angle Sum | Length | Eccentricity | Categorical Eccentricity |
|----|----|-----|----|----|----|-----|----|----|-----------|--------|--------------|--------------------------|
| 0  | 0  | -76 | 0  | 0  | 0  | -12 | 0  | 0  | -88       | 743.61 | -60.46       | -60                      |
| 0  | 0  | -71 | 0  | 0  | 0  | -19 | 0  | 0  | -90       | 746.48 | -58.47       | -60                      |
| 0  | 0  | -60 | 0  | 0  | 0  | -7  | 0  | 0  | -67       | 803.85 | -46.29       | -45                      |
| 0  | 0  | -50 | 0  | 0  | 0  | -30 | 0  | 0  | -80       | 788.03 | -45.01       | -45                      |
| 0  | 0  | -30 | 0  | 0  | 0  | -31 | 0  | 0  | -61       | 835.33 | -30.26       | -30                      |
| 0  | 0  | -34 | 0  | 0  | 0  | -14 | 0  | 0  | -48       | 856.86 | -28.64       | -30                      |
| 0  | 0  | -10 | 0  | 0  | 0  | -36 | 0  | 0  | -46       | 858.20 | -17.00       | -15                      |
| 0  | 0  | -15 | 0  | 0  | 0  | -10 | 0  | 0  | -25       | 888.76 | -13.62       | -15                      |
| 0  | 0  | 15  | 0  | 0  | 0  | 10  | 0  | 0  | 25        | 888.76 | 13.62        | 15                       |
| 0  | 0  | 10  | 0  | 0  | 0  | 36  | 0  | 0  | 46        | 858.20 | 17.00        | 15                       |
| 0  | 0  | 34  | 0  | 0  | 0  | 14  | 0  | 0  | 48        | 856.86 | 28.64        | 30                       |
| 0  | 0  | 30  | 0  | 0  | 0  | 31  | 0  | 0  | 61        | 835.33 | 30.26        | 30                       |
| 0  | 0  | 50  | 0  | 0  | 0  | 30  | 0  | 0  | 80        | 788.03 | 45.01        | 45                       |
| 0  | 0  | 60  | 0  | 0  | 0  | 7   | 0  | 0  | 67        | 803.85 | 46.29        | 45                       |
| 0  | 0  | 71  | 0  | 0  | 0  | 19  | 0  | 0  | 90        | 746.48 | 58.47        | 60                       |
| 0  | 0  | 76  | 0  | 0  | 0  | 12  | 0  | 0  | 88        | 743.61 | 60.46        | 60                       |

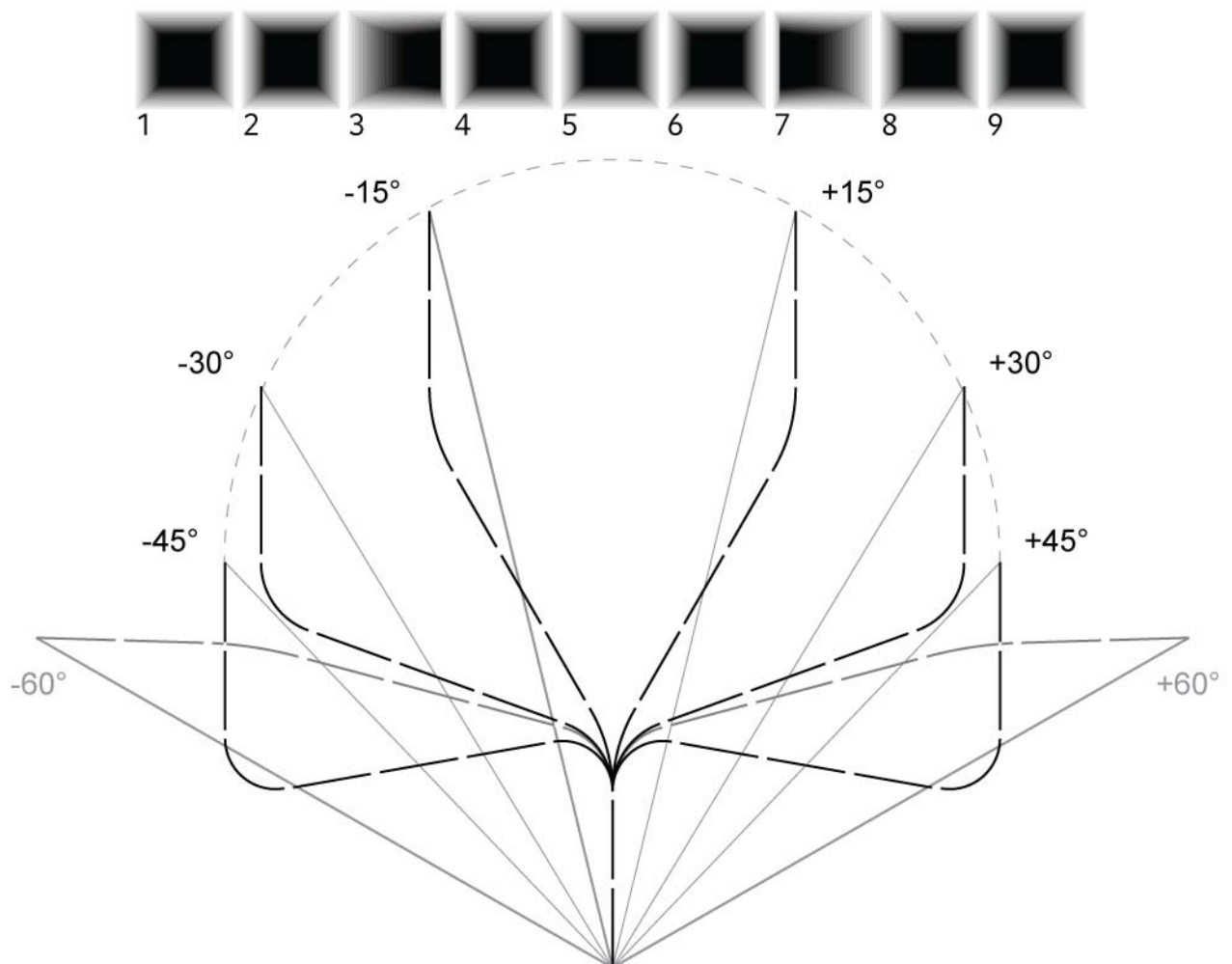
## Angular Specifications

Radii of the turns [standard virtual units; 1 unit = 1 sub-segment]

| First Turn             |        | Second Turn            |         |
|------------------------|--------|------------------------|---------|
| Absolute Turning Angle | Radius | Absolute Turning Angle | Radius  |
| 15                     | 53.480 | 10                     | 80.220  |
| 10                     | 80.220 | 36                     | 22.288  |
| 34                     | 23.590 | 14                     | 57.302  |
| 30                     | 26.740 | 31                     | 25.872  |
| 50                     | 16.044 | 30                     | 26.740  |
| 60                     | 13.370 | 7                      | 114.590 |
| 71                     | 11.298 | 19                     | 42.224  |
| 76                     | 10.556 | 12                     | 66.850  |

### A.2.3 Tunnels with 2 Turns, Opposite Direction (9 Segments)

#### Tunnel Layout



### Tunnel Segments

| 1 | 2 | 3    | 4 | 5 | 6 | 7    | 8 | 9 | Angle Sum | Length | Eccentricity | Categorical Eccentricity |
|---|---|------|---|---|---|------|---|---|-----------|--------|--------------|--------------------------|
| 0 | 0 | -76  | 0 | 0 | 0 | -12  | 0 | 0 | -88       | 743.61 | -60.46       | -60                      |
| 0 | 0 | -71  | 0 | 0 | 0 | -19  | 0 | 0 | -90       | 746.48 | -58.47       | -60                      |
| 0 | 0 | -108 | 0 | 0 | 0 | 108  | 0 | 0 | 0         | 588.71 | -46.10       | -45                      |
| 0 | 0 | -100 | 0 | 0 | 0 | 100  | 0 | 0 | 0         | 630.19 | -43.02       | -45                      |
| 0 | 0 | -70  | 0 | 0 | 0 | 70   | 0 | 0 | 0         | 763.36 | -30.69       | -30                      |
| 0 | 0 | -65  | 0 | 0 | 0 | 65   | 0 | 0 | 0         | 781.67 | -28.56       | -30                      |
| 0 | 0 | -38  | 0 | 0 | 0 | 38   | 0 | 0 | 0         | 858.83 | -16.83       | -15                      |
| 0 | 0 | -31  | 0 | 0 | 0 | 31   | 0 | 0 | 0         | 872.52 | -13.74       | -15                      |
| 0 | 0 | 31   | 0 | 0 | 0 | -31  | 0 | 0 | 0         | 872.52 | 13.74        | 15                       |
| 0 | 0 | 38   | 0 | 0 | 0 | -38  | 0 | 0 | 0         | 858.83 | 16.83        | 15                       |
| 0 | 0 | 65   | 0 | 0 | 0 | -65  | 0 | 0 | 0         | 781.67 | 28.56        | 30                       |
| 0 | 0 | 70   | 0 | 0 | 0 | -70  | 0 | 0 | 0         | 763.36 | 30.69        | 30                       |
| 0 | 0 | 100  | 0 | 0 | 0 | -100 | 0 | 0 | 0         | 630.19 | 43.02        | 45                       |
| 0 | 0 | 108  | 0 | 0 | 0 | -108 | 0 | 0 | 0         | 588.71 | 46.10        | 45                       |
| 0 | 0 | 71   | 0 | 0 | 0 | 19   | 0 | 0 | 90        | 746.48 | 58.47        | 60                       |
| 0 | 0 | 76   | 0 | 0 | 0 | 12   | 0 | 0 | 88        | 743.61 | 60.46        | 60                       |

### Angular Specifications

Radii of the turns [standard virtual units; 1 unit = 1 sub-segment]

| First Turn               |        | Second Turn                     |        |
|--------------------------|--------|---------------------------------|--------|
| Absolute Turning Angle 1 | Radius | Turning Angle 2 (relative to 1) | Radius |
| 31                       | 25.872 | -31                             | 25.872 |
| 38                       | 21.112 | -38                             | 21.112 |
| 65                       | 12.334 | -65                             | 12.334 |
| 70                       | 11.466 | -70                             | 11.466 |
| 100                      | 8.022  | -100                            | 8.022  |
| 108                      | 7.434  | -108                            | 7.434  |
| 71                       | 11.298 | 19                              | 11.298 |
| 76                       | 10.556 | 12                              | 10.556 |

## Appendix B

# EEG-Cap Layout

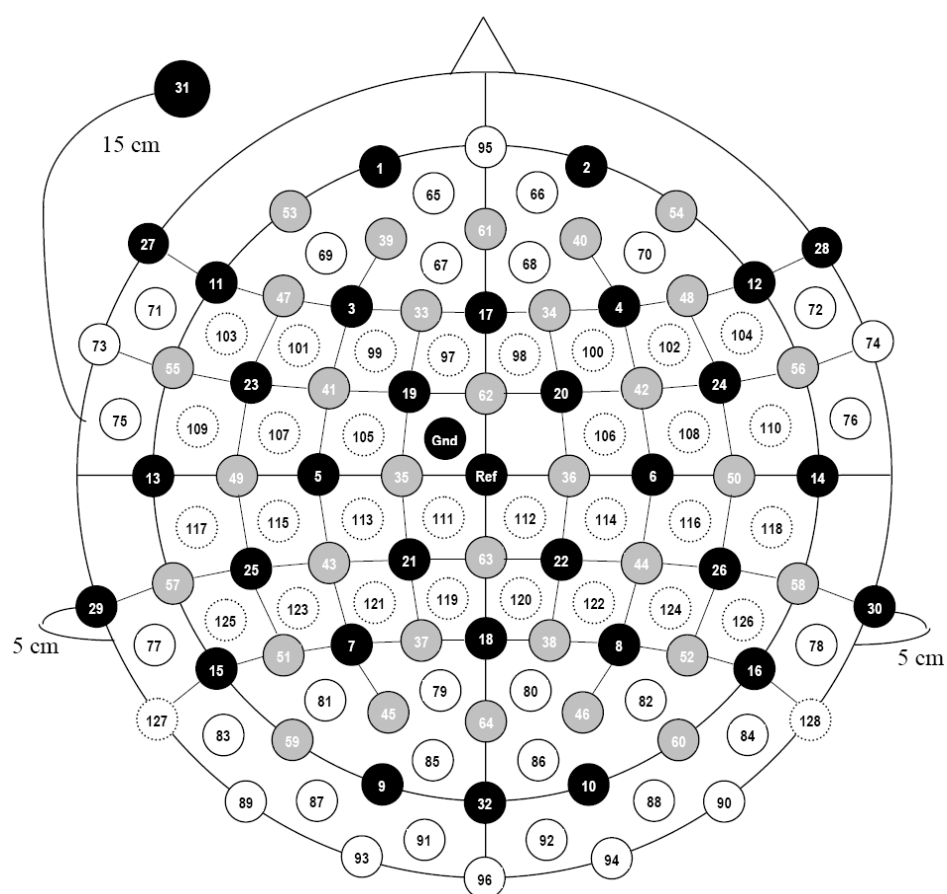


Figure B.1: Electrode designation of the electrode caps used in Experiments 1 and 2 (following the international 5%-system).

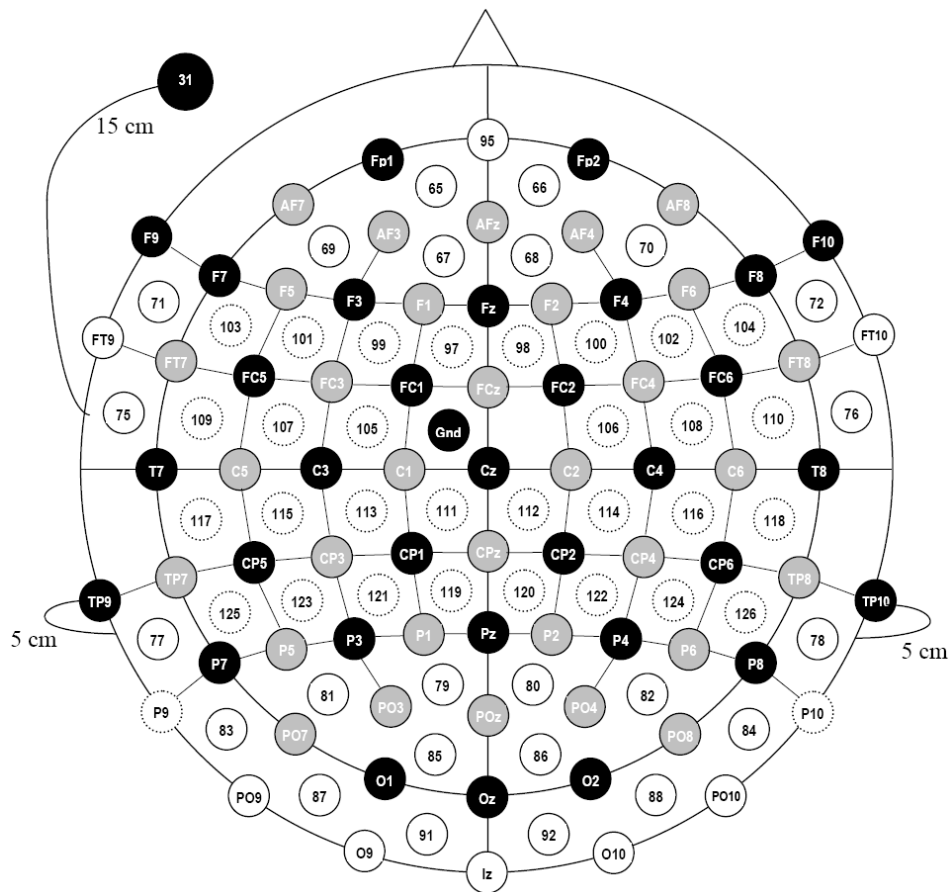


Figure B.2: Channel assignment of the 128 electrodes (+ 1 eye electrode, + ground electrode).

Electrodes were arranged in four bundles with 32 electrodes per bundle for further signal processing to the amplifying system: (1) black filled circles [channels 1 – 32]; (2) grey filled circles [channels 33 – 64]; (3) white circles, solid lines [channels 65 – 96]; (4) white circles, dashed lines [channels 97 – 128]. Reference electrode (Ref/Cz) and ground electrode (Gnd) were connected through all amplifying bundles.

# Eidesstattliche Versicherung

Hiermit versichere ich, Markus Plank, geb. am 10.09.1979 in Villingen-Schwenningen, an Eides Statt, dass ich die vorliegende Dissertation selbstständig und ohne unerlaubte fremde Hilfe angefertigt, keine anderen als die von mir angegebenen Schriften und Hilfsmittel benutzt und die den benutzten Werken wörtlich oder inhaltlich entnommenen Stellen kenntlich gemacht habe.

Weiterhin bestätige ich, dass keine früheren Promotionsversuche unternommen bzw. keine Promotionen abgeschlossen wurden. Diese Dissertation lag zu keinem Zeitpunkt in gleicher oder anderer Form in einem anderen Verfahren vor.

Die Dissertation wird in elektronischer Form veröffentlicht. Daher übertrage ich der Universitätsbibliothek der LMU München, der DDB (Die Deutsche Bibliothek) in Frankfurt/Leipzig und der DFG-Sondersammelgebietsbibliothek das Recht, die elektronische Version (inkl. meines Lebenslaufs) in Datennetzen zu veröffentlichen.

Dies bestätige ich mit meiner Unterschrift.

---

Markus Plank

# Curriculum Vitae

**Markus Plank**  
**(ne Mueller)**

Born on 10. September 1979 in Villingen-Schwenningen (Germany)

## Employment

- |             |  |
|-------------|--|
| 2006 – 2009 | <b>Research Assistant</b><br>Department Psychologie,<br>Ludwig-Maximilians-Universität München |
|-------------|--|

## Research Visits

- |                   |   |
|-------------------|---|
| 04/2008 – 06/2008 | Swartz Center for Computational Neuroscience (SCCN),<br>University of California, San Diego |
| 09/2007 – 11/2007 | Swartz Center for Computational Neuroscience (SCCN),<br>University of California, San Diego |

## Grants and Scholarships

- |                   |  |
|-------------------|--|
| 04/2008 – 06/2008 | G.A.-Lienert-Foundation for Promotion of Young Researchers in Biopsychological Methods |
| 04/2008 – 06/2008 | German Academic Exchange Service [DAAD]  |
| 09/2007 – 11/2007 | Boehringer Ingelheim Fonds, Foundation for Basic Research in Medicine                  |

### **Scientific Education**

|             |  |
|-------------|--|
| 2006 – 2009 | <b>Psychology (Ph.D.)</b>              |
|             | Ludwig-Maximilians-Universität München |
| 2002 – 2006 | <b>Psychology (Dipl.-Psych.)</b>       |
|             | Universität Trier                      |
| 2000 – 2002 | <b>Psychology</b>                      |
|             | Technische Universität Dresden         |
| 1999        | <b>Abitur</b>                          |
|             | Albertus-Magnus-Gymnasium Rottweil     |

### **Memberships**

- Deutsche Gesellschaft für Psychophysiologie und ihre Anwendung (DGPA)